BEILSTEIN JOURNAL OF ORGANIC CHEMISTRY

Sustainable concepts in catalysis: nonprecious metals and visible light

Edited by Osama El-Sepelgy andLuis Miguel Azofra

Imprint

Beilstein Journal of Organic Chemistry
www.bjoc.org
ISSN 1860-5397
Email: journals-support@beilstein-institut.de

The *Beilstein Journal of Organic Chemistry* is published by the Beilstein-Institut zur Förderung der Chemischen Wissenschaften.

Beilstein-Institut zur Förderung der Chemischen Wissenschaften
Trakehner Straße 7–9
60487 Frankfurt am Main
Germany
www.beilstein-institut.de

BEILSTEIN JOURNAL OF ORGANIC CHEMISTRY

Recent advancements in iodide/phosphine-mediated photoredox radical reactions

Tinglan Liu[1], Yu Zhou[2], Junhong Tang[1] and Chengming Wang[*1]

Review

Open Access

Address:
[1]Department of Chemistry, Jinan University, Guangzhou 511443, P. R. China and [2]UNITEST, Weifang 261000, P. R. China

Email:
Chengming Wang[*] - cmwang2019@jnu.edu.cn

* Corresponding author

Keywords:
annulation; decarboxylative; iodide/phosphine; photocatalytic; radical reaction

Beilstein J. Org. Chem. **2023,** *19,* 1785–1803.
https://doi.org/10.3762/bjoc.19.131

Received: 16 September 2023
Accepted: 10 November 2023
Published: 22 November 2023

This article is part of the thematic issue "Sustainable concepts in catalysis: nonprecious metals and visible light".

Guest Editor: O. El-Sepelgy

Abstract

Photoredox catalysis plays a crucial role in contemporary synthetic organic chemistry. Since the groundbreaking work of Shang and Fu on photocatalytic decarboxylative alkylations in 2019, a wide range of organic transformations, such as alkylation, alkenylation, cyclization, amination, iodination, and monofluoromethylation, have been progressively achieved using a combination of iodide and PPh_3. In this review, we primarily focus on summarizing the recent advancements in inexpensive and readily available iodide/phosphine-mediated photoredox radical transformations.

Introduction

Over the past few decades, numerous remarkable breakthroughs and notable progresses have been achieved in the realm of photoredox catalysis [1-3]. This domain has profoundly transformed modern organic synthesis, resulting in a considerable surge in research efforts centered on free radical reactions [4]. Presently, photoredox catalysis has risen to prominence as an incredibly effective methodology, establishing itself as a powerful tool for crafting various C–X (X = C, N, O, F, Cl…) bonds owing to its advantageous traits, such as sustainability, practicality, and environmental compatibility [5].

Despite its broad synthetic utilities, there are still a few drawbacks associated with these photoredox reactions. One of the main limitations is the reliance on precious metals such as Ir, Ru, and Pd, or elaborate organic dyes that act as photosensitizers, which are either limited in abundance or require additional synthetic steps to obtain, thus greatly impeding the widespread application of photoredox catalysis in large-scale industrial processes.

In this context, in 2019, Shang, Fu, and their colleagues made an important breakthrough in addressing these above-mentioned

limitations [6]. They disclosed a photocatalytic decarboxylative alkylation reaction that was facilitated by the synergistic action of a cost-effective and easily accessible NaI/PPh_3 catalyst system (Scheme 1). This system offered an alternative to the use of precious metals or complex organic dyes as catalysts. The developed NaI/PPh_3-based system not only provided a more sustainable and economically viable approach but also demonstrated excellent performance in various transformations. It had been successfully applied to a series of radical reactions, including trifluoromethylation, deaminative alkylation, and asymmetric versions of Minisci reactions, resulting in good to excellent yields and enantioselectivity. This groundbreaking work opened up new possibilities for the practical application of photoredox catalysis in large-scale industrial processes, as it provided a more accessible and cost-effective catalyst system that could be readily utilized for a wide range of transformations [7,8].

Moreover, they proposed a plausible mechanism for the aforementioned conversions (Scheme 2). Initially, an NaI/PPh_3 complex **I** was formed through a cation–π interaction. Subsequently, the combination of complex **I** with *N*-(cyclohexanecarbonyloxy)phthalimide smoothly delivered an electron donor–acceptor (EDA) complex **II** via coulombic interactions. Upon 456 nm blue LED light irradiation, the EDA complex **II** underwent a single electron transfer (SET) process, followed by subsequent decarboxylation to produce the alkyl radical intermediate **A**, accompanied by electron release. The radical intermediate **A** could then be captured by a series of different radical acceptors. Finally, the initial NaI/PPh_3 complex **I** was regenerated from complex **III** through an electron injection/reduction process.

This article aims to provide a comprehensive overview of the latest advancements in the iodide/phosphine catalytic photoredox system. The primary focus of the paper is to delve into the unique catalytic reactivity exhibited by the iodide/phosphine photoredox system, while also exploring potential reaction mechanisms. It is mainly organized around different types of reactions, providing a structured and systematic analysis of each category.

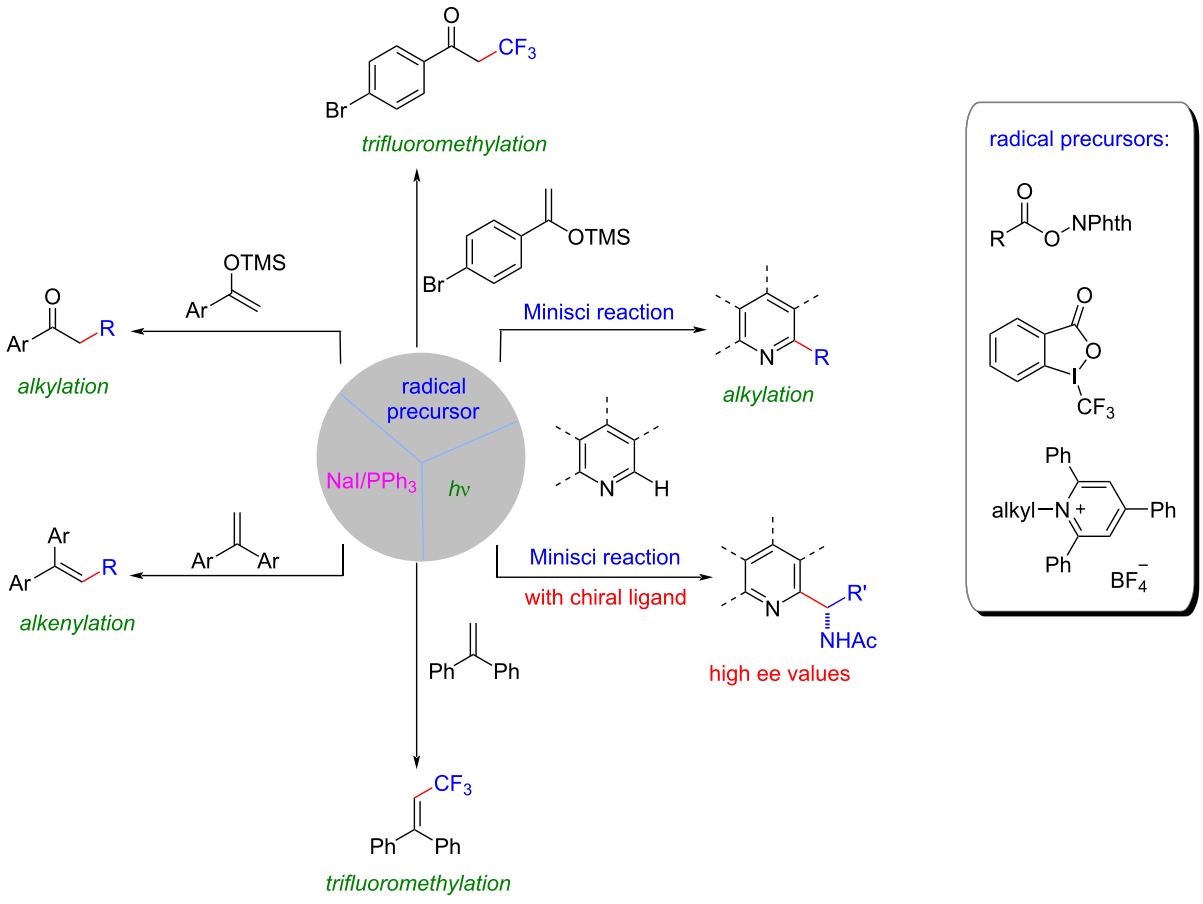

Scheme 1: Photocatalytic decarboxylative transformations mediated by the NaI/PPh_3 catalyst system.

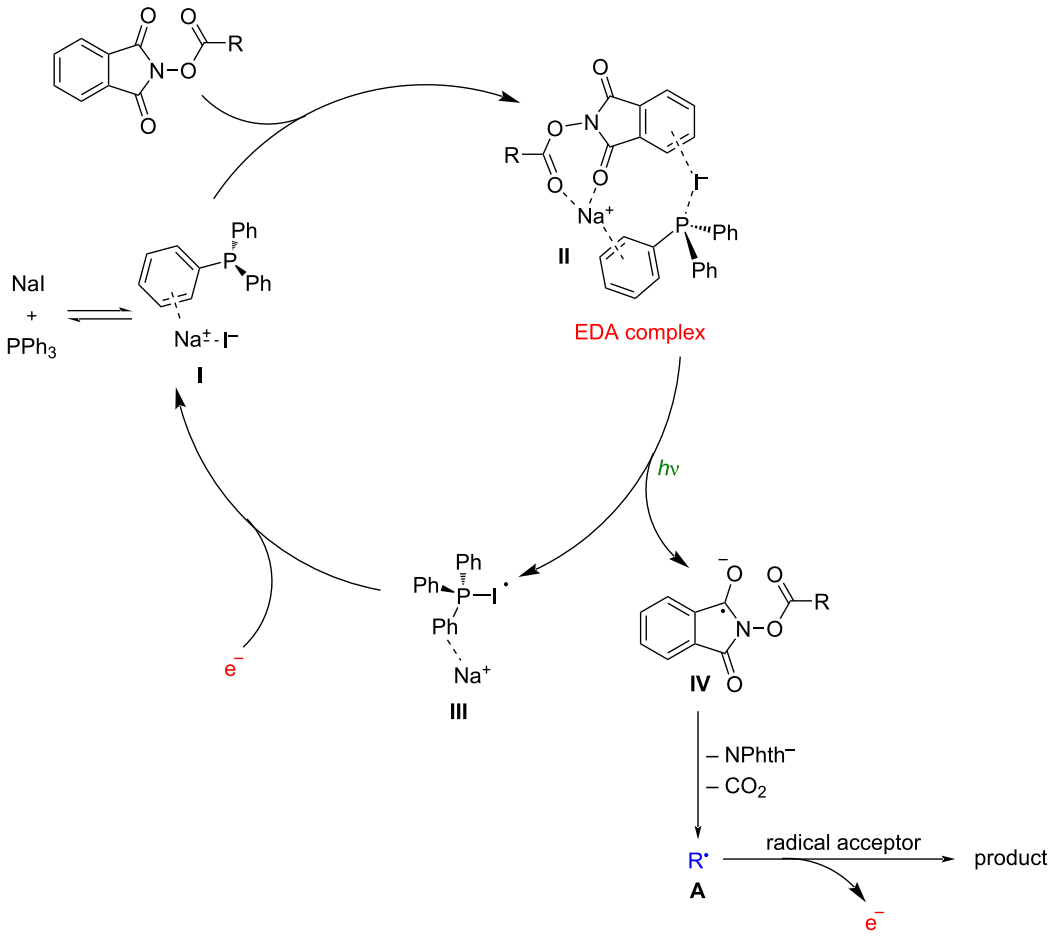

Scheme 2: Proposed catalytic cycle of NaI/PPh_3 photoredox catalysis.

Review

Iodide/phosphine-catalyzed photoredox transformations

Since the seminal work of Shang and Fu, the established NaI/PPh_3 combined system has paved the way for a wide range of photoredox reactions. These reactions encompass diverse transformations such as alkenylation, alkylation, cyclization, amination, iodination, and many others. The discovery of these conversions has significantly expanded the scope and versatility of the NaI/PPh_3 catalytic system, now making it a powerful tool in synthesis.

Alkenylation

In 2020, Shang, Fu, and colleagues reported on the photocatalytic decarboxylative alkenylation reactions facilitated by cooperative NaI/PPh_3 catalysis [9]. These conversions involved the coupling of 1,1-diarylethene/cinnamic acid derivatives (**1**, **2**) with redox-active esters **3** (Scheme 3). Notably, the reactions were driven by blue light irradiation at either 440 nm or 456 nm, and they occurred in acetone at room temperature, without the need for transition metals or organic dyes as photosensitizers. Interestingly, it was discovered that solvation played a vital role in the overall process. These findings shed light on the mechanistic aspects of the reaction and highlighted the potential of the NaI/PPh_3 catalytic system for achieving efficient and transition-metal-free photocatalytic transformations.

Following that, Li and his research group documented similar results (Scheme 4) [10]. They extensively investigated the compatibility and efficiency of a diverse range of redox-active esters **3**, deriving from various aliphatic carboxylic acids (including primary, secondary, and tertiary acids), as well as α-amino acids. Impressively, these redox-active esters exhibited exceptional compatibility, high effectiveness, and remarkable specificity in the synthesis of β-alkylated styrenes **5**. This study underscored the broad applicability and selectivity of the NaI/PPh_3 catalytic system in facilitating the synthesis of β-alkylated styrenes using diverse redox-active esters.

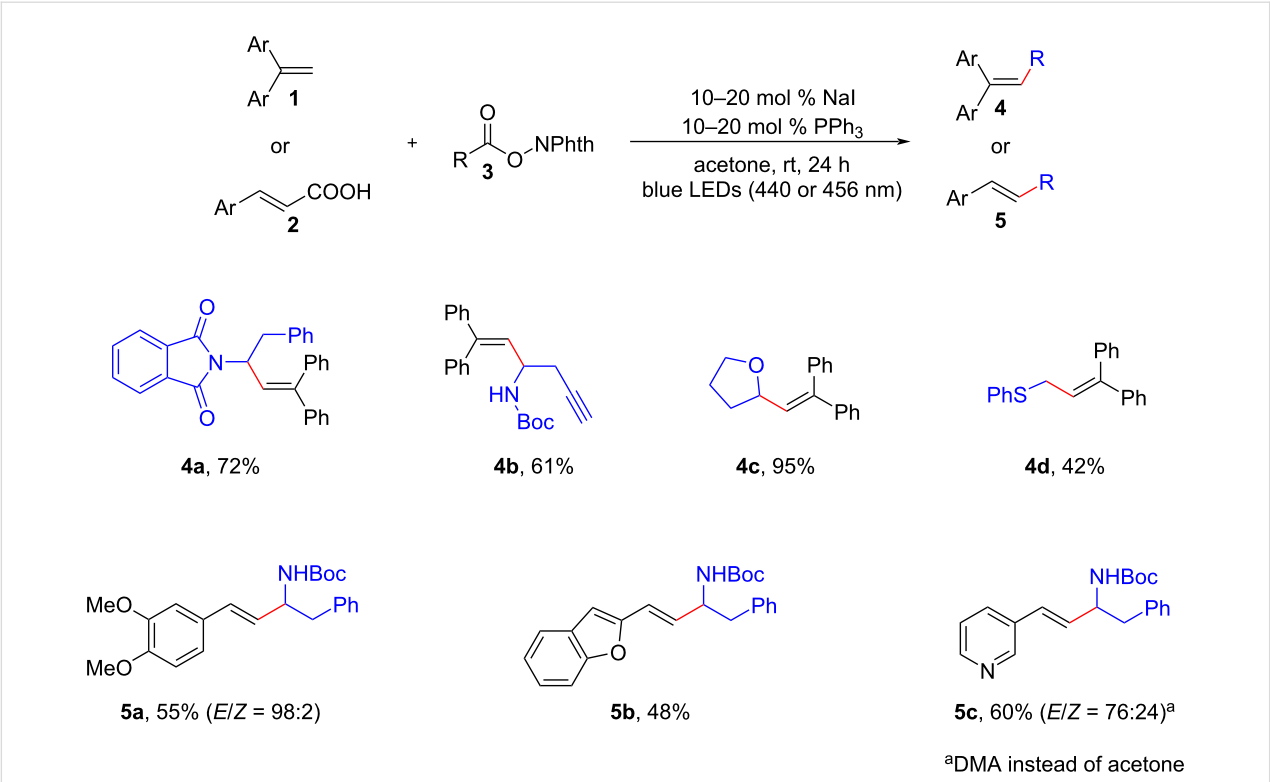

Scheme 3: Decarboxylative alkenylation of redox-active esters by NaI/PPh_3 catalysis.

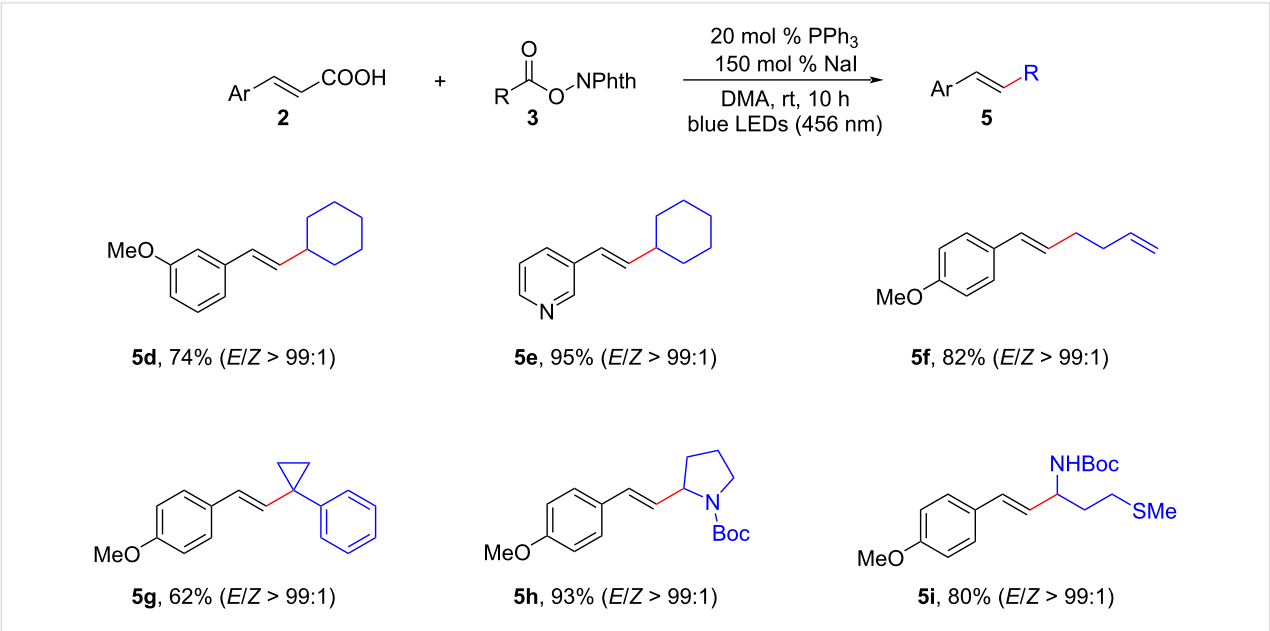

Scheme 4: Decarboxylative alkenylation mediated by NaI/PPh_3 catalysis.

It is worth highlighting that triphenylphosphine is not essential for the photoredox cross-coupling reactions discussed above. A recent elegant study conducted by Chen and colleagues introduced a straightforward method that directly employed sodium iodide for photoinduced deaminative alkenylation processes [11]. This method enabled the synthesis of β,γ-unsaturated esters **8**, **9** without the requirements of phosphine or other photocatalysts (Scheme 5). Through the use of density func-

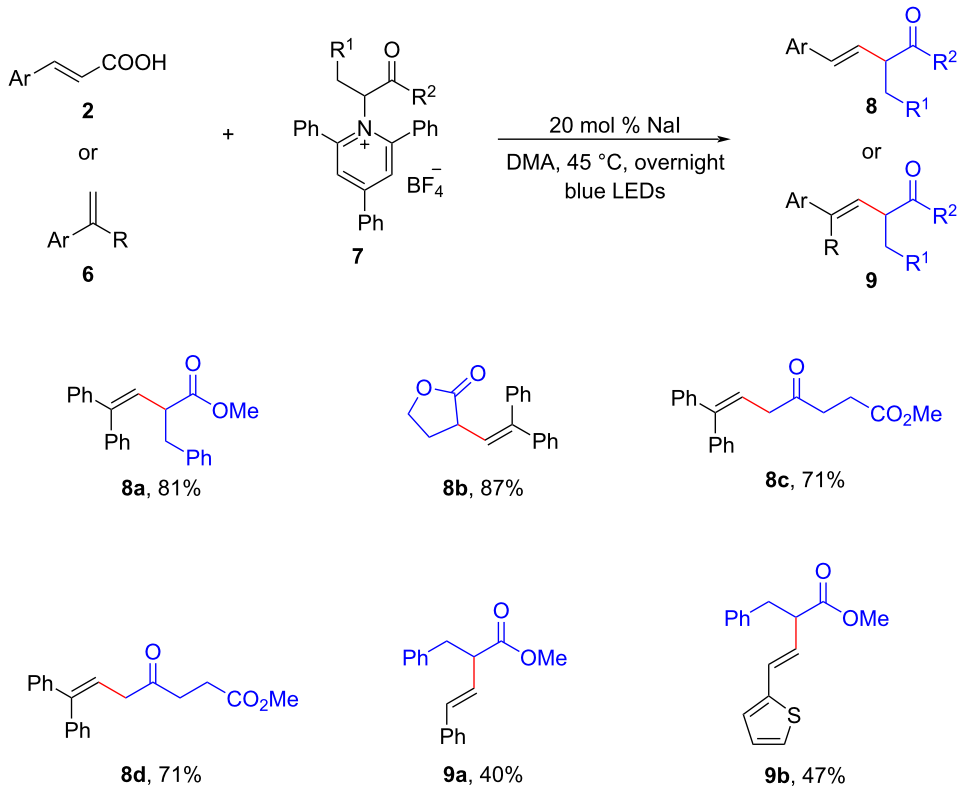

Scheme 5: NaI-mediated photoinduced α-alkenylation of Katritzky salts **7**.

tional theory (DFT) calculations, they elucidated the mechanism behind this process. It was revealed that the formation of a photoactive EDA complex, which subsequently generated alkyl radicals for alkenylation, was primarily facilitated by the electrostatic interaction between NaI and Katritzky salts **7**. This innovative approach not only expanded the scope of photoredox cross-coupling reactions but also offered valuable insights into the role of NaI in facilitating these transformations.

In a recent study, Zheng et al. introduced a highly effective photocatalytic approach for the decarboxylative conversion of redox-active esters **10**, leading to the efficient synthesis of olefins **11**. This process was conducted in the presence of *n*-Bu_4NI, as illustrated in Scheme 6 [12]. The utilization of mild reaction conditions allowed for the application of this method in the modification of complex natural products or pharmaceuticals. Moreover, this photoinduced decarboxylative approach demonstrated the potential for broader utilization in the construction of diverse $C(sp^3)$–N and $C(sp^3)$–X bonds.

An EDA complex was formed through non-covalent interaction between the redox ester **10** and *n*-Bu_4NI (Scheme 7). Subsequently, upon the photoexcitation, radical pairs **I** were generated via a SET process, accompanied by the liberation of CO_2 and the phthalimide anion. The recombination of the alkyl radical and $I^{\bullet}$ played a pivotal as an intermediate step in the production of alkyl iodides **B**. Compound **B** could undergo a further elimination reaction to yield various olefins **11**.

Regarding benzyl substrates, the radical $I^{\bullet}$ demonstrated its efficacy as a reagent for hydrogen atom transfer (HAT), specifically by extracting a hydrogen atom from the α-position of benzyl radicals **A**. The process described above led to the formation of the corresponding olefins **11**, eliminating the need for a carbon–iodine bond formation step.

Alkylation

Diaziridines are highly versatile building blocks in synthesis, with the ability to be readily transformed into various valuable functional molecules, including amines, hydrazines, and nitrogen-containing heterocycles [13]. In a significant advancement in 2021, Lopchuk et al. revealed a novel method for the photodecarboxylative alkylation of diazirines **12** using the readily accessible redox-active esters **3** and cost-effective NaI/PPh_3 photoactivators under mild reaction conditions (Scheme 8) [14]. The methodology exhibited remarkable efficacy when applied to a wide range of natural products and pharmaceuticals, significantly expanding the synthetic utility of this ap-

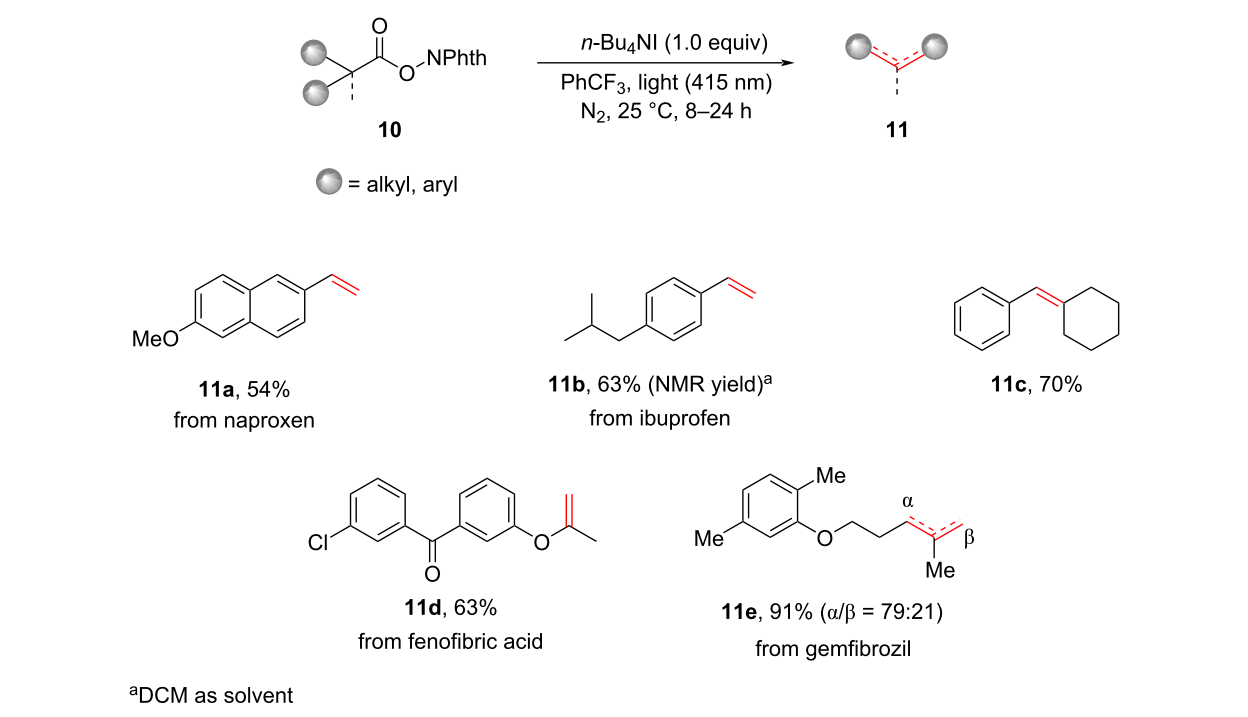

Scheme 6: *n*-Bu_4NI-mediated photoinduced decarboxylative olefination.

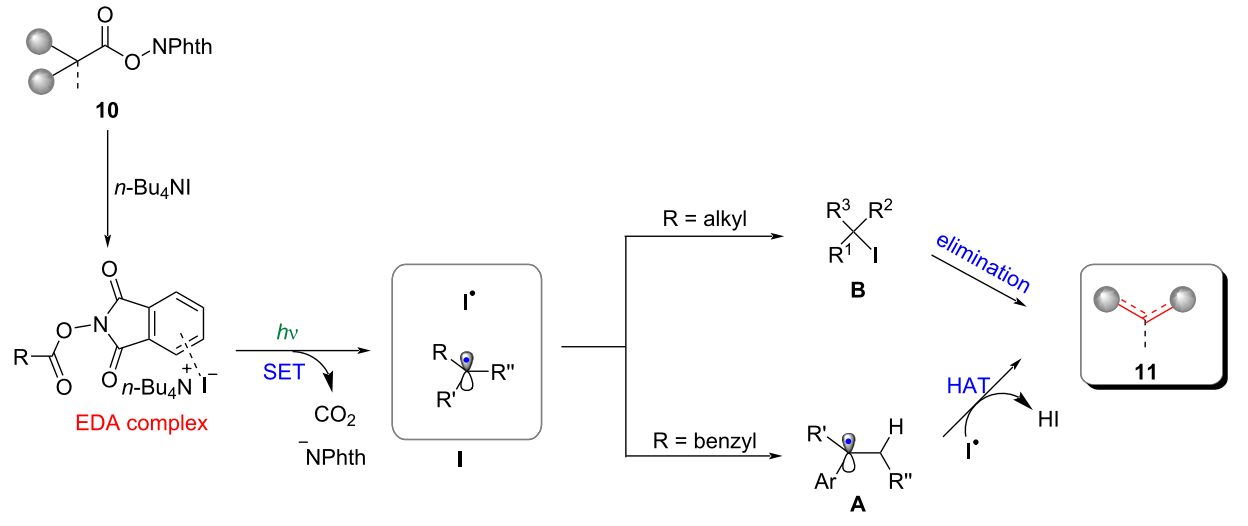

Scheme 7: Proposed mechanism of the *n*-Bu_4NI-mediated photoinduced decarboxylative olefination.

proach. Importantly, the demonstration of the exceptional compatibility between blue LEDs and diazirine compounds also held the promise of inspiring further exploration and development of novel synthetic strategies in this field.

Enamides are commonly found in medicinal compounds and physiologically active natural products. The direct functionalization of C–H bonds in enamides offers a convenient and versatile approach to access a wide range of functionalized enamides. In 2021, Fu and his colleagues successfully developed a novel method for the stereoselective alkylation of enamides **14** using iodine-anion catalysis under visible light irradiation, as depicted in Scheme 9. Subsequent investigations revealed that redox-active esters **3** and Katritzky salts **15** derived from amino acids could be effectively employed in decarboxylative/deaminative cross-coupling reactions [15]. These reactions enabled the effi-

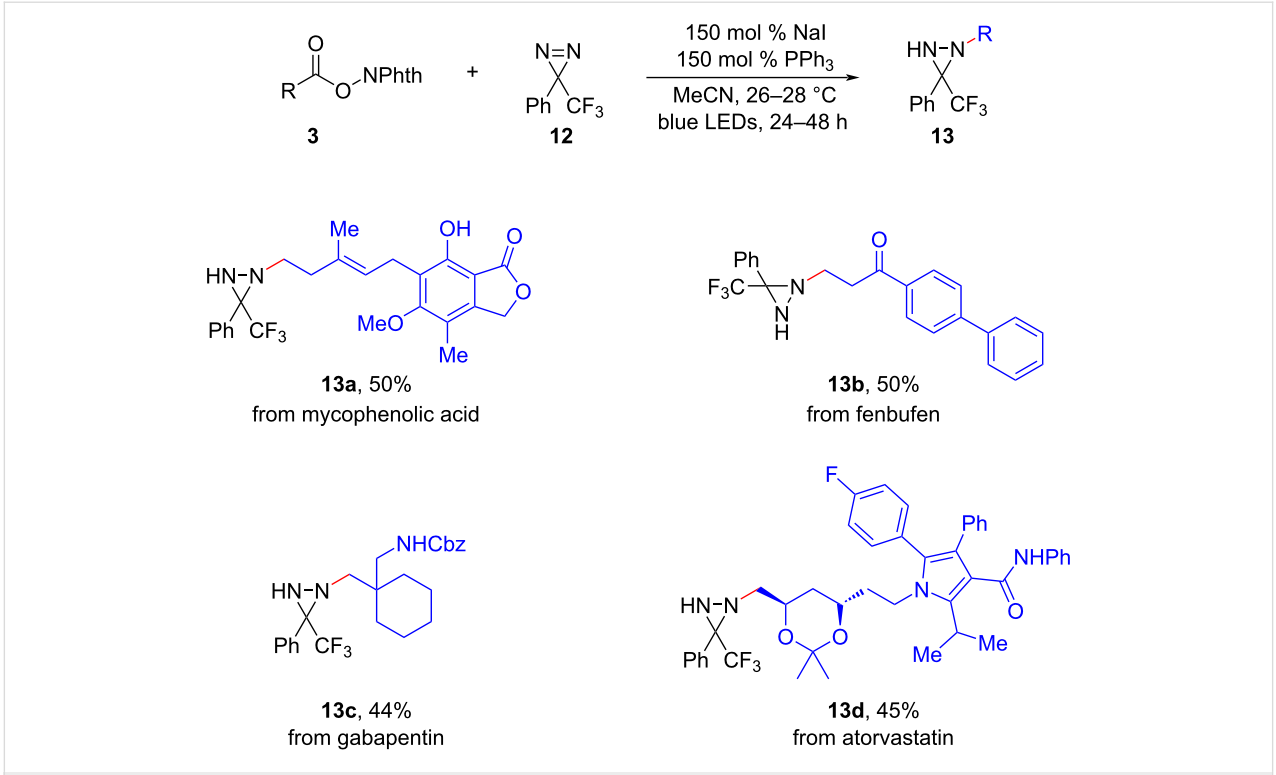

Scheme 8: Photodecarboxylative alkylation of redox-active esters with diazirines.

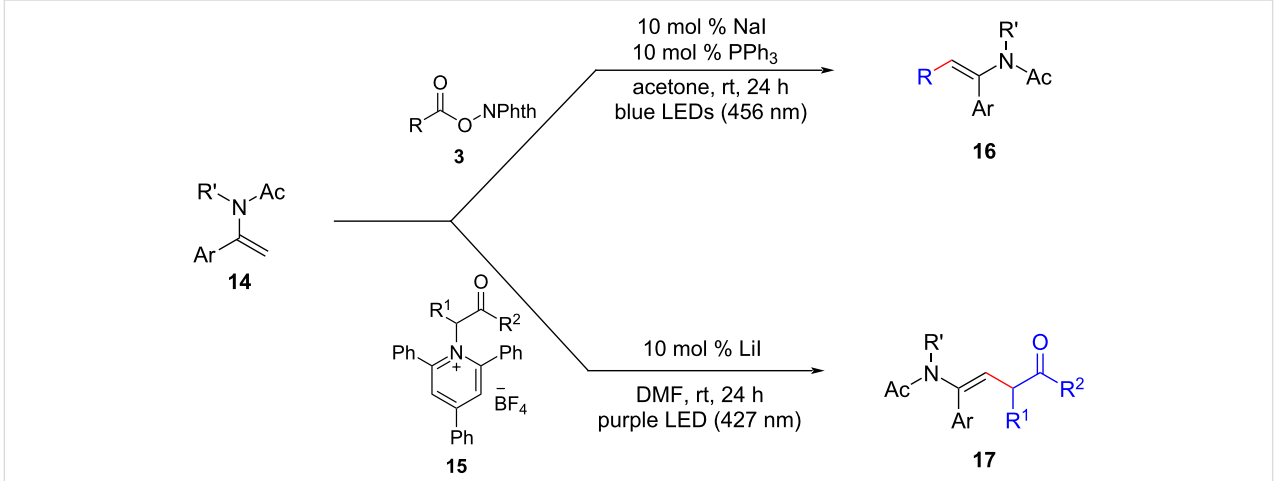

Scheme 9: Photoinduced iodine-anion-catalyzed decarboxylative/deaminative C–H alkylation of enamides.

cient synthesis of diversely functionalized enamides **16** and **17**, demonstrating remarkable tolerance towards various functional groups.

In recent years, there has been a surge of research interest in coumarin derivatives due to their notable biological, pharmacological, and optical properties [16]. Zhou and colleagues introduced an interesting metal- and oxidant-free photocatalytic C–H alkylation method for coumarins **18** [17]. The method utilized triphenylphosphine and sodium iodide, along with readily available alkyl *N*-hydroxyphthalimide esters (NHPIs) **3** as the alkylation reagents (Scheme 10). Impressively, this transformation exhibited exceptional versatility, extending beyond coumarins to encompass other nitrogen-containing heterocycles, including quinoxalinones, with remarkable C-3 regioselectivity. The findings of this study significantly expanded the synthetic toolbox for accessing functionalized coumarin derivatives and related nitrogen-containing heterocycles, opening up exciting possibili-

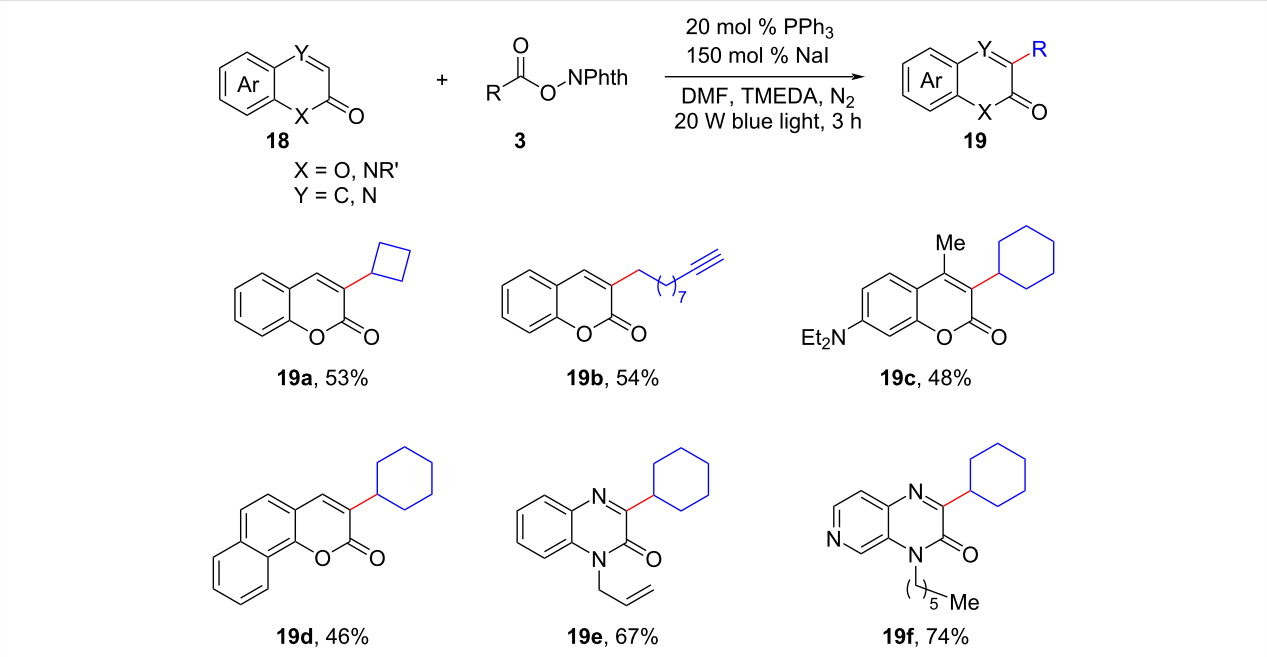

Scheme 10: Photocatalytic C–H alkylation of coumarins mediated by NaI/PPh_3 catalysis.

ties for their diverse applications in other fields. Similarly, the regioselective photodecarboxylative C–H alkylation of 2*H*-indazoles and azauracils using NaI/PPh_3 as mediators and redox esters **3** was reported by the research groups of Murarka [18] and Fan [19], respectively.

Simultaneously, Shen and colleagues made a notable contribution by disclosing a NaI/PPh_3 EDA complex-mediated photoredox alkylation of aldimines **20** (Scheme 11) [20]. This newly developed method offered a reliable and efficient route for the synthesis of unnatural amino acids and amines. Remarkably, the procedure exhibited excellent compatibility with a wide range of alkyl radicals, including primary, secondary, tertiary, and α-heterosubstituted radicals generated from corresponding redox-active esters **3**.

Concurrently, Shang and colleagues achieved a significant breakthrough by sequentially unveiling a series of decarboxylative alkylation reactions involving heteroarenes **22**, enamides **24**, *N*-arylglycine derivatives **26**, and silyl enol ethers **28** [21,22]. Notably, these transformations were accomplished using only a catalytic amount of ammonium iodide under irradiation in the absence of triphenylphosphine (Scheme 12). The generation of alkyl radicals was attributed to the photoactivation of a transient electron donor–acceptor complex formed between iodide and *N*-(acyloxy)phthalimide, in line with earlier findings. These remarkable advances not only highlighted the synthetic potential of photocatalysis but also served as inspiration for future developments of low-cost photocatalysis based on other non-covalent interactions. The simplicity, practicality, and broad substrate scope demonstrated by these approaches further emphasized their significance in facilitating the synthesis of diverse compounds and paving the way for further advancements in the field of photocatalysis.

The highly efficient construction of carbon–heteroatom (C–X) bonds is of significant importance in the fields of natural products, pharmaceuticals, and materials science. In recent years, the combination of dual photoredox with first-row transition-metal catalysis has emerged as a powerful tool for achieving various cross-coupling reactions involving C–N, C–O, C–S, and other chemical bonds [3,23]. In this context, Guan et al. theoretically designed a novel metallaphotoredox catalysis by combining the NaI/PPh_3 photoredox catalyst with a Cu(I) catalyst to accomplish diverse C–O/N cross-couplings of alkyl *N*-hydroxyphthalimide esters **3** with various phenols/secondary amines **30** (Scheme 13) [24]. It was anticipated the utilization of computational methods in organic synthesis would provide new insights and novel concepts for the exploration of other metallaphotoredox catalytic systems, thus greatly speeding up the process of new reaction findings.

An elegant NaI/PPh_3/CuBr metallaphotoredox dual-catalytic system was responsible for the aforementioned transformations, as depicted in Scheme 14. The dual-catalytic cycle comprised a photocatalytic cycle and a copper catalytic cycle, interconnected through an intermolecular single-electron transfer.

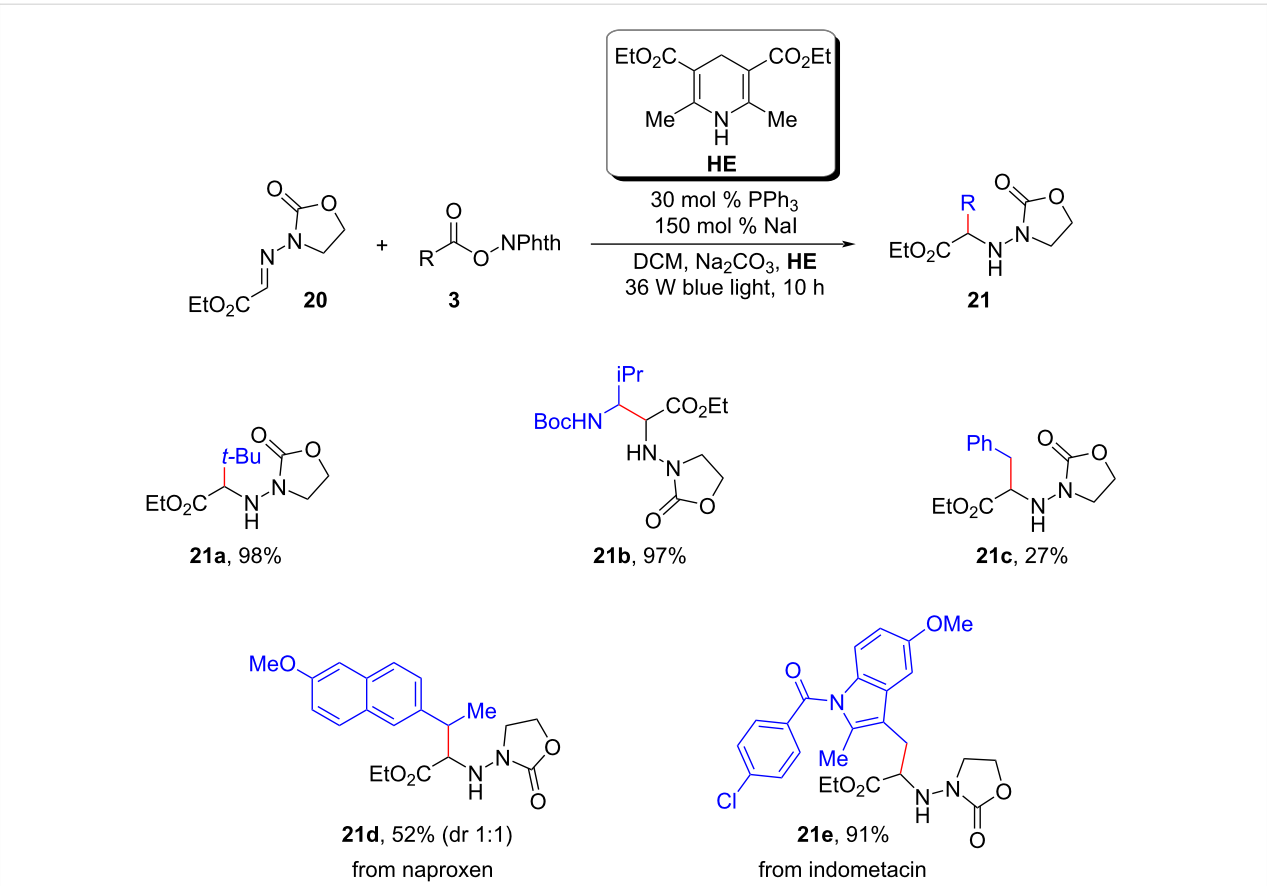

Scheme 11: Photoredox alkylation of aldimines by NaI/PPh_3 catalysis.

Within the context of the photocatalytic cycle, the generation of the C(sp^3)-centered alkyl radical **A** was facilitated by the process of photoexcited radical decarboxylation. On the other hand, the copper catalytic cycle involved the capture of alkyl radicals by the copper complex **B**, the activation of heteroatom-containing substrates **30** by a base-mediated proton transfer, and the subsequent reductive elimination process. This reductive elimination led to the formation of C(sp^3)–X (X = O or N) cross-coupling products **31**.

Cyclization

Radical-involved selective C–H functionalizations [25,26], particularly annulation reactions [26], have emerged as highly effective and powerful techniques in synthesis, possessing notable advantages in terms of both step- and atom-economy.

Taking inspiration from the groundbreaking work of Shang and Fu [6], Li and colleagues demonstrated an innovative approach for the photocatalytic [3 + 2] and [4 + 2] annulation of enynals **32** and γ,σ-unsaturated *N*-(acyloxy)phthalimides **33** (Scheme 15) [27]. This method involved a series of steps, including the formation of an EDA complex, decarboxylation, radical addition, C–H functionalization, and annulation. Various primary, secondary, and tertiary alkyl *N*-hydroxyphthalimide esters **33** showed potential as viable substrates for the synthesis of fused ketones **34**, eliminating the need for transition-metal catalysts or oxidants. The technique offered a broad substrate scope, remarkable selectivity, and simple reaction conditions.

A plausible mechanism had been proposed for the photocatalytic decarboxylative [3 + 2]/[4 + 2] annulation, as depicted in Scheme 16. Initially, a photoactive EDA complex **II** was transiently formed through the combined action of NaI, PPh_3, and the γ,σ-unsaturated phthalimide **33a**. Upon irradiation with blue LEDs, the alkyl radical **A** was generated through a single-electron transfer from the iodide anion to the γ,σ-unsaturated phthalimide **33a**. Simultaneously, radical **III** of the catalyst was also formed, accompanied by the extrusion of CO_2. Subsequently, the alkyl radical **A** added to the carbon–carbon triple bond of enynal **32g**, resulting in the formation of a vinyl radical intermediate **B**, followed by a 5-*exo*-*trig* cyclization to release an active alkyl radical intermediate **C**. Once formed, **C** added to the aldehyde group via a [4 + 2] annulation, releasing the alkoxy radical intermediate **D**. The latter then underwent a

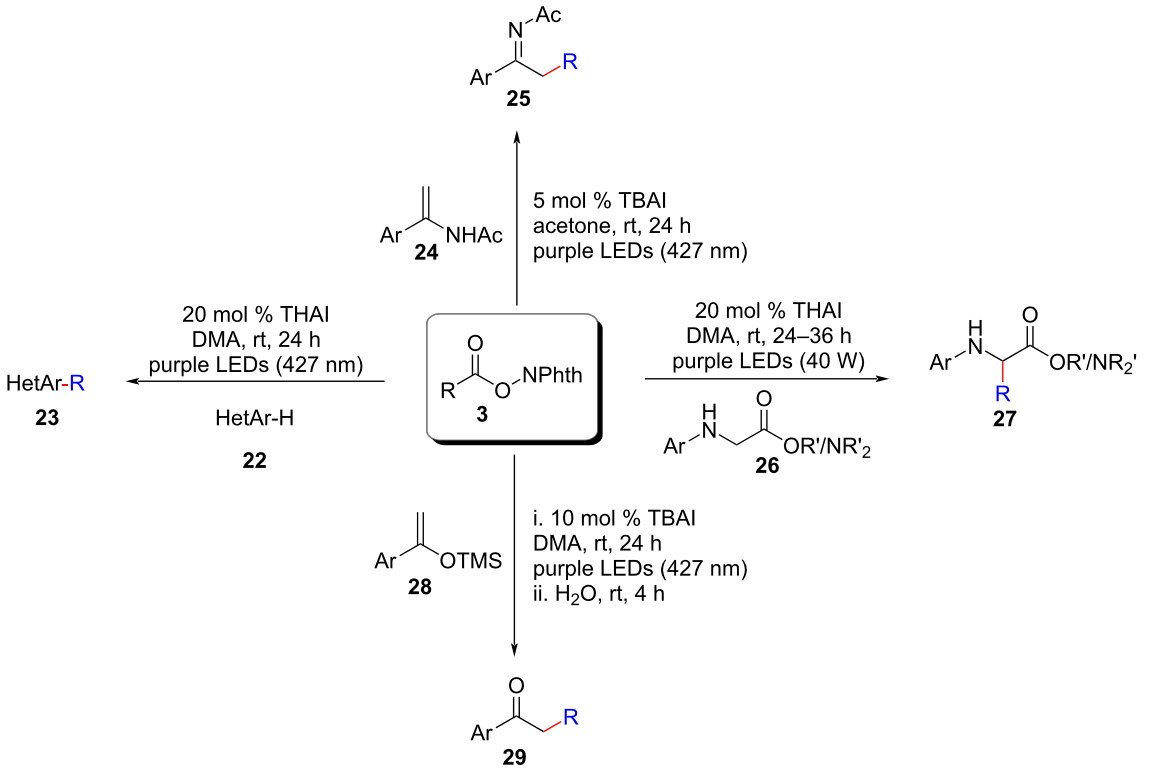

Scheme 12: Photoredox C–H alkylation employing ammonium iodide.

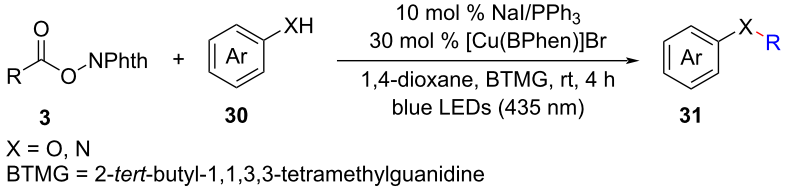

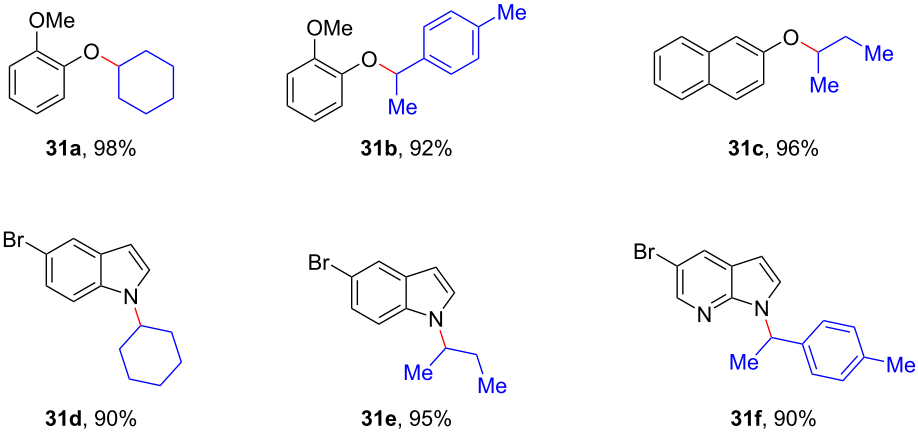

Scheme 13: NaI/PPh_3/CuBr cooperative catalysis for photocatalytic C(sp^3)–O/N cross-coupling reactions.

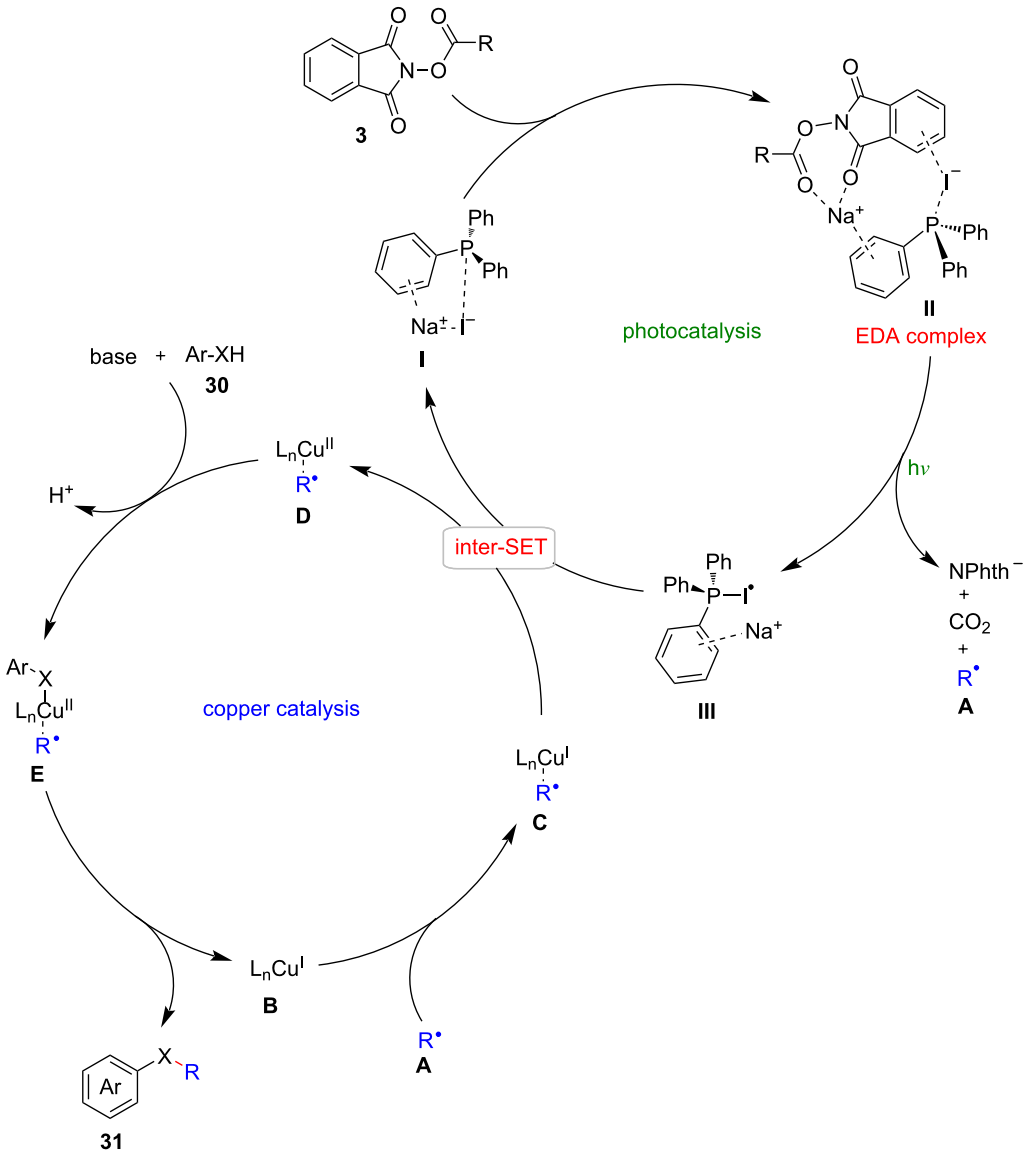

Scheme 14: Proposed mechanism of NaI/PPh_3/CuBr cooperative catalysis for photocatalytic C(sp^3)–O/N cross-couplings.

subsequent 1,2-H atom shift to generate the alkyl radical intermediate **E** which was further oxidized by the $Ph_3P–I^•$ species **III**, forming the cationic intermediate **F**. Finally, deprotonation of intermediate **F** yielded the product **34g**.

Functional polycyclic compounds, such as indene-containing polycyclic motifs and *N*-containing polyheterocycles are commonly found in many natural products and pharmaceuticals, demonstrating significant potential in combating human immunodeficiency virus infections and cardiovascular disorders. The acquisition of these significant structures has predominantly been carried out through a sequential process. Over the decades, chemists have made considerable efforts to improve the construction of these scaffolds [28-31], and one of the most efficient approaches is the cascade cyclization strategy [29-31].

Xu, Li, Wei and their co-workers successfully devised a series of highly regioselective iodide/phosphine synergistically catalyzed photocatalytic cascade annulations for the construction of various nitrogen-containing polycyclic frameworks (**36**, **38**, **39**, **41**) (Scheme 17) [32-34]. These protocols offered a wide range of substrate compatibility in a one-pot reaction, significantly enhancing synthetic efficiency.

Nitrogen-containing heterocycles are abundantly found in nature and represent some of the most prevalent frameworks in

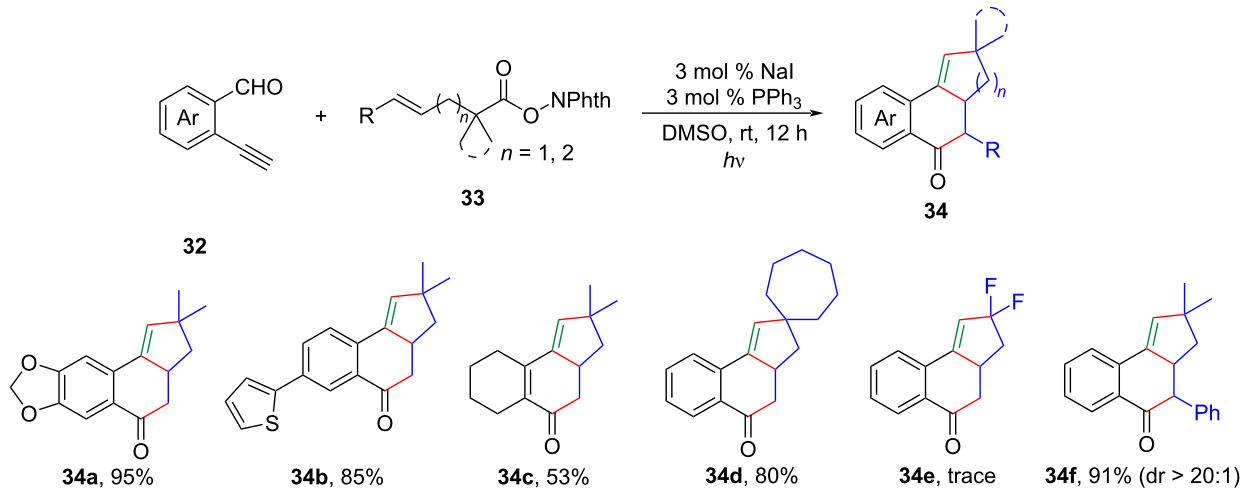

Scheme 15: Photocatalytic decarboxylative [3 + 2]/[4 + 2] annulation between enynals and γ,σ-unsaturated *N*-(acyloxy)phthalimides.

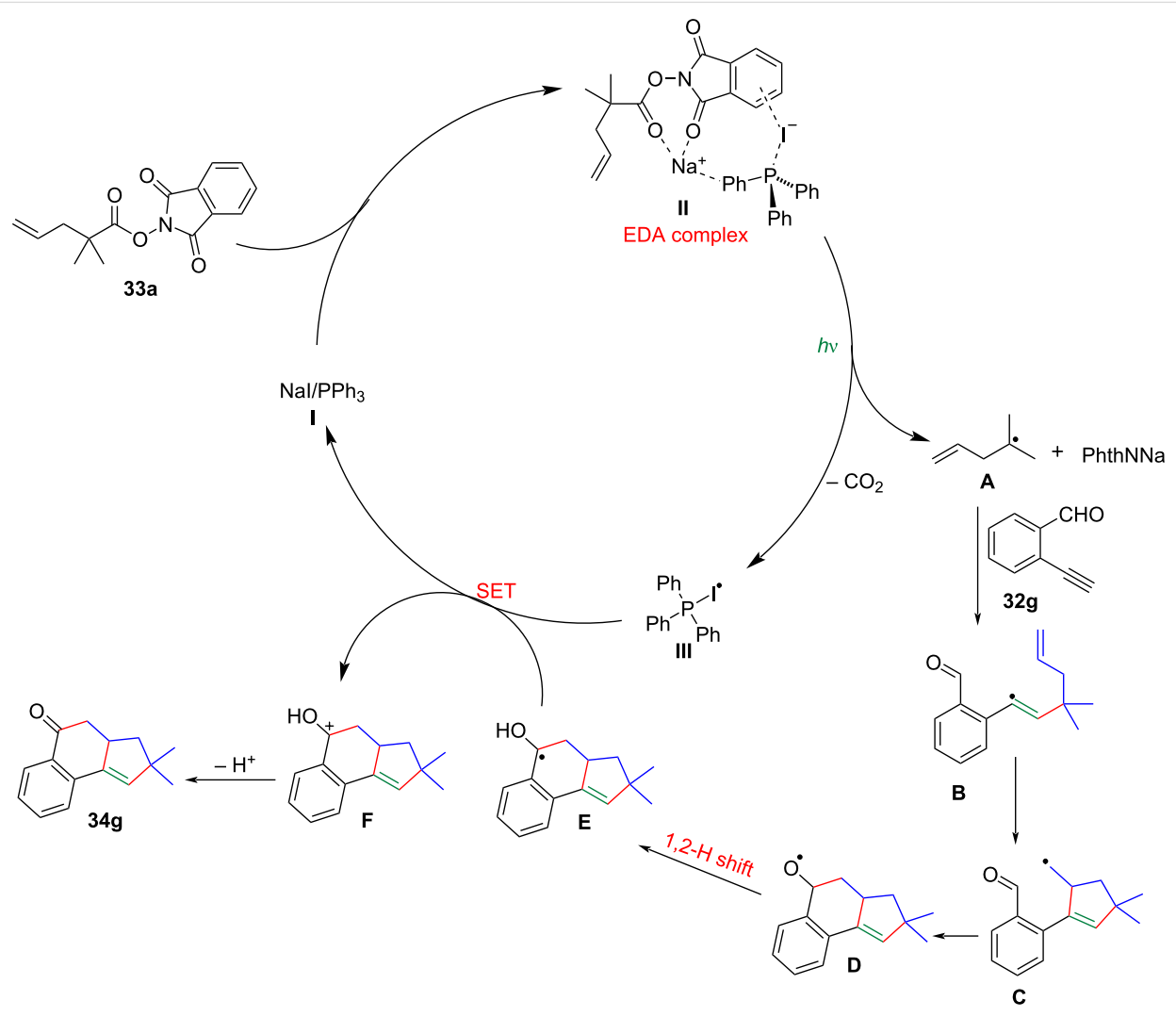

Scheme 16: Proposed mechanism for the decarboxylative [3 + 2]/[4 + 2] annulation.

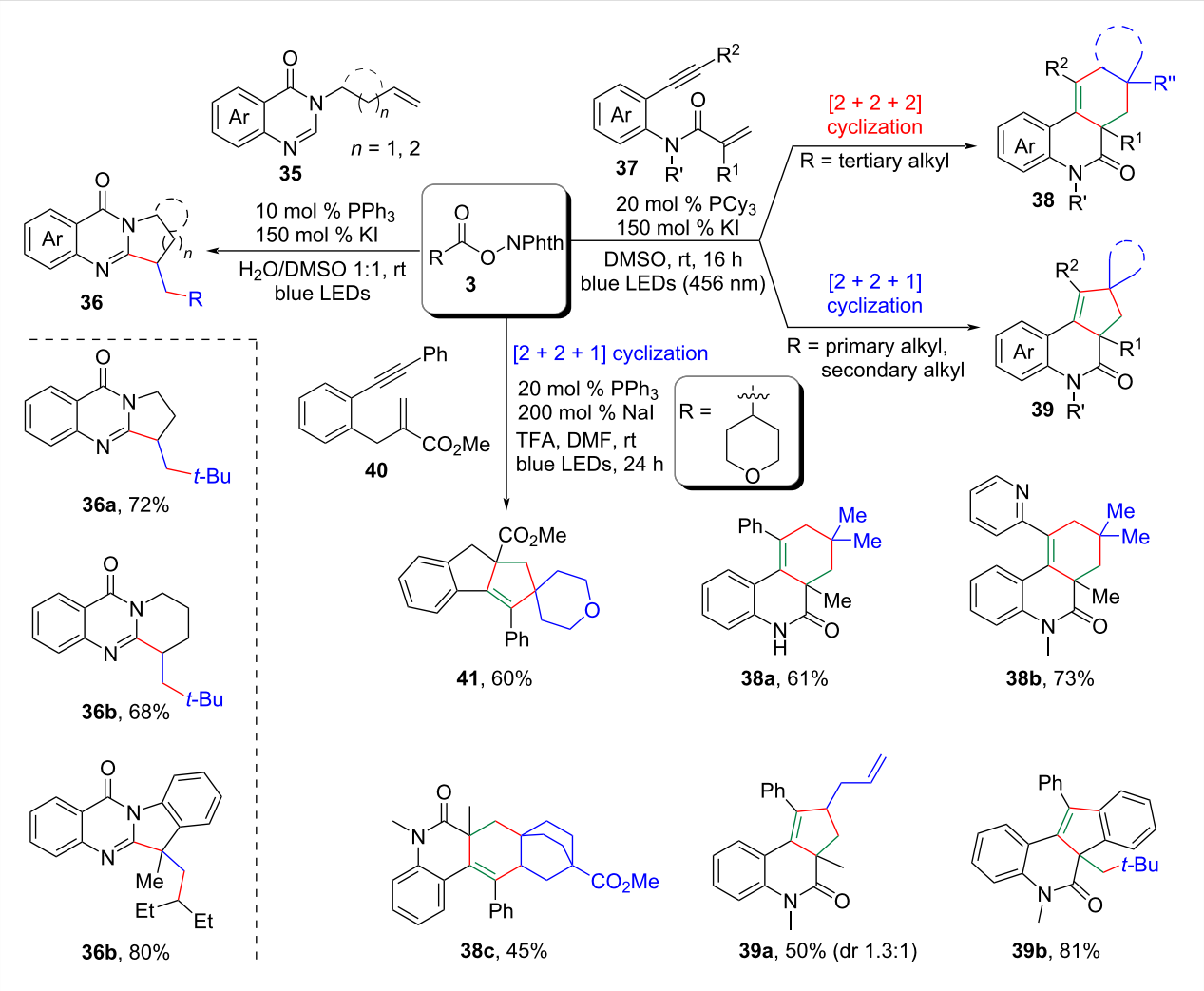

Scheme 17: Decarboxylative cascade annulation of alkenes/1,6-enynes with *N*-hydroxyphthalimide esters.

natural products, medicines, and functional materials. Despite the development of numerous synthetic methods over the past one century, chemists are still seeking more straightforward routes to access these structurally important and useful *N*-heterocycles.

Recently, independent research groups led by Li, Yang, and Patureau separately disclosed a novel approach to 3,3-disubstituted oxindoles **43** through an iodide/phosphine-catalyzed visible-light-mediated decarboxylative radical cascade cyclization of *N*-arylacrylamides **42** (Scheme 18) [35,36]. Importantly, these methodologies could also be smoothly extended to the synthesis of isoquinolinediones, which borne a quaternary carbon center.

Furthermore, Yatham and his colleagues unveiled the first NaI/PPh_3-mediated photocatalytic decarboxylative cascade cyclization of 2-isocyanobiaryls **44** with alkyl *N*-hydroxyphthalimide esters **3**, resulting in the efficient synthesis of various 6-alkylated phenanthridines **45** (Scheme 19) [37]. The protocol exhibited a wide substrate scope, excellent tolerance towards functional groups, and mild reaction conditions.

Based on the experimental observations and a previous report [6], it was proposed that the decarboxylative cascade cyclization reaction proceeded through the formation of a charge-transfer complex (CTC) **II** involving PPh_3, NaI, and NHP ester **3** (Scheme 20). Upon photofragmentation of the CTC complex **II**, two important intermediates were generated: an alkyl radical **A** and a PPh_3–I radical **III**. The subsequent isocyanide **44** SOMOphilic insertion reaction led to the formation of an imidoyl radical **B**. This radical then underwent rapid addition onto the C–C double bond, resulting in the release of the desired phenanthridine products **45**. Importantly, this process also replenished the NaI/PPh_3 catalyst, completing the catalytic cycle.

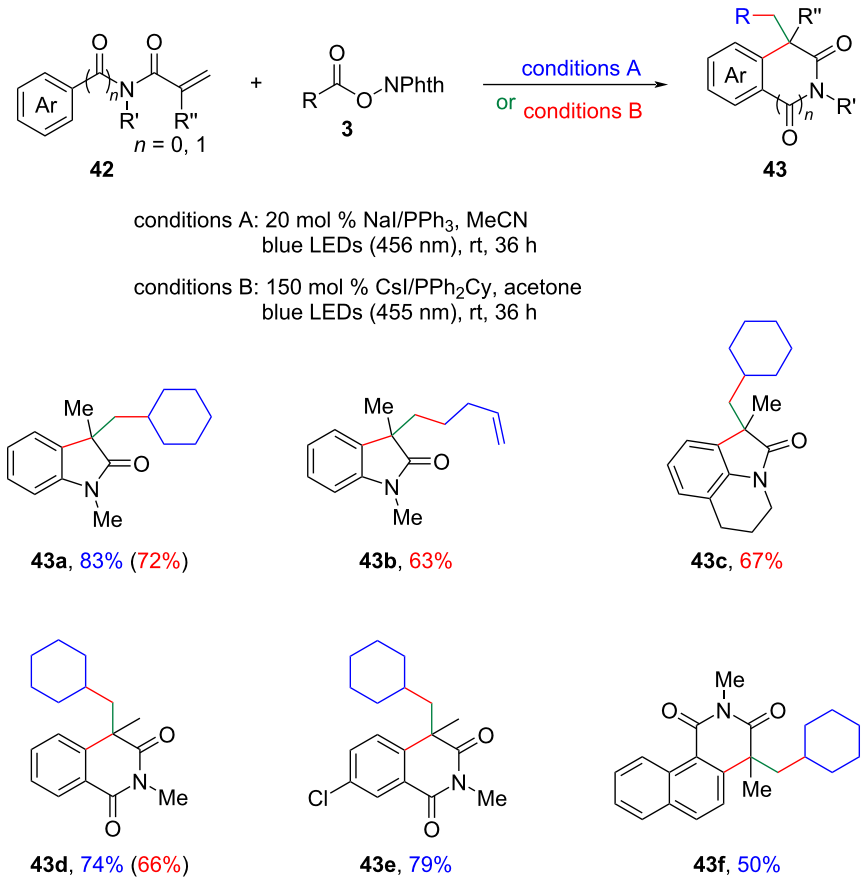

Scheme 18: Decarboxylative radical cascade cyclization of *N*-arylacrylamides.

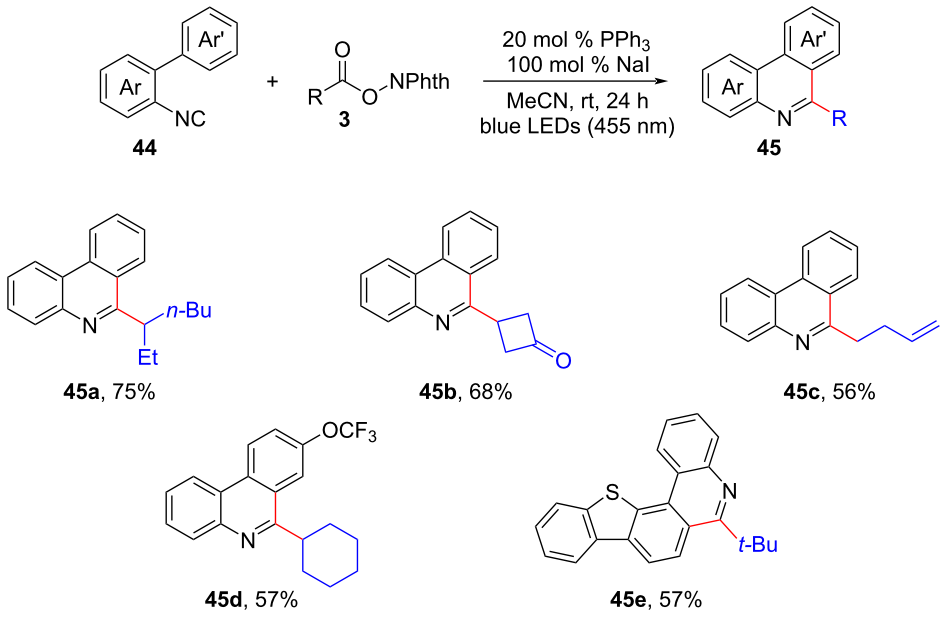

Scheme 19: NaI/PPh_3-driven photocatalytic decarboxylative radical cascade alkylarylation.

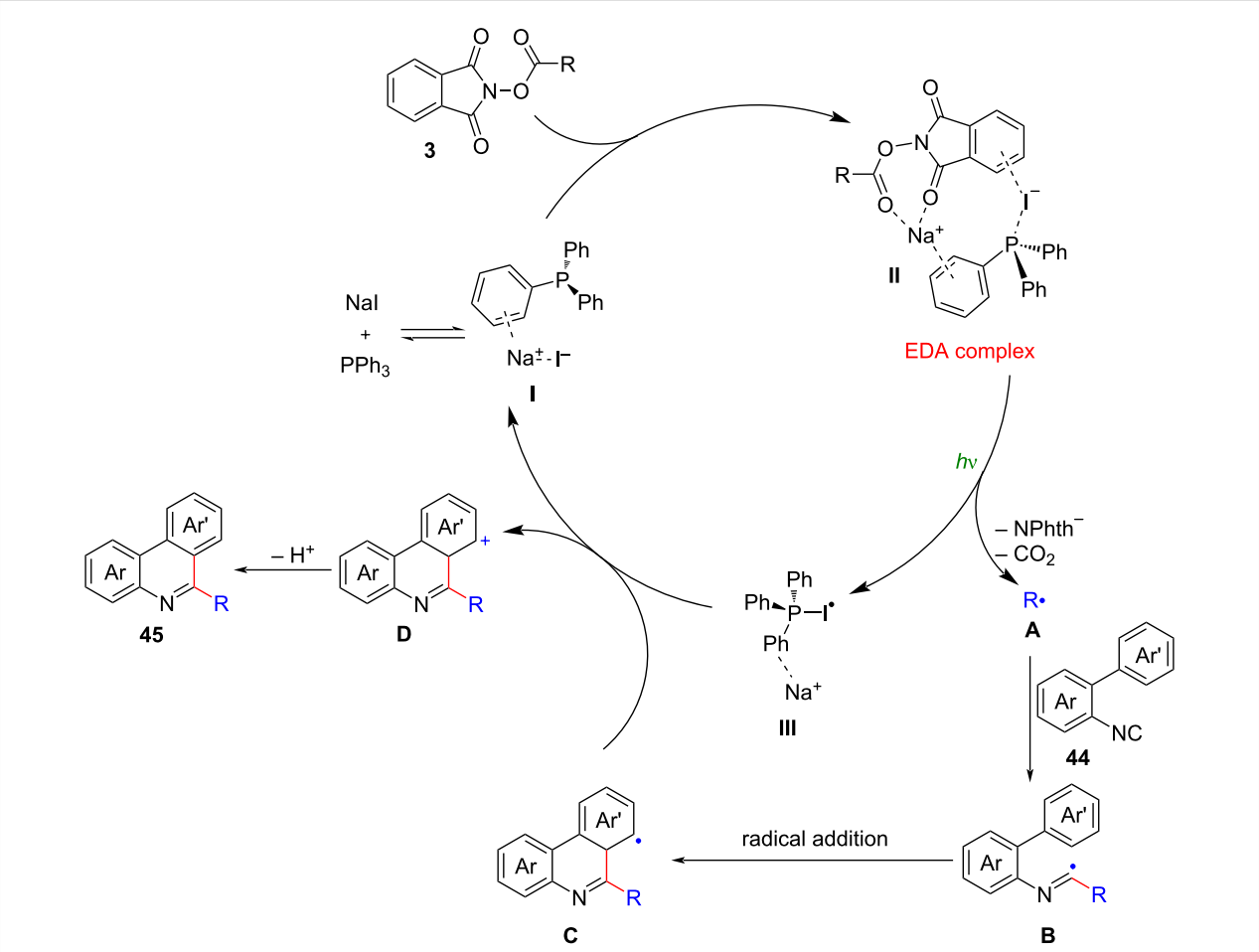

Scheme 20: Proposed mechanism of the NaI/PPh_3-driven photocatalytic decarboxylative radical cascade cyclization.

Very recently, Zhong and his colleagues proposed a decarboxylative alkylation method for vinylcyclopropanes **46** using alkyl *N*-(acyloxy)phthalimide esters **3**. This methodology enabled the synthesis of variously substituted 2-alkylated 3,4-dihydronaphthalenes **47** with yields of up to 92%, as depicted in Scheme 21 [38]. The key aspect of the approach involved the simultaneous cleavage of dual C–C bonds and a single N–O bond, which was facilitated by the utilization of LiI/PPh_3 as the photoredox system.

Amination

Anilines play important roles in both academic research and industrial applications. As a result, significant efforts have been devoted to the development of various methods for the reduction of nitroarenes [39]. Recent advancements in the catalytic reduction of nitroarenes largely rely on transition-metal catalysis through direct hydrogenation or hydrogen transfer [40], electrocatalysis coupled with water oxidation [41], and sustained visible-light-induced photocatalysis [42]. Among the different strategies available, the use of a mild photocatalytic process involving hole-driven hydrogen transfer with hydrogen donors or hole scavengers has emerged as an attractive approach for nitroarene reduction [43,44].

In 2021, Huang and colleagues discovered a photoredox system that did not require any transition metal or other photosensitizers [45]. This system employed a combination of NaI and PPh_3 to achieve highly selective reduction of nitroarenes **48** (Scheme 22). The protocol demonstrated excellent tolerance towards a wide range of reducible functional groups, including halogens (such as chlorine, bromine, and even iodine), aldehydes, ketones, carboxyl groups, and cyano groups.

Iodination

Alkyl iodide is considered to be the most reactive electrophile compared to other alkyl halides, such as related bromides and chlorides. As a result, an effective iododecarboxylation provides a versatile platform for a range of decarboxylative reactions.

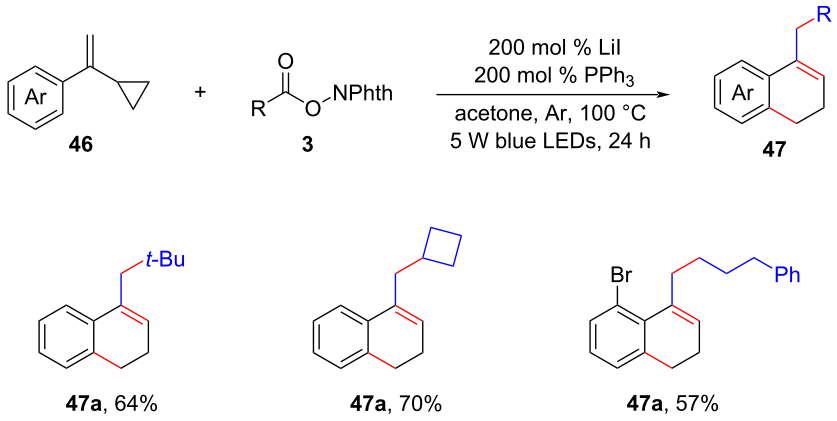

Scheme 21: Visible-light-promoted decarboxylative cyclization of vinylcycloalkanes.

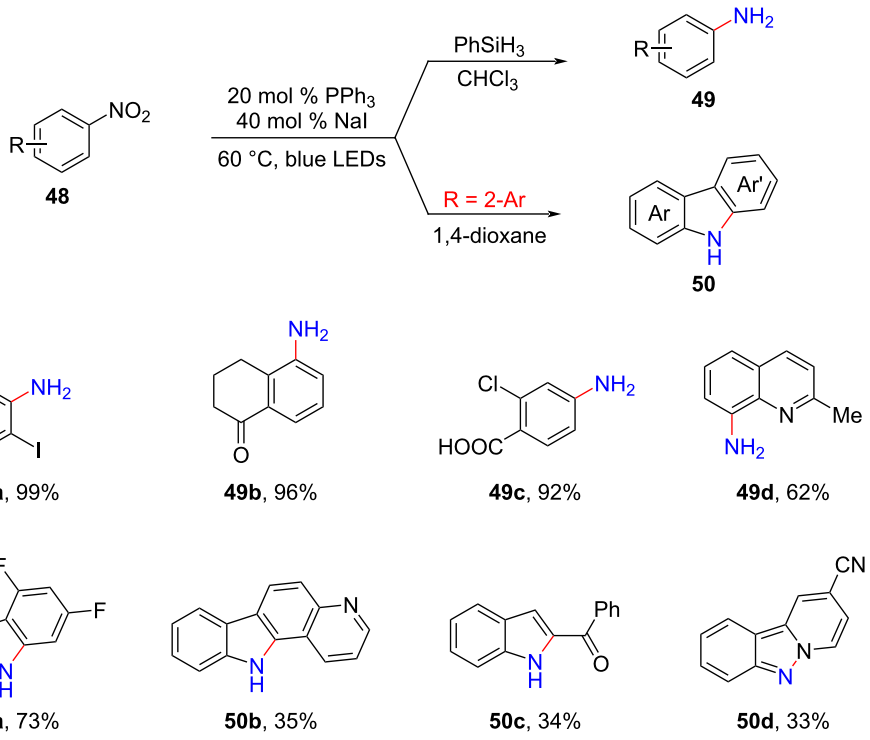

Scheme 22: NaI/PPh_3-mediated photochemical reduction and amination of nitroarenes.

Shang and co-workers recently found that aliphatic carboxylates and lithium iodide could undergo iododecarboxylation under 456 nm blue light irradiation through a PPh_3-catalyzed procedure (Scheme 23) [46]. Moreover, diversely primary, secondary, tertiary alkyl iodides **51** were easily converted to various C–N, C–O, C–F, and C–S bonds, thus greatly enhancing the potential applications of this chemistry.

Meanwhile, the research groups of Chen and Wang demonstrated an elegant use of electrostatic contact to promote radical–radical cross-coupling between *N*-alkenoxypyridinium salts **52** and NaI, resulting in the formation of various α-iodo ketones **53** when exposed to visible light (Scheme 24) [47]. In the process, the NHC catalyst acted as a stabilizer for the EDA complex and generates a radical species, which was confirmed by further computational studies.

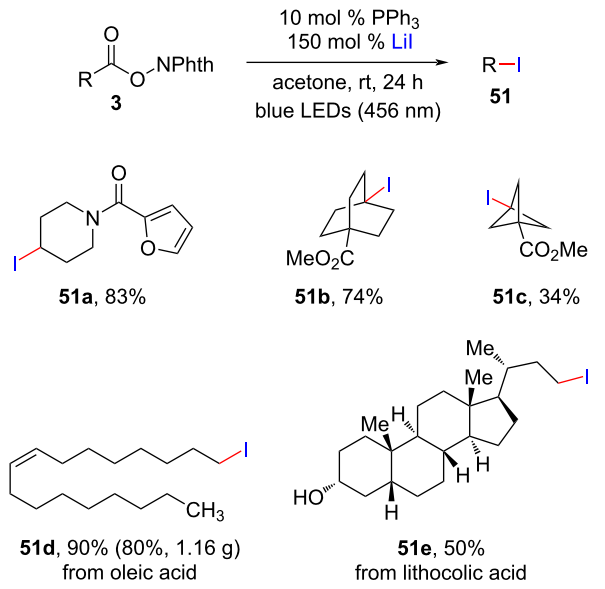

Scheme 23: PPh_3-catalyzed alkylative iododecarboxylation with LiI.

Monofluoromethylation

The monofluoromethyl (CH_2F) group, which is commonly found in a lot of agrochemicals, pharmaceuticals, and materials, serves as a powerful bioisostere for a range of functional groups (such as CH_2OH, CH_2OCH_3, CH_2NH_2, and CH_2SH). Among the various methods available, radical-involving cross-couplings have proven to be the most effective [48,49]. However, the generation of the CH_2F radical remains to be a challenging task. Therefore, there is an urgent need to develop diverse monofluoromethylation methods.

In this context, Chen and his colleagues recently developed a concise photocatalytic procedure for achieving monofluoromethylation, as well as di- and trifluoromethylation of various alkenes (Scheme 25) [50]. The synthetic method also showcased broad applicability, operational simplicity, and utilized easily obtainable and air-stable phosphonium salts **54** as convenient photoinduced R_f radical reagents.

Conclusion

In recent years, the field of synthetic chemistry has experienced significant advancements in iodide/phosphine-based photoredox radical reactions. These reactions have garnered much attention due to their cost-effectiveness, low toxicity, and widespread availability. Notably, the NaI/PPh_3 combined system has been successfully employed in the photofixation of nitrogen [51].

Despite these remarkable progresses made, there remain several synthetic challenges that require further investigation and resolution: First, the current reliance on redox-active esters as radical precursors in iodide/phosphine-mediated conversions restricts the potential applications of these conversions in synthesis. Therefore, it is highly recommended to develop other alternative radical precursors, explore new different reaction types (rather than the decarboxylative process), and design novel EDA complexes for photoredox catalysis, in addition to the well-established methods mentioned earlier.

Moreover, asymmetric versions of iodide/phosphine-mediated photoredox radical reactions are relatively scarce [52], representing an unexplored area that requires further investigation. Developing asymmetric methodologies in this domain holds great promise for future exploration.

Last but not the least, conducting detailed mechanistic studies on iodide/phosphine-involved reactions is crucial for gaining a deeper understanding of their underlying mechanisms and expediting the process of designing new reactions.

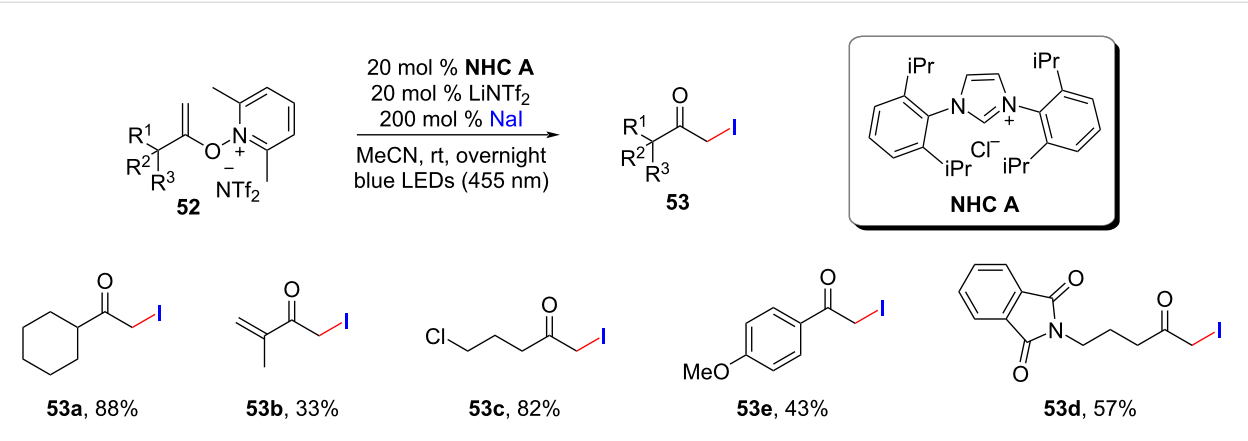

Scheme 24: Visible-light-triggered iodination facilitated by N-heterocyclic carbenes.

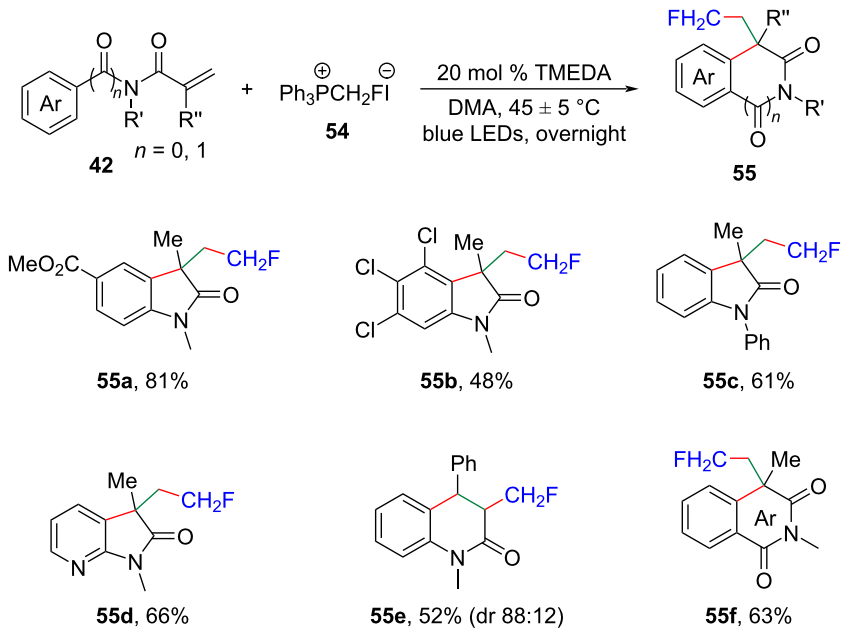

Scheme 25: Visible-light-induced photolysis of phosphonium iodide salts for monofluoromethylation.

Overall, addressing these challenges and advancing the field through innovative approaches and mechanistic insights will contribute to the continued progresses and applications of iodide/phosphine-based photoredox radical reactions in synthetic chemistry.

Funding

This work was financially supported by the Central University Basic Research Fund of China (21620318, 2019QNGG22 and 21623414).

ORCID® iDs

Chengming Wang - https://orcid.org/0000-0002-0201-1526

References

1. Romero, N. A.; Nicewicz, D. A. *Chem. Rev.* **2016,** *116,* 10075–10166. doi:10.1021/acs.chemrev.6b00057
2. Bell, J. D.; Murphy, J. A. *Chem. Soc. Rev.* **2021,** *50,* 9540–9685. doi:10.1039/d1cs00311a
3. Chan, A. Y.; Perry, I. B.; Bissonnette, N. B.; Buksh, B. F.; Edwards, G. A.; Frye, L. I.; Garry, O. L.; Lavagnino, M. N.; Li, B. X.; Liang, Y.; Mao, E.; Millet, A.; Oakley, J. V.; Reed, N. L.; Sakai, H. A.; Seath, C. P.; MacMillan, D. W. C. *Chem. Rev.* **2022,** *122,* 1485–1542. doi:10.1021/acs.chemrev.1c00383
4. Matsui, J. K.; Lang, S. B.; Heitz, D. R.; Molander, G. A. *ACS Catal.* **2017,** *7,* 2563–2575. doi:10.1021/acscatal.7b00094
5. Shaw, M. H.; Twilton, J.; MacMillan, D. W. C. *J. Org. Chem.* **2016,** *81,* 6898–6926. doi:10.1021/acs.joc.6b01449
6. Fu, M.-C.; Shang, R.; Zhao, B.; Wang, B.; Fu, Y. *Science* **2019,** *363,* 1429–1434. doi:10.1126/science.aav3200
7. Noble, A.; Aggarwal, V. K. *Sci. China: Chem.* **2019,** *62,* 1083–1084. doi:10.1007/s11426-019-9489-4
8. List, B.; Li, Y. *Synfacts* **2019,** *15,* 791. doi:10.1055/s-0039-1689888
9. Wang, Y.-T.; Fu, M.-C.; Zhao, B.; Shang, R.; Fu, Y. *Chem. Commun.* **2020,** *56,* 2495–2498. doi:10.1039/c9cc09654j
10. Wang, H.-Y.; Zhong, L.-J.; Lv, G.-F.; Li, Y.; Li, J.-H. *Org. Biomol. Chem.* **2020,** *18,* 5589–5593. doi:10.1039/d0ob01242d
11. Zhang, C.-S.; Bao, L.; Chen, K.-Q.; Wang, Z.-X.; Chen, X.-Y. *Org. Lett.* **2021,** *23,* 1577–1581. doi:10.1021/acs.orglett.0c04287
12. Luo, J.-j.; Jing, D.; Lu, C.; Zheng, K. *Eur. J. Org. Chem.* **2023,** *26,* e202300167. doi:10.1002/ejoc.202300167
13. Ravindra, S.; Jesin, C. P. I.; Shabashini, A.; Nandi, G. C. *Adv. Synth. Catal.* **2021,** *363,* 1756–1781. doi:10.1002/adsc.202001372
14. Maharaj, V.; Chandrachud, P. P.; Che, W.; Wojtas, L.; Lopchuk, J. M. *Org. Lett.* **2021,** *23,* 8838–8842. doi:10.1021/acs.orglett.1c03344
15. Wang, J.-X.; Wang, Y.-T.; Zhang, H.; Fu, M.-C. *Org. Chem. Front.* **2021,** *8,* 4466–4472. doi:10.1039/d1qo00660f
16. Bouhaoui, A.; Eddahmi, M.; Dib, M.; Khouili, M.; Aires, A.; Catto, M.; Bouissane, L. *ChemistrySelect* **2021,** *6,* 5848–5870. doi:10.1002/slct.202101346
17. Gan, X.; Wu, S.; Geng, F.; Dong, J.; Zhou, Y. *Tetrahedron Lett.* **2022,** *96,* 153720. doi:10.1016/j.tetlet.2022.153720
18. Panda, S. P.; Hota, S. K.; Dash, R.; Roy, L.; Murarka, S. *Org. Lett.* **2023,** *25,* 3739–3744. doi:10.1021/acs.orglett.3c01210
19. Wang, J.; Song, Q.; He, X.; Ma, C.; Jiang, Y.; Fan, J. *New J. Chem.* **2022,** *46,* 16436–16439. doi:10.1039/d2nj02766f
20. Shao, Z.; Zhou, Q.; Wang, J.; Tang, R.; Shen, Y. *Chin. J. Org. Chem.* **2021,** *41,* 2676–2683. doi:10.6023/cjoc202102039
21. Liu, C.; Shen, N.; Shang, R. *Org. Chem. Front.* **2021,** *8,* 4166–4170. doi:10.1039/d1qo00648g
22. Wang, G.-Z.; Fu, M.-C.; Zhao, B.; Shang, R. *Sci. China: Chem.* **2021,** *64,* 439–444. doi:10.1007/s11426-020-9905-1

23. Prier, C. K.; Rankic, D. A.; MacMillan, D. W. C. *Chem. Rev.* **2013,** *113,* 5322–5363. doi:10.1021/cr300503r
24. Li, R.-H.; Zhao, Y.-L.; Shang, Q.-K.; Geng, Y.; Wang, X.-L.; Su, Z.-M.; Li, G.-F.; Guan, W. *ACS Catal.* **2021,** *11,* 6633–6642. doi:10.1021/acscatal.1c01222
25. Yi, H.; Zhang, G.; Wang, H.; Huang, Z.; Wang, J.; Singh, A. K.; Lei, A. *Chem. Rev.* **2017,** *117,* 9016–9085. doi:10.1021/acs.chemrev.6b00620
26. Murray, P. R. D.; Leibler, I. N.-M.; Hell, S. M.; Villalona, E.; Doyle, A. G.; Knowles, R. R. *ACS Catal.* **2022,** *12,* 13732–13740. doi:10.1021/acscatal.2c04316
27. Liu, X.-J.; Zhou, S.-Y.; Xiao, Y.; Sun, Q.; Lu, X.; Li, Y.; Li, J.-H. *Org. Lett.* **2021,** *23,* 7839–7844. doi:10.1021/acs.orglett.1c02858
28. Ibarra, I. A.; Islas-Jácome, A.; González-Zamora, E. *Org. Biomol. Chem.* **2018,** *16,* 1402–1418. doi:10.1039/c7ob02305g
29. Liao, J.; Yang, X.; Ouyang, L.; Lai, Y.; Huang, J.; Luo, R. *Org. Chem. Front.* **2021,** *8,* 1345–1363. doi:10.1039/d0qo01453b
30. Bur, S. K.; Padwa, A. *Adv. Heterocycl. Chem.* **2007,** *94,* 1–105. doi:10.1016/s0065-2725(06)94001-x
31. Lu, L.-Q.; Chen, J.-R.; Xiao, W.-J. *Acc. Chem. Res.* **2012,** *45,* 1278–1293. doi:10.1021/ar200338s
32. Jiao, M.-J.; Liu, D.; Hu, X.-Q.; Xu, P.-F. *Org. Chem. Front.* **2019,** *6,* 3834–3838. doi:10.1039/c9qo01166h
33. Liu, H.-Y.; Lu, Y.; Li, Y.; Li, J.-H. *Org. Lett.* **2020,** *22,* 8819–8823. doi:10.1021/acs.orglett.0c03182
34. Zhang, W.-K.; Li, J.-Z.; Zhang, C.-C.; Zhang, J.; Zheng, Y.-N.; Hu, Y.; Li, T.; Wei, W.-T. *Eur. J. Org. Chem.* **2022,** e202200523. doi:10.1002/ejoc.202200523
35. Fan, X.; Liu, H.; Ma, S.; Wang, F.; Yang, J.; Li, D. *Tetrahedron* **2022,** *117–118,* 132849. doi:10.1016/j.tet.2022.132849
36. Liu, D.; Zhao, Y.; Patureau, F. W. *Beilstein J. Org. Chem.* **2023,** *19,* 57–65. doi:10.3762/bjoc.19.5
37. Wadekar, K.; Aswale, S.; Yatham, V. R. *RSC Adv.* **2020,** *10,* 16510–16514. doi:10.1039/d0ra03211e
38. Liu, Y.; Sui, J.-L.; Yu, W.-Q.; Xiong, B.-Q.; Tang, K.-W.; Zhong, L.-J. *J. Org. Chem.* **2023,** *88,* 8563–8575. doi:10.1021/acs.joc.3c00486
39. Tafesh, A. M.; Weiguny, J. *Chem. Rev.* **1996,** *96,* 2035–2052. doi:10.1021/cr950083f
40. Formenti, D.; Ferretti, F.; Scharnagl, F. K.; Beller, M. *Chem. Rev.* **2019,** *119,* 2611–2680. doi:10.1021/acs.chemrev.8b00547
41. Song, J.; Huang, Z.-F.; Pan, L.; Li, K.; Zhang, X.; Wang, L.; Zou, J.-J. *Appl. Catal., B* **2018,** *227,* 386–408. doi:10.1016/j.apcatb.2018.01.052
42. Guo, Q.; Ma, Z.; Zhou, C.; Ren, Z.; Yang, X. *Chem. Rev.* **2019,** *119,* 11020–11041. doi:10.1021/acs.chemrev.9b00226
43. Xiao, Q.; Sarina, S.; Waclawik, E. R.; Jia, J.; Chang, J.; Riches, J. D.; Wu, H.; Zheng, Z.; Zhu, H. *ACS Catal.* **2016,** *6,* 1744–1753. doi:10.1021/acscatal.5b02643
44. Tsutsumi, K.; Uchikawa, F.; Sakai, K.; Tabata, K. *ACS Catal.* **2016,** *6,* 4394–4398. doi:10.1021/acscatal.6b00886
45. Qu, Z.; Chen, X.; Zhong, S.; Deng, G.-J.; Huang, H. *Org. Lett.* **2021,** *23,* 5349–5353. doi:10.1021/acs.orglett.1c01654
46. Fu, M.-C.; Wang, J.-X.; Shang, R. *Org. Lett.* **2020,** *22,* 8572–8577. doi:10.1021/acs.orglett.0c03173
47. Sheng, H.; Liu, Q.; Su, X.-D.; Lu, Y.; Wang, Z.-X.; Chen, X.-Y. *Org. Lett.* **2020,** *22,* 7187–7192. doi:10.1021/acs.orglett.0c02523
48. Liang, T.; Neumann, C. N.; Ritter, T. *Angew. Chem., Int. Ed.* **2013,** *52,* 8214–8264. doi:10.1002/anie.201206566
49. Reichel, M.; Karaghiosoff, K. *Angew. Chem., Int. Ed.* **2020,** *59,* 12268–12281. doi:10.1002/anie.201913175
50. Liu, Q.; Lu, Y.; Sheng, H.; Zhang, C.-S.; Su, X.-D.; Wang, Z.-X.; Chen, X.-Y. *Angew. Chem., Int. Ed.* **2021,** *60,* 25477–25484. doi:10.1002/anie.202111006
51. Hou, T.; Peng, H.; Xin, Y.; Wang, S.; Zhu, W.; Chen, L.; Yao, Y.; Zhang, W.; Liang, S.; Wang, L. *ACS Catal.* **2020,** *10,* 5502–5510. doi:10.1021/acscatal.0c00920
52. Yao, W.; Bazan-Bergamino, E. A.; Ngai, M.-Y. *ChemCatChem* **2022,** *14,* e202101292. doi:10.1002/cctc.202101292

License and Terms

BEILSTEIN JOURNAL OF ORGANIC CHEMISTRY

Visible-light-induced radical cascade cyclization: a catalyst-free synthetic approach to trifluoromethylated heterocycles

Chuan Yang[‡1,2], Wei Shi[‡1,2], Jian Tian[2], Lin Guo[2], Yating Zhao[*1] and Wujiong Xia[*2,3]

Full Research Paper

Open Access

Address:
[1]College of Chemical and Material Engineering, Quzhou University, Quzhou 324000, China, [2]State Key Lab of Urban Water Resource and Environment, School of Science, Harbin Institute of Technology (Shenzhen), Shenzhen, 518055, China and [3]School of Chemistry and Chemical Engineering, Henan Normal University, Xinxiang, Henan 453007, China

Email:
Yating Zhao[*] - liveagain@126.com; Wujiong Xia[*] - xiawj@hit.edu.cn

* Corresponding author ‡ Equal contributors

Keywords:
cascade reaction; indole derivatives; photocatalysis; radical chain process; trifluoromethylation

Beilstein J. Org. Chem. **2024,** *20,* 118–124.
https://doi.org/10.3762/bjoc.20.12

Received: 03 November 2023
Accepted: 10 January 2024
Published: 19 January 2024

This article is part of the thematic issue "Sustainable concepts in catalysis: nonprecious metals and visible light".

Guest Editor: O. El-Sepelgy

Abstract

A visible-light-promoted research protocol for constructing dihydropyrido[1,2-*a*]indolone skeletons is herein described proceeding through a cascade cyclization mediated by trifluoromethyl radicals. This method allows the efficient synthesis of various indole derivatives without the need of photocatalysts or transition-metal catalysts. Mechanism experiments indicate that the process involves a radical chain process initiated by the homolysis of Umemoto's reagent. This straightforward method enables a rapid access to heterocycles containing a trifluoromethyl group.

Introduction

Dihydropyrido[1,2-*a*]indolone (DHPI) skeletons are commonly found in natural products and pharmaceutical compounds (Figure 1) [1-3], which exhibit a wide range of biological and pharmaceutical activities [4]. For example, mersicarpine has been found to inhibit protein translation and induce apoptosis [5] and vinburnine acts as a vasodilator for the treatment of cerebrovascular insufficiency [6,7].

Given their biological activity and potential applications, continuous efforts have been dedicated to the synthesis of DHPI derivatives. Various synthetic strategies have been explored (Scheme 1), including transition-metal-catalyzed cross-coupling reactions [8-10], annulation reaction of carbenoids [11], Friedel–Crafts acylation [12], radical cascade reactions [2,13], and photoinduced radical cyclizations [14-17]. However, these methods often suffer from drawbacks such as harsh reaction conditions and the requirement of transition-metal catalysts. Although photocatalyzed cyclization reactions usually occur under mild conditions, they typically require expensive metal-based photocatalysts or structurally complex organic dyes

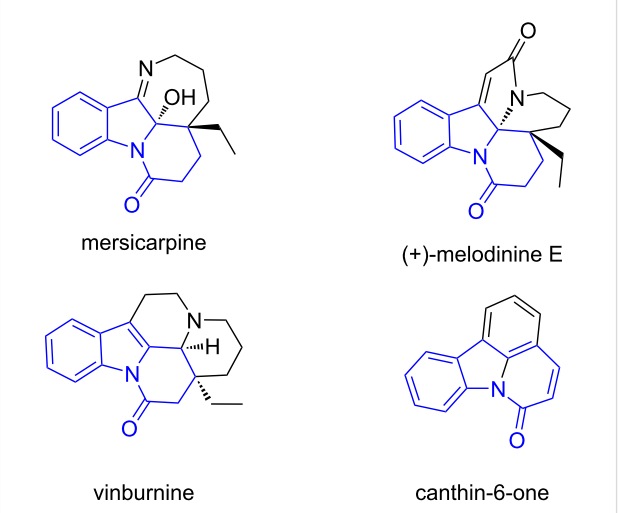

Figure 1: Representative dihydropyrido[1,2-*a*]indolone derivatives.

[18]. Therefore, the development of a photoinduced cascade reaction without the need of additional catalysts or additives remains highly desirable [19].

The introduction of an electron-withdrawing functional moiety into drug molecules would increase their metabolic stability [20], by avoiding, e.g., fast oxidation by cytochrome P450 oxidases [21]. In particular, the introduction of a trifluoromethyl group (–CF_3) was shown to increase the metabolic stability of molecules and at the same time improved cell membrane permeability. Therefore, it became a commonly used strategy to modify medicine candidates [22-24]. Based on these advantages, we envisioned a one-step synthesis of dihydropyrido[1,2-*a*]indolone skeletons utilizing an indole substrate and a trifluoromethyl radical source under light irradiation. Umemoto's reagent, which is capable of releasing a trifluoromethyl radical via a photoinduced single-electron-transfer (SET) process, is usually employed to enable the trifluoromethylation of unsaturated substrates [25-27]. Herein, we report a protocol to furnish trifluoromethylated dihyropyrido[1,2-*a*]indolones under mild conditions, without the need of photocatalysts or transition metals [28].

Results and Discussion

We initialized our study by employing $Ru(bpy)_3Cl_2{\cdot}6H_2O$ and Umemoto's reagent to generate trifluoromethyl radicals via a photo-reductive quench process (Table 1). The indole substrate **1a** was chosen as a model substrate, and the reaction mixture was irradiated under 450 nm visible light for 12 h, resulting in the formation of the desired product **3a**, albeit in a relatively low yield (Table 1, entry 1). Control experiments revealed that omitting the photocatalyst led to an even higher yield (Table 1, entry 2), but light irradiation was essential to the reaction (Table 1, entries 3 and 4). Initially, some bases were added into the reaction system considering a deprotonation process, but subsequent investigations indicated that bases were not required. Among the solvents examined, DCM was found to be the most effective (Table 1, entries 5–8). However, due to the low boiling point of DCM, more solvent was added to avoid complete volatilization (Table 1, entry 8). The screening of dif-

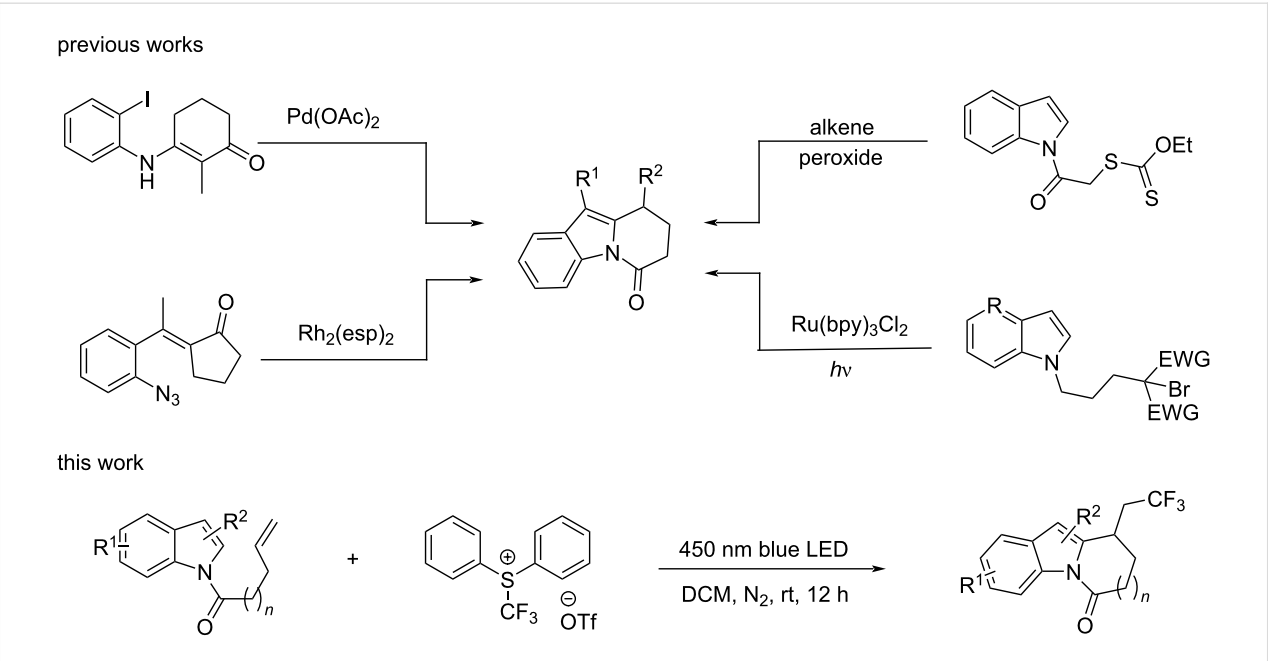

Scheme 1: Selected works for the construction of dihydropyrido[1,2-*a*]indolones and current methodology.

Table 1: Optimization of reaction conditions.[a]

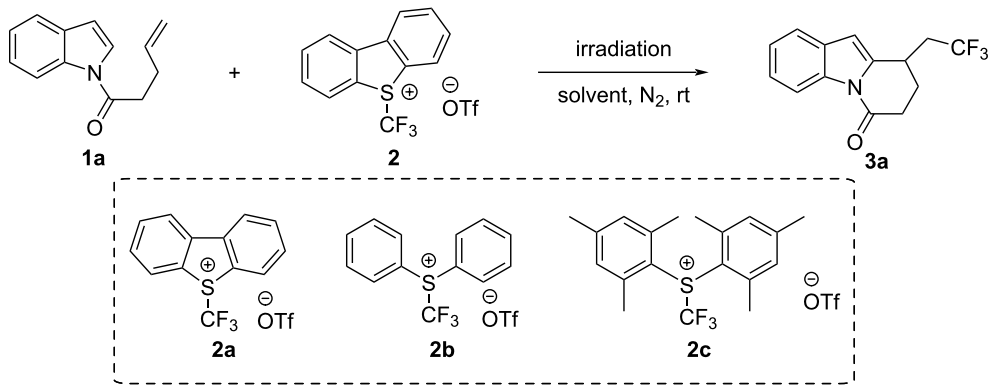

Entry	$CF_3^{\cdot}$ source (equiv)	Photocatalyst	Solvent	λ Irradiation (nm)	Time	Yield **3a**
1	**2a** (2)	$Ru(bpy)_3Cl_2$	MeCN	450	12 h	21%
2	**2a** (2)	–	MeCN	450	12 h	43%
3[b]	**2a** (2)	–	MeCN	450	12 h	52%
4[b]	**2a** (2)	–	MeCN	dark	12 h	trace
5[b]	**2a** (2)	–	1,4-dioxane	450	12 h	trace
6[b]	**2a** (2)	–	toluene	450	12 h	trace
7[b]	**2a** (2)	–	DCM (1 mL)	450	12 h	45%
8[b]	**2a** (2)	–	DCM (2 mL)	450	12 h	55%
9[b]	**2a** (2)	–	DCM (2 mL)	365	12 h	33%
10[b]	**2a** (2)	–	DCM (2 mL)	390	12 h	40%
11[b]	**2a** (2)	–	DCM (2 mL)	420	12 h	51%
12[c]	**2a** (1)	–	DCM (2 mL)	450	22 h	68%
13[b,c]	**2a** (1)	–	DCM (2 mL)	450	22 h	68%
14[c]	**2b** (1)	–	DCM (2 mL)	450	18 h	67%
15[c]	**2c** (1)	–	DCM (2 mL)	450	18 h	58%
16[c]	**2b** (1)	–	dry DCM	450	12 h	72%

[a]Standard reaction conditions: **1a** (0.1 mmol, 1.0 equiv), **2a** (0.2 mmol, 2.0 equiv), solvent (1 mL). [b]2.0 equiv of KH_2PO_4 were added. [c]3.0 equiv of substrate **1a** were utilized in the reaction.

ferent irradiation wavelengths revealed that 450 nm visible light irradiation is optimal (Table 1, entries 9–12). Furthermore, various types of Umemoto's reagent were also screened (Table 1, entries 13–15). As Umemoto's reagent **2b** was easier to prepare [29] and the use of **2b** did not significantly affect the reaction yield, it was chosen as the most suitable CF_3 radical source. Further optimization involved screening the substrates' ratios, which revealed that an excess of substrate **1a** resulted in improved yields. Finally, experimenting with anhydrous DCM as the solvent showed that anhydrous conditions were not necessary for the reaction (Table 1, entry 16).

With the optimized conditions in hand, we started to explore the scope of this photoinduced transformation. Various alkene-tethered indole derivatives were subjected to the reaction. Remarkably, a range of dihydropyrido[1,2-*a*]indolones bearing a trifluoromethyl group were obtained in moderate to good yields (Scheme 2). In general, substrates with electron-withdrawing groups delivered the products in lower yields, such as -CN (**3d**, 42%) and -CHO (**3j**, 28%), while the substrates with electron-donating groups gave higher yields, such as -Me (**3b**, 70%; **3e**, 79%), -OMe (**3f**, 59%; **3k**, 55%). Most of the substrates bearing substituents at the C5 position on the indole skeleton reacted well, furnishing the products in moderate to good yields from 53–79% (**3e**–**i**) except the 5-CHO-substituted substrate which afforded product **3j** in 28% yield. Indoles with substituents at the C7 position of the indole ring (**3m** and **3n**) furnished the products in moderate yields. The structure of compound **3m** (4-Br) was confirmed by X-ray single crystal diffraction (CCDC: 2304916). Reactions of substrates with a longer carbon chain and a branched chain also proceeded well and afforded the products in 43% (**3o**) and 52% (**3p**) yields, respec-

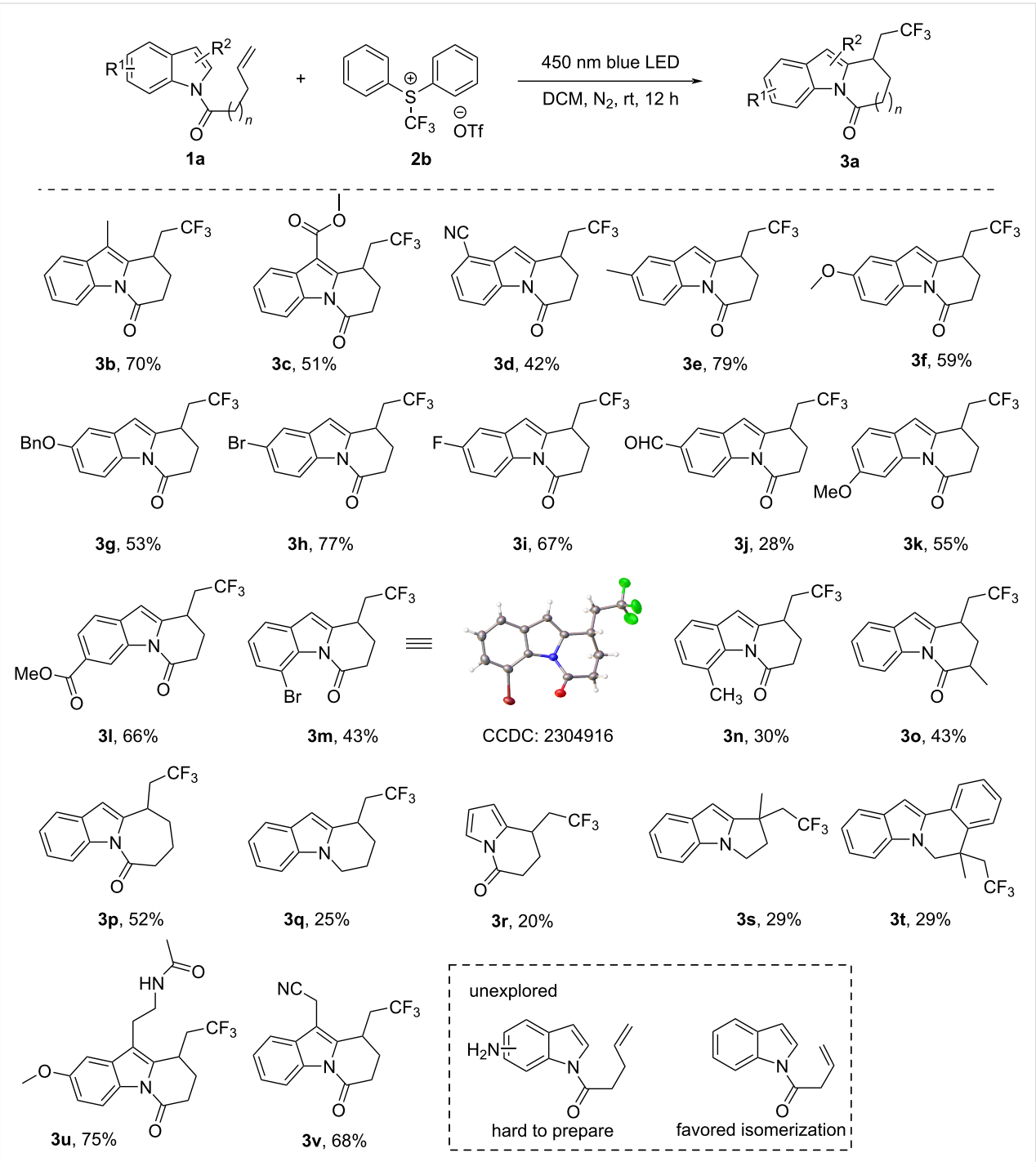

Scheme 2: Substrate scope of the cascade reaction.

tively. If the chains did not involve a carbonyl group, the yields were much lower (**3q**, 25%; **3s**, 29%, and **3t**, 29%). When a pyrrole ring was used instead of indole, the reaction proceeded but gave the product in low yield (**3r**).

We did not explore the reaction with a primary amine functionalized substrate, because of competition of the reaction site during the synthesis of substrates. However, an amide-substituted indole furnished a clean product without competition; for example, product **3u** was derived from melatonin with an amide functional group, whose reaction to the desired product was clean without competitive byproducts. Finally, 3-indoleacetonitrile, a plant growth hormone, furnished the desired product in good yield (**3v**, 68%). Combined with melatonin,

these examples demonstrate the suitability of our approach to be used in drug modification and development. In short, this reaction tolerates different substituents on the indole ring, including electron-donating and electron-withdrawing groups, providing access to a diverse array of dihydropyrido[1,2-*a*]indolone derivatives.

To gain insight into the reaction process, we performed a series of control experiments. The addition of a typical radical scavenger – TEMPO (2,2,6,6-tetramethylpiperidin-1-yloxyl) significantly inhibited the reaction (as shown in Scheme 3), suggesting the involvement of radical species during the reaction process. Moreover, the radical trapping product was detected and confirmed via ^{19}F NMR (Figure S3 in Supporting Information File 1) [30] and high-resolution mass spectrometry.

You and co-workers proposed a reaction pathway involving the combination of the indole substrate and Umemoto's reagent to form an electron donor–acceptor (EDA) complex [31]. We excluded the possibility of an EDA charge transfer complex because there was no obvious EDA charge transfer band in the UV–vis spectra (Figure 2). Their indole substrate was more electron-rich in structure. The quantum yield was measured to investigate whether there was a radical chain process or not. The procedure was following a precedent work [32] (see Supporting Information File 1), and the calculated quantum yield was 2.2, which revealed that one photon generates more than one product molecule.

Based on preliminary experiments and previous reports [33,34], we propose a plausible mechanism (Scheme 4). Upon light irradiation, Umemoto's reagent undergoes a homolysis process to generate the trifluoromethyl radical species. The trifluoromethyl radical is trapped by the terminal alkene and forms a relayed radical intermediate **6**, which is intercepted by the indole ring realizing an intramolecular cyclization (6-*exo*-*trig*). The newly formed radical **7** can be oxidized by **2a** or **4** giving a cation **8**, which undergoes a deprotonation process and formation of the desired product.

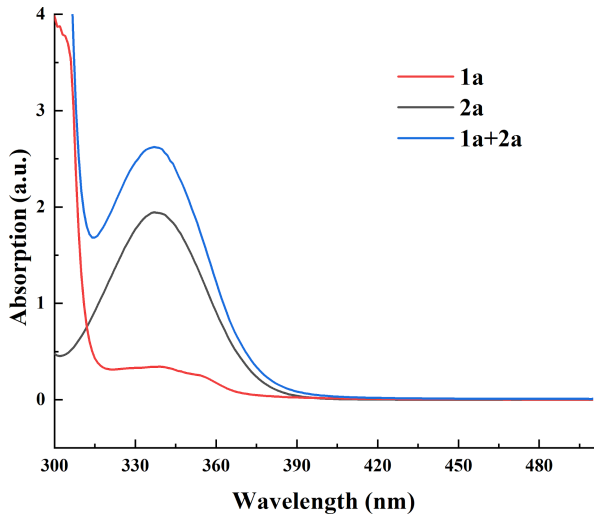

Figure 2: UV–vis spectra of substrates; [**1a**] 0.33 M, [**2a**] 0.11 M.

Conclusion

In conclusion, we have developed a visible-light-promoted protocol for the synthesis of dihydropyrido[1,2-*a*]indolones bearing a trifluoromethyl group at room temperature without additives. Mechanistic investigations support a photochemical process initiated by the homolysis of Umemoto's reagent under visible light irradiation. This method provides rapid access to a diverse range of trifluoromethylated dihydropyrido[1,2-*a*]indolone derivatives in moderate to good yields.

Experimental

To a vial equipped with a stirring bar, alkene-tethered indole substrate **1a** (0.3 mmol), Umemoto's reagent (**2b**, 0.1 mmol), and DCM (2 mL) were added. Then, the vial was degassed and backfilled with N_2 three times to remove oxygen. The reaction mixture was stirred at room temperature for 12 hours under visible light irradiation (450 nm). After completion, the reaction mixture was concentrated, and the crude product was purified by column chromatography to afford the desired dihydropyrido[1,2-*a*]indolone product.

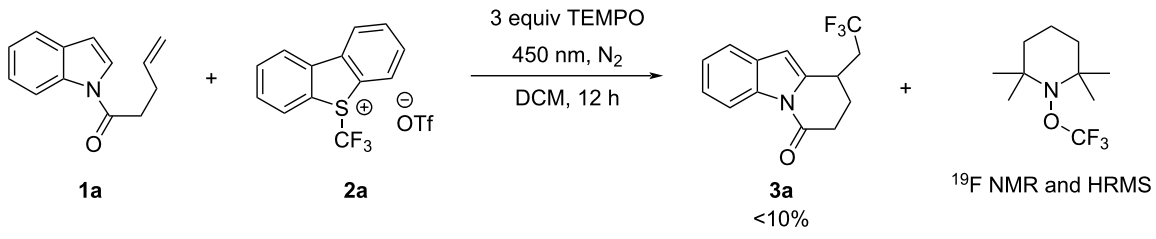

Scheme 3: Radical trapping experiment.

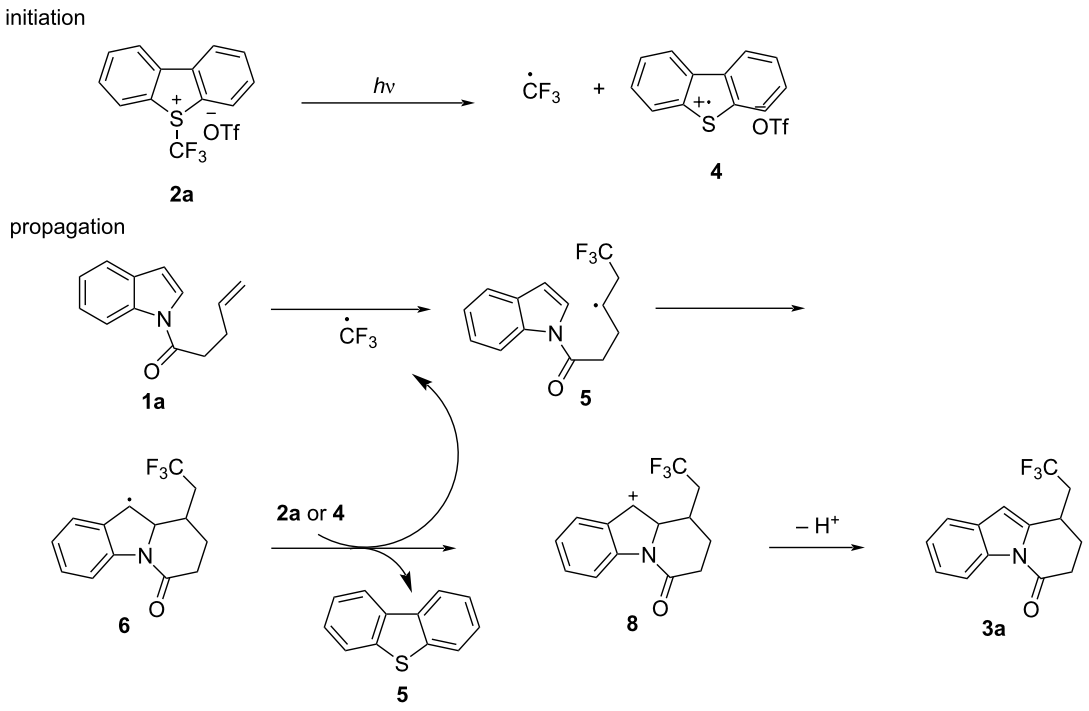

Scheme 4: Plausible reaction mechanism.

Supporting Information

Supporting Information File 1

Characterization data and copies of spectra.
[https://www.beilstein-journals.org/bjoc/content/supplementary/1860-5397-20-12-S1.pdf]

Supporting Information File 2

Crystallographic information file (cif) of X-ray structure for compound **3m**.
[https://www.beilstein-journals.org/bjoc/content/supplementary/1860-5397-20-12-S2.cif]

Funding

We are grateful for the financial support from the Science and Technology Plan of Shenzhen (No. JCYJ20210324133001004 and GXWD20220817131550002), the Natural Science Foundation of Guangdong (No. 2020A1515010564), and Guangdong Basic and Applied Basic Research Foundation (No. 2021A1515220069). W.X. is grateful for the Talent Recruitment Project of Guangdong (No. 2019QN01L753). The project was also supported by State Key Laboratory of Urban Water Resource and Environment (Harbin Institute of Technology) (No.2022TS23), and the Open Research Fund of the School of Chemistry and Chemical Engineering, Henan Normal University.

ORCID® iDs

Wujiong Xia - https://orcid.org/0000-0001-9396-9520

Data Availability Statement

The data that supports the findings of this study is available from the corresponding author upon reasonable request.

References

1. Xu, Z.; Wang, Q.; Zhu, J. *J. Am. Chem. Soc.* **2015,** *137,* 6712–6724. doi:10.1021/jacs.5b03619
2. Kim, R.; Ferreira, A. J.; Beaudry, C. M. *Angew. Chem., Int. Ed.* **2019,** *58,* 12595–12598. doi:10.1002/anie.201907455
3. Pritchett, B. P.; Kikuchi, J.; Numajiri, Y.; Stoltz, B. M. *Angew. Chem., Int. Ed.* **2016,** *55,* 13529–13532. doi:10.1002/anie.201608138
4. Park, S.-a.; Park, J.-U.; Kim, Y. L.; Kim, J. H. *J. Org. Chem.* **2021,** *86,* 17050–17062. doi:10.1021/acs.joc.1c02176
5. Shiobara, T.; Nagumo, Y.; Nakajima, R.; Fukuyama, T.; Yokoshima, S.; Usui, T. *Biosci., Biotechnol., Biochem.* **2021,** *85,* 92–96. doi:10.1093/bbb/zbaa070
6. Benzi, G.; Arrigoni, E.; Dagani, F.; Marzatico, F.; Curti, D.; Manzini, A.; Villa, R. F. *Biochem. Pharmacol.* **1979,** *28,* 2703–2708. doi:10.1016/0006-2952(79)90550-1
7. Villa, R. F.; Strada, P.; Marzatico, F.; Dagani, F. *Eur. Neurol.* **1978,** *17* (Suppl. 1), 97–112. doi:10.1159/000115013

8. Dong, Z.; Zhang, X.-W.; Li, W.; Li, Z.-M.; Wang, W.-Y.; Zhang, Y.; Liu, W.; Liu, W.-B. *Org. Lett.* **2019,** *21,* 1082–1086. doi:10.1021/acs.orglett.8b04128
9. Pritchett, B. P.; Kikuchi, J.; Numajiri, Y.; Stoltz, B. M. *Heterocycles* **2017,** *95,* 1245–1253. doi:10.3987/com-16-s(s)80
10. Zhou, B.; Du, J.; Yang, Y.; Li, Y. *Chem. – Eur. J.* **2014,** *20,* 12768–12772. doi:10.1002/chem.201403973
11. Li, H.; Cheng, P.; Jiang, L.; Yang, J.-L.; Zu, L. *Angew. Chem., Int. Ed.* **2017,** *56,* 2754–2757. doi:10.1002/anie.201611830
12. Zhong, X.; Qi, S.; Li, Y.; Zhang, J.; Han, F.-S. *Tetrahedron* **2015,** *71,* 3734–3740. doi:10.1016/j.tet.2014.07.095
13. Biechy, A.; Zard, S. Z. *Org. Lett.* **2009,** *11,* 2800–2803. doi:10.1021/ol900996k
14. Tucker, J. W.; Narayanam, J. M. R.; Krabbe, S. W.; Stephenson, C. R. J. *Org. Lett.* **2010,** *12,* 368–371. doi:10.1021/ol902703k
15. Saget, T.; König, B. *Chem. – Eur. J.* **2020,** *26,* 7004–7007. doi:10.1002/chem.202001324
16. Wei, Y.-L.; Chen, J.-Q.; Sun, B.; Xu, P.-F. *Chem. Commun.* **2019,** *55,* 5922–5925. doi:10.1039/c9cc02388g
17. Chen, J.-Q.; Tu, X.; Qin, B.; Huang, S.; Zhang, J.; Wu, J. *Org. Lett.* **2022,** *24,* 642–647. doi:10.1021/acs.orglett.1c04082
18. Yang, R.; Yi, D.; Shen, K.; Fu, Q.; Wei, J.; Lu, J.; Yang, L.; Wang, L.; Wei, S.; Zhang, Z. *Org. Lett.* **2022,** *24,* 2014–2019. doi:10.1021/acs.orglett.2c00472
19. Liao, J.; Yang, X.; Ouyang, L.; Lai, Y.; Huang, J.; Luo, R. *Org. Chem. Front.* **2021,** *8,* 1345–1363. doi:10.1039/d0qo01453b
20. Xiao, H.; Zhang, Z.; Fang, Y.; Zhu, L.; Li, C. *Chem. Soc. Rev.* **2021,** *50,* 6308–6319. doi:10.1039/d1cs00200g
21. Nagib, D. A.; MacMillan, D. W. C. *Nature* **2011,** *480,* 224–228. doi:10.1038/nature10647
22. Kornfilt, D. J. P.; MacMillan, D. W. C. *J. Am. Chem. Soc.* **2019,** *141,* 6853–6858. doi:10.1021/jacs.9b03024
23. Yin, D.; Su, D.; Jin, J. *Cell Rep. Phys. Sci.* **2020,** *1,* 100141. doi:10.1016/j.xcrp.2020.100141
24. Qi, X.-K.; Zhang, H.; Pan, Z.-T.; Liang, R.-B.; Zhu, C.-M.; Li, J.-H.; Tong, Q.-X.; Gao, X.-W.; Wu, L.-Z.; Zhong, J.-J. *Chem. Commun.* **2019,** *55,* 10848–10851. doi:10.1039/c9cc04977k
25. Xu, J.; Fu, Y.; Luo, D.-F.; Jiang, Y.-Y.; Xiao, B.; Liu, Z.-J.; Gong, T.-J.; Liu, L. *J. Am. Chem. Soc.* **2011,** *133,* 15300–15303. doi:10.1021/ja206330m
26. Pan, X.; Xia, H.; Wu, J. *Org. Chem. Front.* **2016,** *3,* 1163–1185. doi:10.1039/c6qo00153j
27. Merino, E.; Nevado, C. *Chem. Soc. Rev.* **2014,** *43,* 6598–6608. doi:10.1039/c4cs00025k
28. Xia, W. Green Preparation of Pyrido[1,2-*a*]Indole Compounds. Chin. Patent CN115947726A, April 11, 2023.
29. Wang, S.-M.; Wang, X.-Y.; Qin, H.-L.; Zhang, C.-P. *Chem. – Eur. J.* **2016,** *22,* 6542–6546. doi:10.1002/chem.201600991
30. Wang, X.; Ye, Y.; Zhang, S.; Feng, J.; Xu, Y.; Zhang, Y.; Wang, J. *J. Am. Chem. Soc.* **2011,** *133,* 16410–16413. doi:10.1021/ja207775a
31. Zhu, M.; Zhou, K.; Zhang, X.; You, S.-L. *Org. Lett.* **2018,** *20,* 4379–4383. doi:10.1021/acs.orglett.8b01899
32. Cismesia, M. A.; Yoon, T. P. *Chem. Sci.* **2015,** *6,* 5426–5434. doi:10.1039/c5sc02185e
33. Wang, H.; Xu, Q.; Yu, S. *Org. Chem. Front.* **2018,** *5,* 2224–2228. doi:10.1039/c8qo00430g
34. Chen, L.; Ma, P.; Yang, B.; Zhao, X.; Huang, X.; Zhang, J. *Chem. Commun.* **2021,** *57,* 1030–1033. doi:10.1039/d0cc07502g

License and Terms

BEILSTEIN JOURNAL OF ORGANIC CHEMISTRY

Manganese-catalyzed C–C and C–N bond formation with alcohols via borrowing hydrogen or hydrogen auto-transfer

Mohd Farhan Ansari‡, Atul Kumar Maurya‡, Abhishek Kumar and Saravanakumar Elangovan*

Review

Open Access

Address:
Department of Chemistry, Indian Institute of Technology (BHU), Varanasi, Uttar Pradesh 221005, India

Email:
Saravanakumar Elangovan* - saravana.chy@itbhu.ac.in

* Corresponding author ‡ Equal contributors

Keywords:
alcohols; alkylation; amines; borrowing hydrogen; hydrogen auto-transfer; manganese

Beilstein J. Org. Chem. **2024,** *20,* 1111–1166.
https://doi.org/10.3762/bjoc.20.98

Received: 27 January 2024
Accepted: 24 April 2024
Published: 21 May 2024

This article is part of the thematic issue "Sustainable concepts in catalysis: nonprecious metals and visible light".

Guest Editor: O. El-Sepelgy

Abstract

Transition-metal-mediated “borrowing hydrogen" also known as hydrogen auto-transfer reactions allow the sustainable construction of C–C and C–N bonds using alcohols as hydrogen donors. In recent years, manganese complexes have been explored as efficient catalysts in these reactions. This review highlights the significant progress made in manganese-catalyzed C–C and C–N bond-formation reactions via hydrogen auto-transfer, emphasizing the importance of this methodology and manganese catalysts in sustainable synthesis strategies.

Introduction

The construction of C–C and C–N bonds is of utmost importance in organic synthesis and is widely used in the pharmaceutical and other chemical industries. Palladium-catalyzed cross-coupling reactions are one of the compelling methods for building C–C and C–N bonds [1,2]. However, using organohalide reagents and harsh reaction conditions in this process results in the co-production of a significant amount of waste or side-products. Borrowing hydrogen (BH) or hydrogen auto-transfer (HA) reactions have emerged as the most elegant and powerful strategy to overcome this drawback [3-5]. Furthermore, this method has been considered an environmentally friendly and atom-economical process for C–C and C–N bond formations utilizing alcohol as an alkylating agent and hydrogen donor, producing water as the only side-product [6-9]. Notably, alcohols are inexpensive, abundant and can be obtained from biomass, which makes this method even more attractive to the scientific community [10-12]. In this process, first, the metal-catalyzed dehydrogenation of the alcohol provides a reactive substrate for coupling with nucleophiles and the active metal hydride species. Later, the borrowed hydrogen is used in the final step to reduce unsaturated compounds. To achieve the selective C–C and C–N bond formation via hydrogen borrowing, controlling the selectivity is an important factor since the formation of possible side-products such as overreduc-

tion of unsaturated compounds or dialkylation. Hence, developing an efficient catalyst, capable of achieving both selective dehydrogenation and hydrogenation is highly important. A typical BH process is demonstrated in Scheme 1.

Several precious transition-metal catalysts have been used successfully in this area, including iridium, rhodium, ruthenium, and osmium [4]. However, these noble metals are toxic, expensive, and limited in availability. Hence, replacing them with the first row of transition metals would increase the sustainability and profitability of this procedure [13]. Indeed, many 3d-metal-based homogeneous catalysts have been documented for BH reactions [14,15] since these metals are considerably inexpensive, eco-friendly and more abundant in the Earth's crust. According to this viewpoint, manganese is biocompatible and less expensive than noble metals. Also, it is the third most abundant transition metal, behind titanium and iron. After the independent pioneering works of Beller [16] and Milstein [17] in hydrogenation and dehydrogenation reactions with pincer-decorated manganese complexes, significant progress has been made in manganese catalysis [18-20]. Notably, well-defined low-valent diamagnetic manganese(I) complexes have been studied in many catalytic transformations, and several reviews have been reported on their applications in dehydrogenative coupling reactions [21-24]. This review focuses mainly on the BH reaction to create sustainable C–C and C–N bonds with manganese catalysts.

Review

C–N bond formation with alcohols and amines

Amines and their derivatives are of substantial importance for the fine chemical industry, pharmaceuticals, agrochemicals, dyes, and natural products [25]. The synthesis of amine derivatives can be accomplished using many powerful techniques, including Buchwald–Hartwig and Ullmann cross-coupling reactions, hydroamination, hydroaminomethylation, reduction of nitriles and nitro compounds or through reductive amination of carbonyl derivatives [26-30]. However, for example, cross-coupling reactions with alkyl or aryl halides generate considerable amounts of waste (Scheme 2A). Even though many different approaches exist for synthesizing amines, the borrowing hydrogen approach is becoming increasingly popular in catalysis since this method provides an excellent example of a green chemistry and atom-efficient reaction [31-33]. This section focuses on manganese-catalyzed C–N bond formation reactions via BH or HA using alcohols as hydrogen donors and alkylating agents.

In general, low-valent manganese complexes are used as pre-catalysts in this reaction and are activated using a strong base to generate the active amido complexes, which in turn activate the alcohols. Then, the formed dehydrogenation products, such as aldehydes or ketones, undergo base-assisted condensation reactions with amines providing the corresponding imines. In the last step, the active manganese hydride complexes reduce the imine compounds and afford the desired alkylated amine products (Scheme 2B). Several well-defined manganese complexes have been developed for the N-alkylation of amines with alcohols, including methanol (Figure 1).

Beller and co-workers introduced the first intriguing manganese-catalyzed BH for the N-alkylation of amines with alcohols in 2016 [34]. The potential Mn(I)-pincer complex **Mn1** (3 mol %) catalyzed the coupling of the several alcohols and primary amines in the presence of *t*-BuOK (0.75 equiv) in toluene at 80 °C for 24–48 h and selectively produced the N-alky-

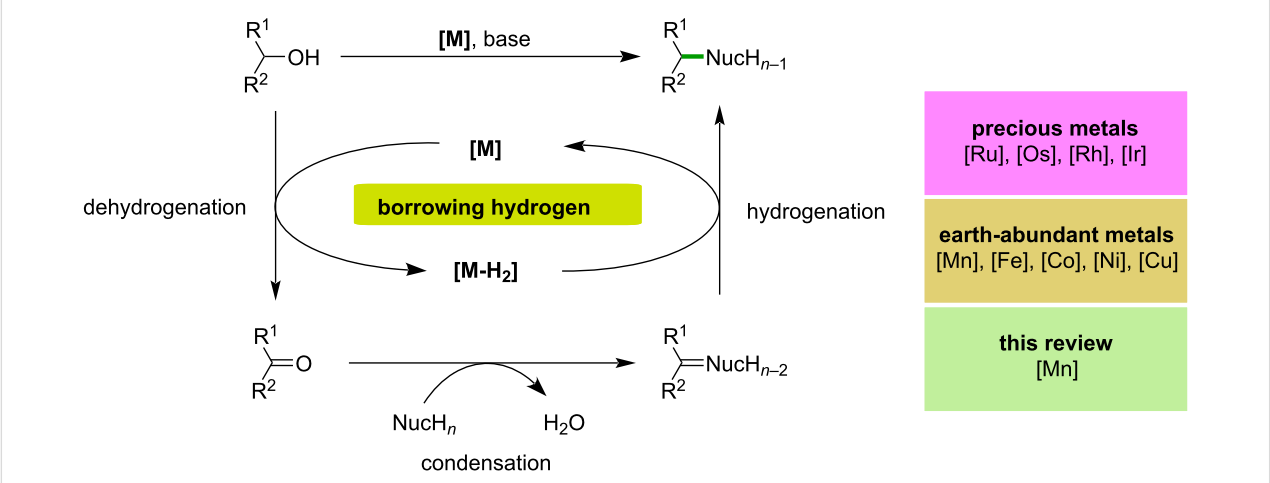

Scheme 1: General scheme of the borrowing hydrogen (BH) or hydrogen auto-transfer (HA) methodology.

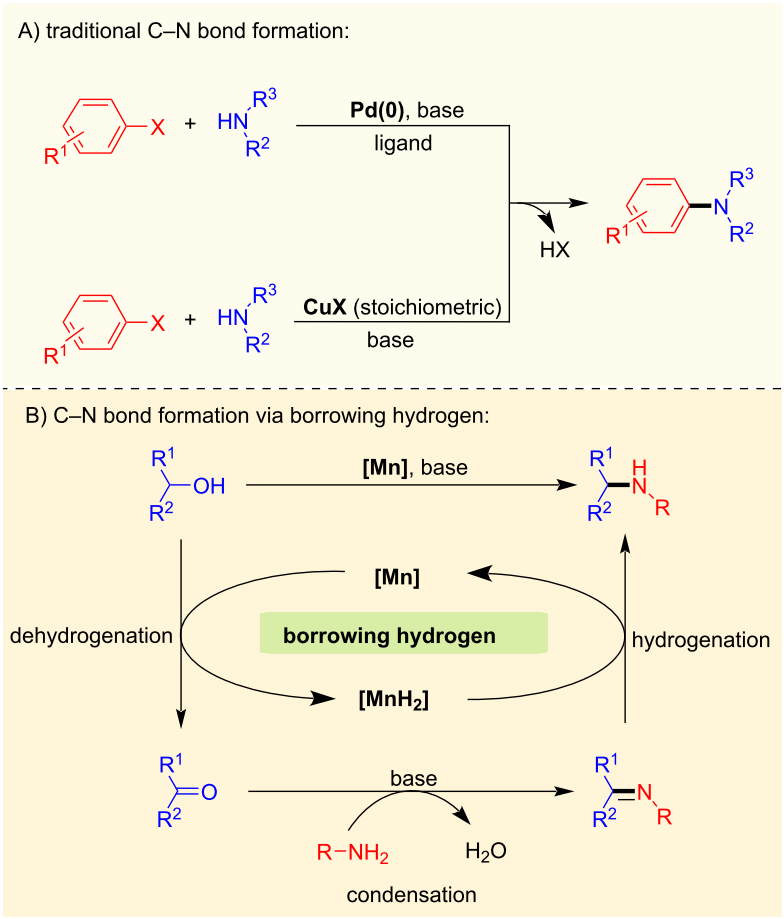

Scheme 2: General scheme for C–N bond formation. A) Traditional cross-couplings with alkyl or aryl halides. B) Borrowing hydrogen with alcohols and amines.

lated products with good yields (Scheme 3). More interestingly, the first non-noble-metal catalyzed the most challenging N-methylation of amines with methanol was achieved at 100 °C with one equivalent of *t*-BuOK. In all the cases, the catalytic system selectively yielded mono-N-alkylated and N-methylated products under mild conditions. Noteworthy, high functional group tolerance, such as alkenes, halogens, thioethers, and benzodioxane derivatives was observed under the established reaction conditions. This pioneering work opened the door for manganese catalysis in BH reactions. However, the high base loading (0.75–1 equiv) was required for this system to attain good yields of the N-alkylated products.

Later, the same group developed the second generation of manganese PNP pincer complexes for the N-methylation of aromatic amines with methanol [35]. Various primary anilines were methylated selectively with good yields using **Mn2** (2 mol %) and *t*-BuOK (0.5 equiv) as a base at 100 °C for 16 h (Scheme 4). Compared to their previous report, the N-methylation of amines with methanol was achieved with lower catalyst and base loading.

Sortais et al. reported an elegant example of a manganese-catalyzed N-methylation of primary amines with methanol using catalytic amounts of base. They synthesized a novel Mn(I) complex bearing a bis(diaminopyridine)phosphine ligand (PN^3P) (**Mn3**) and studied N-methylation reactions in the presence of *t*-BuOK (20 mol %) at 120 °C for 24 h in toluene [36]. This catalytic system tolerated various functional groups, including nitro, ester, amide, and ketones and gave moderate to good yields (42–98%) of the mono-N-methylated products (Scheme 5). Interestingly, the dearomatized intermediate resulting from the reaction of base and **Mn3** was isolated and characterized by X-ray analysis during the mechanistic investigation.

In 2018, Kempe et al. disclosed that the choice of the base plays a critical role in the BH method for the synthesis of amines and imines using Mn-pincer catalyst [37]. When *t*-BuOK (1 equiv)

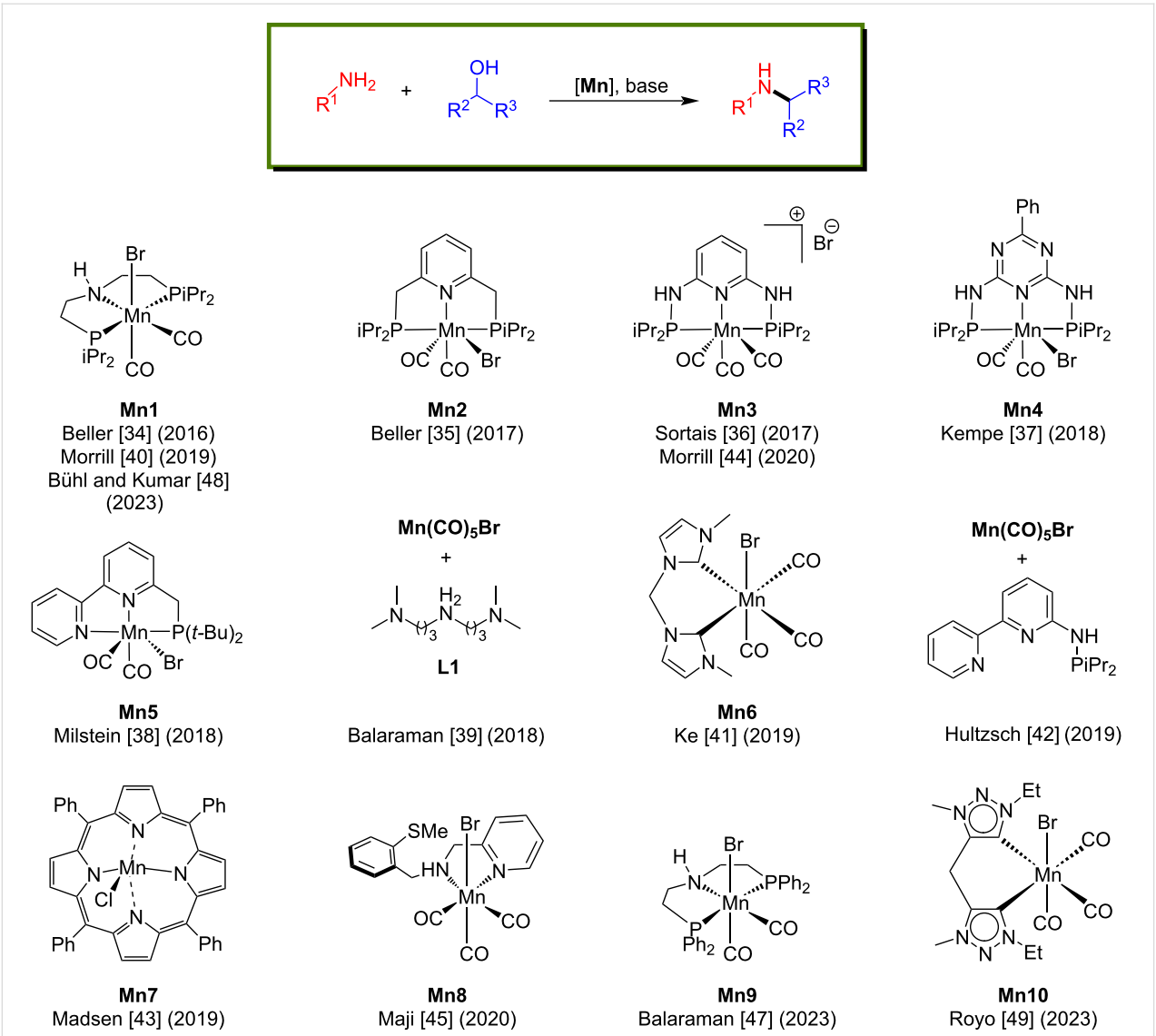

Figure 1: Manganese pre-catalysts used for the N-alkylation of amines with alcohols.

was used as a base, alkylated amine products were observed selectively using alcohol as an alkylating agent, whereas when *t*-BuONa (1.5 equiv) was used as base, alkylated imine products were isolated (Scheme 6). This indicates that the cation-coordinative interaction with the catalyst plays a significant role. Moreover, the mechanistic investigation suggested that the observed selectivity is due to the more reactive potassium manganate hydride towards the hydrogenation of imines to amines than the sodium manganate hydride.

In 2018, the Milstein group demonstrated a partial hydrogen-borrowing reaction with a manganese-pincer complex by coupling alcohols and hydrazine to form N-substituted hydrazones. Benzylic and aliphatic alcohols were studied with hydrazine using Mn(*t*-Bu-PNN)$(CO)_2$Br (**Mn5**, 3 mol %) and a catalytic amount of *t*-BuOK (5 mol %) at 110 °C [38]. Benzylic alcohols bearing electron-donating and withdrawing groups afforded 65–92% yields of the product within 24 h (Scheme 7). However, aliphatic alcohols such as 1-hexanol and 1-octanol required 36 h to give the corresponding products with 77% and 65% yields, respectively.

The proposed mechanism suggested that the active amido species (**Mn5-a**) was formed by treating **Mn5** with the base. Then, the alkoxy intermediate **Mn5-b** is formed by reaction with the alcohol followed by release of an aldehyde and formation of the manganese hydride **Mn5-c**. The released aldehyde condenses with hydrazine followed by reduction and condensation with another aldehyde to afford the N-substituted hydrazones (Scheme 8).

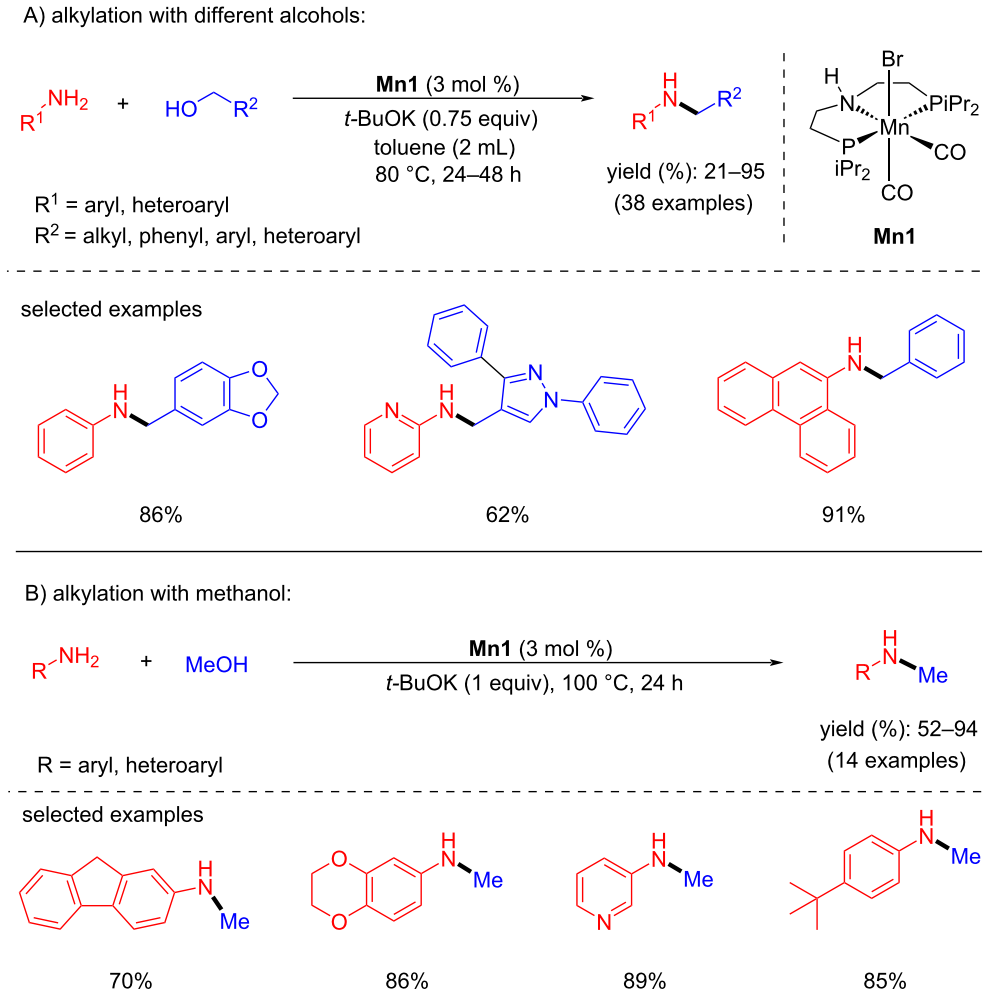

Scheme 3: Manganese(I)-pincer complex **Mn1** used for the N-alkylation of amines with alcohols and methanol.

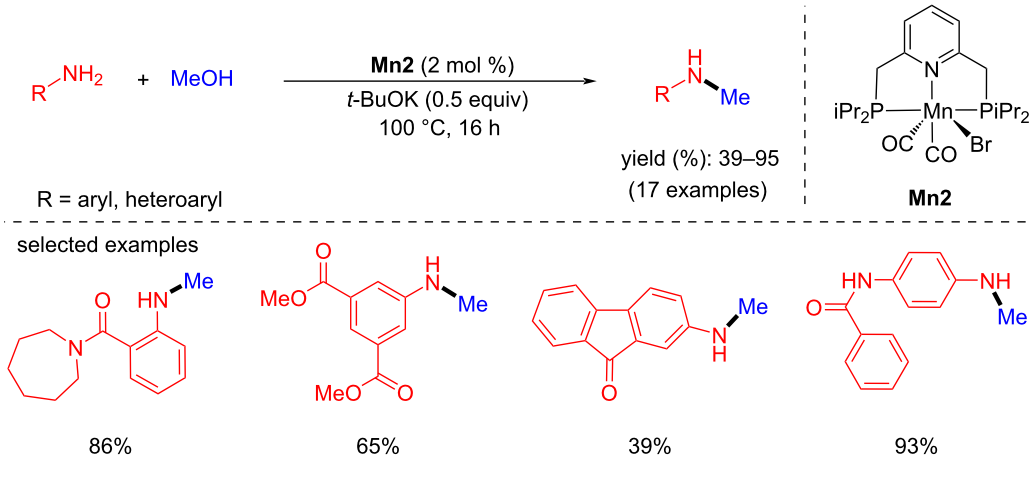

Scheme 4: N-Methylation of amines with methanol using **Mn2**.

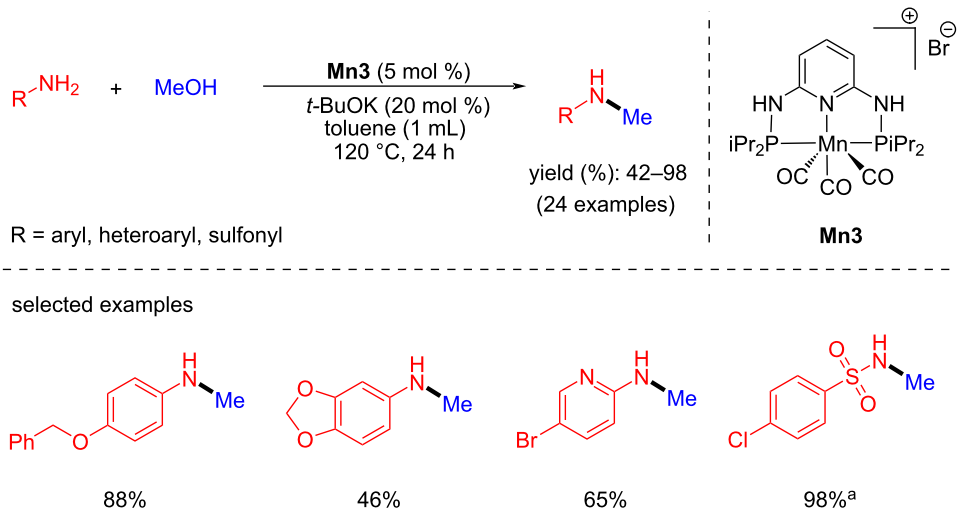

Scheme 5: C–N-Bond formation with amines and methanol using PN^3P-Mn complex **Mn3** reported by Sortais et al. [36]. [a]1.2 Equiv *t*-BuOK, 60 h.

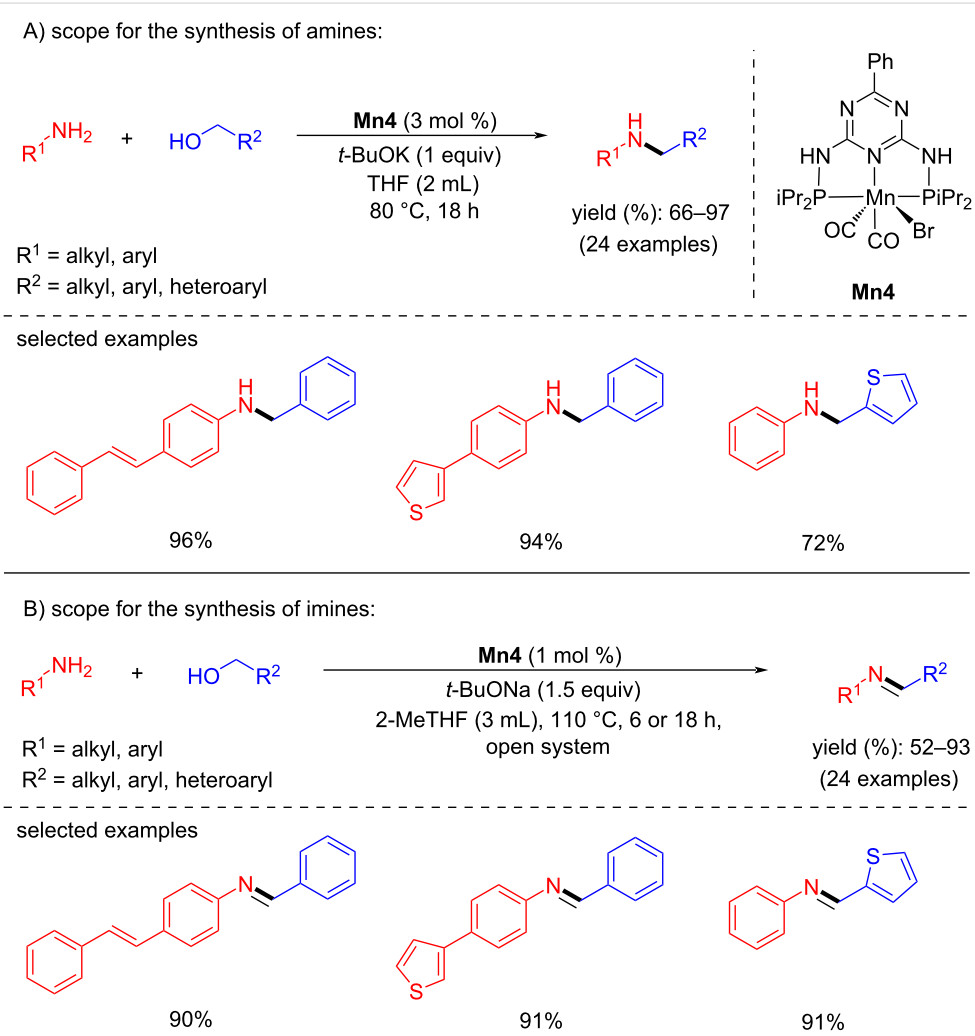

Scheme 6: Base-assisted synthesis of amines and imines with **Mn4**. Reaction assisted by A) *t*-BuOK and B) *t*-BuONa as base.

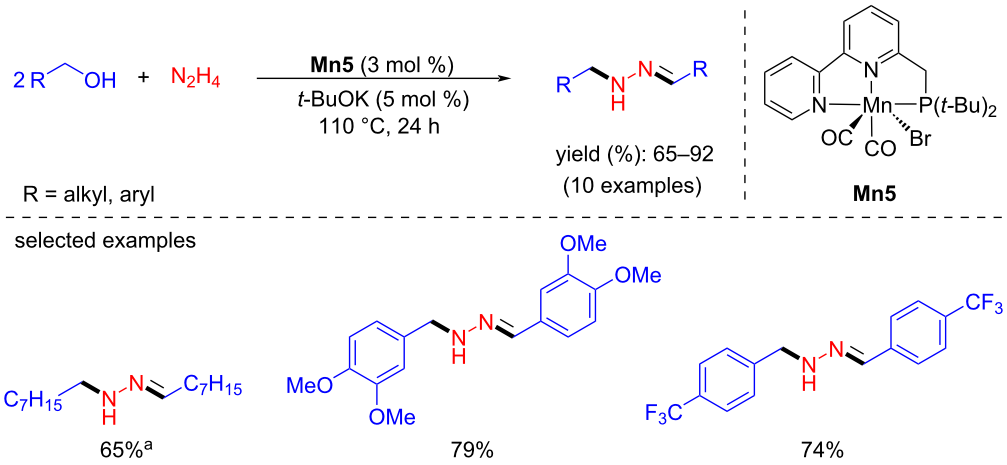

Scheme 7: Coupling of alcohols and hydrazine via the HB approach reported by Milstein et al. [38]. [a]Reaction time was 36 h

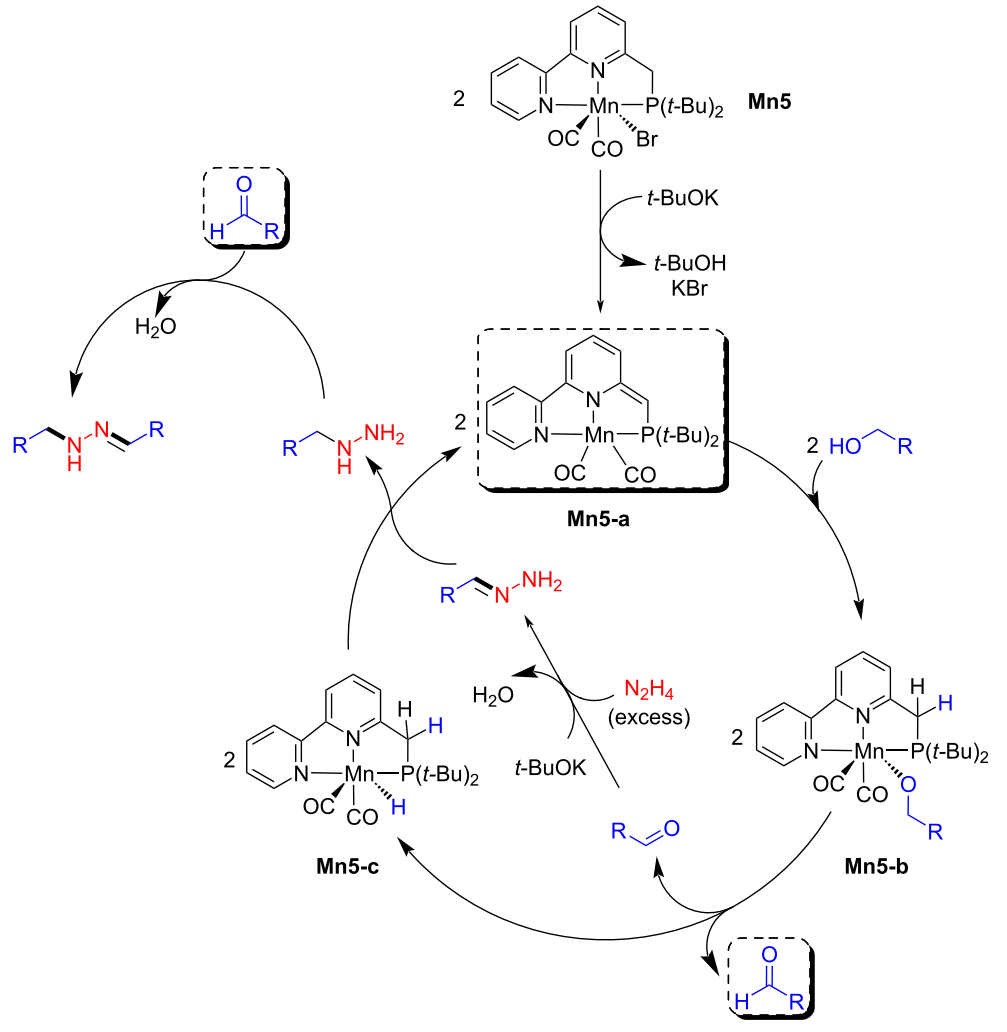

Scheme 8: Proposed mechanism for the coupling of alcohols and hydrazine catalyzed by **Mn5**.

Balaraman and co-workers established a phosphine-free manganese catalyst generated in situ from a manganese precursor and a ligand for the N-alkylation of anilines with alcohols [39]. Various ligands were screened for the N-alkylation of *m*-toluidine with benzyl alcohol using $Mn(CO)_5Br$ (5 mol %) and *t*-BuOK (1 equiv) in toluene at 140 °C (Scheme 9). Among these, **L1** and **L2** showed better activity for the N-alkylation reactions. Different substituted anilines and alcohols, including aliphatic alcohols, were tested and afforded moderate to good yields (up to 95%) of the N-alkylated products using **L1** (5 mol %) and $Mn(CO)_5Br$ (5 mol %). Notably, heteroaromatic amines provided a good yield with **L2** (5 mol %) under the same reaction conditions. The poisoning test with Hg showed the homogeneous nature of the catalytic system. The mechanistic investigation suggested that the reaction proceeds via a dehydrogenative pathway confirmed by forming an aldehyde product and H_2 gas which was detected by GC.

In 2019, Morrill's group reported the N-alkylation of sulfonamides using **Mn1**. The reaction optimized with 5 mol % of **Mn1** and 10 mol % of K_2CO_3 in xylene at high temperature (150 °C) for 24 h afforded the desired N-alkylated sulfonamide compounds [40]. A wide range of aryl and alkyl sulfonamides were alkylated with various benzylic and aliphatic alcohols, providing good to excellent yields (Scheme 10). However, sulfonamides with electron-withdrawing groups attached to the aromatic ring (e.g., 4-NO_2, 4-CN) were found incompatible with the conditions.

Ke and co-workers described an exciting example of a phosphine-free Mn(I)-NHC catalyst for the N-alkylation of amines with alcohols at room temperature [41]. The coupling of several aromatic amines with aliphatic and benzylic alcohols was studied with bis-NHC-manganese complex (**Mn6**). A catalyst loading of 1.5 mol % in the presence of *t*-BuOK (1 equiv) at room temperature produced the corresponding N-alkylated amines with 40–93% yield (Scheme 11). However, N-methylation of anilines with methanol required 100 °C to yield the selective N-methylated products.

The same year, Hultzsch et al. designed PN^3-pincer ligand-supported Mn(I) complexes for the alkylation of amines with primary and secondary alcohols [42]. Most interestingly, a low catalyst loading (0.5 mol %) and mild reaction conditions (60–100 °C) were employed for this transformation. Aromatic amines gave good yields with benzyl alcohol at 60 °C, but 1,1-phenylethylamine, linear aliphatic amine and benzylamine required 100 °C to achieve the good yields (Scheme 12). Similarly, the N-alkylation of aniline with secondary alcohols required a high temperature (100 °C) compared to substituted benzylic alcohols (60 °C). Interestingly, this protocol was used to synthesize the drug cinacalcet, via alkylating the challenging benzylamine substrate under non-optimized conditions.

Later, Madsen's team introduced a manganese(III) porphyrin system as a catalyst for the BH methodology to achieve C–N coupling reactions [43]. Various tertiary amines were isolated by coupling secondary amines and benzylic alcohols using **Mn7** (3 mol %) in the presence of K_2CO_3 (20 mol %) under reflux conditions in mesitylene (Scheme 13).

The formation of manganese(III) alkoxide intermediate **Mn7-a**, was believed to be the first step in the reaction mechanism which then releases the aldehyde under formation of hydride

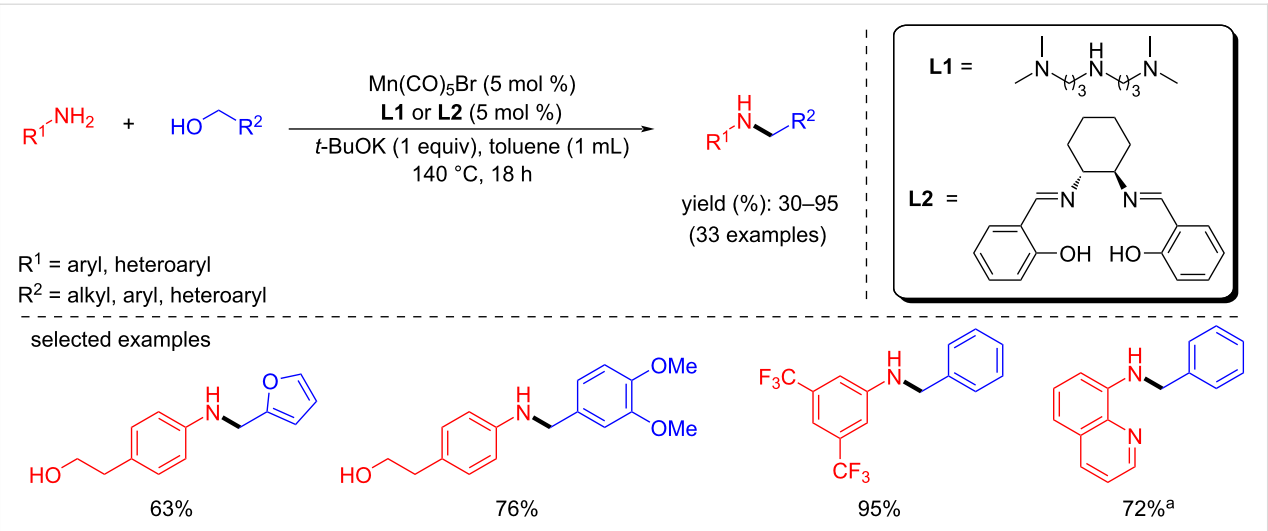

Scheme 9: Phosphine-free manganese catalyst for N-alkylation of amines with alcohols reported by Balaraman and co-workers [39]. [a]Ligand **L2** was used.

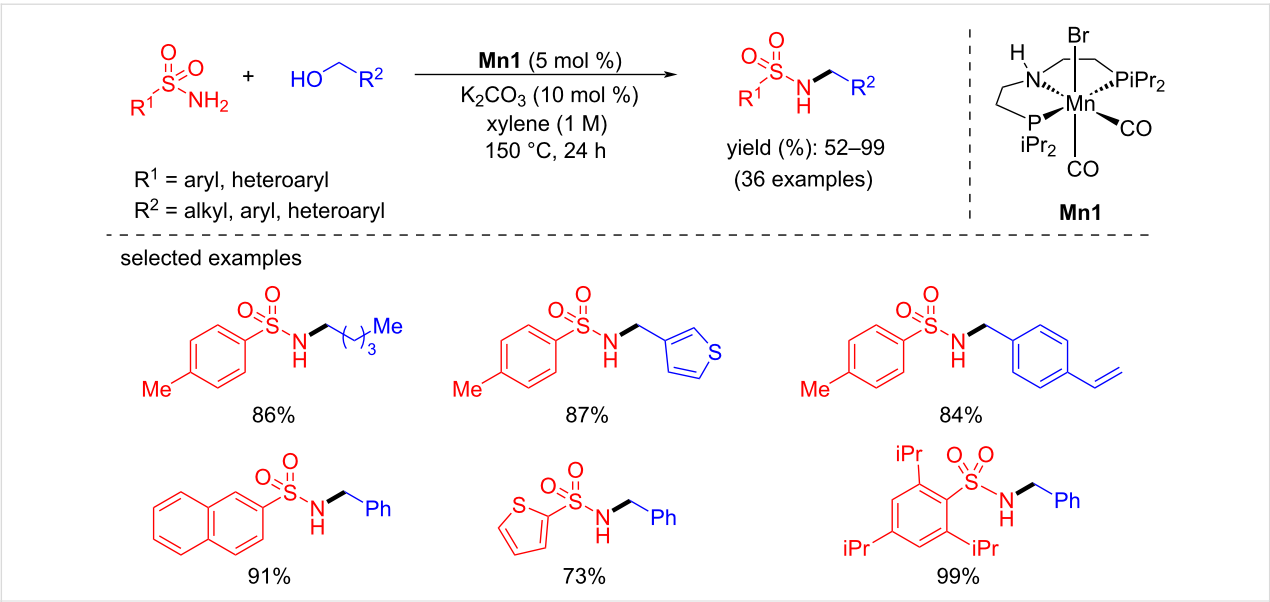

Scheme 10: N-Alkylation of sulfonamides with alcohols.

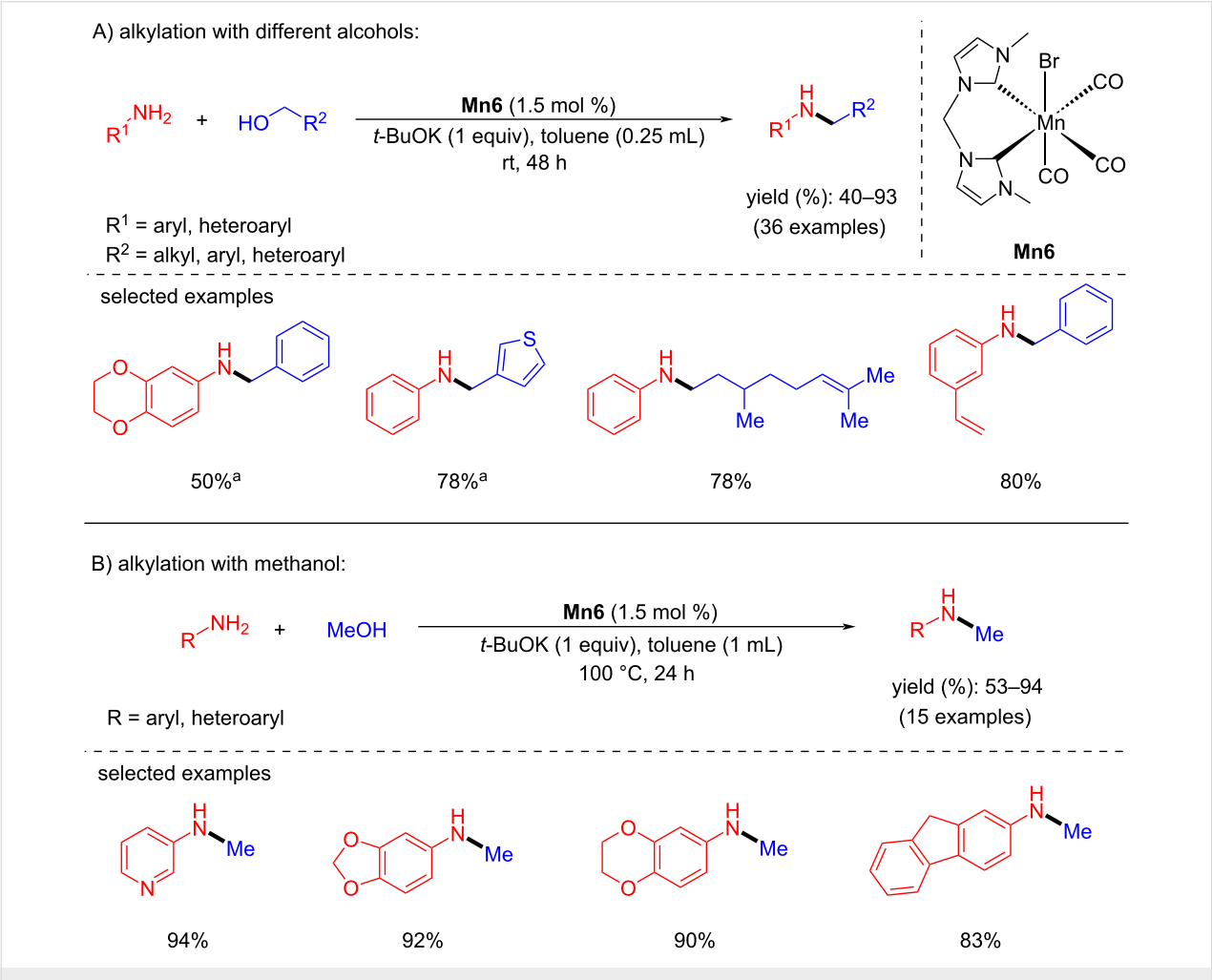

Scheme 11: Mn–NHC catalyst **Mn6** applied for the N-alkylation of amines with alcohols. [a]3 mol % of **Mn6** were used.

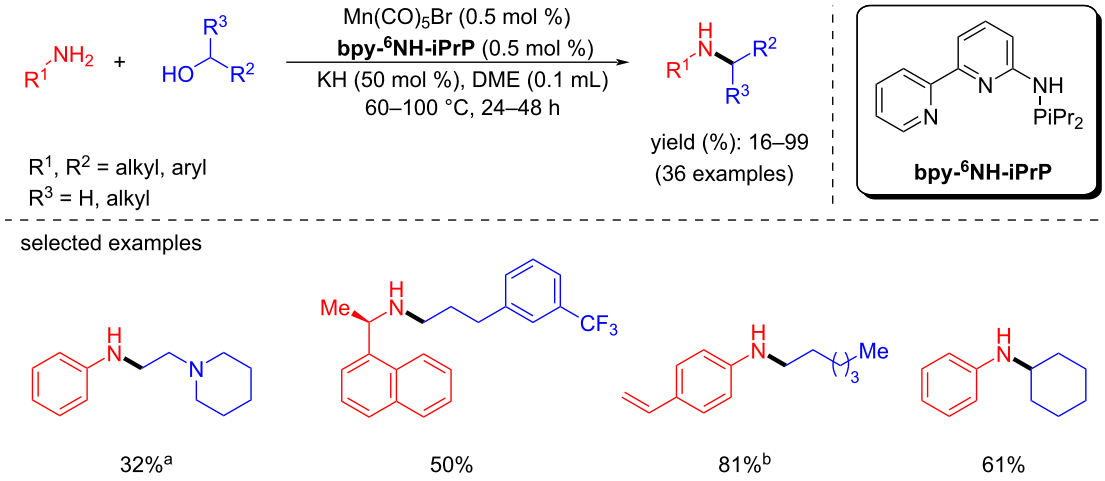

Scheme 12: N-Alkylation of amines with primary and secondary alcohols. [a]80 °C, [b]100 °C.

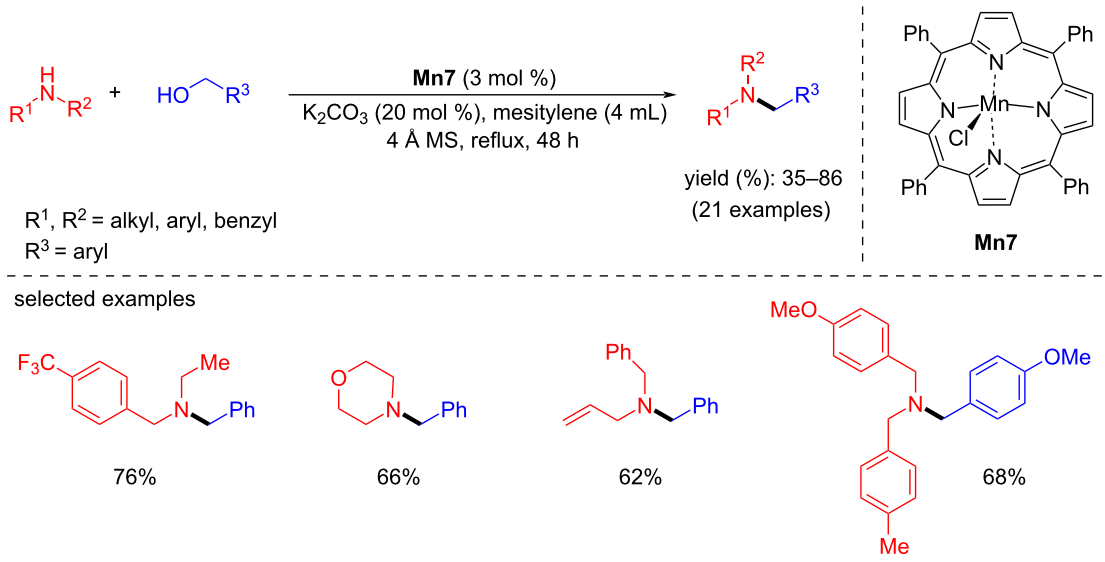

Scheme 13: Manganese(III)-porphyrin catalyst for synthesis of tertiary amines.

complex, **Mn7-b**. Then, the alcohol reacts with the hydride complex under release of hydrogen gas and regeneration of complex **Mn7-a** (Scheme 14).

In 2020, Morrill's group reported the one-pot synthesis of *N*-methylarylamines from nitroarenes using methanol as a methylating agent and reductant [44]. When substituted nitroarenes were methylated with methanol under optimal conditions (5 mol % **Mn3**, 2 equiv of KOH at 110 °C for 16 h), moderate to good yields of *N*-methylamines were produced (Scheme 15).

The mechanistic studies suggested that the base activates the complex **Mn3**. The active catalyst dehydrogenates methanol into formaldehyde and converts nitroarenes to anilines via transfer hydrogenation. The latter then undergo condensation with formaldehyde providing an *N*-phenylmethanimine intermediate which was confirmed by ^{1}H NMR spectroscopy. In the final step, the imine undergoes hydrogenation with **Mn3-b** to yield the N-methylated product (Scheme 16).

In 2020, Maji et al. synthesized manganese(I) complexes bearing bidentate amine-based ligands and studied them in the

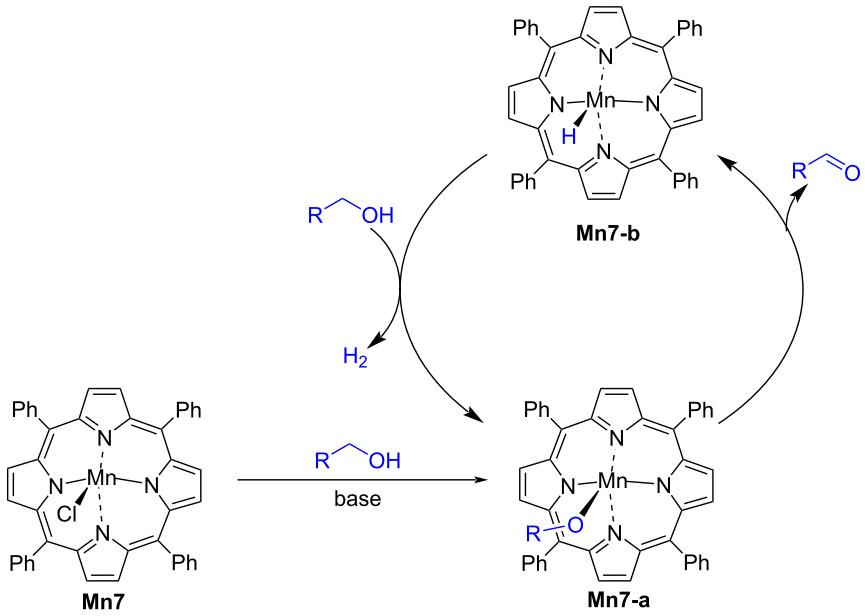

Scheme 14: Proposed mechanism for the alcohol dehydrogenation with Mn(III)-porphyrin complex **Mn7**.

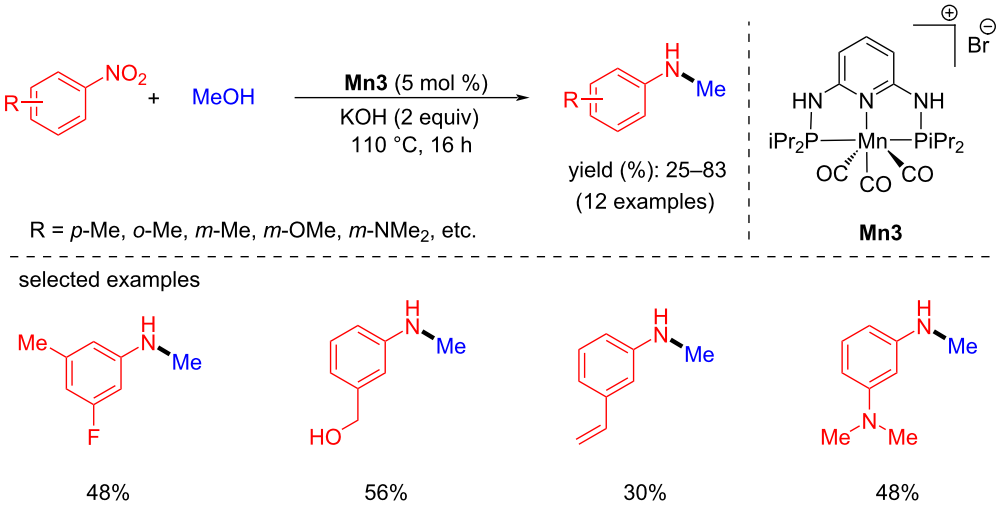

Scheme 15: N-Methylation of nitroarenes with methanol using catalyst **Mn3**.

N-alkylation of aromatic amines with benzylic alcohols (Scheme 17). Under the optimized reaction conditions (140 °C, 24 h), complex **Mn8** (2 mol %) was successfully applied for the coupling of various electron-donating and withdrawing primary amines and aromatic alcohols in the presence of *t*-BuOK (40 mol %) in toluene to give the corresponding secondary amines with up to 98% yield [45].

In 2021, Peng and co-workers demonstrated a practical and operationally simple approach for the N-alkylation of aromatic amines with alcohols using inexpensive and commercially available manganese salts such as $MnCl_2$ or $Mn(CO)_5Br$ and triphenylphosphine (PPh_3) as ligand [46]. Using this catalytic system (10 mol % Mn precursor, 20 mol % PPh_3, 1.2 equiv *t*-BuOK, 130 °C, 20 h), a variety of (hetero)aromatic and aliphatic amines were selectively alkylated in moderate-to-high yields with aliphatic and aromatic alcohols (Scheme 18). In addition, this protocol allowed for the synthesis of indole through an intramolecular reaction and a resveratrol-derived amine. However, this catalytic method did not tolerate some functional

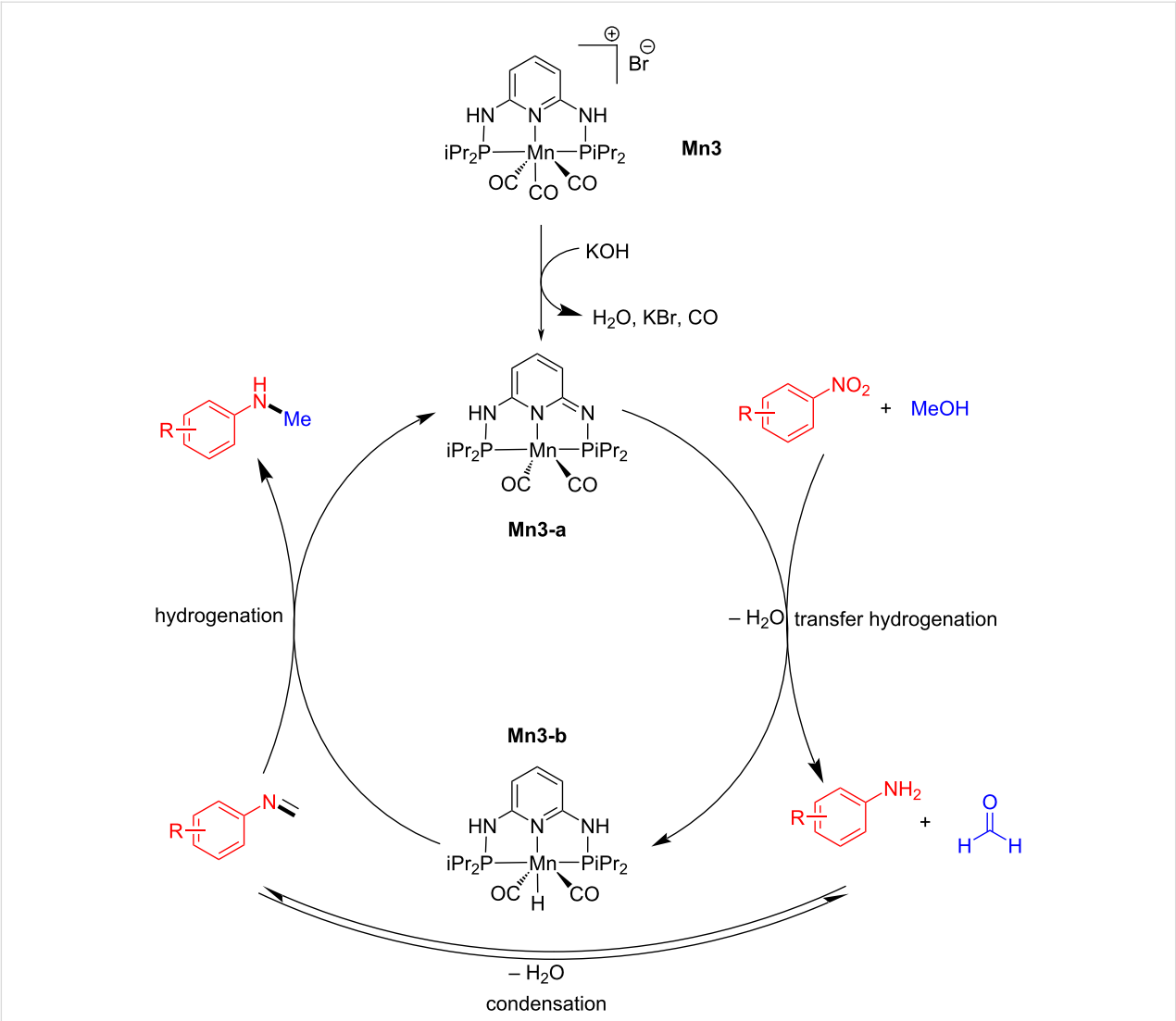

Scheme 16: Mechanism of manganese-catalyzed methylation of nitroarenes using **Mn3** as the catalyst.

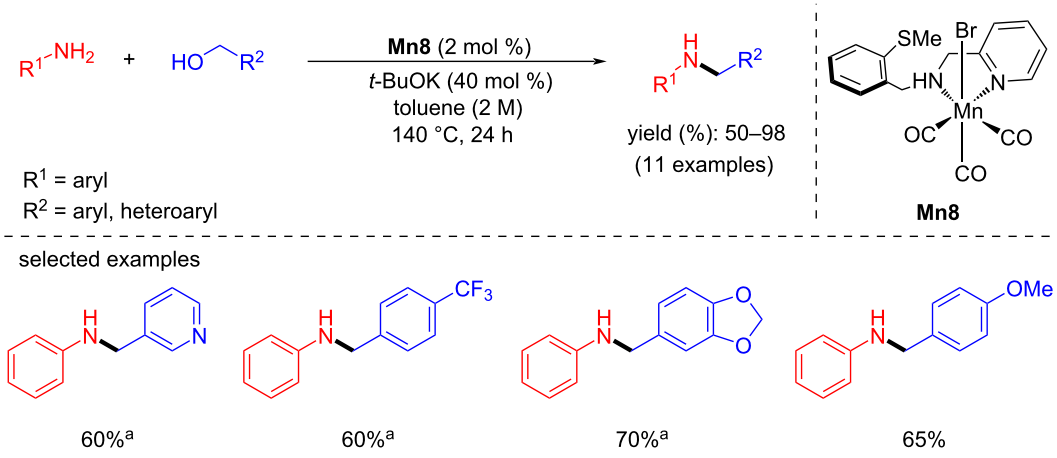

Scheme 17: Bidentate manganese complex **Mn8** applied for the N-alkylation of primary anilines with alcohols. [a]One equiv of *t*-BuOK was used.

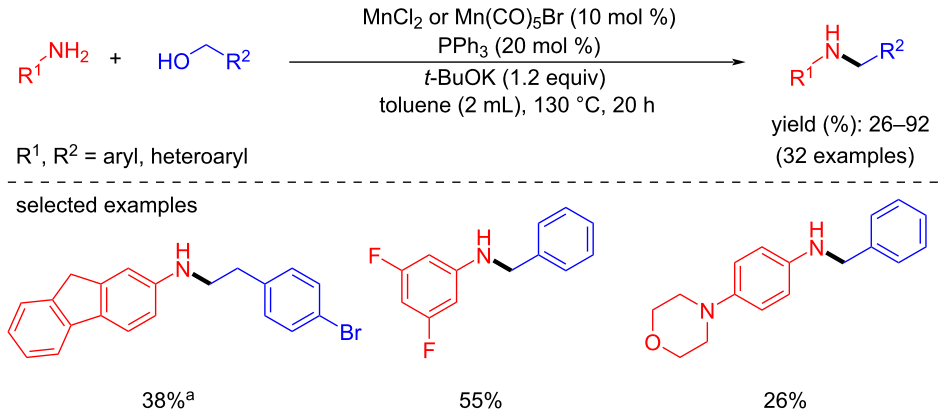

Scheme 18: N-Alkylation of amines with alcohols in the presence of manganese salts and triphenylphosphine as the catalytic system. [a]10 mol % $Mn(CO)_5Br$ was used.

groups such as nitro, ester, and hydroxy groups and it did not need a prior synthesis of molecularly defined manganese complexes.

Recently, Balaraman's group introduced a new method for N-alkylation with diazo compounds as an amine source and alcohols as alkylating agents via a tandem process using a manganese(I)-PNP pincer complex [47]. Symmetrical, unsymmetrical, and cyclic azoarenes were studied with benzyl alcohol using catalyst **Mn9** (5 mol %) and *t*-BuOK (2 equiv) at 130 °C for 24 h in octane, resulting in the corresponding N-alkylated amines with up to 96% yield (Scheme 19). On the other hand, various aromatic and aliphatic primary and secondary alcohols were studied with diazobenzene compounds under the same reaction conditions. Remarkably, the N-methylation was carried out with methanol and deuterated methanol and afforded N-methylated/deuterated products with good yields.

The proposed catalytic cycle showed the formation of the amido complex **Mn9-a** via the debromination of the pre-catalyst **Mn9** with the help of a strong base. Then, **Mn9-a** treated with an alcohol provided a manganese alkoxy complex **Mn9-b,** which then undergoes β-hydride elimination to give the manganese hydride complex **Mn9-c** and the corresponding aldehyde. Further, the azo compound coordinates with the hydride complex **Mn9-c** to give **Mn9-d,** from which the hydrazo compound is released with regeneration of the active amido species **Mn9-a**. Next, the semi-hydrogenated hydrazo compound further undergoes complete hydrogenation. It provides the amine compounds, which condense with aldehydes, leading to the corresponding imine intermediate, which again undergoes hydrogenation by **Mn9-c** and yield the N-alkylated product and the regeneration of complex **Mn9-a** (Scheme 20).

Very recently, Bühl and Kumar reported a novel and efficient methodology for the synthesis of branched polyethyleneimine derivatives by coupling ethylene glycol and ethylenediamine using manganese-pincer catalyst **Mn1** (1 mol %), *t*-BuOK (10 mol %) in toluene at 150 °C (Scheme 21) [48]. The mechanistic investigation based on the experimental and DFT calculations suggested a BH pathway. First, dehydrogenation of the ethylene glycol followed by condensation with ethylenediamine generated the corresponding imine intermediates. The subsequent hydrogenation with borrowed hydrogen finally formed the polyethyleneimine product.

In 2023, Royo and co-workers conveyed the N-alkylation of amines with alcohols using the bis-triazolylidene manganese complexes [49]. Complex **Mn10** showed superior activity with low catalyst loading (1.5 mol %) and base (50 mol % of *t*-BuOK) at 100 °C for 2 h to afford the N-alkylated products (Scheme 22). Under this protocol, several substituted amines were N-alkylated with various benzyl and aliphatic alcohols and afforded a good to excellent yield. Unfortunately, aliphatic amines such as isopropylamine and cyclohexylamine showed poor activity.

C–C Bond formation via borrowing hydrogen

Building C–C bonds by selective, efficient, and environmentally benign processes has been challenging and the most commonly used reaction in synthetic chemistry [50,51]. The selective α-functionalization of carbonyl compounds with organohalides in the presence of bases is one of the most fundamental reactions. This methodology usually suffers from the use of stoichiometric amounts of bases and the use of halides, which leads to the formation of a considerable amount of waste [52-54]. The BH approach allows a sustainable way for build-

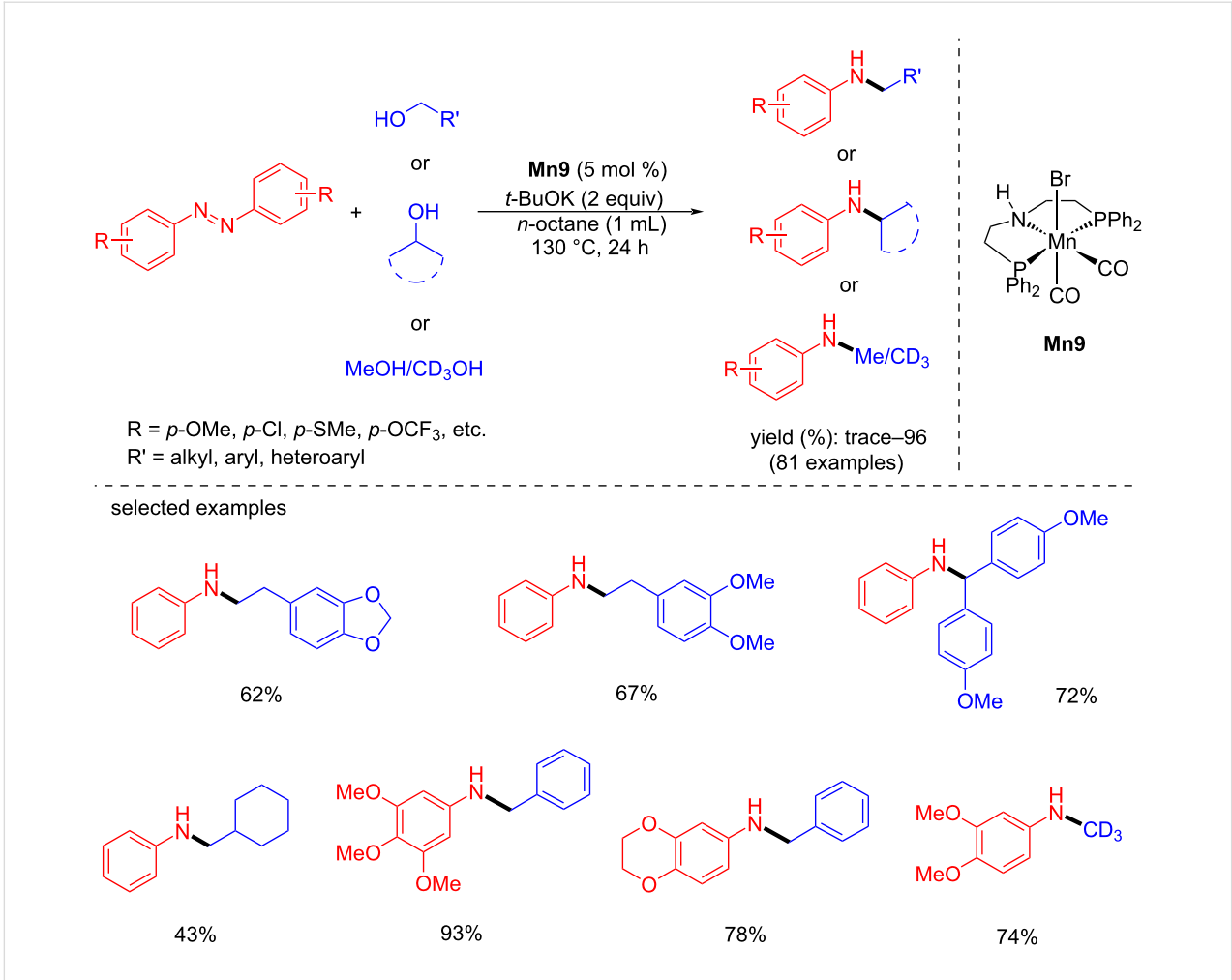

Scheme 19: N-Alkylation of diazo compounds with alcohols using catalyst **Mn9**.

ing C–C bonds by coupling abundant and cheap alcohols with ketones, nitriles, esters, and amides [4].

C–C Bond formation via alkylation of ketones with alcohols

Several homogeneous catalysts, including noble and non-noble metals, have been studied for the alkylation of ketones with primary and secondary alcohols [55,56]. In this section, we discuss the development of manganese complexes (Figure 2) for coupling primary and secondary alcohols with ketones to give the corresponding alkylated ketones or alcohols.

As depicted in the general Scheme 23, in the first step, the manganese-catalyzed dehydrogenation of alcohols delivers carbonyl compounds, which condense with other carbonyl compounds in the presence of a base to afford unsaturated intermediate compounds. In the final step, reduction of unsaturated compounds with manganese hydride complexes giving the desired C-alkylated products.

In 2016, Beller and co-workers introduced the first air-stable manganese(I)-PNP-pincer pre-catalyst for the α-alkylation of ketones with primary alcohols [57]. The reaction conditions were investigated using four different well-defined phosphine substituents-containing Mn complexes with acetophenone and benzyl alcohol as model substrates. Among these, complex **Mn1** showed better results with 2 mol % loading and at low base concentration (Cs_2CO_3; 5 mol %) in *tert*-amyl alcohol at 140 °C for 22 h, giving 88% yield of the desired alkylated product. Several ketones were studied under the same conditions, with substituted benzyl and aliphatic alcohols giving up to 92% yield of the corresponding C-alkylated products (Scheme 24).

The proposed mechanism showed that the pre-catalyst **Mn1** was first activated by the base, affording the active amido complex **Mn1-a** which reacts with the alcohol to form the alkoxo-type complex **Mn1-b**. An intramolecular ligand-assisted mechanism produced the aldehyde and manganese hydride complex **Mn1-c** after protonation of the intermediate. The aldehyde then under-

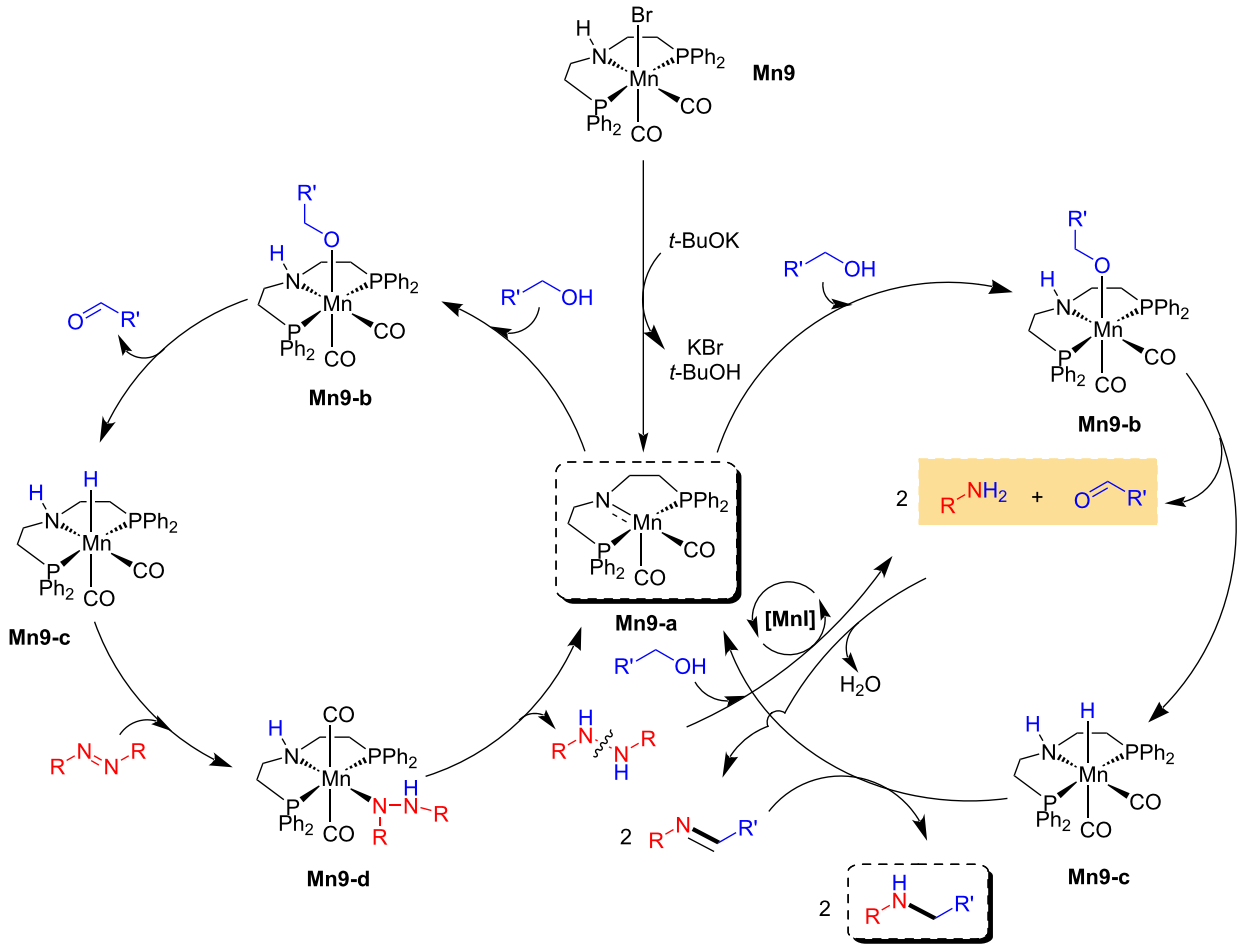

Scheme 20: Proposed mechanism for the amination of alcohols with diazo compounds catalyzed by catalyst **Mn9**.

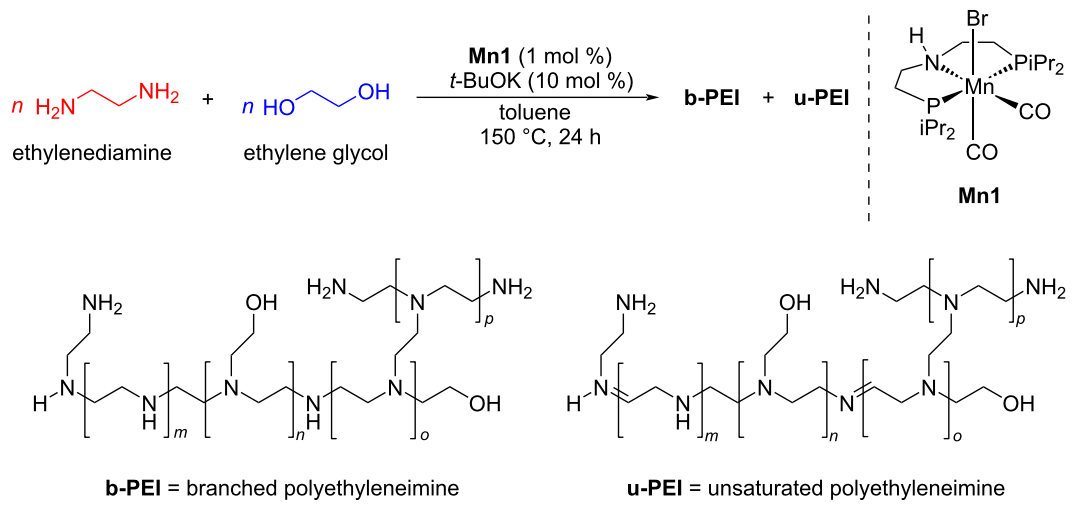

Scheme 21: Mn1 complex-catalyzed synthesis of polyethyleneimine from ethylene glycol and ethylenediamine.

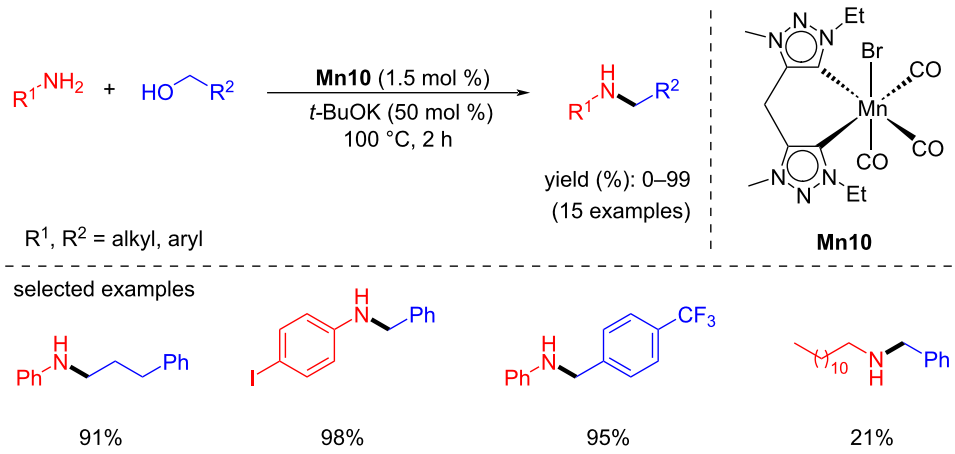

Scheme 22: Bis-triazolylidene-manganese complex **Mn10** for the N-alkylation of amines with alcohols.

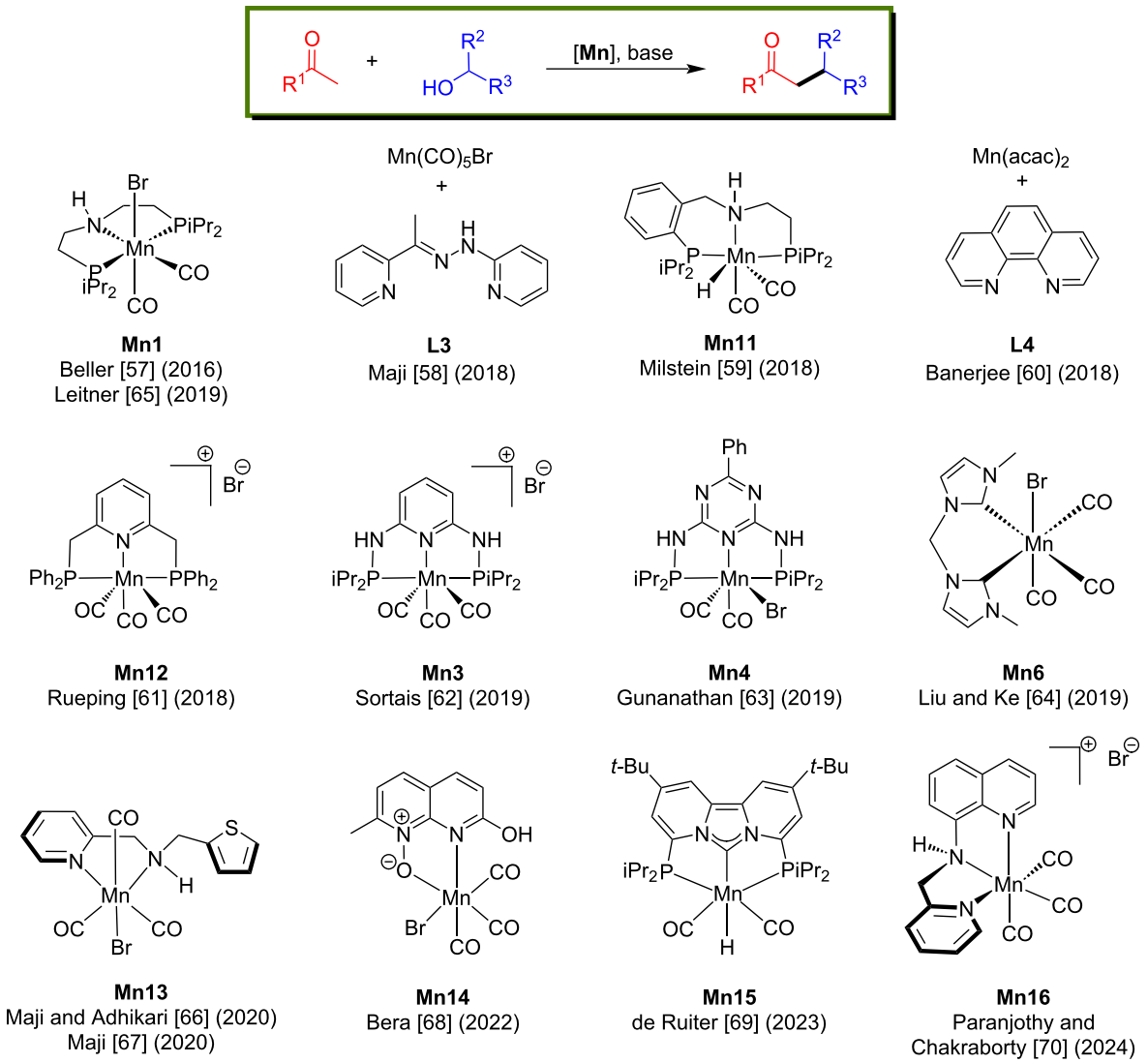

Figure 2: Manganese complexes applied for C-alkylation reactions of ketones with alcohols.

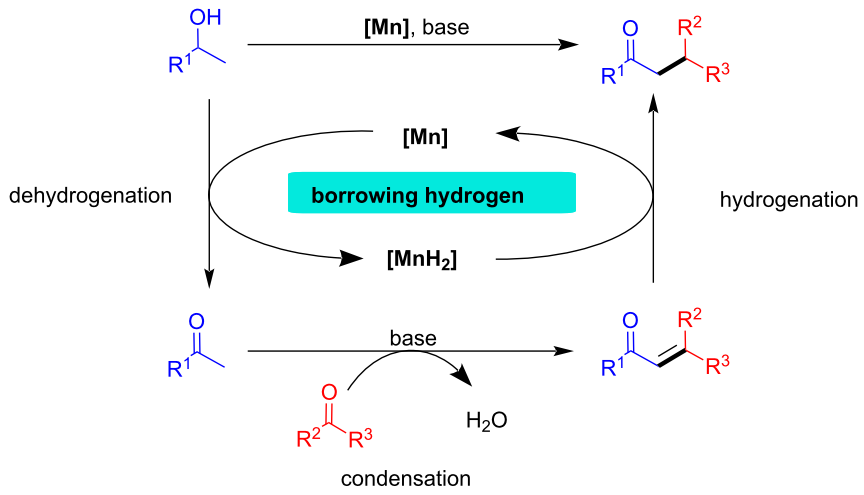

Scheme 23: General scheme for the C–C bond formation with alcohols and ketones.

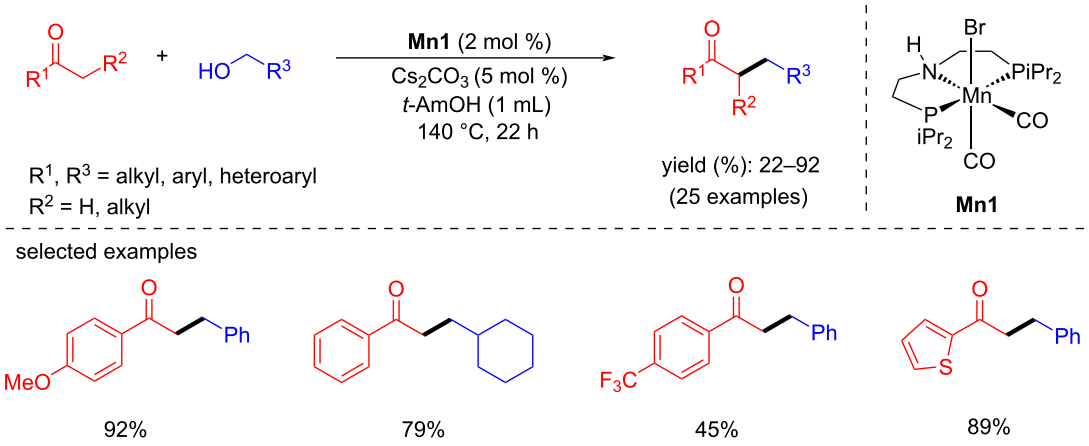

Scheme 24: Mn1 complex-catalyzed α-alkylation of ketones with primary alcohols.

went aldol condensation with ketones, yielding an α,β-unsaturated compound, which was hydrogenated by the manganese hydride species, resulting in the final alkylated product (Scheme 25). A set of deuterium labelling tests and additional control studies determined that the alcohol dehydrogenation was aided by an intramolecular manganese amidate rather than the traditional β-hydride elimination process.

In 2018, Maji's group reported the α-alkylation of ketones with primary alcohols using a phosphine-free manganese catalyst generated in situ from $Mn(CO)_5Br$ and **L3** [58]. Under optimized conditions (2 mol % $Mn(CO)_5Br$, 10 mol % *t*-BuOK, *t*-AmOH, argon atmosphere), various substituted ketones were selectively alkylated with benzyl alcohols as alkyl source and hydrogen donor at 140 °C for 24 h and afforded up to 98% yield of the C-alkylated products (Scheme 26). In addition, numerous substituted benzylic, aliphatic, and heterocyclic alcohols were tested and showed good functional group tolerances. However, ester and nitrile-substituted ketones were not alkylated with this protocol.

The proposed mechanism showed that the $Mn(CO)_5Br$ reacted with ligand **L3** to generate the active complex **Mn-L3-I** in the presence of a base. The formed active catalyst dehydrogenates the alcohol to generate the alkoxy complex **Mn-L3-II**. The liberated aldehyde undergoes aldol condensation with the ketone to afford the α,β-unsaturated ketone, followed by the selective hydrogenation with **Mn-L3-III** to give the desired alkylated product (Scheme 27).

In the same year, Milstein and co-workers accomplished the α-alkylation of esters, ketones, and amides using alcohols as

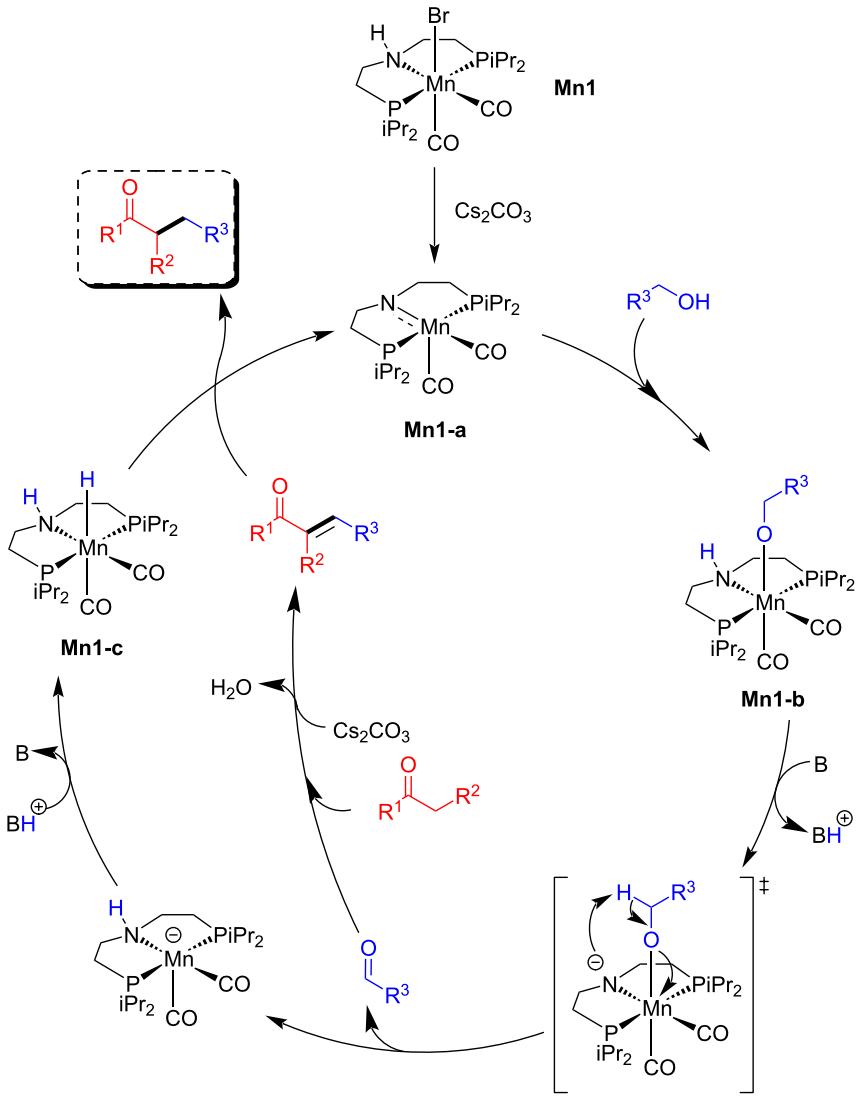

Scheme 25: Mechanism for the **Mn1**-catalyzed alkylation of ketones with alcohols.

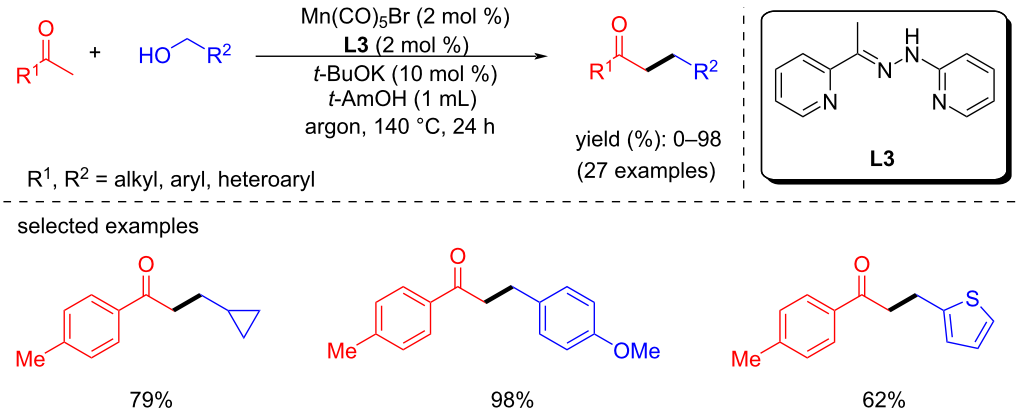

Scheme 26: Phosphine-free in situ-generated manganese catalyst for the α-alkylation of ketones with primary alcohols.

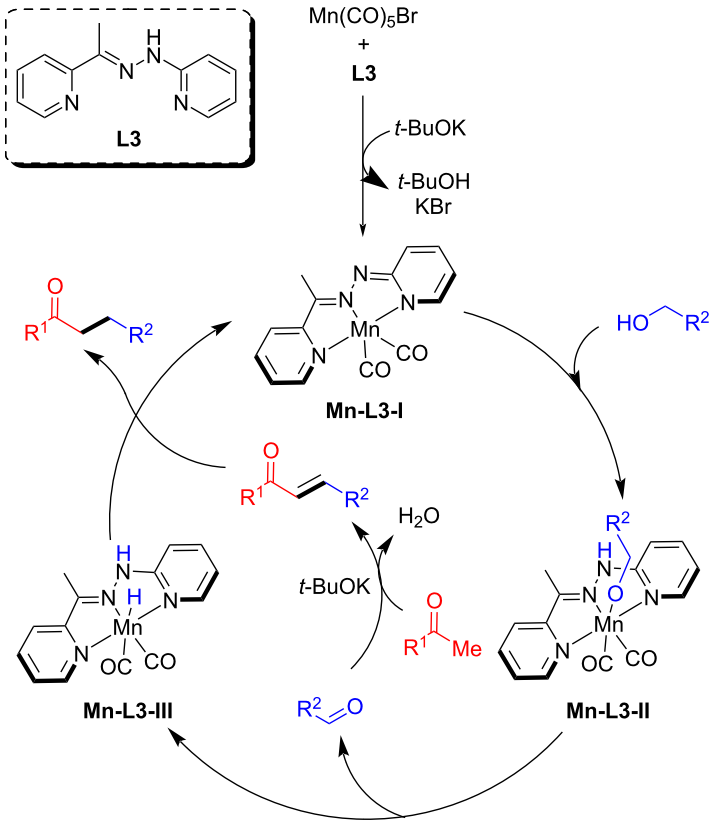

Scheme 27: Plausible mechanism for the Mn-catalyzed α-alkylation of ketones with alcohols.

alkylating agents with a PNP-pincer-supported manganese catalyst [59]. First, the α-alkylation of ketones with benzylic and aliphatic alcohols was studied using **Mn11** (1 mol %) as catalyst and *t*-BuOK as a base at 125 °C for 18 h in toluene which afforded up to 95% yield of the desired alkylated ketones (Scheme 28A). Later, the more challenging esters and amides were selectively alkylated with alcohols, however, required higher catalyst loading (5 mol %) and a stoichiometric amount of *t*-BuOK (1.5 equiv) at 125 °C for 18 h (Scheme 28B). The proposed mechanism suggested the formation of α,β-unsaturated ketones as the intermediates, similar to the previous report [58] and the selective hydrogenation of the C=C bond was the last step.

In 2018, Banerjee's group developed the alkylation of methylene ketones with primary alcohols using a phosphine-free and commercially available $Mn(acac)_2$/1,10-phenanthroline system [60]. Various methylene ketones and alcohols were investigated with $Mn(acac)_2$ (2.5 mol %) as a precursor, 1,10-phenanthroline (3 mol %) as ligand, and *t*-BuOK (1 equiv) as a base in toluene at 140 °C for 36 h that gave up to 84% yield (Scheme 29A). More interestingly, double alkylation also occurred in one pot using acetophenone and 4-methoxyacetophenone with different benzyl alcohols under the optimized conditions. In the first step, monoalkylation of the methyl ketone led to the linear α-alkylated product, followed by the alkylation of the methylene ketone with the second benzyl alcohol then afforded the dialkylated product. Remarkably, the drug donepezil, a steroid derivative and a fatty acid derivative were synthesized using this procedure (Scheme 29B).

In 2018, Rueping and co-workers reported a manganese-catalyzed α-methylation of ketones with methanol and deuterated methanol. Many ketones were investigated with methanol under the optimized conditions (2.5 mol % of **Mn12**, 2 equiv of Cs_2CO_3, 85 °C for 24 h) providing yields up to 94% [61]. Interestingly, trideuteromethylation of ketones were studied with 5 mol % of **Mn12** and 4 equiv of Cs_2CO_3 at 105 °C for 24 h giving up to 89% yield. More interestingly, the double trideuteromethylation of ketones was also reported (Scheme 30).

In 2019, Sortais reported the α-methylation of several ketones with methanol as a C1 source. Under the optimized reaction

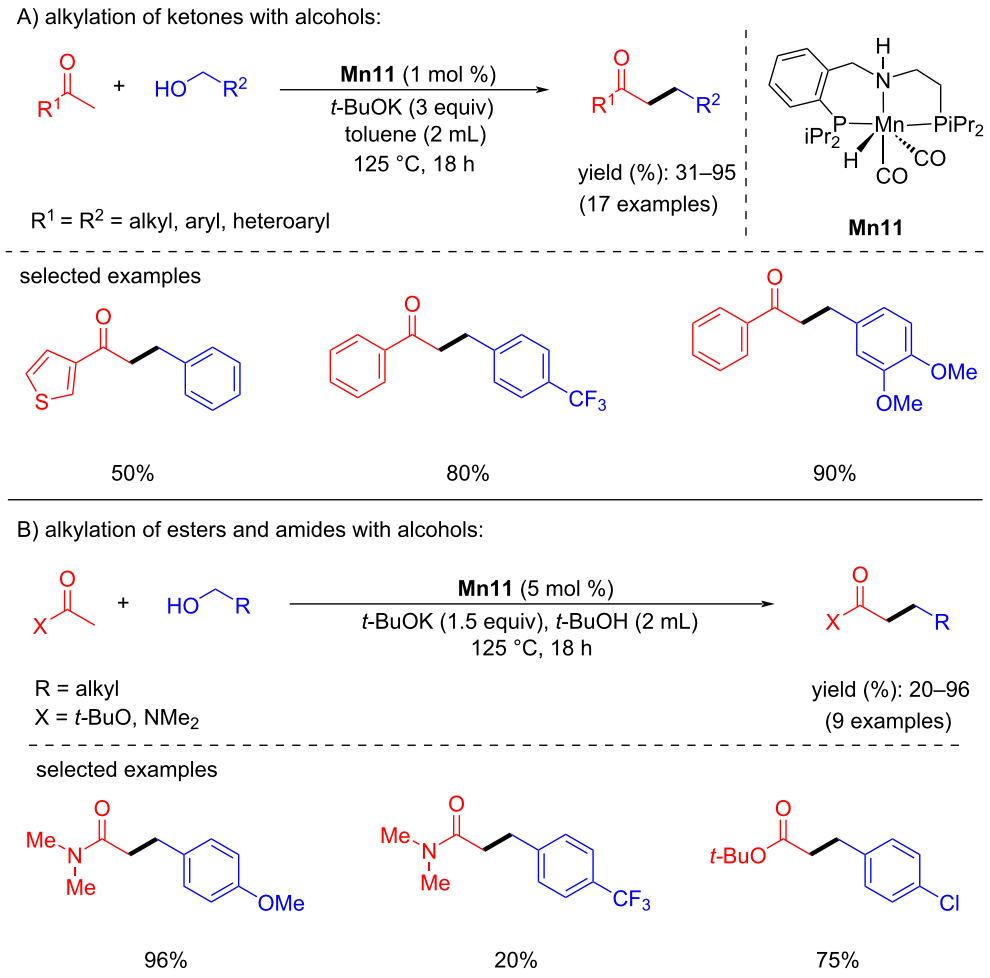

Scheme 28: α-Alkylation of esters, ketones, and amides using alcohols catalyzed by **Mn11**.

conditions, they achieved good yields (23–93%) of the desired methylated products that could be obtained with 3 mol % catalyst loading and 50 mol % *t*-BuONa in a closed pressure tube at 120 °C for 20 h [62]. In addition, the α-methylation of esters was studied under the optimized conditions with 100 mol % of the base, however, only a poor yield was obtained (Scheme 31).

Later, Gunanathan and co-workers reported an efficient method for the chemoselective alkylation of ketones and secondary alcohols with primary alcohols using a Mn(I)-PNP pincer complex [63]. The reaction of different ketones with several alcohols (aliphatic and benzylic) was carried out at 140 °C for 24 h in the presence of 2 mol % **Mn4** and 10 mol % of Cs_2CO_3 and provided up to 97% of the desired alkylated products. Notably, the alkylation of ketones using ethanol as a coupling partner was also established. Furthermore, β-alkylation of 1-phenyl-1-ethanol with benzylic alcohols was also studied with 2 mol % of the **Mn4** pre-catalyst, 5 mol % of Cs_2CO_3 in *t*-AmOH at 135 °C for 20 h (Scheme 32). NMR studies endorsed the formation of intermediates such as aldehyde, ketone, and α,β-unsaturated ketone. The proposed mechanism suggested that dearomatization–aromatization pathways operated for the dehydrogenation of the alcohol and C–C bond formations.

After the successful attempt of bidentate N-heterocyclic carbene-manganese complex-catalyzed N-alkylation of amines with alcohols at room temperature [41], Liu and Ke's group planned the α-alkylation of ketones using alcohols as an alkylating agent [64]. A number of substituted aromatic and heterocyclic ketones with different alcohols were tested and gave good to excellent yields (38–96%) using 4 mol % of **Mn6** and 50 mol % of NaOH in toluene at 110 °C for 2 h (Scheme 33). The reaction proceeded via the dehydrogenation of the alcohol, aldol condensation, and hydrogenation of α,β-unsaturated ketones.

In 2019, Leitner and his group introduced an outstanding cascade BH approach for the synthesis of various substituted

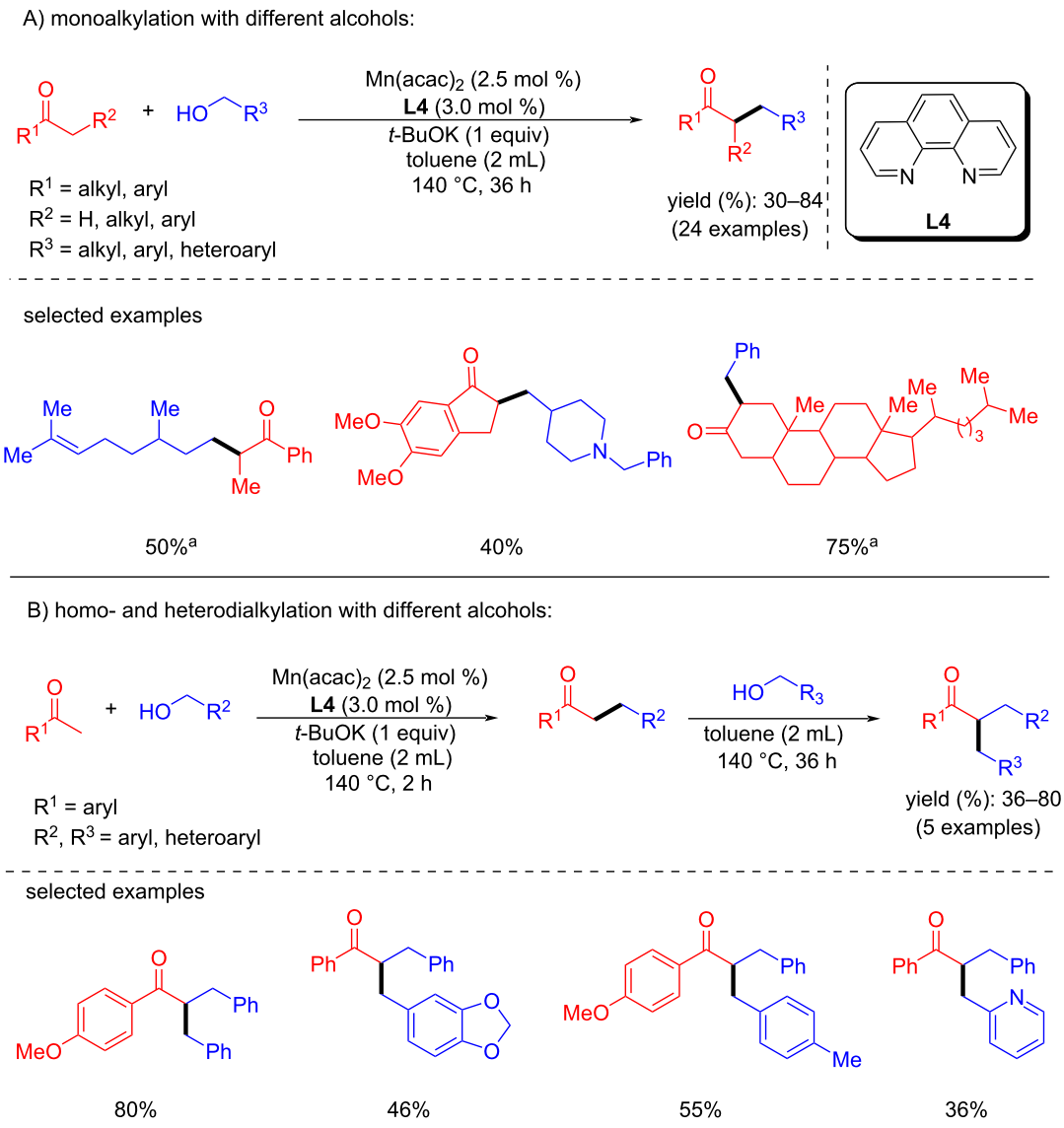

Scheme 29: Mono- and dialkylation of methylene ketones with primary alcohols using the $Mn(acac)_2$/1,10-phenanthroline system. [a]24 h reaction time.

cycloalkanes by coupling diols and secondary alcohols or ketones [65]. Various substituted secondary alcohols were treated with 1,5-pentanediol in the presence of 2 mol % of **Mn1** and 4 equiv of *t*-BuOK as base in toluene at 150 °C for 32 h to afford the desired products with moderate to good yields (40–83%). In addition, five to seven-membered rings were constructed by treating aromatic ketones with substituted diols. However, a stoichiometric amount of the base (4 equiv), excess of diols (4 equiv), and long reaction time (32 h) were required to deliver the desired products (Scheme 34).

The proposed mechanism demonstrated that the active amido complex **Mn1-a** dehydrogenated secondary alcohols into ketone **B** and diol into aldehyde **A**. Further, aldol condensation occurred between the ketone and aldehyde and produced α,β-unsaturated ketone **C**, which was subsequently hydrogenated by complex **Mn1-c**, followed by allyl isomerization, which led to the formation of hydroxy ketone compound **E**. Cyclization occurred via dehydrogenation and intramolecular aldol condensation and in the last step hydrogen transfer provided the desired cyclic product **H** (Scheme 35).

In 2020, Maji and Adhikari reported a phosphine-free *N*,*N*-amine–manganese complex-catalyzed stereoselective intermolecular and intramolecular BH reaction for the formation of cycloalkanes from ketones and 1,*n*-diols [66]. Different substi-

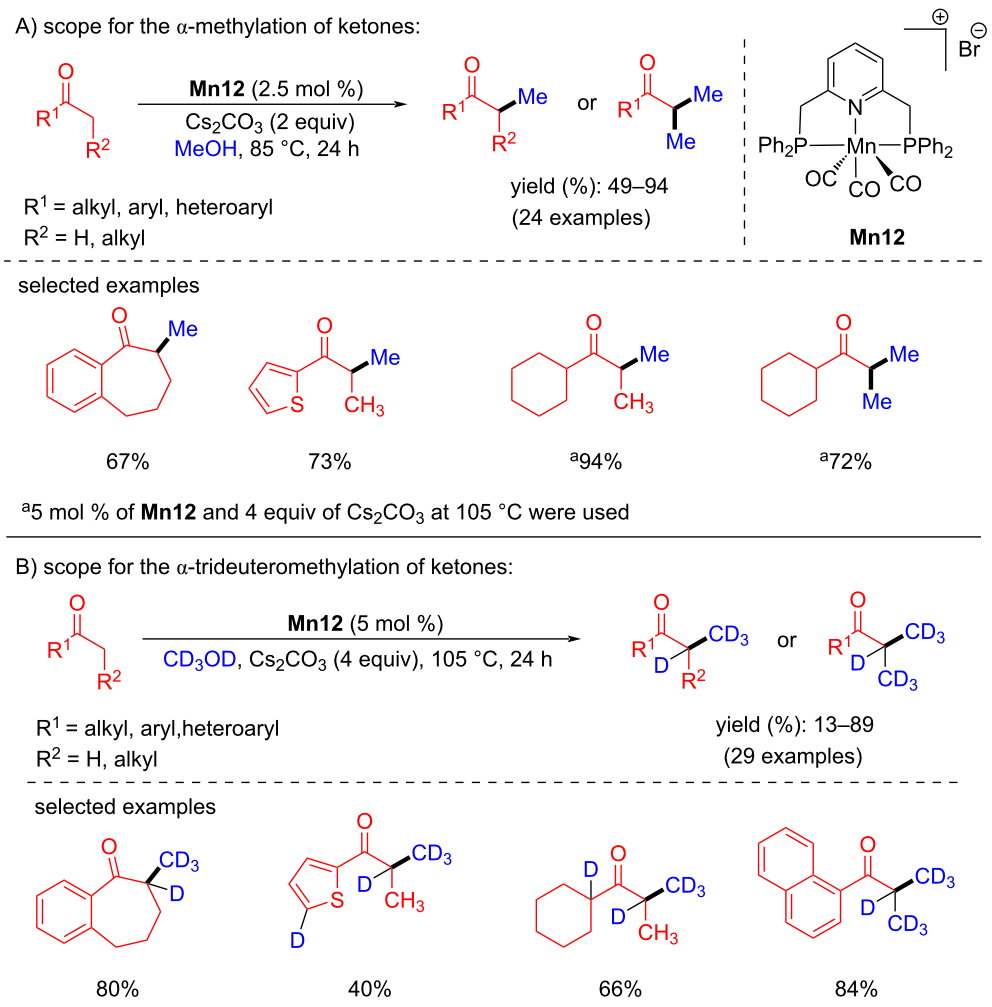

Scheme 30: Methylation of ketones with methanol and deuterated methanol.

tuted 1,5-diols were coupled with 1-(2,3,4,5,6-pentamethylphenyl)ethan-1-one using 4 mol % of catalyst **Mn13** and 2 equiv of *t*-BuOK as base in *t*-AmOH at 140 °C for 36 h to give 51–98% yield of the six-membered ring products. They isolated cyclic five to seven-membered ring products by changing the lengths of the diols. For example, for the formation of cyclopentane products, butane-1,4-diol was used as the alcohol under the same reaction conditions, giving 31 to 70% yield of the desired products. Seven-membered rings were also formed only by changing the alcohols to hexane-1,6-diol under the same conditions as above, giving yields up to 80%. In addition, several ketones were investigated under these conditions with different diol systems, giving 55–80% yields of the cyclic products (Scheme 36). DFT studies showed that the hemilability and bifunctionality of the thiophene arm attached to the metal play an important role in this transformation for the dehydrogenation and hydrogenation steps.

Later, the same complex was successfully used for the α-alkylation of ketones with secondary alcohols to synthesize β-branched carbonyl compounds [67]. The reaction conditions were optimized by treating the 2,3,4,5,6-pentamethylacetophenone with cyclohexanol by different manganese complexes. Among all the complexes, 2 mol % of **Mn13** and one equiv of *t*-BuOK as base in toluene at 140 °C for 24 h under an argon atmosphere afforded 85% yield of the desired alkylated product. Pentamethylacetophenone was alkylated with several secondary alcohols, giving yields between 30 and 93%, which included aliphatic and heteroaryl secondary alcohols (Scheme 37).

In 2022, Bera's group reported the α-alkylation of ketones with alcohols as an alkylating agent using the protic functionality on a naphthyridine-*N*-oxide manganese complex [68]. The reaction conditions were optimized using acetophenone and benzyl

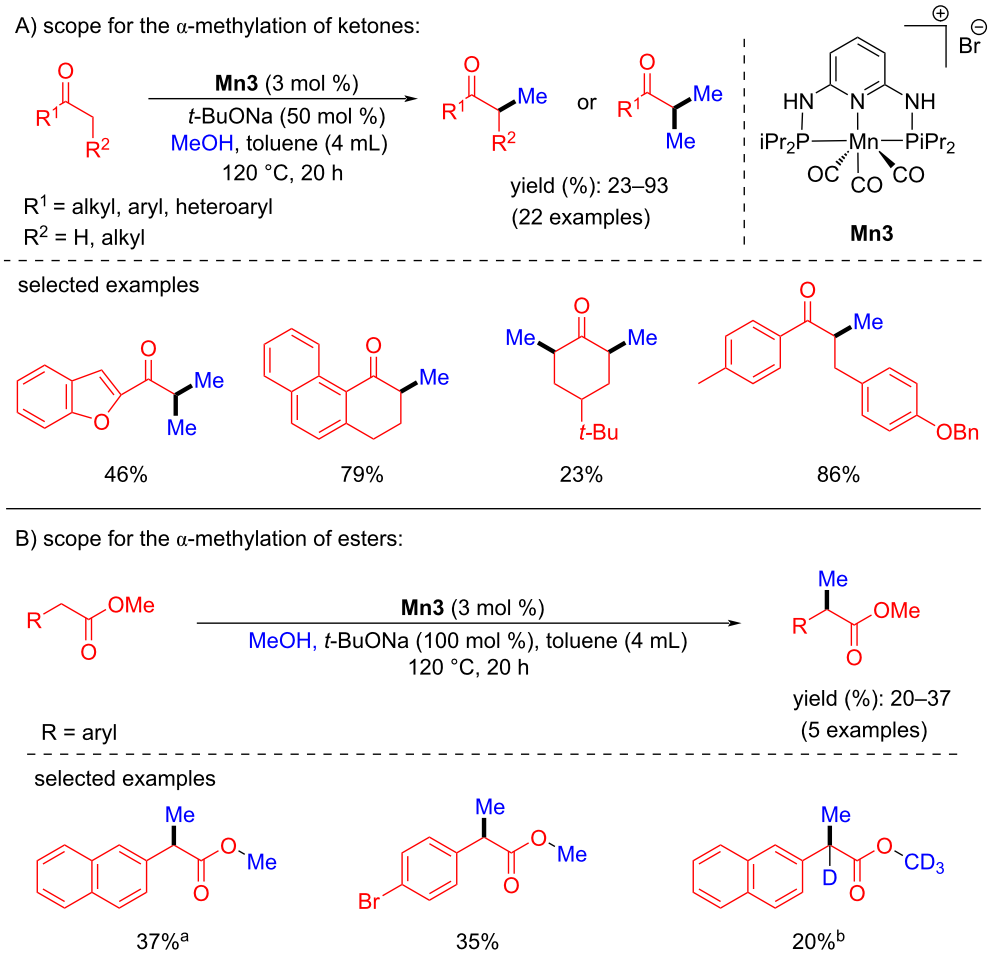

Scheme 31: Methylation of ketones and esters with methanol. [a]50 mol % of *t*-BuOK were used, [b]CD_3OD was used instead of CH_3OH, 48 h.

alcohol as model substrates. After optimizing various reaction parameters, 2 mol % of **Mn14** and 20 mol % of KOH in toluene afforded the α-alkylated product with 96% yield. Under the optimized catalytic conditions, various substituted alcohols were investigated with acetophenone, which gave good to excellent yields of the alkylated products (Scheme 38). The scope of ketones was also tested with benzyl alcohols, which gave yields up to 85%. The proposed mechanism suggested the formation of the dehydrogenation product and the desired product due to the metal–ligand cooperation (Scheme 39).

de Ruiter and co-workers studied PCNHCP-based manganese complexes for the α-methylation of ketones and indoles with methanol as a C1 source in 2023 [69]. The reaction conditions were optimized using three different Mn catalysts and bases. Among them, complex **Mn15** gave the better yield with 1 mol % of **Mn15**, Cs_2CO_3 (1 equiv) as a base in methanol at 110 °C for 24 h under N_2 atmosphere, giving 99% of the methylated product. The same conditions were followed for the methylation of several ketones with methanol, which gave yields of up to 99% (Scheme 40).

Very recently, a quinoline-based manganese catalyst was studied by Chakraborty and co-workers for the alkylation of methyl aryl ketones with alcohols (Scheme 41) [70]. Several methyl ketones and alcohols were studied using 2.5 mol % of **Mn16** and 30 mol % of NaOH in toluene and yields up to 90% were achieved at high temperature (150 °C) and long reaction time (48 h).

C–C Bond formation through coupling of various alcohols

Cross-coupling of two different alcohols to build C–C bonds is challenging because of the formation of undesired side products from aldol condensation. Herein, we summarized the reported manganese complexes applied for the coupling of secondary and primary alcohols to form a C–C bond (Figure 3).

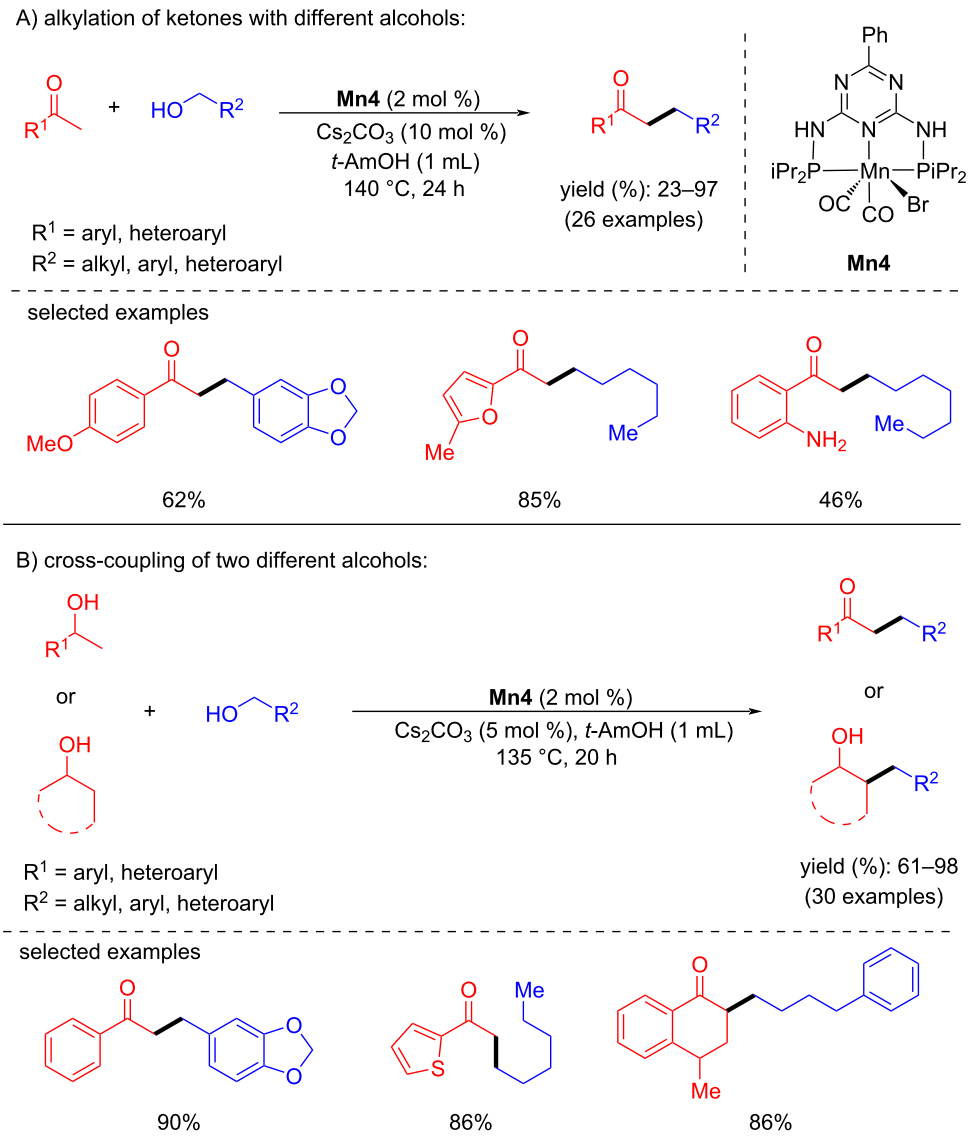

Scheme 32: Alkylation of ketones and secondary alcohols with primary alcohols using **Mn4**.

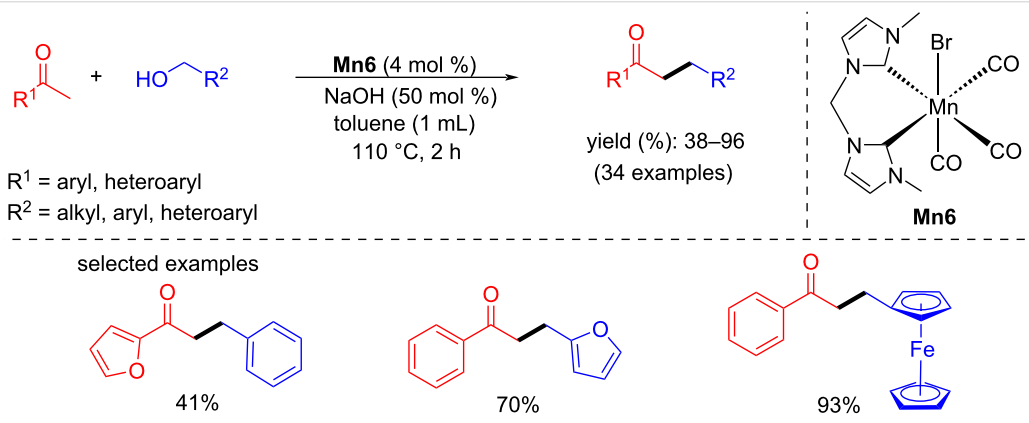

Scheme 33: Bidentate manganese-NHC complex **Mn6** applied for the synthesis of alkylated ketones using alcohols.

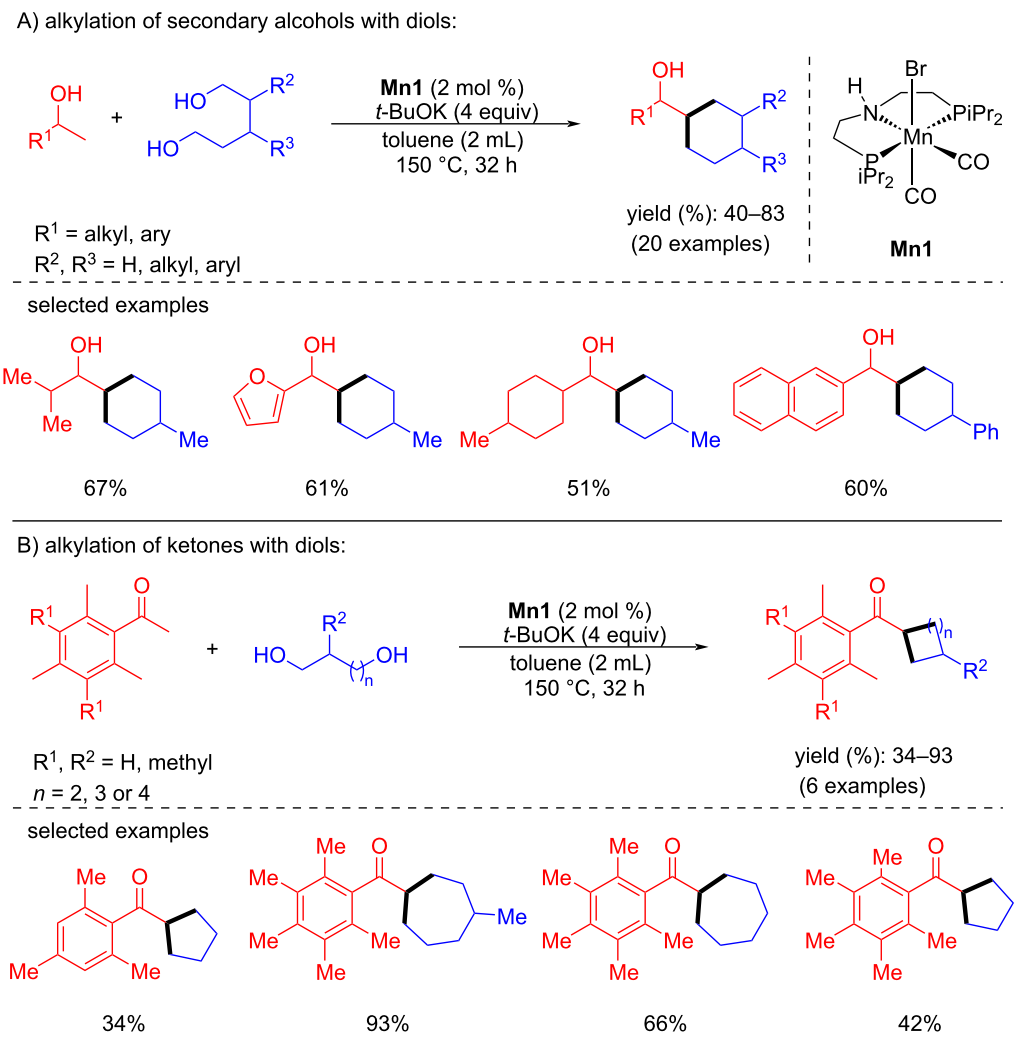

Scheme 34: Mn1-catalyzed synthesis of substituted cycloalkanes by coupling diols and secondary alcohols or ketones.

In 2018, Yu's group introduced phosphine-free manganese(I) catalytic systems for the direct β-alkylation of secondary alcohols with primary alcohols [71]. The reaction conditions were investigated for the alkylation of 1-phenylethanol with benzyl alcohol using manganese complexes containing pyridyl-supported pyrazolyl-imidazolyl ligands and bases. Among these complexes, **Mn17** gave an isolated yield of 90% with 2.1 mol % of **Mn17** and 30 mol % of *t*-BuOK in toluene at 110 °C for 24 h. Various benzylic, heteroaromatic, and aliphatic alcohols were reacted with 1-phenylethanol, giving the products with up to 90% yield. Similarly, variation of the secondary alcohols in the reaction with benzyl alcohol gave good to excellent product yields of 54–93%. Interestingly, dialkylated products were achieved when cyclopentanol was treated with benzylic alcohols at 140 °C for 48 h. In addition, 5α-cholestan-3β-ol was also selectively monoalkylated with benzylic alcohols (Scheme 42).

In 2019, El-Sepelgy and Rueping's team reported that a stable PNN-manganese-pincer complex catalyzed the C-alkylation of secondary alcohols with primary alcohols [72]. Four different manganese catalysts were investigated for the alkylation of 1-phenylethanol with benzyl alcohol. Among these, **Mn18** showed excellent activity with low catalyst loading (1 mol %), *t*-BuOK (25 mol %) as base, and toluene as solvent at 135 °C for 20 h under argon conditions, giving a yield of 82% (Scheme 43). Substituted aromatic and aliphatic secondary alcohols with benzyl alcohol gave 40 to 82% yields, and 1-phenylethanol with substituted primary alcohols gave moderate to good yields (50–82%). Deuterium-labelling experiments with deuterated 1-phenylethanol-α-d_1 and benzyl alcohol-α,α-d_2 suggested a hydrogen auto-transfer and dehydrogenation process. The amido species **Mn18-a** generated from **Mn18** by the base is responsible for the dehydrogenation of alcohol-yielding **Mn18-b** species. Mn–H complex reduced the C=C and

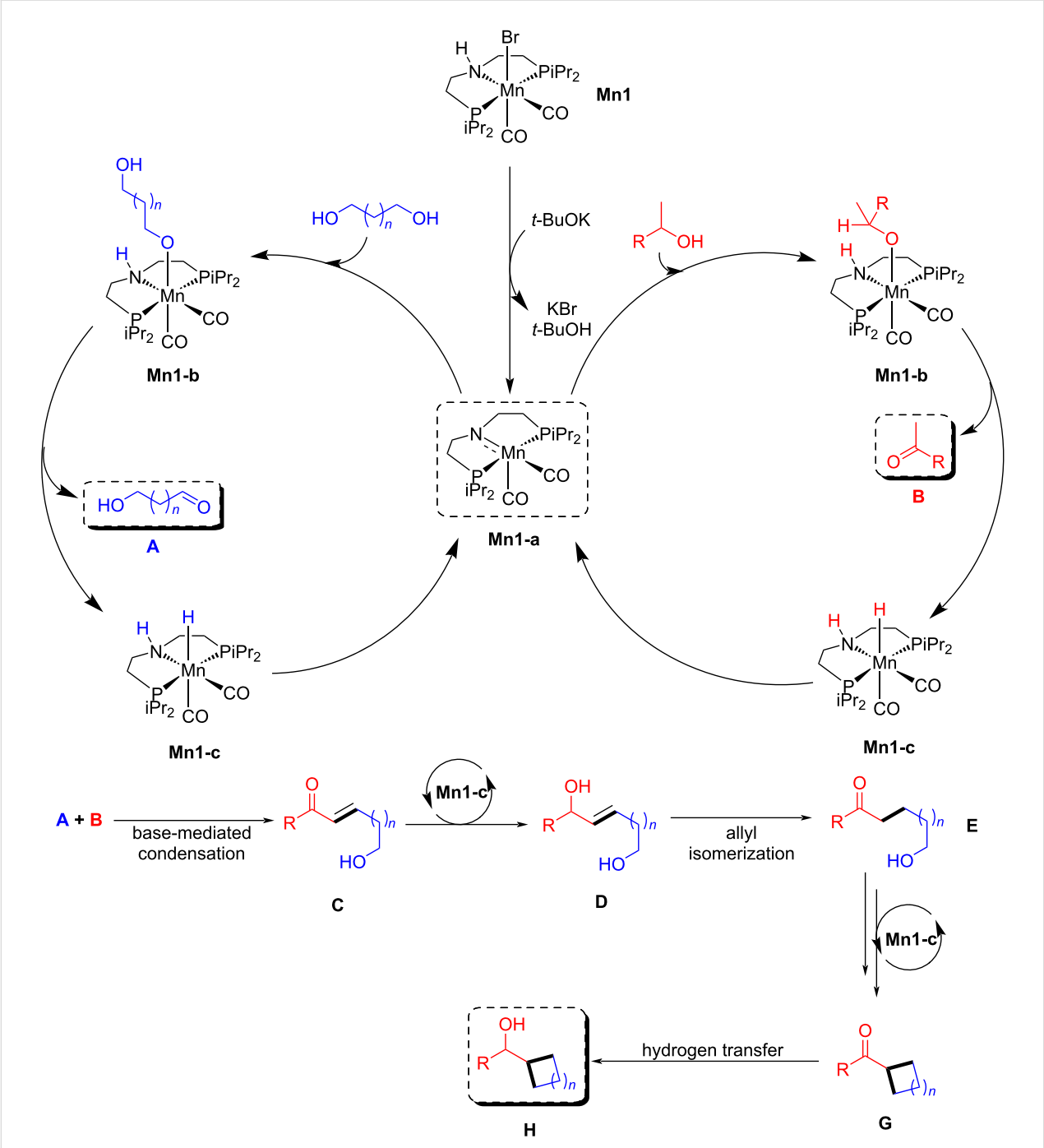

Scheme 35: Proposed mechanism for the synthesis of cycloalkanes via BH method.

C=O bonds, yielding the fully reduced saturated alcohol products (Scheme 44).

In 2019, the upgrading of bio-derived ethanol with widely available methanol for the production of isobutanol was developed by Liu and co-workers using Mn-pincer (PNP) complex **Mn1** at various concentrations. An extraordinary TON (9233) could be achieved at low catalyst loading using 3.5 equiv NaOMe at 200 °C for 48 h with 91% selectivity and 29% yield (Scheme 45) [73].

In 2020, Kempe's group reported an elegant example for the β-methylation of alcohols by methanol as a methylating agent using a manganese PN^5P pincer complex [74]. First, the double

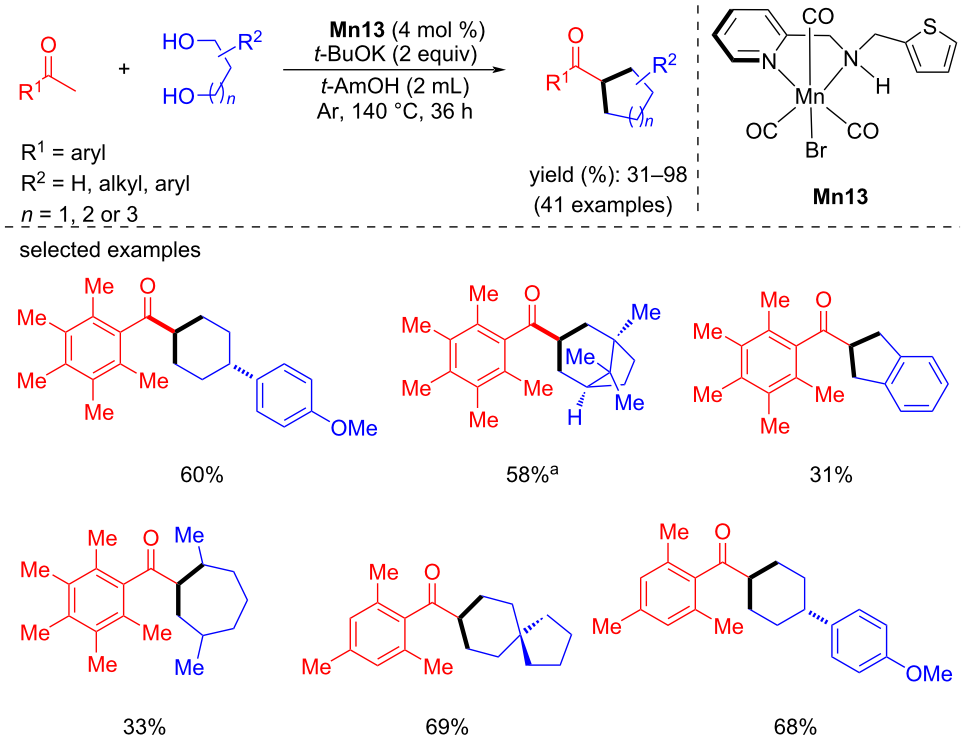

Scheme 36: Synthesis of various cycloalkanes from methyl ketones and diols catalyze by **Mn13**. [a]Reaction time was 6 h.

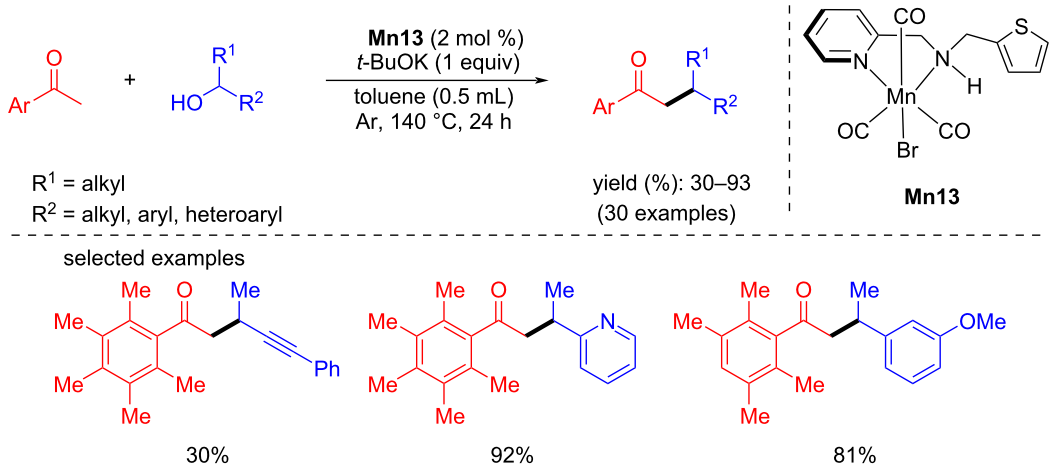

Scheme 37: *N*,*N*-Amine–manganese complex (**Mn13**)-catalyzed alkylation of ketones with alcohols.

methylation of the primary carbon atoms of various secondary alcohols was investigated with methanol using very low catalyst loading (0.1 mol % of **Mn19**) and 1.5 equiv of *t*-BuOK in diglyme as solvent at 140 °C for 3 h and gave up to 96% yield of the dimethylated products. Interestingly, under the same reaction conditions, monomethylation of the secondary carbon atom of the alcohols afforded up to 98% yield (Scheme 46).

In 2020, Liu and Ke reported that a phosphine-free manganese complex catalyzed the coupling of secondary and primary alcohols for the formation of ketones [75]. The reaction conditions

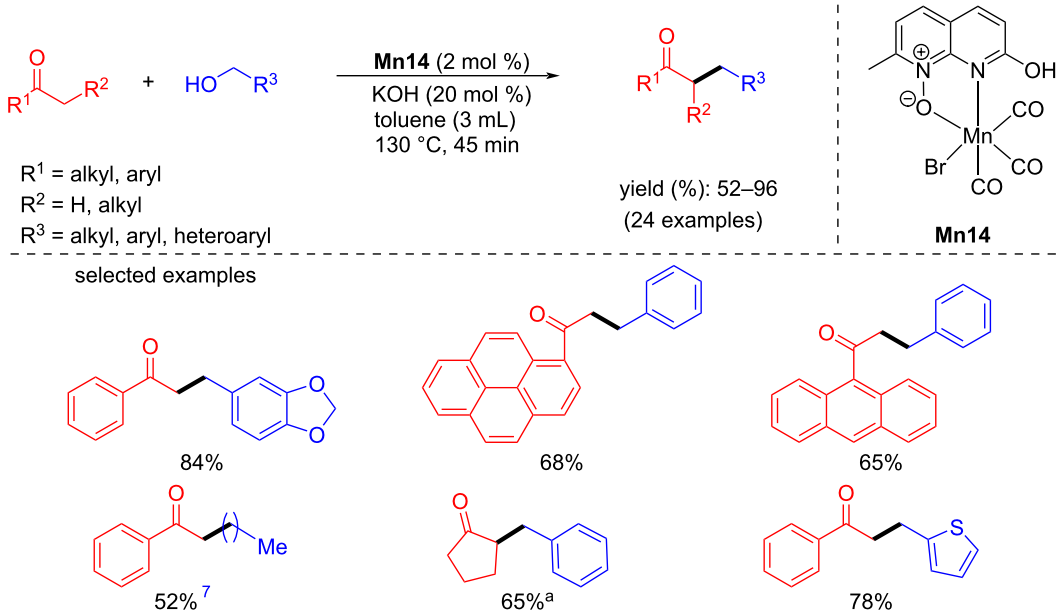

Scheme 38: Naphthyridine-*N*-oxide manganese complex **Mn14** applied for the alkylation of ketones with alcohols. [a]Reaction time was 6 h.

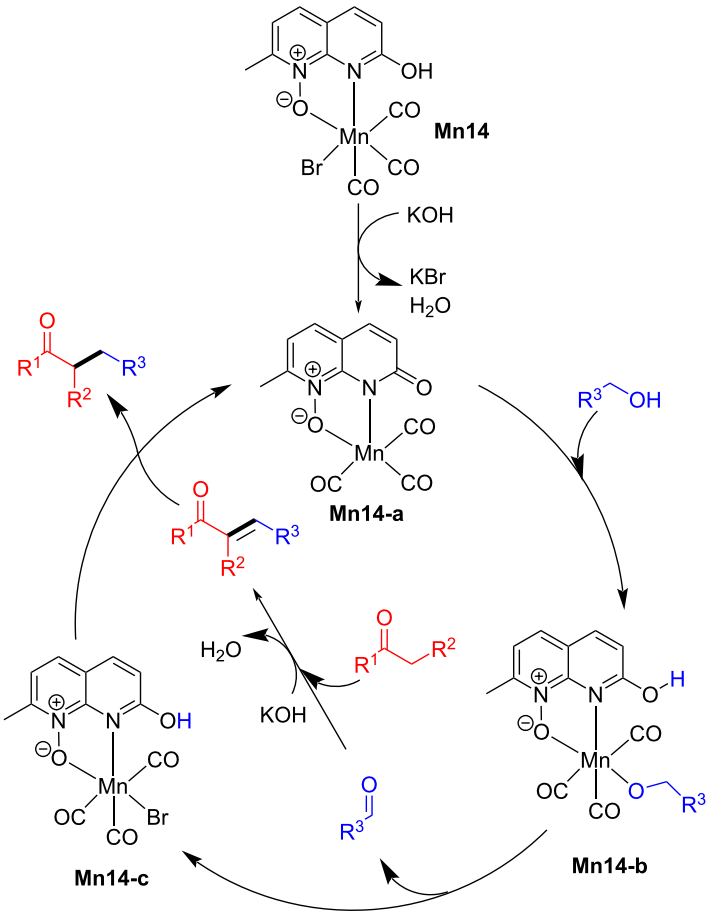

Scheme 39: Proposed mechanism of the naphthyridine-*N*-oxide manganese complex (**Mn14**)-catalyzed alkylation of ketones with alcohols.

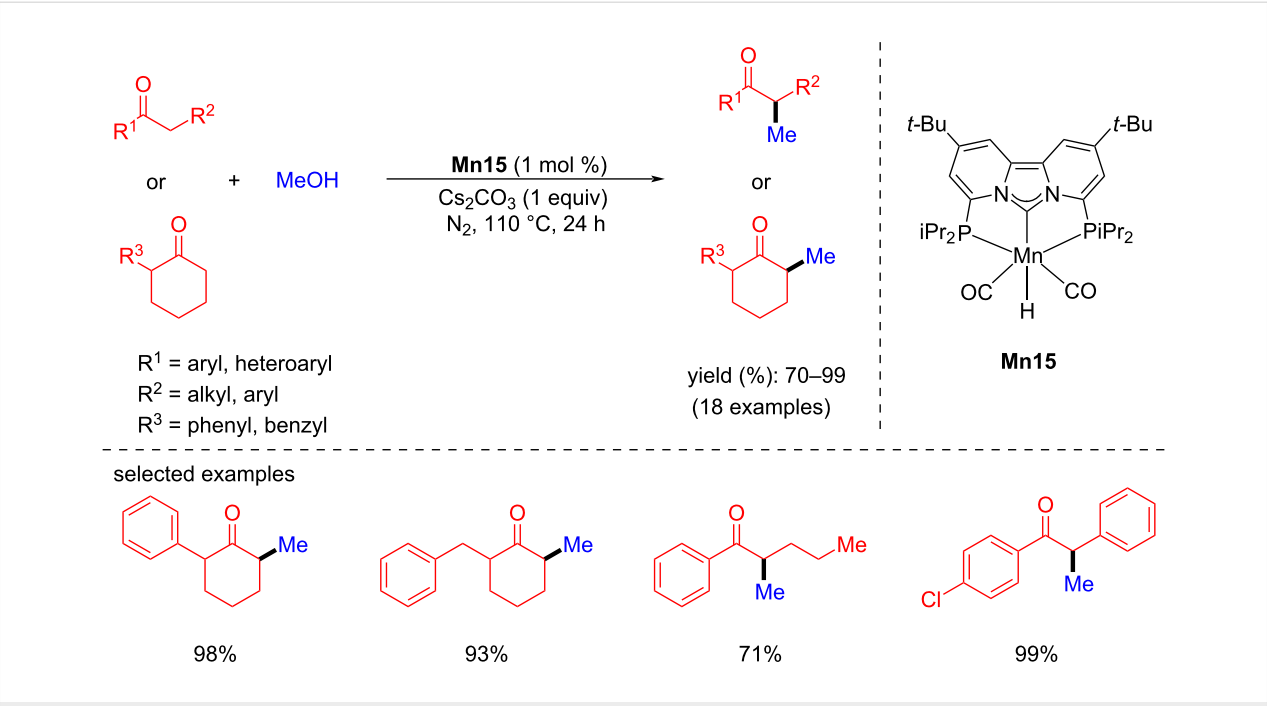

Scheme 40: α-Methylation of ketones and indoles with methanol using **Mn15**.

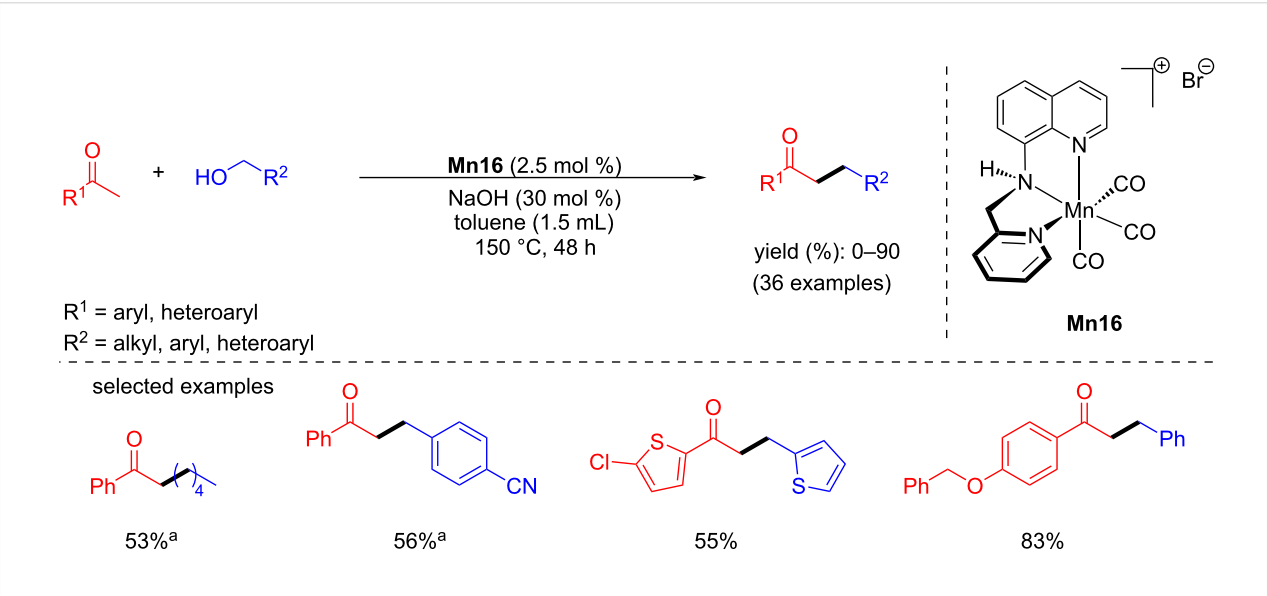

Scheme 41: α-Alkylation of ketones with primary alcohols using **Mn16**. [a]NMR yield.

were optimized with 1-phenylethan-1-ol and benzyl alcohols using several manganese complexes. Among all, 1 mol % of **Mn20**, 0.3 equiv of NaOH in *t*-AmOH at 110 °C for 6 h afforded the alkylated ketone with 88% yield. Under the same conditions, several primary alcohols were tested and gave good to excellent yields (up to 95%) of the desired products. Various substituted secondary alcohols were also tested, giving the alkylated ketones in yields up to 87% (Scheme 47).

Tang and Liu reported the divergent synthesis of γ-disubstituted alcohols and β-disubstituted ketones via coupling the two secondary alcohols [76]. The selectivity was obtained by controlling the reaction conditions. Using the catalyst **Mn9** (2 mol %) and a stoichiometric amount of *t*-BuONa (1 equiv) at 140 °C for 16 h in a sealed system, several γ-disubstituted alcohols were isolated from moderate to high yield (Scheme 48). Notably, the reduced temperature to 60 °C for 6 h is necessary

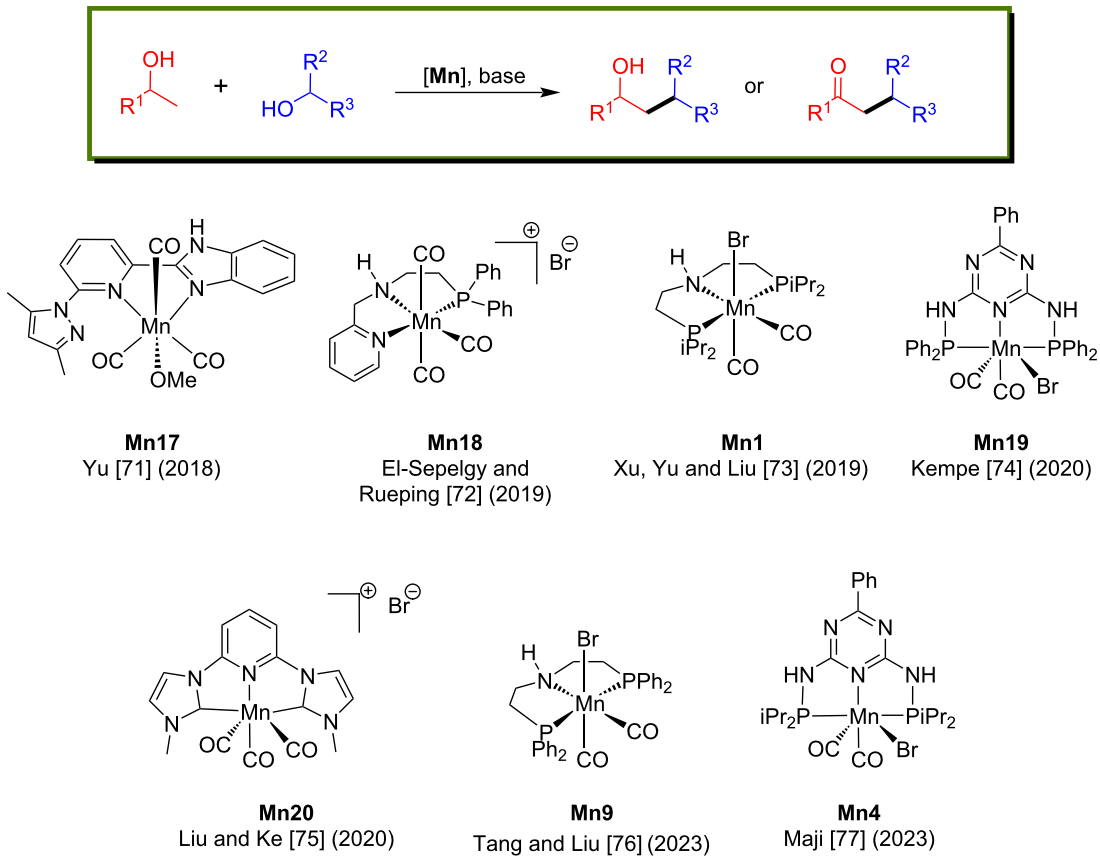

Figure 3: Manganese complexes used for coupling of secondary and primary alcohols.

to achieve the excellent yield of the desired γ-disubstituted alcohol products. To access the β-disubstituted ketones from secondary alcohols, 3 mol % of the manganese catalyst, a catalytic amount of *t*-BuONa (10 mol %) and an open reflux system (120 °C in toluene) under argon flow were required. Utilizing this unique method, many aromatic, aliphatic, and acyclic alcohols were cross-coupled, furnishing a library of disubstituted alcohols and ketones in moderate to good yields with good functional group tolerance.

The proposed mechanism showed that the amido complex dehydrogenated the secondary alcohols into the corresponding carbonyl compounds, which undergo base-assisted aldol condensation, providing the unsaturated ketone compounds. Then, **Mn9-c** hydrogenated the C=C and C=O bonds delivering the desired alkylated alcohol products (Scheme 49).

Recently, Maji's group showed environmentally benign examples of the manganese-catalyzed dehydrogenative coupling of ethylene glycol and primary alcohols producing value-added α-hydroxycarboxylic acid molecules [77]. Several alcohols, including long-chain aliphatic alcohols, were coupled with ethylene glycol using manganese-pincer complex **Mn4** (0.5 mol %), KOH (5 equiv) in *t*-BuOH at 140 °C for 8 h under argon. Excitingly, lactic acid synthesized by treating methanol with ethylene glycol provided a very high TON of 12125. A mechanistic investigation showed the possible characteristic ^{31}P NMR signals of the amido (126.5 ppm) and alkoxy (at 132.7 and 134.9 ppm) manganese complexes (Scheme 50).

C–C Bond formation via alkylation of esters and amides with alcohols

Rueping and El-Sepelgy described an exciting protocol for the C-alkylation of unactivated esters and amides with alcohols using a PNN-Mn complex [78]. The alkylation of several amides with aliphatic, benzylic, and heteroaromatic alcohols gave good to excellent yields (52–92%) using **Mn18** (3 mol %) and *t*-BuOK (1.2 equiv) at 130 °C for 15 h. In the same way, alkylation of *tert*-butyl acetate with numerous alcohols was also tested using catalyst **Mn18** (5 mol %), *t*-BuOK (2 equiv) in toluene at 100 °C for 4 h and gave moderate yields of 39 to 61%. Compared to the alkylation of amides, the alkylation of esters

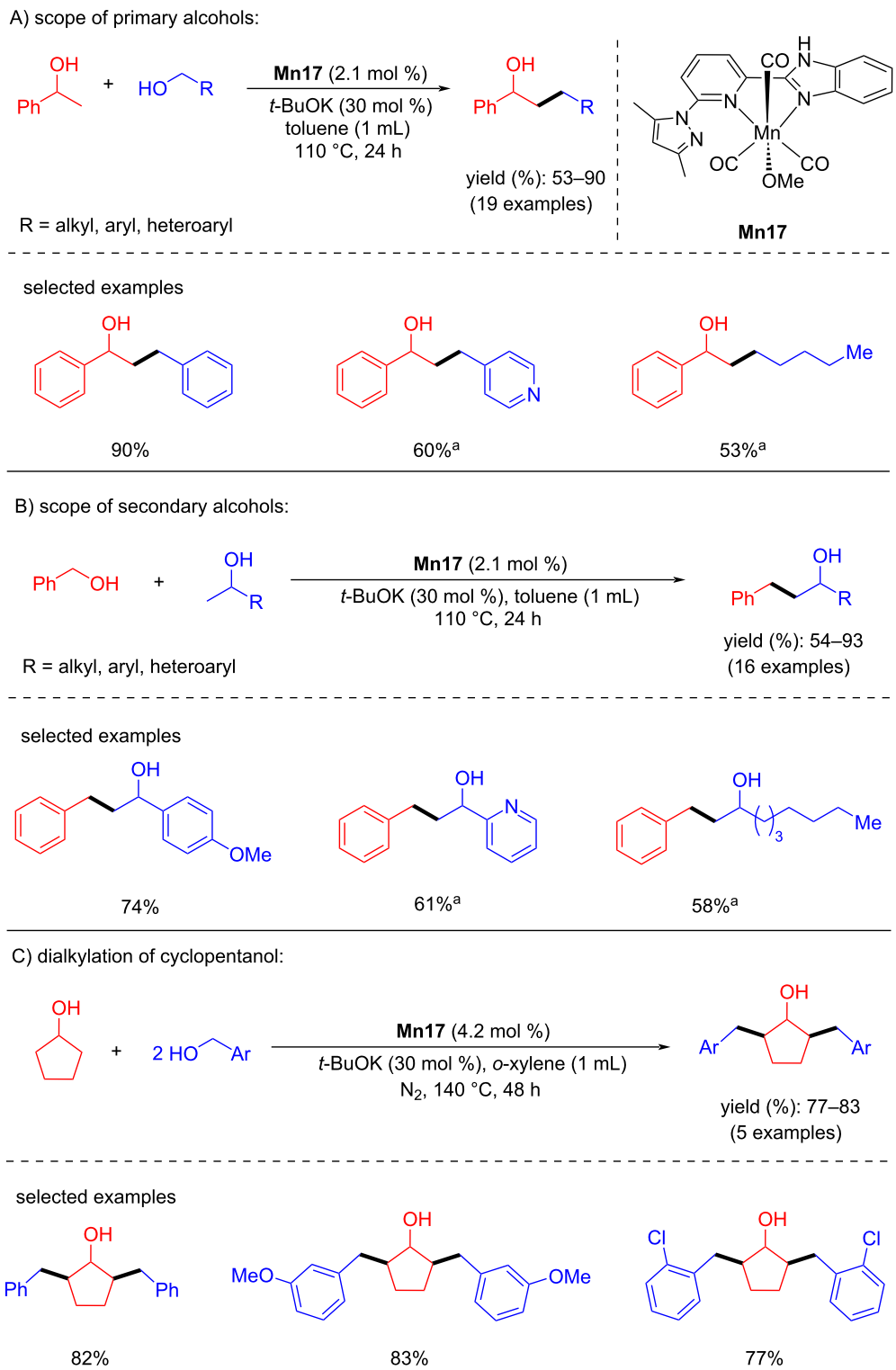

Scheme 42: Alkylation of secondary alcohols with primary alcohols catalyzed by phosphine-free catalyst **Mn17**. [a]4.2 mol % of **Mn17** were used.

required higher catalyst and base loading. However, the reaction proceeded at a low temperature and less reaction time (Scheme 51).

In addition, Balaraman and co-workers reported the C-alkylation of unactivated amides and *tert*-butyl acetate using primary alcohols as alkylating agents catalyzed by an aliphatic PNP-

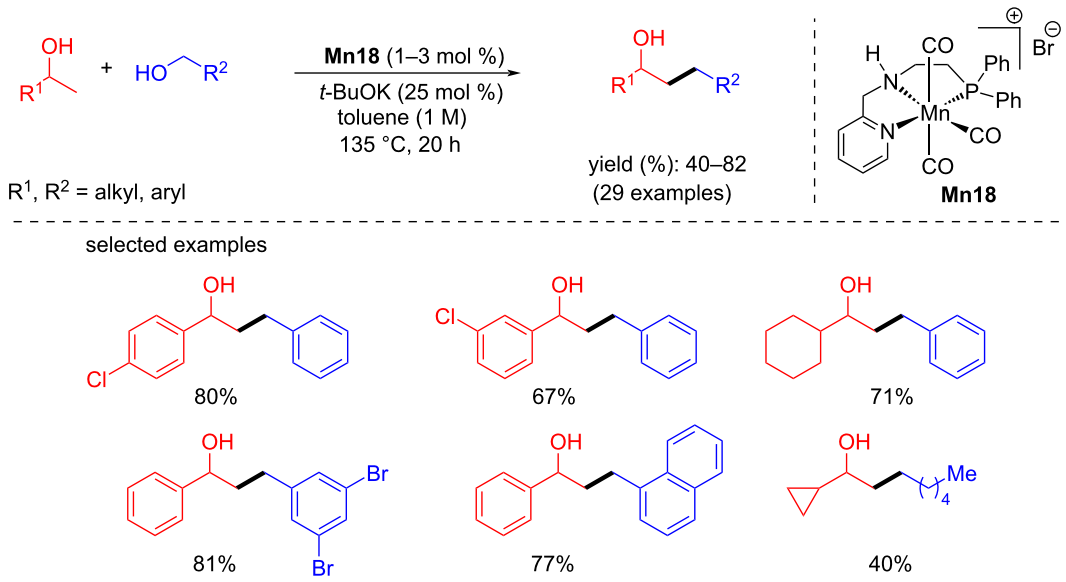

Scheme 43: PNN-Manganese complex **Mn18** for the alkylation of secondary alcohols with primary alcohols.

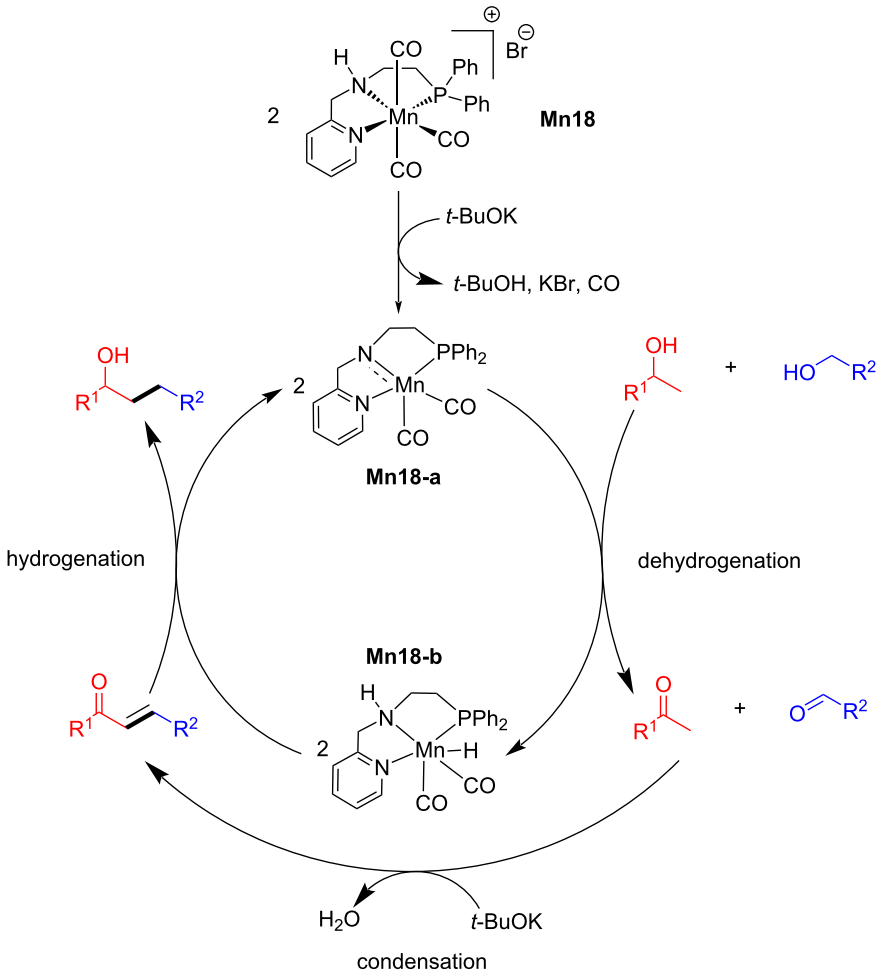

Scheme 44: Mechanism for the Mn-pincer catalyzed C-alkylation of secondary alcohols with primary alcohols.

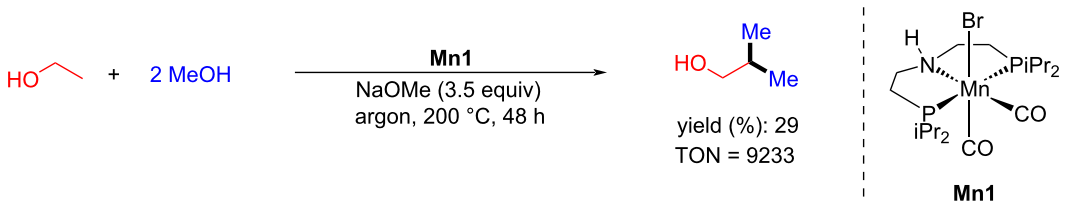

Scheme 45: Upgrading of ethanol with methanol for isobutanol production.

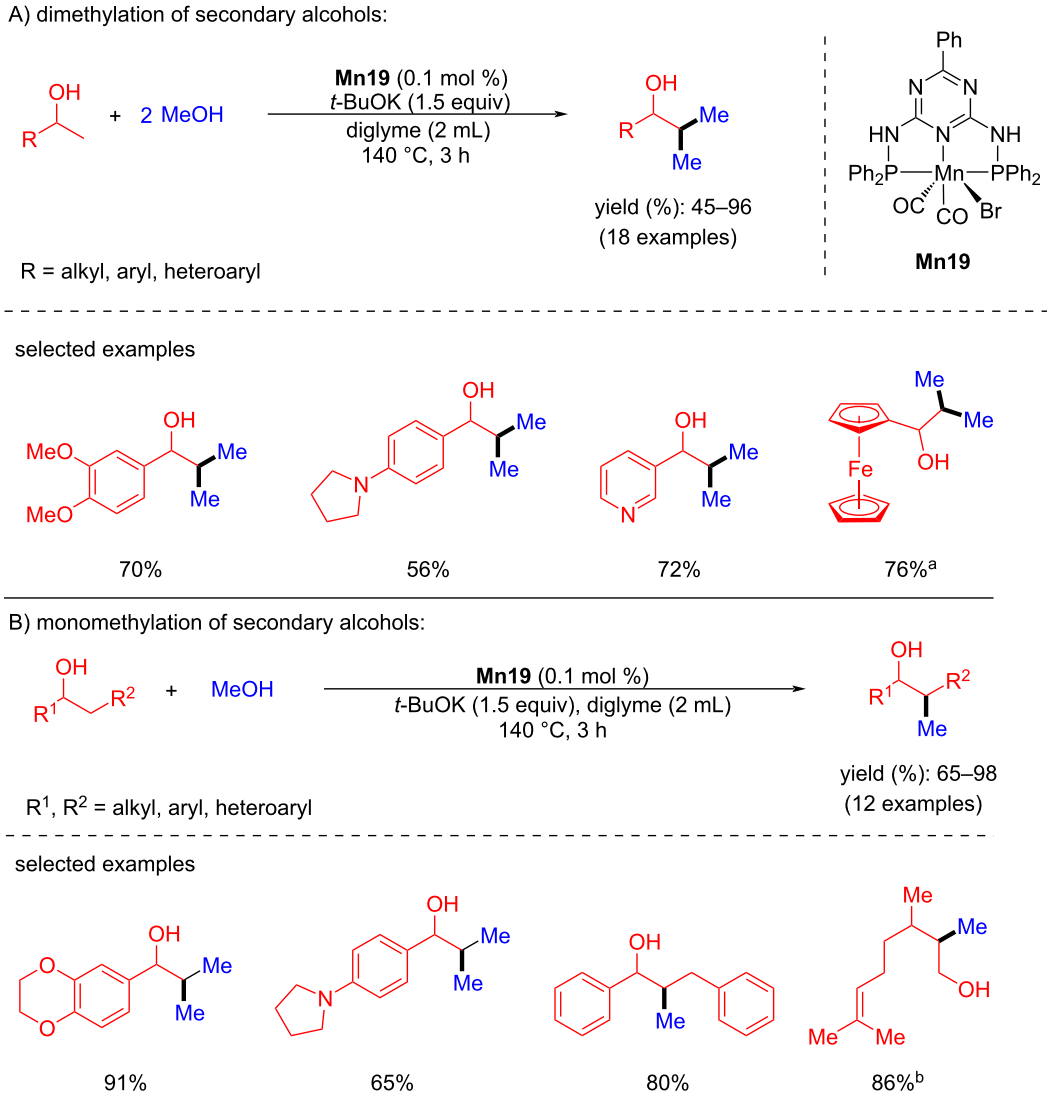

Scheme 46: Mn-Pincer catalyst **Mn19** applied for the β-methylation of alcohols with methanol. [a]2.0 mol % of **Mn19** were used, 12 h. [b]Reaction time was 6 h.

Mn pincer catalyst [79]. Various alcohols, including aliphatic alcohols, were coupled with *N*,*N*-dimethylacetamide using low catalyst loading (0.5 mol % **Mn21**) and *t*-BuOK as base (1.2 equiv) at 110 °C for 16 h and furnished the products in good yields (up to 88%). The alkylation of *tert*-butyl acetate with alcohols under the same reaction conditions provi-

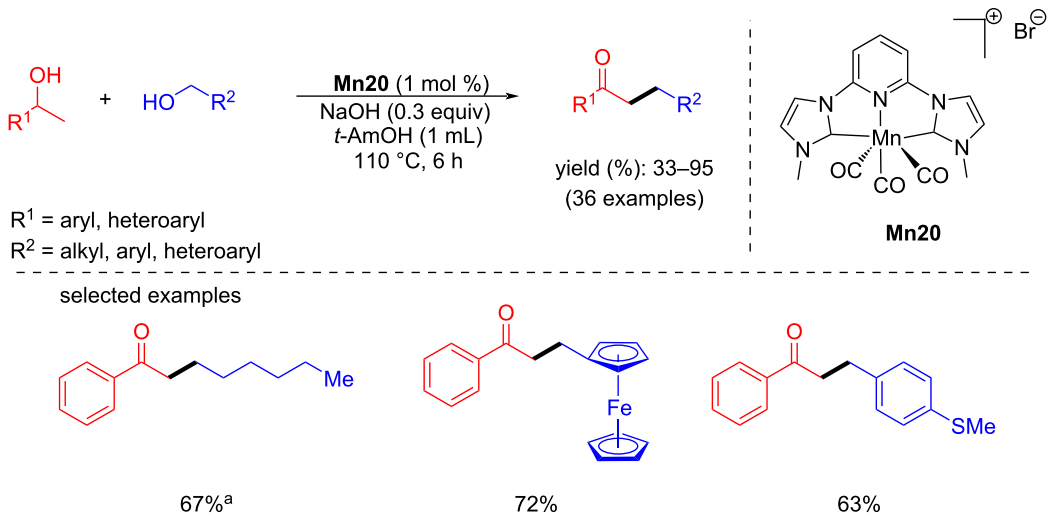

Scheme 47: Functionalized ketones from primary and secondary alcohols catalyzed by **Mn20**. [a]**Mn20** (5 mol %), NaOH (0.5 equiv), 130 °C.

ded the alkylated products with up to 72% yield at 80 °C (Scheme 52).

C-C Bond formation via alkylation of nitriles with alcohols

In 2018, an in situ-generated manganese catalytic system for the α-alkylation of nitriles using primary alcohols was studied [80]. Various substituted nitriles were selectively alkylated in the α-position with 4-methoxybenzyl alcohol as alkyl source using $Mn(CO)_5Br$ (2 mol %), *t*-BuOK (20 mol %) as base in *t*-AmOH as solvent at 140 °C for 24 h to afford the products with up to 88% yield. Furthermore, several benzylic and aliphatic alcohols were used as an alkylating agent (Scheme 53).

The proposed mechanism suggested that the dehydrogenation of the alcohol took place first using the active amido manganese complex. The formed carbonyl compound then condensed with the alkylnitrile and generated the unsaturated compound in the presence of a base. In the final step, the hydrogenation of the formed intermediate took place via the outer sphere mechanism to deliver the desired alkylated nitrile products (Scheme 54).

In 2019, Rueping and El-Seplegy reported the well-defined manganese-PNP complex-catalyzed alkylation of nitriles with alcohols as a hydrogen donor [81]. Three different manganese catalysts were screened for the alkylation of phenylacetonitrile in the presence of a base. Several alcohols and nitriles were tested and showed better functional tolerance with up to 99% yield under the optimized conditions (1 mol % of **Mn9** and 10 mol % of Cs_2CO_3 in toluene at 135 °C for 18 h) (Scheme 55). The mechanistic investigation discussed the formation of a manganese imido complex by treating **Mn9** with 1 equiv of *t*-BuOK at room temperature (rt) for 1 h in C_6D_6. The signal at 91.02 ppm in the ^{31}P NMR spectrum confirmed the formation of the imido compound.

C-Alkylation of heterocyclic compounds with alcohols

Functionalized heterocyclic compounds are omnipresent structural skeletons in bioactive compounds [82]. Remarkably, the alkylation of indoles and quinolines received significant interest since they are common compounds in pharmaceutical and agrochemical industries [83-85]. Various manganese catalysts have been reported (Figure 4) for the C-alkylation of heterocyclic compounds with several alcohols, including indoles and quinolines.

In 2017, Kirchner's group established a new method for the aminomethylation of aromatic compounds with secondary amines and methanol as a C1 source [86]. A total of 28 desired aminomethylated aromatic products were isolated with moderate to good yields (Scheme 56).

Later, Rueping and co-workers developed the regioselective alkylation of indolines with alcohols as the alkylating agent using a manganese-pincer catalyst [87]. Interestingly, the **Mn9**-catalyzed dehydrogenation of alcohols and indolines provided selectively the C3- or N-alkylated products depending on the solvent. For example, the alkylation of indolines with several alcohols using 1 mol % of **Mn9**, 60 mol % of $CsOH{\cdot}H_2O$ in toluene as solvent at 135 °C for 20 h afforded the C3-alkylated indole products in up to 98% yield (Scheme 57).

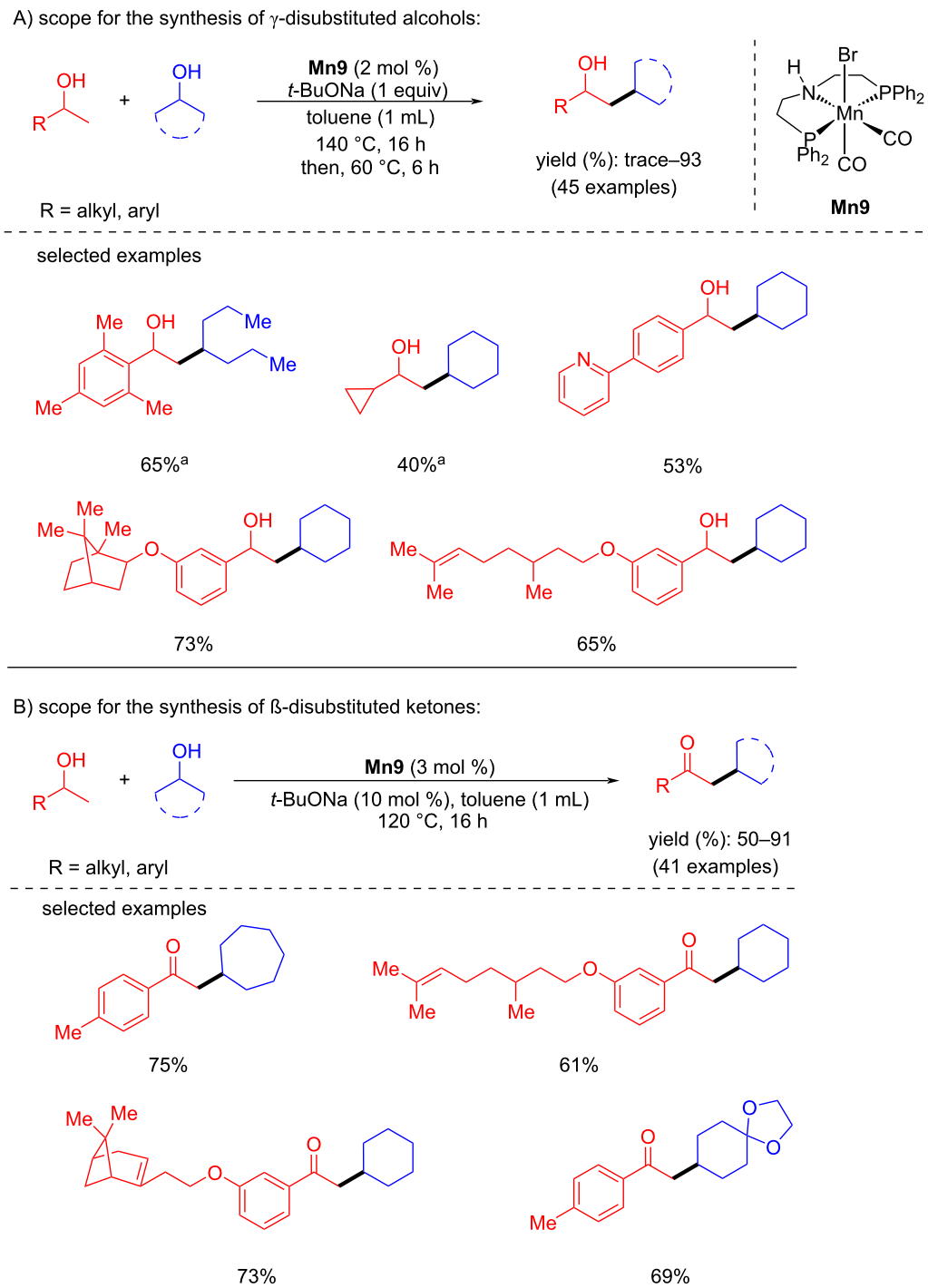

Scheme 48: Synthesis of γ-disubstituted alcohols and β-disubstituted ketones through **Mn9**-catalyzed coupling of two secondary alcohols. [a]4.0 mol % of **Mn9** were used.

Similarly, the alkylation of indolines with various alcohols using 3 mol % of **Mn9** in a TFE/toluene 2:1 mixture provided the corresponding N-alkylated products.

The mechanistic investigation showed that the metal complex activated by the base dehydrogenates the alcohol to the aldehyde and indoline to indole by acceptorless dehydrogenation. Moreover, C3 alkylation proceeded via BH (Scheme 58).

In early 2021, Maji's group demonstrated an efficient approach for the C-alkylation of methyl *N*-heteroarenes with primary alcohols using a manganese-pincer complex [88]. Various

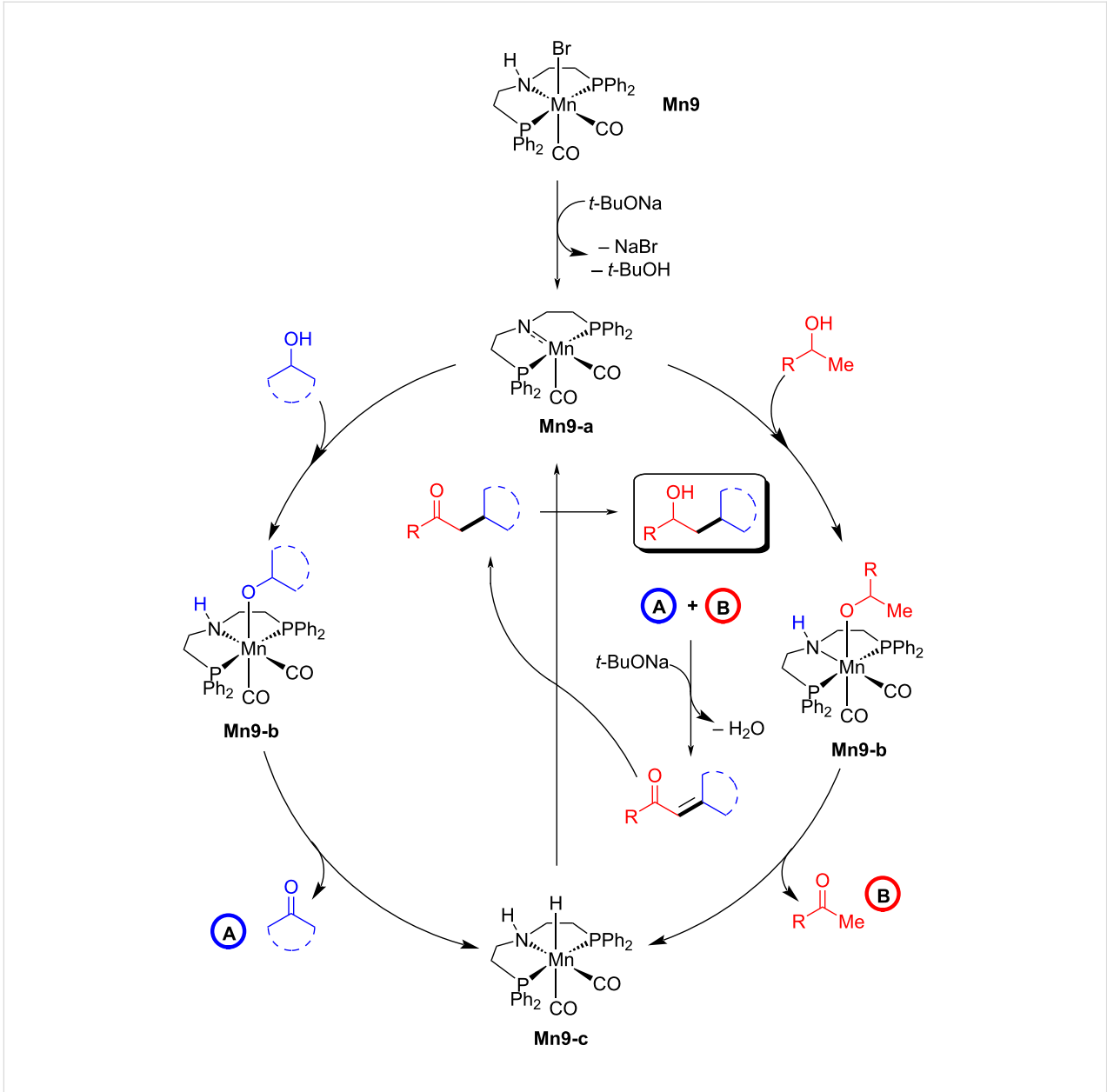

Scheme 49: Proposed mechanism for the **Mn9**-catalyzed synthesis of γ-disubstituted alcohols and β-disubstituted ketones.

methyl-substituted N-heteroarenes were coupled with several alcohols using **Mn1** (2 mol %), *t*-BuOK (1 equiv) as a base in *t*-AmOH at 140 °C under argon atmosphere for 24 h to give moderate to excellent yields (53–98%) of the desired C-alkylated N-heteroarene products (Scheme 59).

The same year, Balaraman and co-workers reported the selective C-alkylation of oxindole with unactivated secondary alcohols catalyzed by a phosphine-free NNN-Mn(II) catalyst [89]. Various cyclic and aliphatic secondary alcohols were coupled with different oxindoles using 2 mol % of **Mn23** and *t*-BuOK (30 mol %) in toluene at 110 °C for 8 h to afford the C3-alkylated oxindoles with up to 85% yield (Scheme 60). However, secondary alcohols substituted with reducible (nitro, amide, aldehyde) groups and −OH, −SH, and –NHMe groups did not provide any expected C-alkylated product.

Like the previous C–C bond forming mechanism, the base-assisted aldol condensation of the ketone with the oxindole generated the unsaturated C-alkylated intermediate and H_2O. Finally, the unsaturated product is hydrogenated to the saturated C-alkylated product by the manganese hydride complex **Mn23-c** with regeneration of the active catalyst **Mn23-a** (Scheme 61).

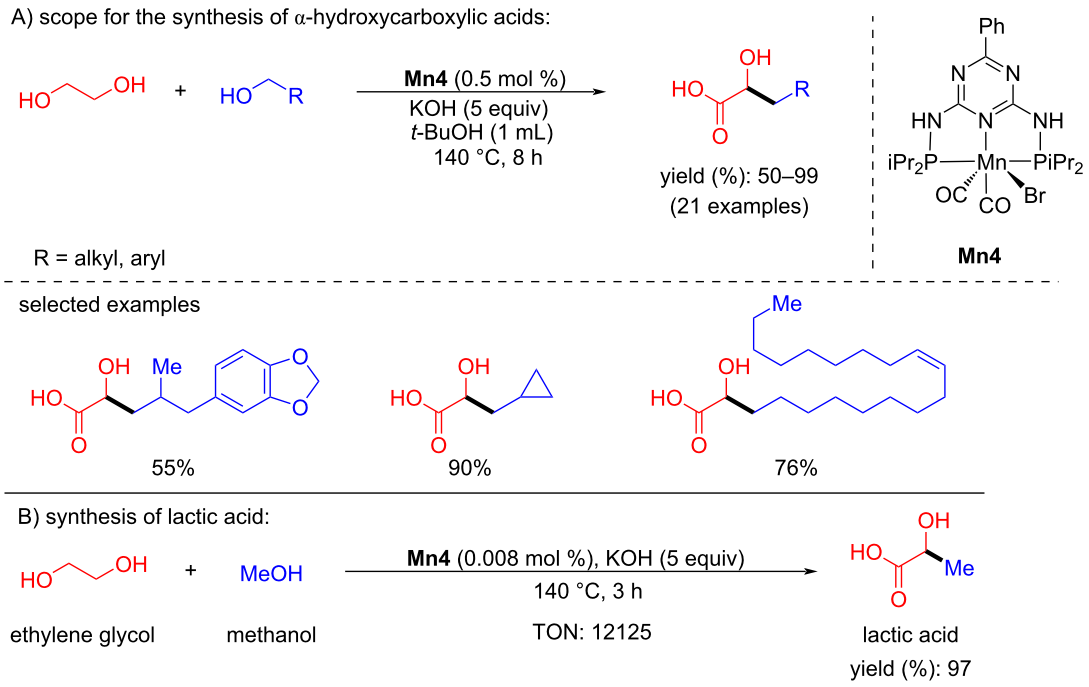

Scheme 50: Dehydrogenative coupling of ethylene glycol and primary alcohols catalyzed by **Mn4**.

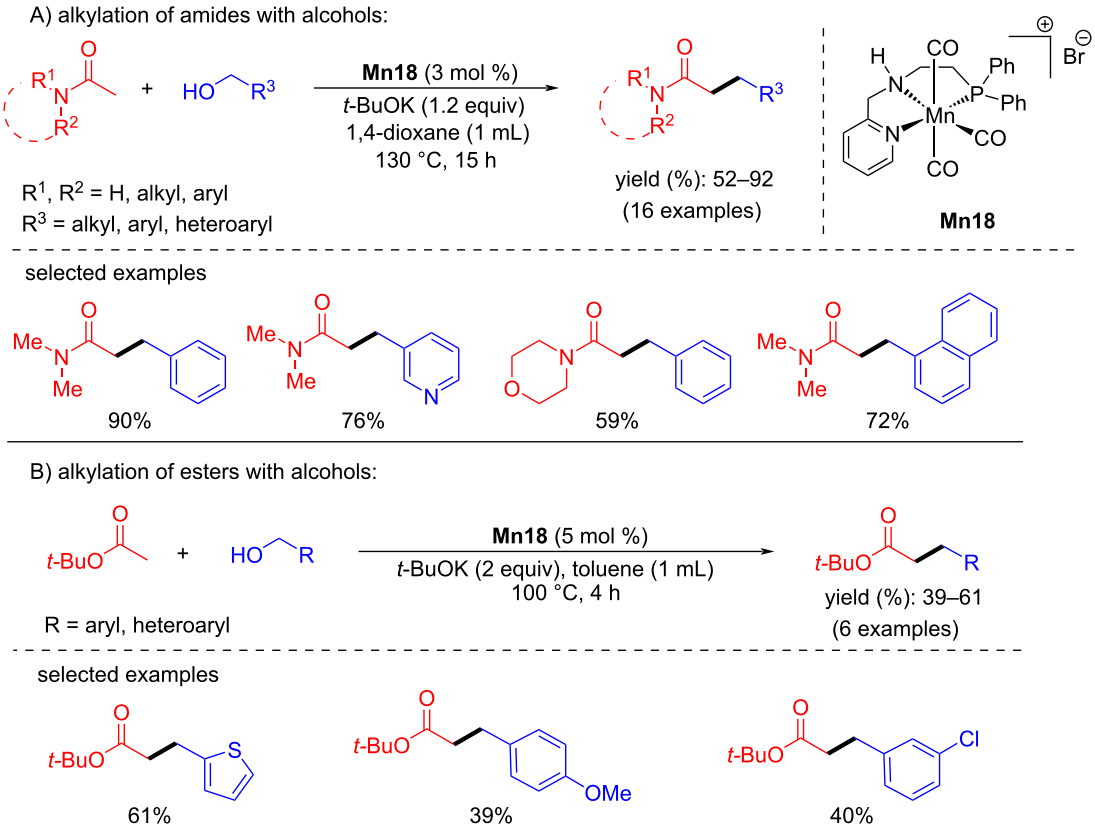

Scheme 51: Mn18-catalyzed C-alkylation of unactivated esters and amides with alcohols.

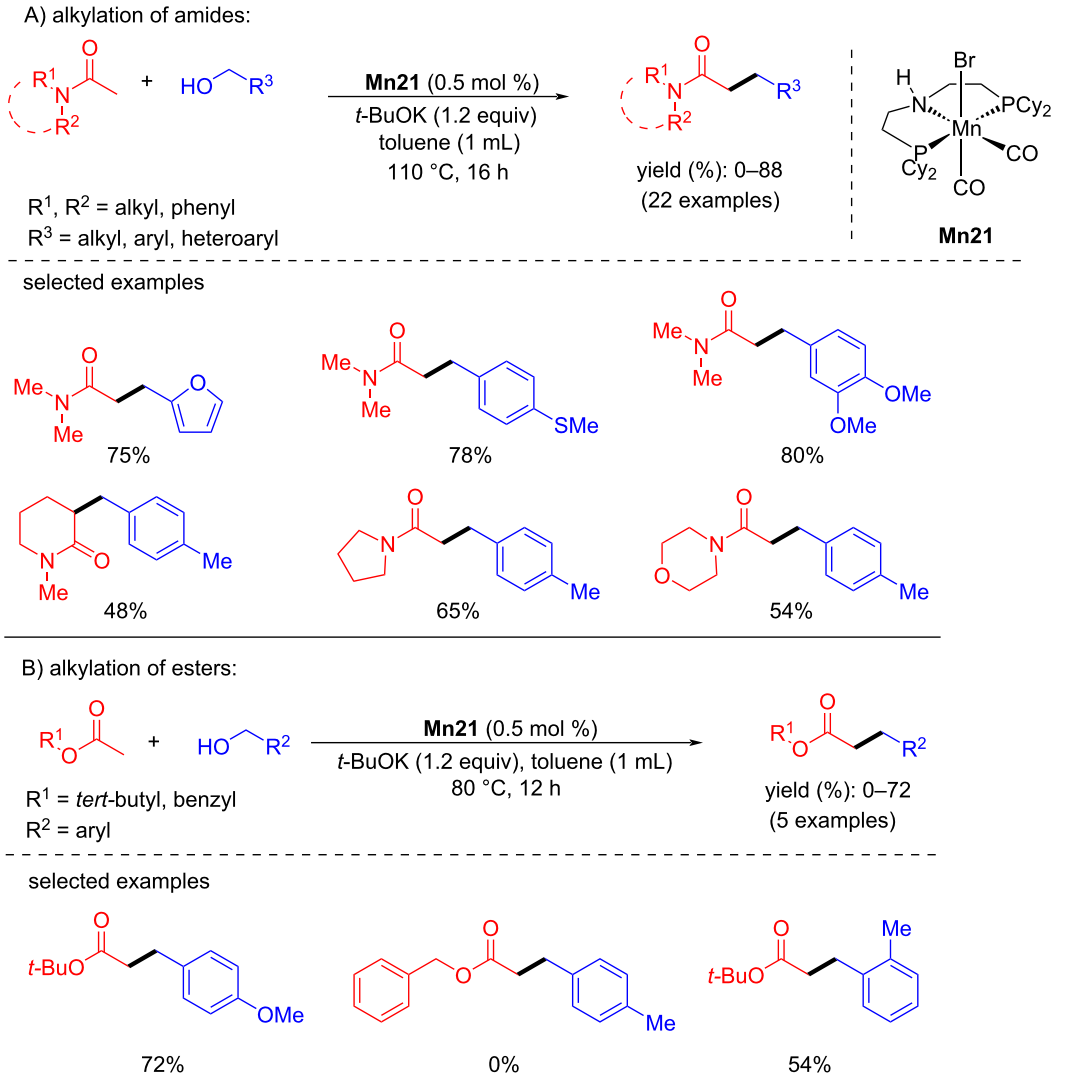

Scheme 52: Alkylation of amides and esters using **Mn21**.

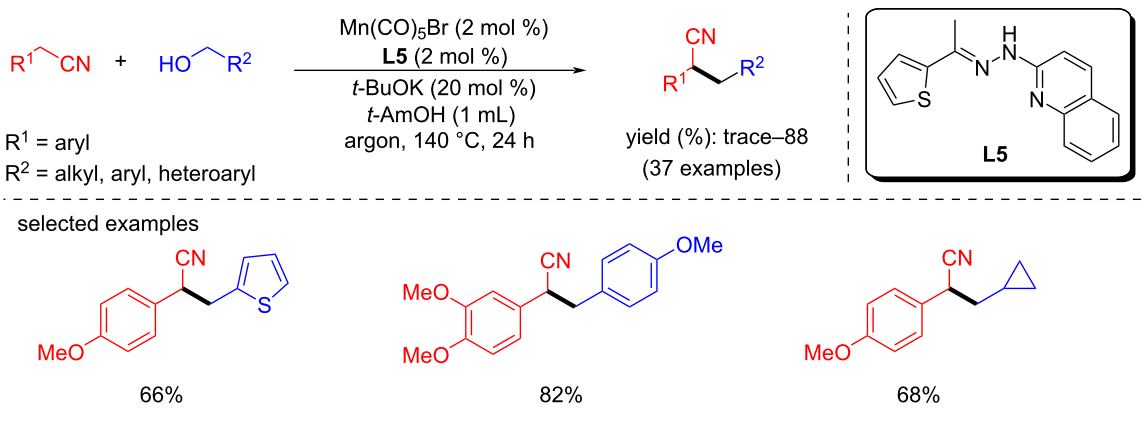

Scheme 53: α-Alkylation of nitriles with primary alcohols using in situ-generated manganese catalyst.

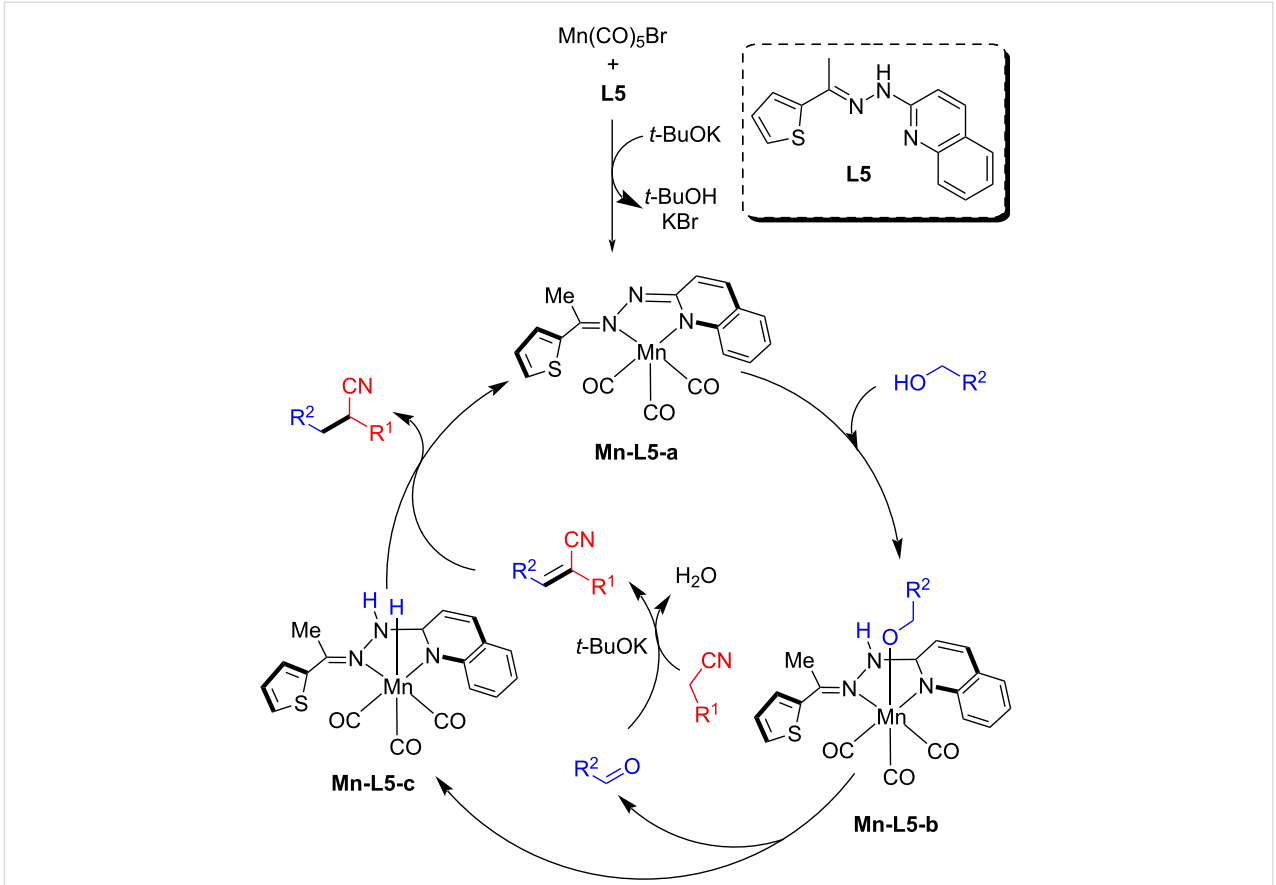

Scheme 54: Proposed mechanism for the α-alkylation of nitriles with primary alcohols.

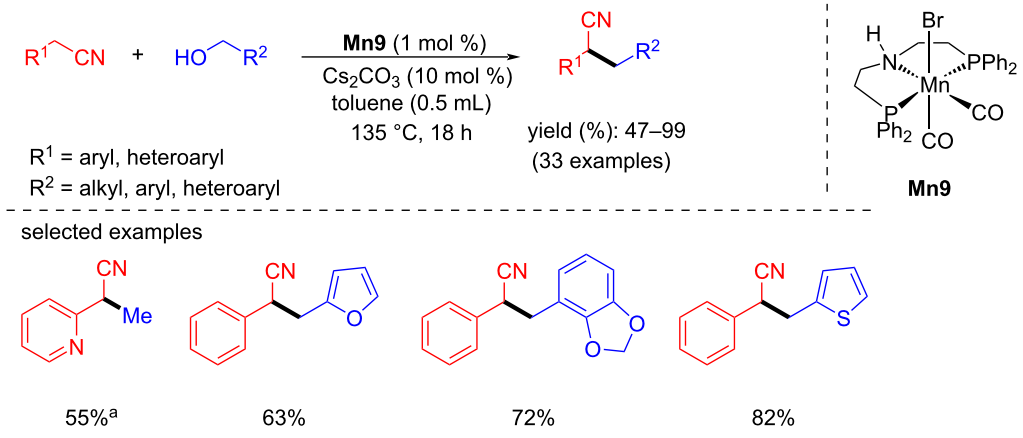

Scheme 55: Mn9-catalyzed α-alkylation of nitriles with primary alcohols. [a]1,4-Dioxane was used as solvent, 24 h.

Later, Srimani and co-workers studied the C-3 alkylation of indoles with various primary and secondary alcohols using **Mn24** (5 mol %) and KOH (0.6 equiv) under neat conditions for 36 h at 130 °C (Scheme 62) [90]. The same cationic complex was used for the synthesis of bis(indolyl)methane by coupling the same substrate using *t*-BuOK (50 mol %) as the base in toluene.

In 2022, Shao and co-workers reported the C-3 alkylation of indoles with primary and secondary benzylic alcohols using an

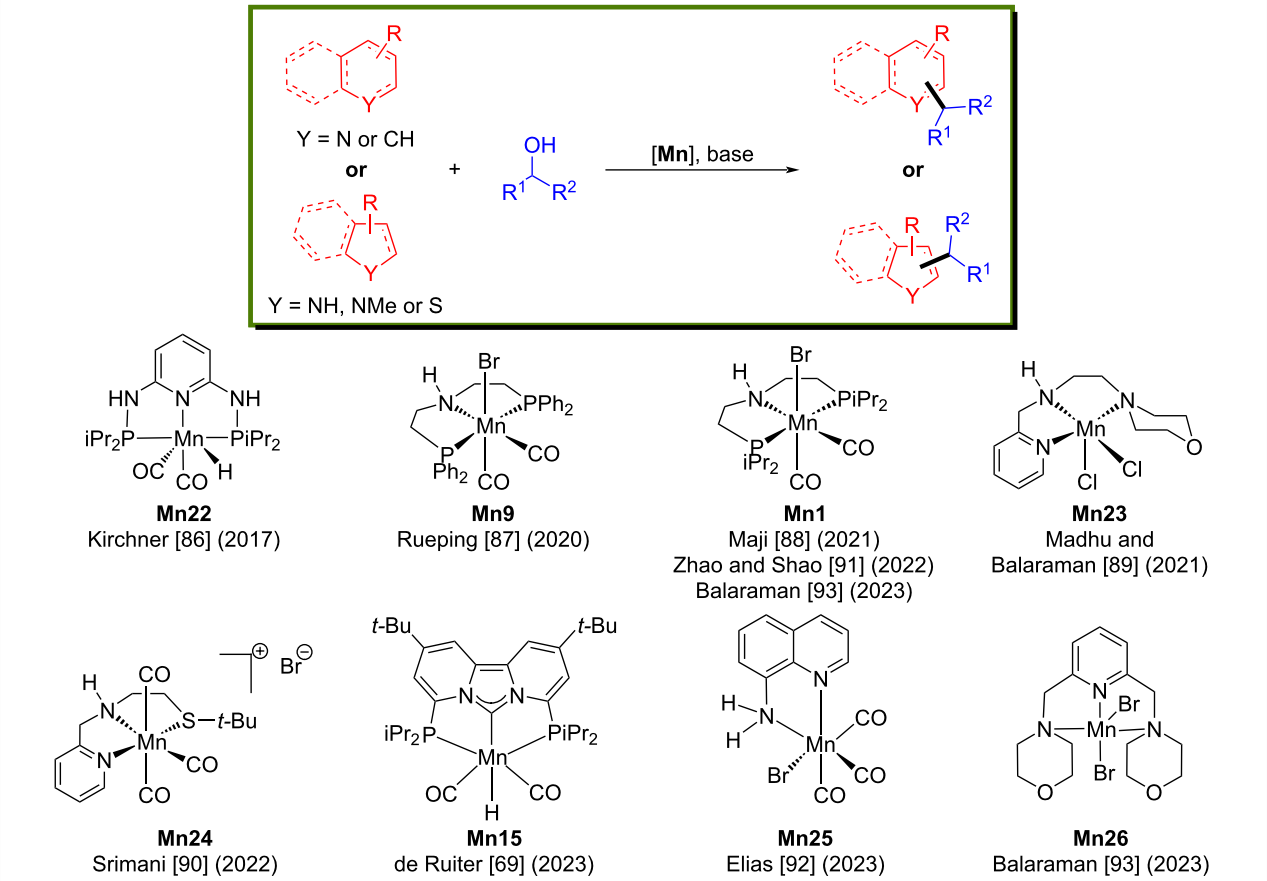

Figure 4: Manganese complexes used for alkylation of heterocyclic compounds.

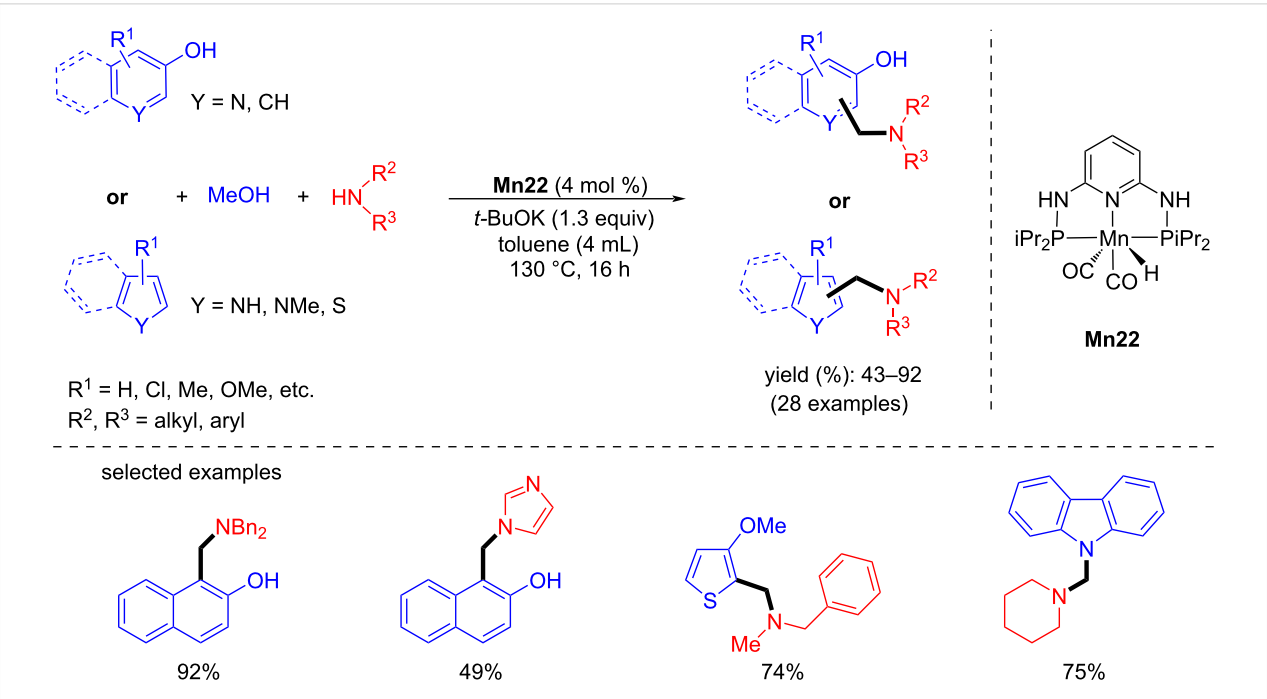

Scheme 56: Aminomethylation of aromatic compounds with secondary amines and methanol catalyzed by **Mn22**.

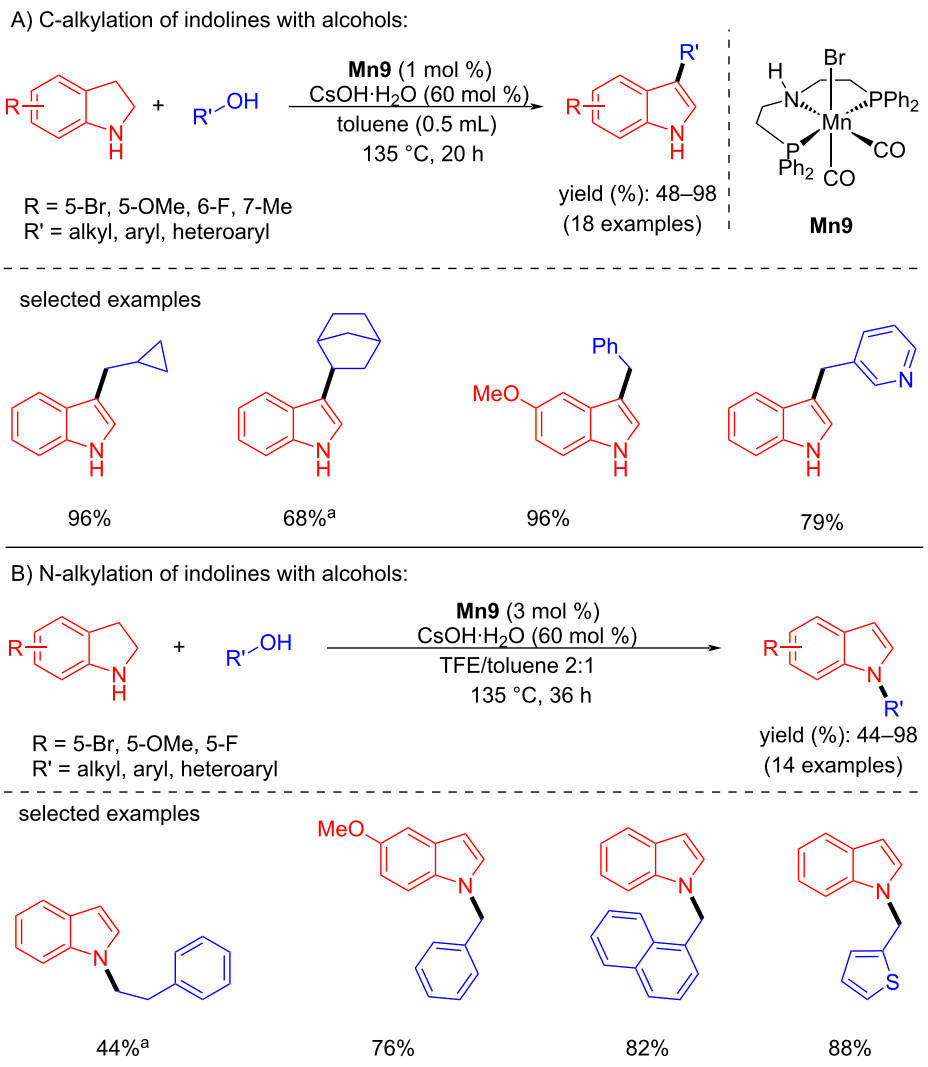

Scheme 57: Regioselective alkylation of indolines with alcohols catalyzed by **Mn9**. [a]**Mn9** (4 mol %), 48 h.

iPrPNP pincer-manganese complex. Three different pincer-Mn complexes were investigated for the alkylation of indole with benzyl alcohol. Among them, **Mn1** demonstrated an excellent activity with 1 mol % of **Mn1**, 1.2 equiv of KOH as base in dioxane at 165 °C for 16 h giving a 99% yield [91]. Further investigation of indole with primary benzyl alcohols under the same conditions gave up to 93% yield of the desired products (Scheme 63), whereas a secondary benzylic alcohol gave the product in 68% yield. When substituted indoles were reacted with benzyl alcohol the C-3-benzylated indole products were obtained with up to 96% yield under the same reaction conditions.

After the successful attempt of using PCNHCP-based manganese complexes for the α-methylation of ketones with methanol as a C1 source by de Ruiter et al., the methylation of indole was also studied [69]. Methylation of substituted indoles with methanol was achieved using 1 mol % of **Mn15** with Cs_2CO_3 (1 equiv) as a base in methanol at 110 °C for 24 h under a N_2 atmosphere, giving the desired products with 60 to 99% yields (Scheme 64).

In 2023, Elias et al. reported that an air-stable, phosphine-free manganese complex generated from 8-quinoline could α-alkylate 2-oxindole with primary and secondary alcohols [92]. Various secondary alcohols were tested with oxindoles using 4 mol % of **Mn25** as a pre-catalyst, *t*-BuOK (1.5–2 equiv.) as a base in toluene at 125 °C for 18 h to provide the C-3-alkylated oxindoles with good yields (70–87%). Moreover, substituting oxindole with different primary alcohols gave up to 85% yield of the isolated products (Scheme 65).

Balaraman and co-workers established an innovative protocol for achieving manganese-catalyzed divergence in the C3-alkyl-

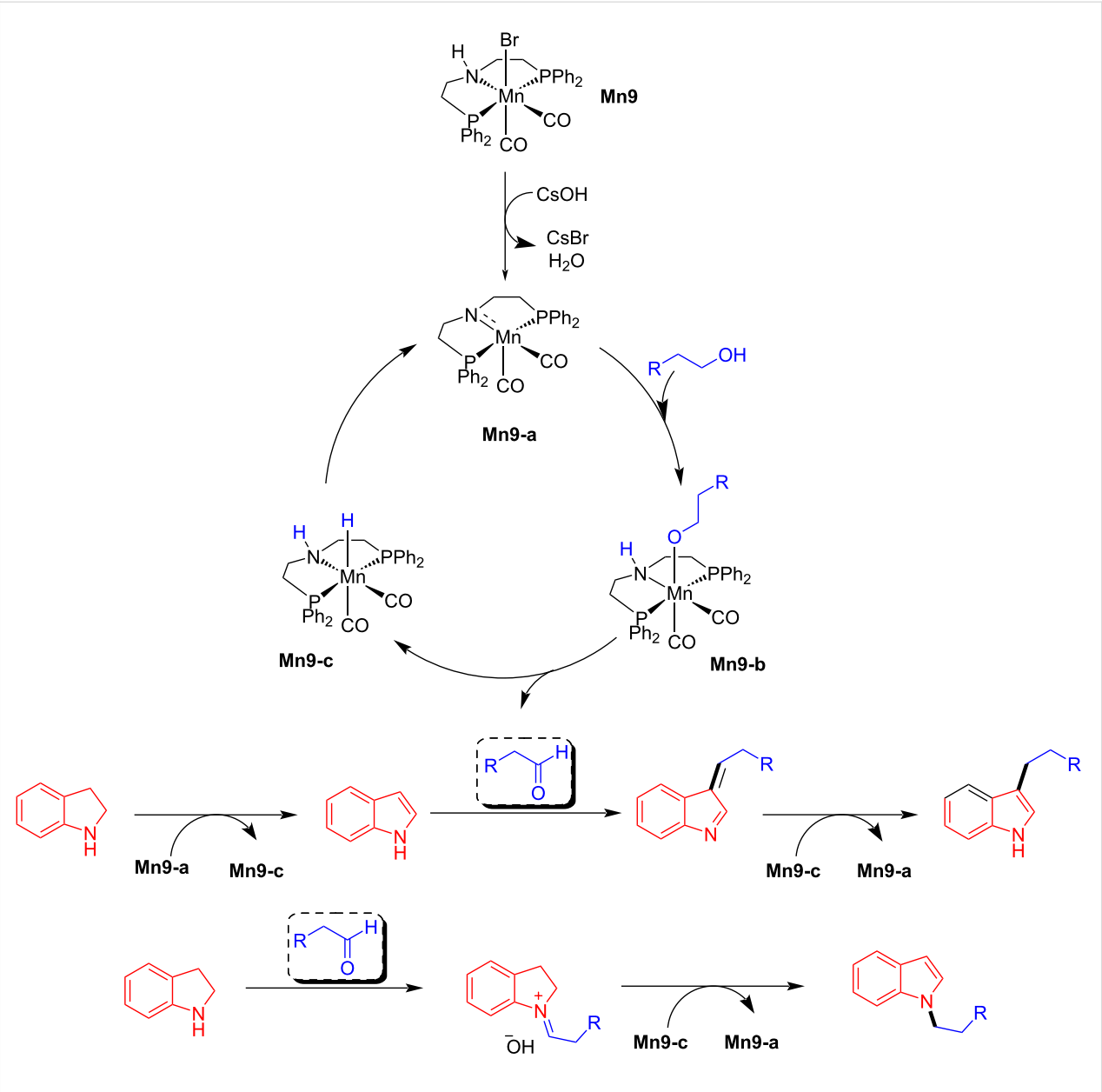

Scheme 58: Proposed mechanism for the C- and N-alkylation of indolines with alcohols.

ation of indoles with alcohols. Various functionalized (hetero)aromatic and aliphatic alcohols were used as an alkylating agent for the double dehydrogenative alkylation of indolines with manganese-pincer complex **Mn1** (2.5 mol %) and *t*-BuOK (40 mol %) in toluene at 140 °C for 36 h under an argon atmosphere (Scheme 66) [93].

On the other hand, numerous bis(indolyl)methane derivatives were synthesized from indoles and alcohols via an interrupted BH approach using **Mn26** (3 mol %) and *t*-BuOK (50 mol %) in toluene at 130 °C for 24 h (Scheme 67). Fascinatingly, this process was used to synthesize pharmacologically active compounds like vibrindole A and turbomycin B alkaloids and natural products like gramine and dipterine analogues. Discrete control studies with Hg and TEMPO indicated that the reactions were homogeneous and did not proceed through a radical pathway.

Synthesis of heterocycles via C–C and C–N bond formation

In 2016, Beller and co-workers reported an intramolecular cyclization using 2-(2-aminophenyl)ethanol for the synthesis of the corresponding indole (98% yield) at 100 °C for 48 h [34]. One year later, Kempe and co-workers showed the multicompo-

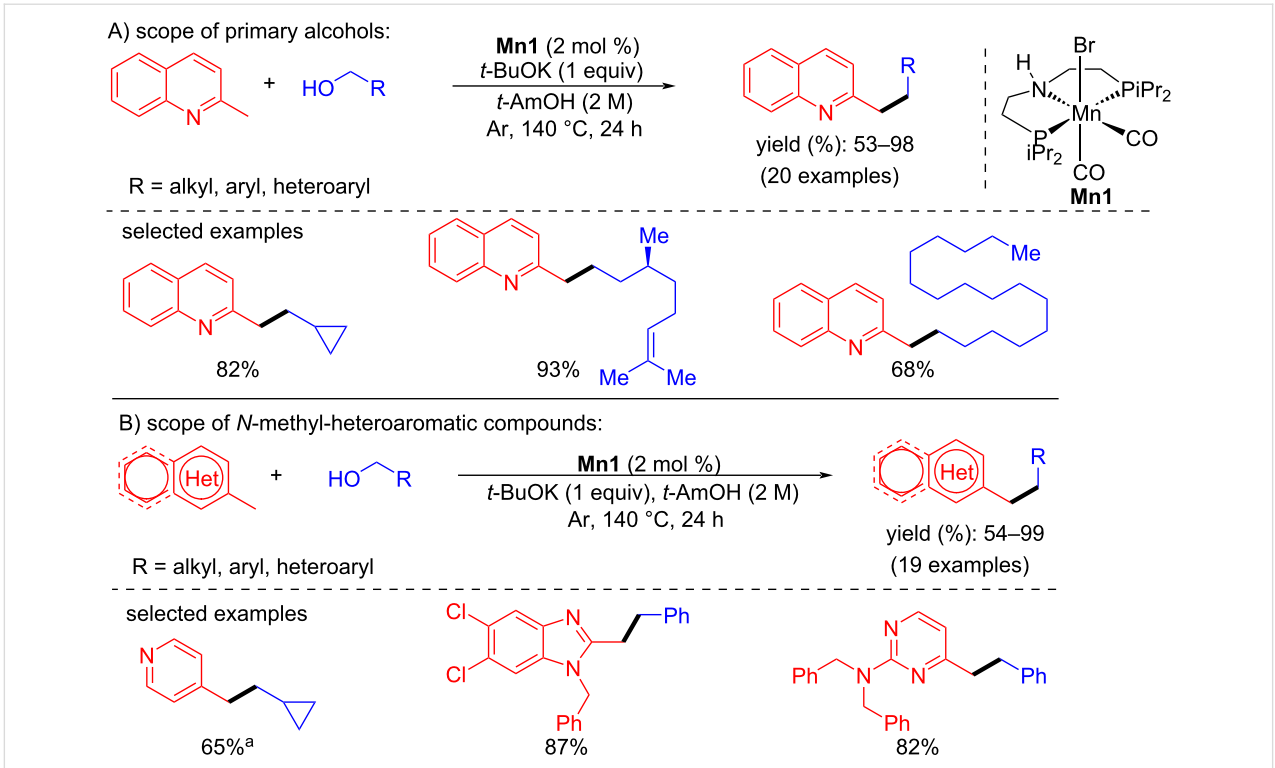

Scheme 59: C-Alkylation of methyl *N*-heteroarenes with primary alcohols catalyzed by **Mn1**. [a]Time was 60 h.

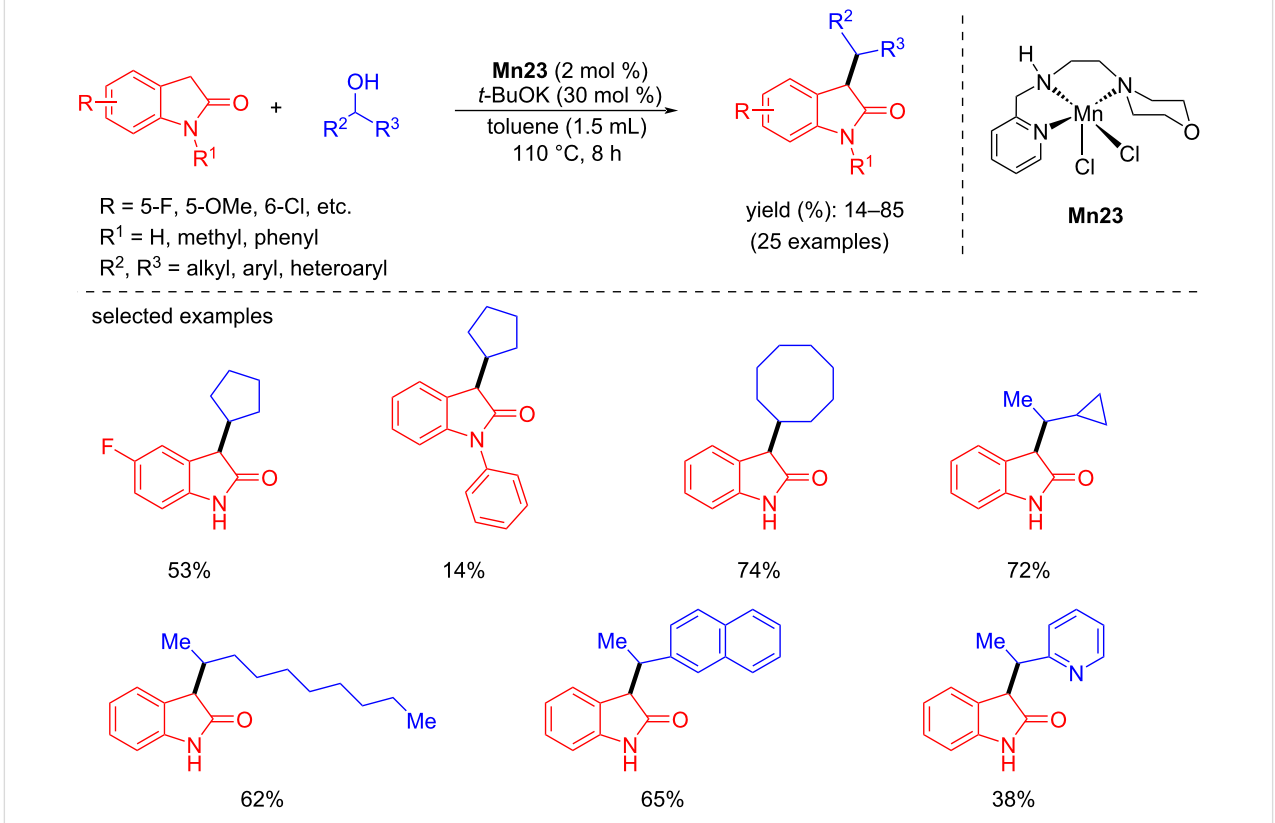

Scheme 60: C-Alkylation of oxindoles with secondary alcohols.

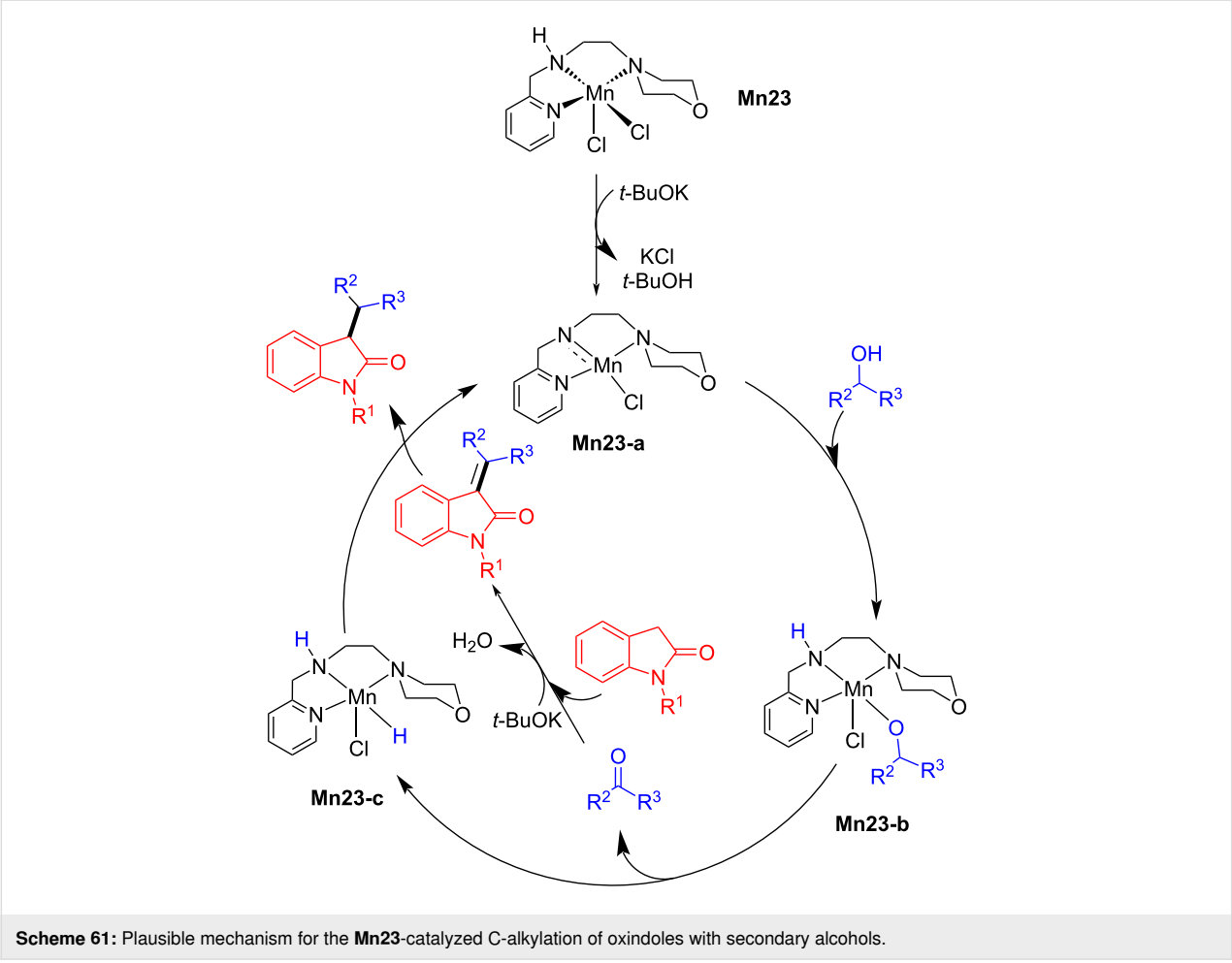

Scheme 61: Plausible mechanism for the **Mn23**-catalyzed C-alkylation of oxindoles with secondary alcohols.

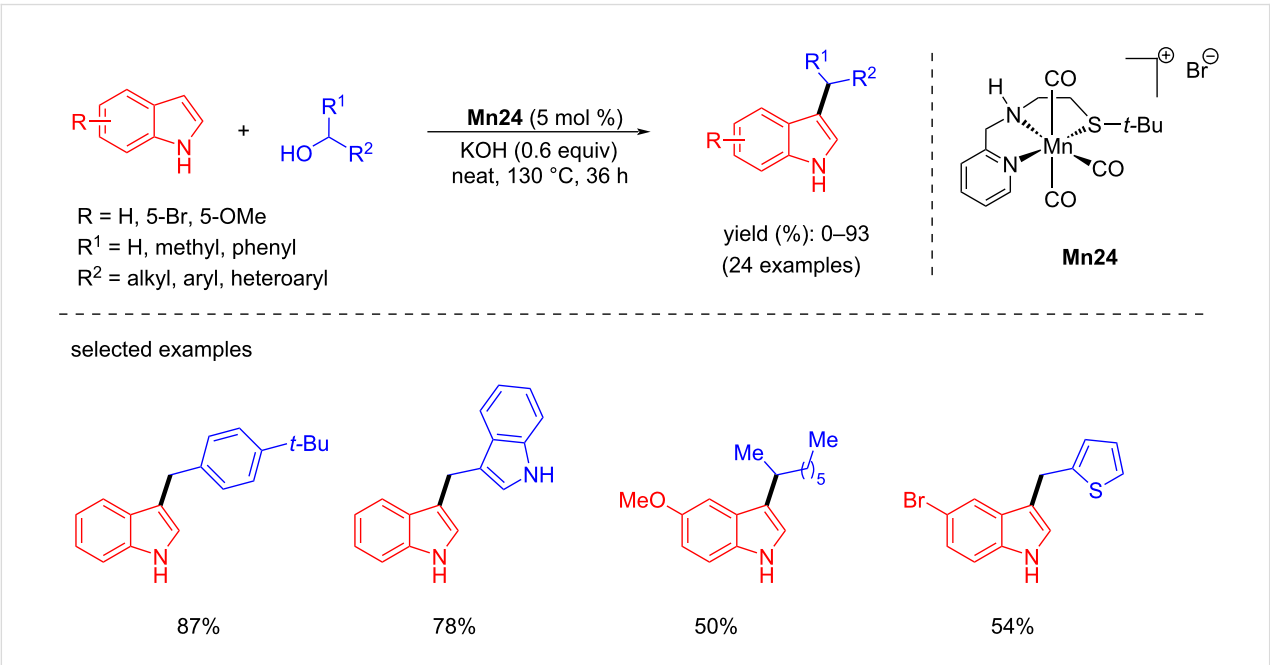

Scheme 62: Synthesis of C-3-alkylated products by coupling alcohols with indoles and aminoalcohols.

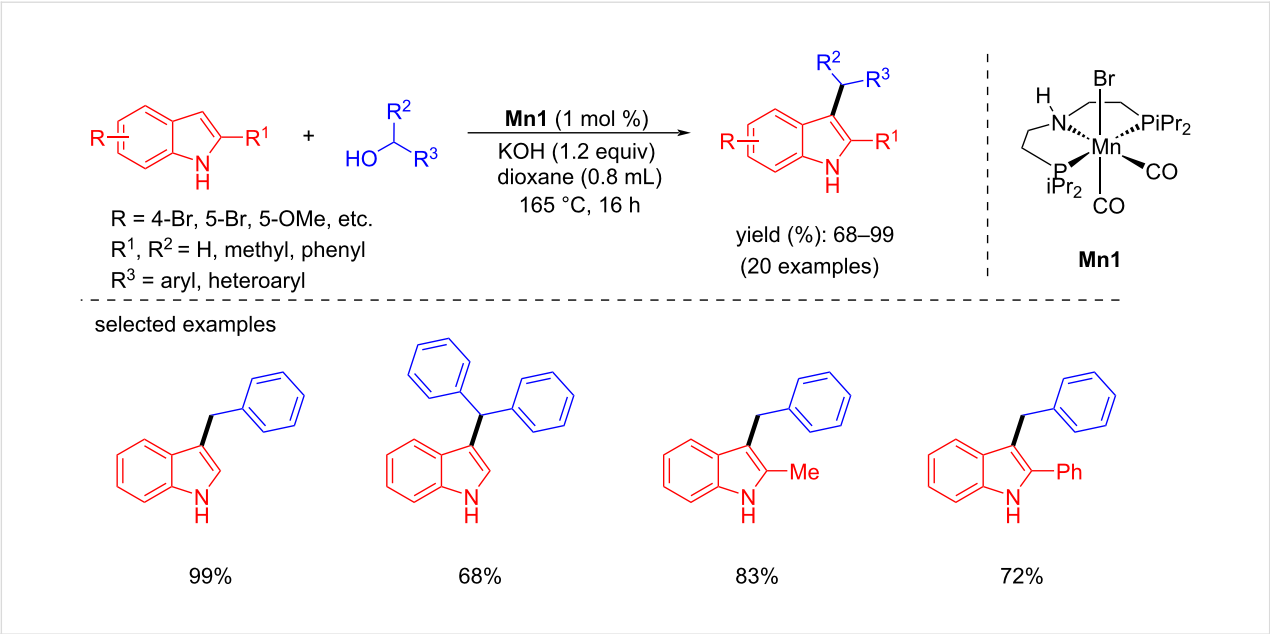

Scheme 63: C3-Alkylation of indoles using **Mn1**.

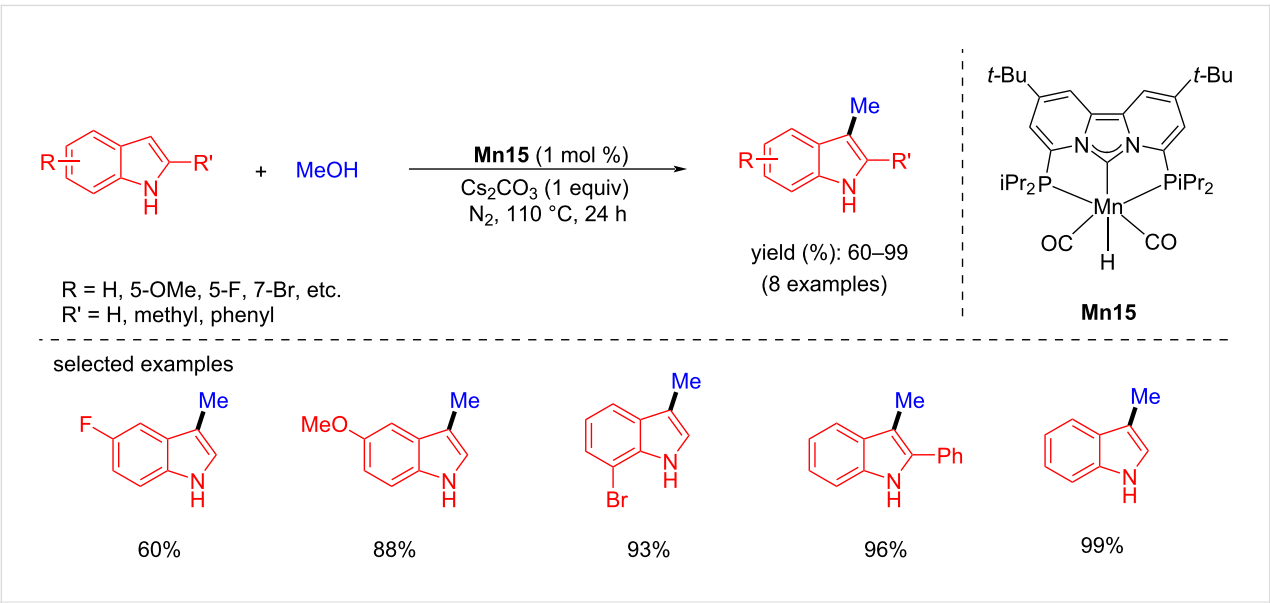

Scheme 64: C-Methylation of indoles with **Mn15** and methanol.

nent synthesis of pyrimidines from amidines and alcohols using **Mn4** via C–C and C–N bond formations [94]. Various amidines were selectively coupled with different alcohols using 2 mol % of **Mn4** and 1.1–1.5 equiv of *t*-BuOK in 1,4-dioxane at 120 °C for 20 h, affording good to excellent yields of the substituted pyrimidines (Scheme 68).

The same group disclosed an efficient synthesis of substituted pyrroles from aminoalcohols and secondary alcohols using **Mn4** under mild conditions [95]. A variety of amino alcohols and alcohols were investigated with **Mn4** (0.5 mol %) and *t*-BuOK (1.5 equiv) in 2-MeTHF under reflux conditions and the corresponding pyrroles were isolated with up to 93% yield (Scheme 69). Notably, the same pincer ligand-supported Co and Fe complexes showed no activity in pyrrole synthesis under the same reaction conditions.

In 2019, Rueping, El-Sepelgy and co-workers achieved the sustainable multicomponent synthesis of pyrroles from readily available substrates catalyzed by manganese-pincer complex

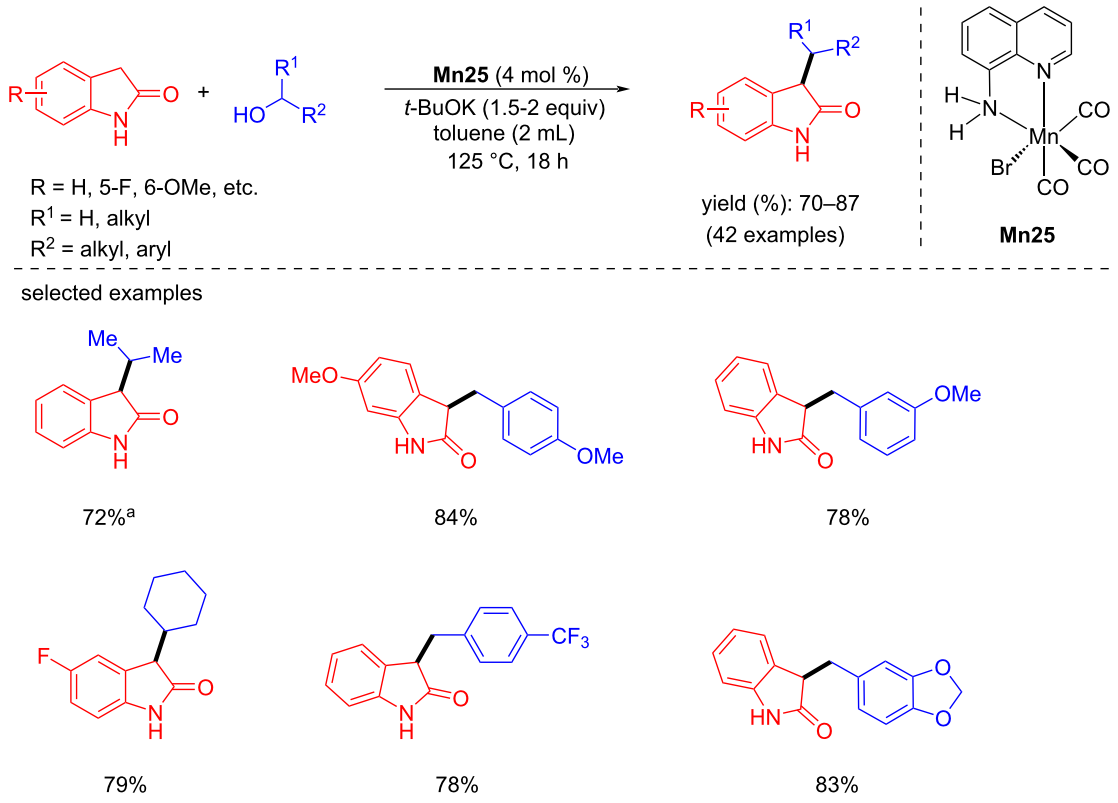

Scheme 65: α-Alkylation of 2-oxindoles with primary and secondary alcohols catalyzed by **Mn25**. [a]Reaction carried out without solvent.

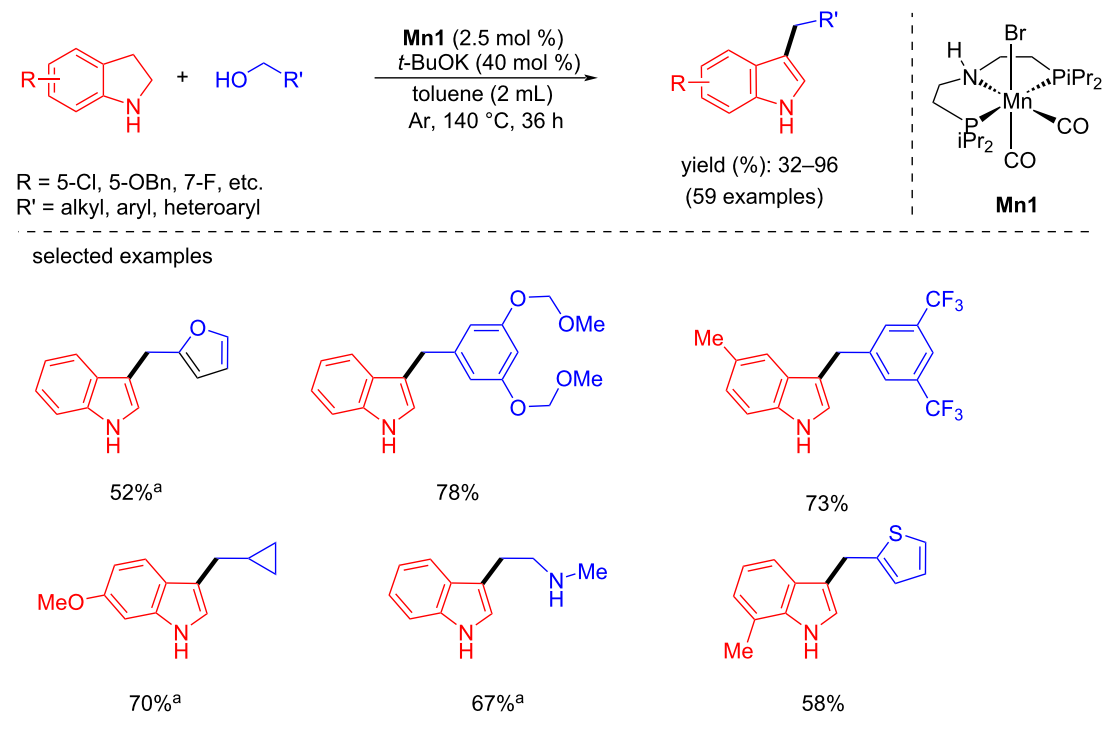

Scheme 66: Dehydrogenative alkylation of indolines with **Mn1**. [a]**Mn1** (5.0 mol %) was used.

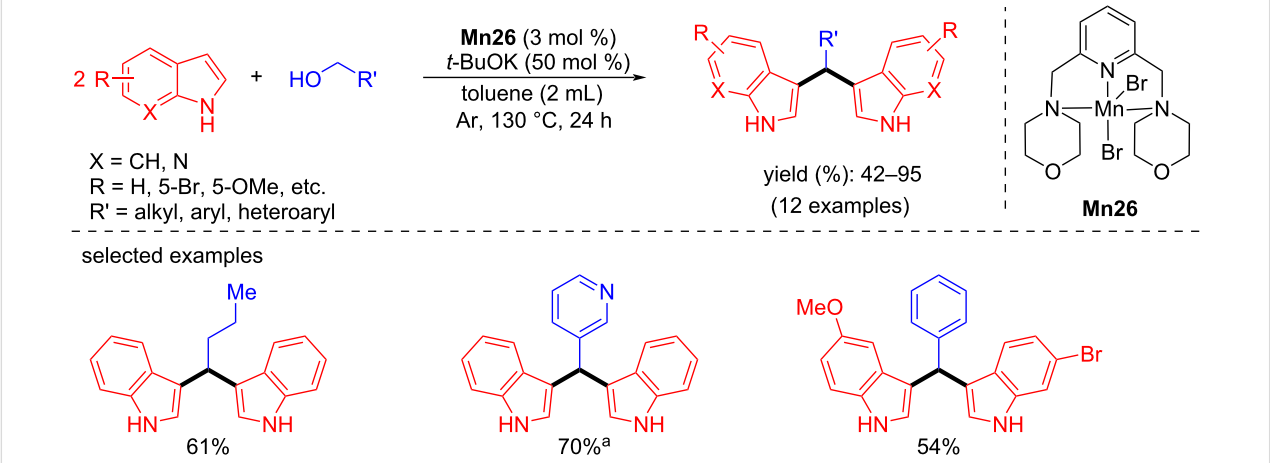

Scheme 67: Synthesis of bis(indolyl)methane derivatives from indoles and alcohols catalyzed by **Mn26**. [a]**Mn26** (5.0 mol %) was used.

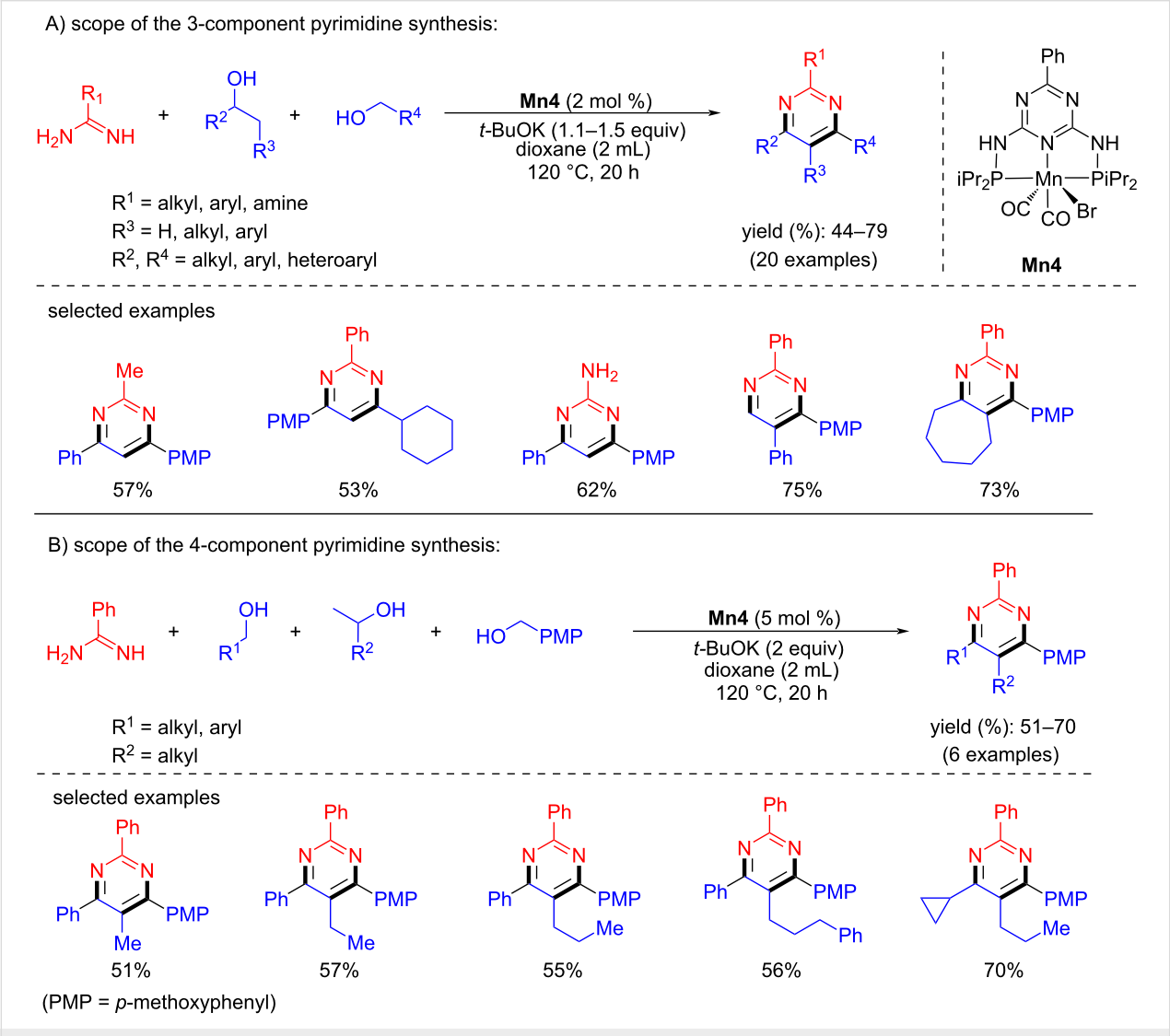

Scheme 68: One-pot synthesis of pyrimidines via BH.

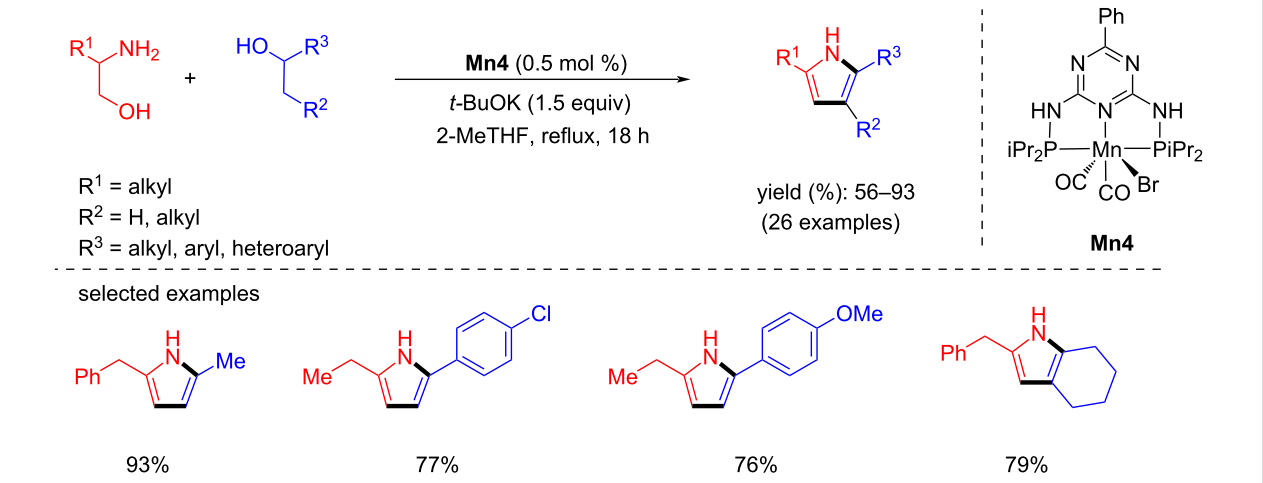

Scheme 69: Synthesis of pyrroles from alcohols and aminoalcohols using **Mn4**.

Mn12 [96]. The use of 2 mol % of **Mn12** in combination with a catalytic amount of *t*-BuOK (20 mol %) in *t*-AmOH at 135 °C for 24 h allowed for the investigation of several alkyl and aryl ketones with amines and vicinal diols yielding good to excellent yields of the desired pyrroles (Scheme 70) with water and hydrogen gas being the only byproducts. DFT calculations suggested that the metal–ligand cooperation plays a crucial role in the acceptorless dehydrogenation of ethylene glycol to glycolaldehyde and the HA process.

In 2018, Maji's group reported the Friedländer quinoline synthesis using a phosphine-free manganese catalyst generated in situ from $Mn(CO)_5Br$ and **L3** [58]. Under optimized conditions (2 mol % $Mn(CO)_5Br$, 10 mol % *t*-BuOK, *t*-AmOH, argon atmosphere), various quinoline derivatives were successfully synthesized with this protocol (Scheme 71).

In 2019, Liu et al. used a bis-N-heterocyclic carbene-supported manganese complex for quinoline synthesis by coupling aminobenzyl alcohols and methyl ketones with **Mn6** (4 mol %), NaOH (50 mol %) in toluene at 110 °C for 2 h [64]. Moderate to good yields (46–86%) of the 2-substituted quinoline derivatives were isolated (Scheme 72).

In the same year, Madsen's team introduced a manganese(III)-porphyrin catalyst for the synthesis of quinoline derivatives from 2-aminobenzyl alcohols and secondary alcohols in the combination of KOH/*t*-BuOK 1:1 with 5 mol % **Mn7** catalyst

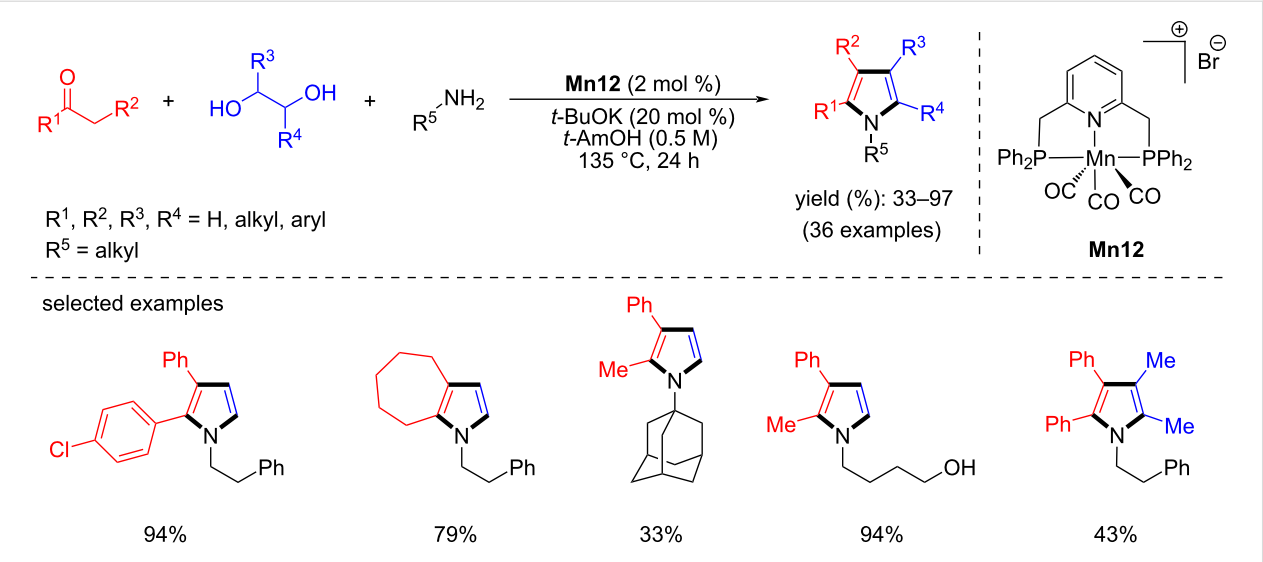

Scheme 70: Synthesis of pyrroles via multicomponent reaction catalyzed by **Mn12**.

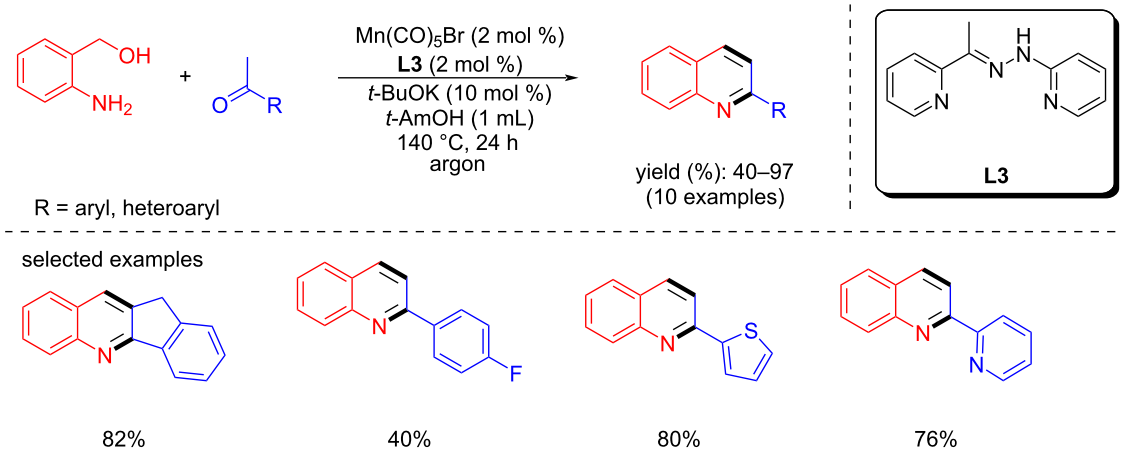

Scheme 71: Friedländer quinoline synthesis using an in situ-generated phosphine-free manganese catalyst.

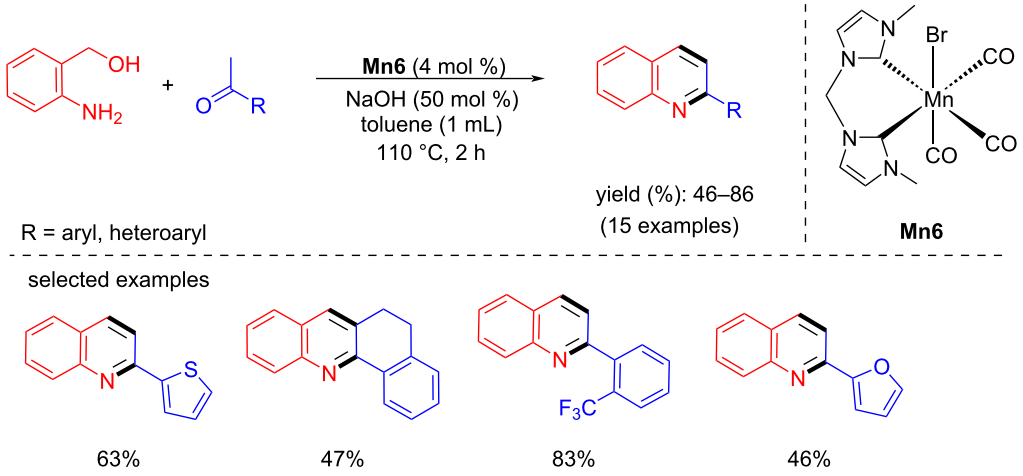

Scheme 72: Quinoline synthesis using bis-N-heterocyclic carbene-manganese catalyst **Mn6**.

loading [43]. However, a high temperature (reflux with mesitylene) and long reaction time (60 h) were required to achieve a moderate to high yields (48–93%) (Scheme 73).

Later, Hultzsch and co-workers reported a PN3 pincer-supported manganese complex for the synthesis of tetrahydroquinolines via BH methodology [97]. The reaction conditions were optimized with 2-aminobenzyl alcohol and 1-phenylethanol using **Mn27**. Among the several bases tested in DME at 120 °C for 24 h, a mixture of KH and KOH (1:5) together with 2 mol % of Mn complex **Mn27** afforded 2-phenyl-1,2,3,4-tetrahydroquinoline as product with 78% yield. Several aromatic and aliphatic substituted alcohols were studied, and the results showed good to exceptional yields of the substituted tetrahydroquinolines (Scheme 74). The active amido complex **Mn27-a** dehydrogenated the amino alcohol and secondary alcohol into the corresponding carbonyl compounds, and the subsequent base-assisted condensation allowed the formation of the quinoline product, which was further hydrogenated into the target compound (Scheme 75).

In 2022, Srimani and co-workers showed the synthesis of C3-functionalized indoles by coupling of (2-aminophenyl)ethanol with various alcohols, including aliphatic alcohols, using **Mn24** (8 mol %) and KOH (1 equiv) under neat conditions for 36 h at 130 °C and afforded yields up to 78% (Scheme 76) [90].

In 2022, Shao and co-workers synthesized C3-alkylated indoles by coupling 2-aminophenethanol with several substituted

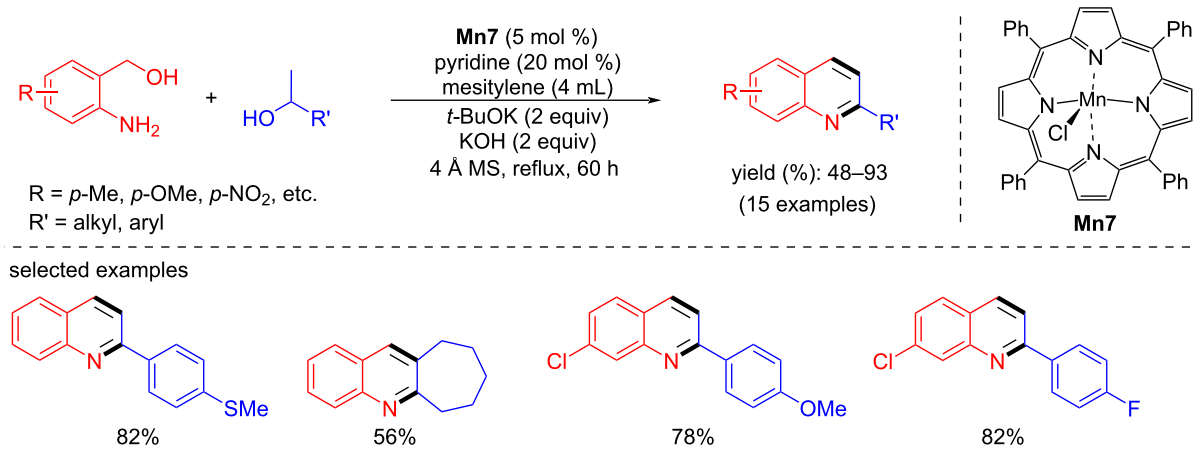

Scheme 73: Quinoline synthesis using manganese(III)-porphyrin catalyst **Mn7**.

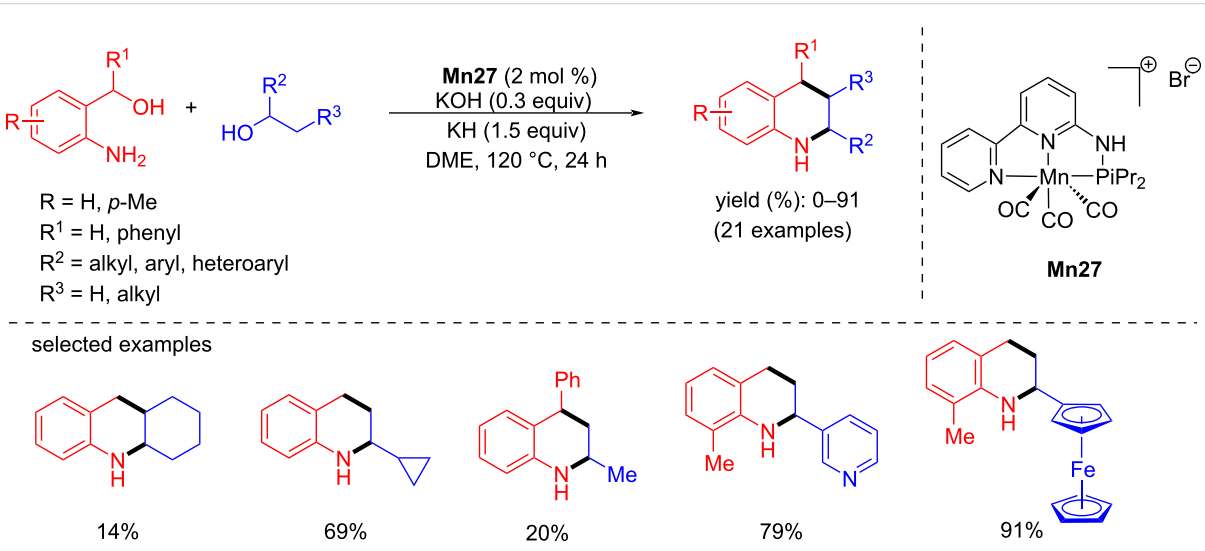

Scheme 74: Manganese-catalyzed tetrahydroquinoline synthesis via borrowing BH.

benzyl alcohols, including heteroaromatic alcohols, in good to excellent yield (69–89%) using 1 mol % of **Mn1**, 1.2 equiv of KOH as base in dioxane at 165 °C for 16 h (Scheme 77) [91].

Miscellaneous C-alkylation reactions

In 2020, Werner used a Mn-PNP pincer catalyst for the coupling of alcohols and ylides to build C–C and C=C bonds via BH and dehydrogenative coupling (not shown), respectively [98]. Using catalyst **Mn1** and *t*-BuOK (1:1) in 1,4-dioxane at 110–120 °C for 12–16 h, some substituted benzylic alcohols and ylides were screened to produce the desired products with a yield of up to 91% (Scheme 78). However, a high temperature (140 °C), a prolonged reaction time (30 h), and an excess of base (1.1 equiv of *t*-BuOK) were needed for the coupling of secondary alcohols with secondary ylides. The observed moderate yields (46–69%) of the desired products were due to the formation of dehydrogenative side products.

In 2021, Srimani and co-workers reported the C-alkylation and olefination (not shown) of fluorene and indene with alcohols using phosphine-free and air-stable Mn-NNS complexes [99]. Various types of alcohols, including aliphatic and secondary alcohols, were coupled with fluorene and indene, giving good to excellent yields (35–98%) of the desired alkylated products using **Mn24** (5 mol %), *t*-BuOK (1 equiv) in toluene at 130 °C for 24–36 h (Scheme 79). A similar C–C bond-formation mechanism was proposed in earlier reports. Fluorene coupled with the carbonyl compound in the presence of base led to the unsaturated compound, which was hydrogenated by **Mn24-c** to deliver the desired final product (Scheme 80).

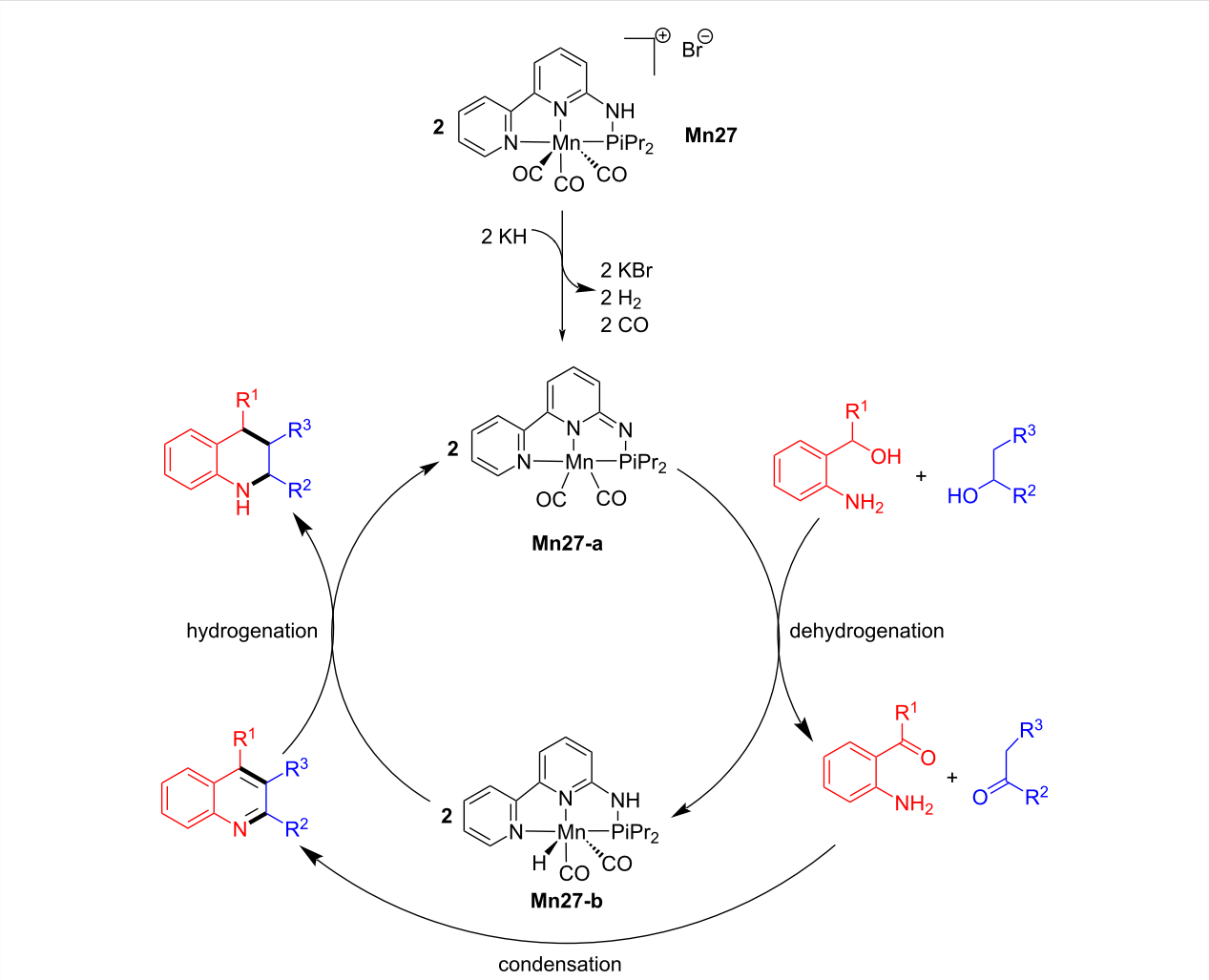

Scheme 75: Proposed mechanism for the manganese-catalyzed tetrahydroquinoline synthesis.

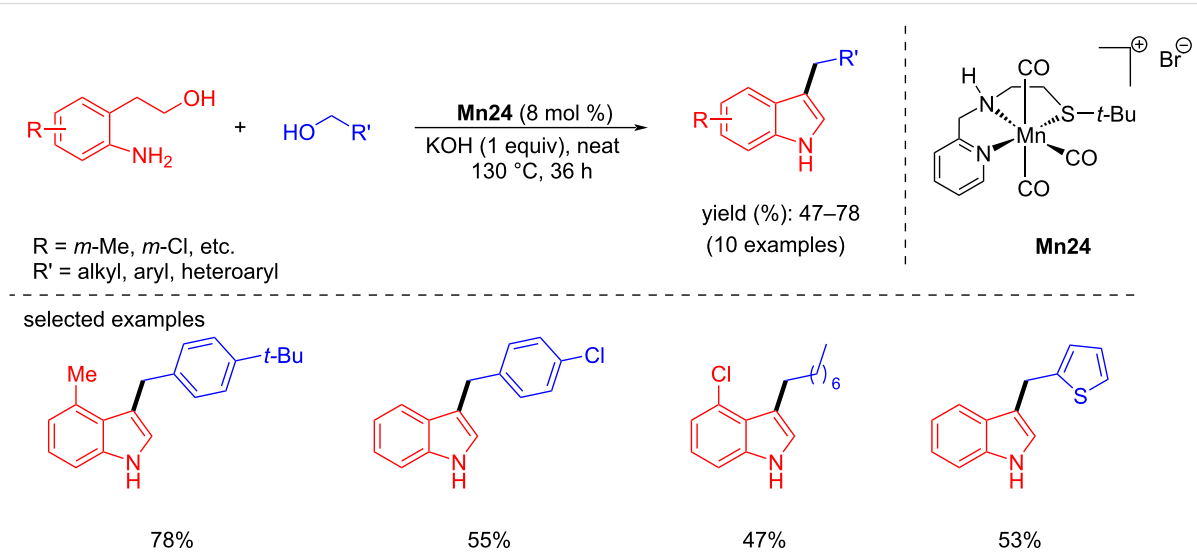

Scheme 76: Synthesis of C3-alkylated indoles using **Mn24**.

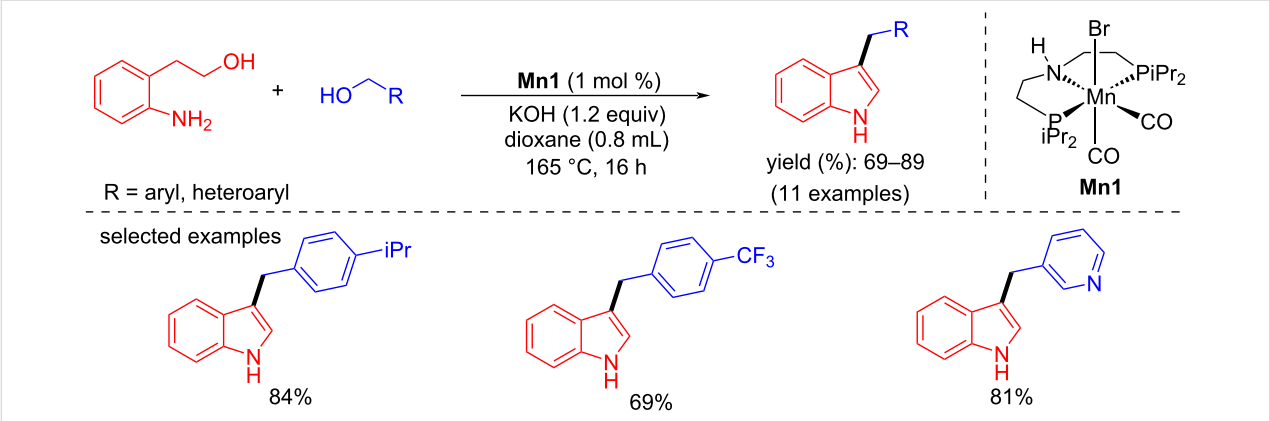

Scheme 77: Synthesis of C-3-alkylated indoles using **Mn1**.

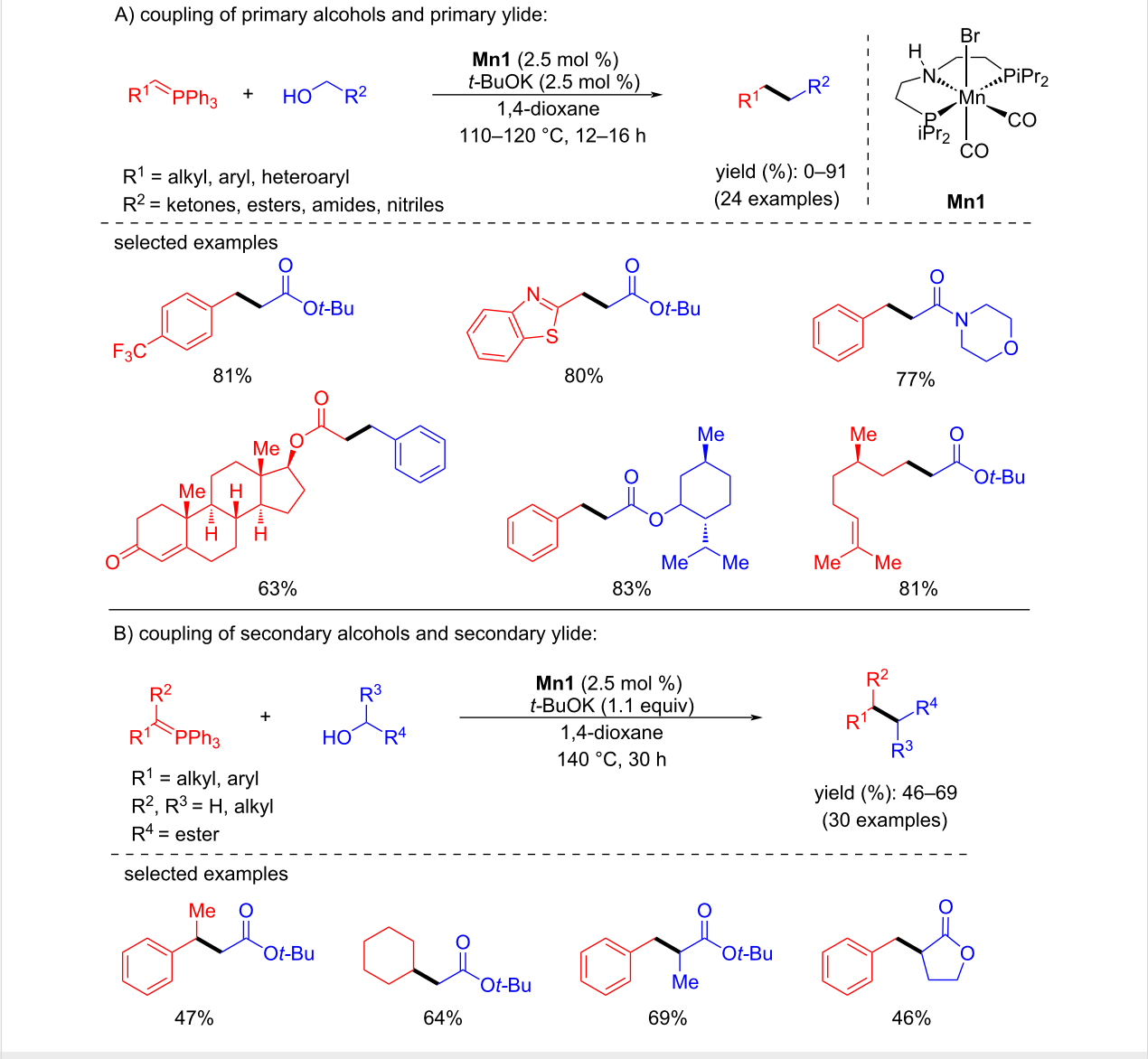

Scheme 78: C–C Bond formation by coupling of alcohols and ylides.

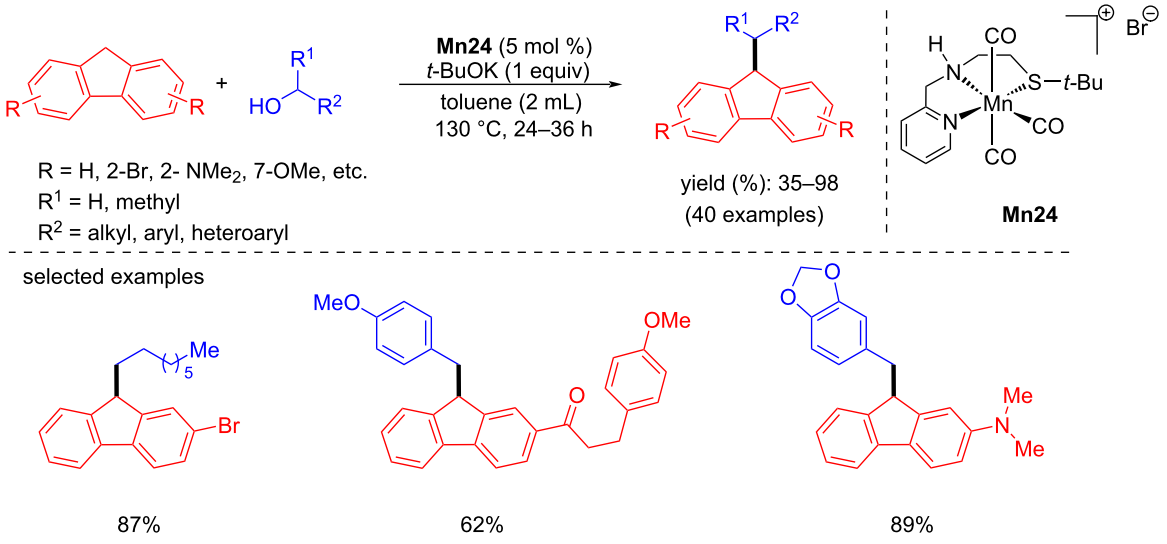

Scheme 79: C-Alkylation of fluorene with alcohols catalyzed by **Mn24**.

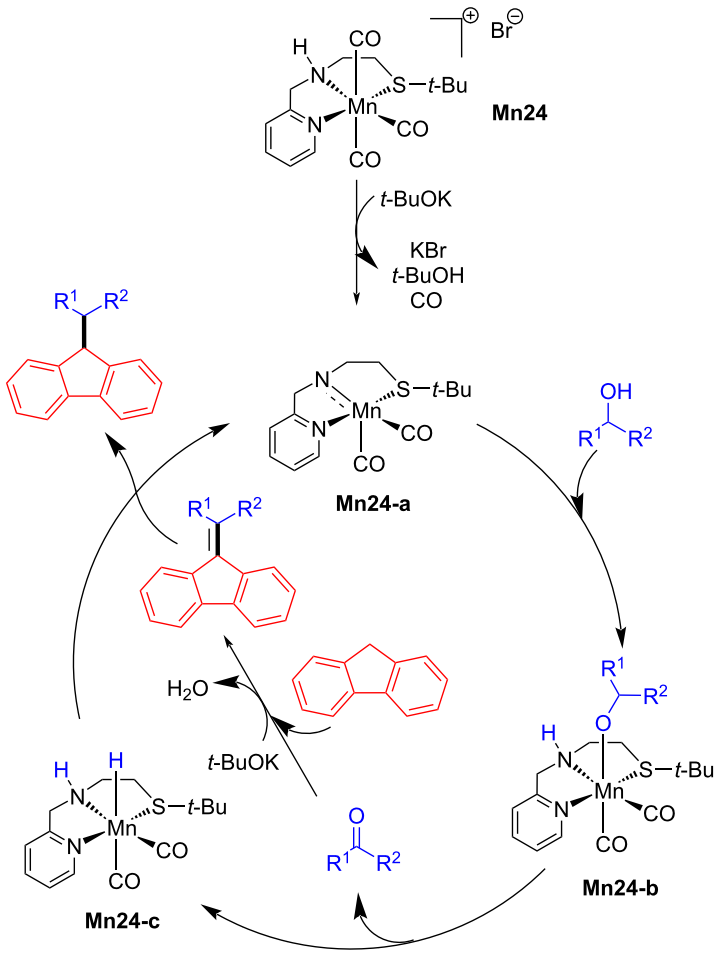

Scheme 80: Proposed mechanism for the C-alkylation of fluorene with alcohols catalyzed by **Mn24**.

In 2023, Milstein et al. reported the α-alkylation of sulfones catalyzed by a Mn-PNN catalyst using alcohols as an alkylating agent [100]. The reaction conditions were optimized with benzyl alcohols and methyl phenyl sulfones using four different catalysts. Among all, 0.5 mol % of **Mn28** and 20 mol % of NaOH in toluene at high temperature (150 °C) for 24 h gave better selectivity and yields towards the desired alkylated products. Under the optimized conditions, several alcohols were investigated and gave the products in isolated yields up to 99% (Scheme 81).

Conclusion

Manganese-catalyzed borrowing hydrogen reactions have emerged as powerful tools for C–C and C–N bond formation from readily available alcohols. A series of homogeneous manganese catalyst systems have been successfully established, and good catalytic activity and selectivity have been obtained for C-alkylation and N-alkylation reactions. As evident in the multicomponent reactions, manganese is recognized as a potent catalyst to replace the expensive iridium metal in BH reactions.

Though remarkable advances have been realized in manganese catalysis, the development of new and inexpensive ligand-supported manganese catalysts and a deeper understanding of the reaction mechanisms are expected to expand the efficiency and scope of this process. Compared to the classical BH with benzylic alcohols, the use of methanol and ethanol is really challenging since it requires a higher energy for the activation. Hence, increased catalyst or base loading and elevated temperature are needed for the N-methylation of amines with methanol compared to benzylic alcohols [41,44]. Similarly, to access heterocycles by coupling of amino alcohols and primary or secondary alcohols required harsh reaction conditions and high catalyst loading [43,90]. Hence, the development of efficient catalytic systems with base-free and mild reaction conditions for various applications such as multicomponent reactions, heterocycle synthesis, polymer synthesis, and upgrading of alcohols present exciting opportunities for future research in this field. We sincerely hope this review will provide insight towards the design of the new manganese catalysts and the study of C–C and C–N bond formation via BH reaction.

Funding

M. F. A. and A. K. M. thank IIT (BHU) for providing a research fellowship. S. E. thanks the Indian Institute of Technology (BHU), Varanasi, for the institute Seed grant and the Science and Engineering Research Board (SERB), India, for the start-up research grant (SRG/2023/000181).

Conflict of Interest

No interests are declared.

ORCID® iDs

Saravanakumar Elangovan - https://orcid.org/0000-0003-2694-9989

Data Availability Statement

Data sharing is not applicable as no new data was generated or analyzed in this study.

References

1. Ruiz-Castillo, P.; Buchwald, S. L. *Chem. Rev.* **2016,** *116,* 12564–12649. doi:10.1021/acs.chemrev.6b00512
2. Devendar, P.; Qu, R.-Y.; Kang, W.-M.; He, B.; Yang, G.-F. *J. Agric. Food Chem.* **2018,** *66,* 8914–8934. doi:10.1021/acs.jafc.8b03792
3. Leonard, J.; Blacker, A. J.; Marsden, S. P.; Jones, M. F.; Mulholland, K. R.; Newton, R. *Org. Process Res. Dev.* **2015,** *19,* 1400–1410. doi:10.1021/acs.oprd.5b00199
4. Corma, A.; Navas, J.; Sabater, M. J. *Chem. Rev.* **2018,** *118,* 1410–1459. doi:10.1021/acs.chemrev.7b00340

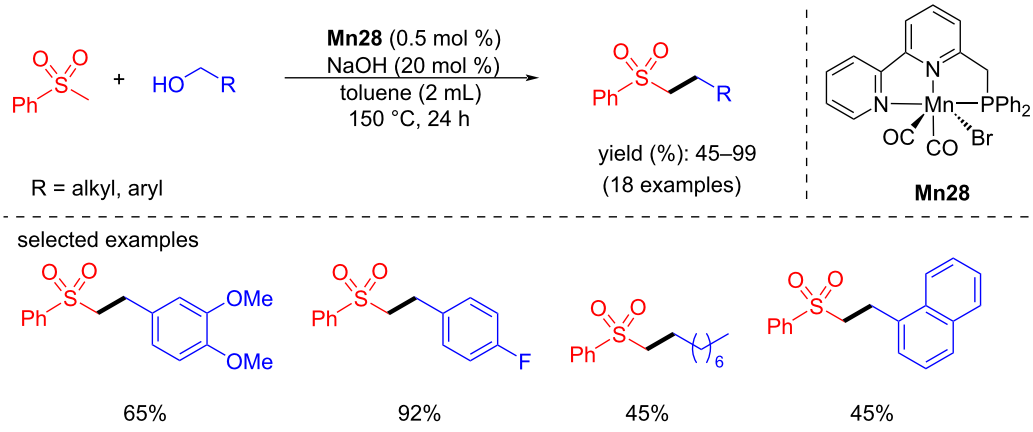

Scheme 81: α-Alkylation of sulfones using Mn-PNN catalyst **Mn28**.

5. Reed-Berendt, B. G.; Latham, D. E.; Dambatta, M. B.; Morrill, L. C. *ACS Cent. Sci.* **2021,** *7,* 570–585. doi:10.1021/acscentsci.1c00125
6. Nixon, T. D.; Whittlesey, M. K.; Williams, J. M. J. *Dalton Trans.* **2009,** 753–762. doi:10.1039/b813383b
7. Jafarzadeh, M.; Sobhani, S. H.; Gajewski, K.; Kianmehr, E. *Org. Biomol. Chem.* **2022,** *20,* 7713–7745. doi:10.1039/d2ob00706a
8. Nallagangula, M.; Subaramanian, M.; Kumar, R.; Balaraman, E. *Chem. Commun.* **2023,** *59,* 7847–7862. doi:10.1039/d3cc01517c
9. Yan, Q.; Wu, X.; Jiang, H.; Wang, H.; Xu, F.; Li, H.; Zhang, H.; Yang, S. *Coord. Chem. Rev.* **2024,** *502,* 215622. doi:10.1016/j.ccr.2023.215622
10. Corma, A.; Iborra, S.; Velty, A. *Chem. Rev.* **2007,** *107,* 2411–2502. doi:10.1021/cr050989d
11. Hamid, M. H. S. A.; Slatford, P. A.; Williams, J. M. J. *Adv. Synth. Catal.* **2007,** *349,* 1555–1575. doi:10.1002/adsc.200600638
12. Hameury, S.; Bensalem, H.; De Oliveira Vigier, K. *Catalysts* **2022,** *12,* 1306. doi:10.3390/catal12111306
13. Bullock, R. M. *Science* **2013,** *342,* 1054–1055. doi:10.1126/science.1247240
14. Reed-Berendt, B. G.; Polidano, K.; Morrill, L. C. *Org. Biomol. Chem.* **2019,** *17,* 1595–1607. doi:10.1039/c8ob01895b
15. Subaramanian, M.; Sivakumar, G.; Balaraman, E. *Chem. Rec.* **2021,** *21,* 3839–3871. doi:10.1002/tcr.202100165
16. Elangovan, S.; Topf, C.; Fischer, S.; Jiao, H.; Spannenberg, A.; Baumann, W.; Ludwig, R.; Junge, K.; Beller, M. *J. Am. Chem. Soc.* **2016,** *138,* 8809–8814. doi:10.1021/jacs.6b03709
17. Mukherjee, A.; Nerush, A.; Leitus, G.; Shimon, L. J. W.; Ben David, Y.; Espinosa Jalapa, N. A.; Milstein, D. *J. Am. Chem. Soc.* **2016,** *138,* 4298–4301. doi:10.1021/jacs.5b13519
18. Maji, B.; Barman, M. K. *Synthesis* **2017,** *49,* 3377–3393. doi:10.1055/s-0036-1590818
19. Wang, Y.; Wang, M.; Li, Y.; Liu, Q. *Chem* **2021,** *7,* 1180–1223. doi:10.1016/j.chempr.2020.11.013
20. Das, K.; Waiba, S.; Jana, A.; Maji, B. *Chem. Soc. Rev.* **2022,** *51,* 4386–4464. doi:10.1039/d2cs00093h
21. Rohit, K. R.; Radhika, S.; Saranya, S.; Anilkumar, G. *Adv. Synth. Catal.* **2020,** *362,* 1602–1650. doi:10.1002/adsc.201901389
22. Waiba, S.; Maji, B. *ChemCatChem* **2020,** *12,* 1891–1902. doi:10.1002/cctc.201902180
23. Nad, P.; Mukherjee, A. *Asian J. Org. Chem.* **2021,** *10,* 1958–1985. doi:10.1002/ajoc.202100249
24. Das, K.; Barman, M. K.; Maji, B. *Chem. Commun.* **2021,** *57,* 8534–8549. doi:10.1039/d1cc02512k
25. Lawrence, S. A. *Amines: Synthesis Properties, and Applications;* Cambridge University Press: Cambridge, UK, 2004.
26. Monnier, F.; Taillefer, M. *Angew. Chem., Int. Ed.* **2009,** *48,* 6954–6971. doi:10.1002/anie.200804497
27. Bagal, D. B.; Bhanage, B. M. *Adv. Synth. Catal.* **2015,** *357,* 883–900. doi:10.1002/adsc.201400940
28. Heravi, M. M.; Kheilkordi, Z.; Zadsirjan, V.; Heydari, M.; Malmir, M. *J. Organomet. Chem.* **2018,** *861,* 17–104. doi:10.1016/j.jorganchem.2018.02.023
29. Kalck, P.; Urrutigoïty, M. *Chem. Rev.* **2018,** *118,* 3833–3861. doi:10.1021/acs.chemrev.7b00667
30. Afanasyev, O. I.; Kuchuk, E.; Usanov, D. L.; Chusov, D. *Chem. Rev.* **2019,** *119,* 11857–11911. doi:10.1021/acs.chemrev.9b00383
31. Guillena, G.; Ramón, D. J.; Yus, M. *Chem. Rev.* **2010,** *110,* 1611–1641. doi:10.1021/cr9002159
32. Bähn, S.; Imm, S.; Neubert, L.; Zhang, M.; Neumann, H.; Beller, M. *ChemCatChem* **2011,** *3,* 1853–1864. doi:10.1002/cctc.201100255
33. Podyacheva, E.; Afanasyev, O. I.; Vasilyev, D. V.; Chusov, D. *ACS Catal.* **2022,** *12,* 7142–7198. doi:10.1021/acscatal.2c01133
34. Elangovan, S.; Neumann, J.; Sortais, J.-B.; Junge, K.; Darcel, C.; Beller, M. *Nat. Commun.* **2016,** *7,* 12641. doi:10.1038/ncomms12641
35. Neumann, J.; Elangovan, S.; Spannenberg, A.; Junge, K.; Beller, M. *Chem. – Eur. J.* **2017,** *23,* 5410–5413. doi:10.1002/chem.201605218
36. Bruneau-Voisine, A.; Wang, D.; Dorcet, V.; Roisnel, T.; Darcel, C.; Sortais, J.-B. *J. Catal.* **2017,** *347,* 57–62. doi:10.1016/j.jcat.2017.01.004
37. Fertig, R.; Irrgang, T.; Freitag, F.; Zander, J.; Kempe, R. *ACS Catal.* **2018,** *8,* 8525–8530. doi:10.1021/acscatal.8b02530
38. Das, U. K.; Ben-David, Y.; Diskin-Posner, Y.; Milstein, D. *Angew. Chem., Int. Ed.* **2018,** *57,* 2179–2182. doi:10.1002/anie.201712593
39. Landge, V. G.; Mondal, A.; Kumar, V.; Nandakumar, A.; Balaraman, E. *Org. Biomol. Chem.* **2018,** *16,* 8175–8180. doi:10.1039/c8ob01886c
40. Reed-Berendt, B. G.; Morrill, L. C. *J. Org. Chem.* **2019,** *84,* 3715–3724. doi:10.1021/acs.joc.9b00203
41. Huang, M.; Li, Y.; Li, Y.; Liu, J.; Shu, S.; Liu, Y.; Ke, Z. *Chem. Commun.* **2019,** *55,* 6213–6216. doi:10.1039/c9cc02989c
42. Homberg, L.; Roller, A.; Hultzsch, K. C. *Org. Lett.* **2019,** *21,* 3142–3147. doi:10.1021/acs.orglett.9b00832
43. Azizi, K.; Akrami, S.; Madsen, R. *Chem. – Eur. J.* **2019,** *25,* 6439–6446. doi:10.1002/chem.201900737
44. Reed-Berendt, B. G.; Mast, N.; Morrill, L. C. *Eur. J. Org. Chem.* **2020,** 1136–1140. doi:10.1002/ejoc.201901854
45. Das, K.; Kumar, A.; Jana, A.; Maji, B. *Inorg. Chim. Acta* **2020,** *502,* 119358. doi:10.1016/j.ica.2019.119358
46. Wei, D.; Yang, P.; Yu, C.; Zhao, F.; Wang, Y.; Peng, Z. *J. Org. Chem.* **2021,** *86,* 2254–2263. doi:10.1021/acs.joc.0c02407
47. Babu, R.; Sukanya Padhy, S.; Kumar, R.; Balaraman, E. *Chem. – Eur. J.* **2023,** *29,* e202302007. doi:10.1002/chem.202302007
48. Brodie, C. N.; Owen, A. E.; Kolb, J. S.; Bühl, M.; Kumar, A. *Angew. Chem., Int. Ed.* **2023,** *62,* e202306655. doi:10.1002/anie.202306655
49. Friães, S.; Gomes, C. S. B.; Royo, B. *Organometallics* **2023,** *42,* 1803–1809. doi:10.1021/acs.organomet.3c00046
50. Miyaura, N.; Suzuki, A. *Chem. Rev.* **1995,** *95,* 2457–2483. doi:10.1021/cr00039a007
51. Zheng, Y.-L.; Newman, S. G. *Chem. Commun.* **2021,** *57,* 2591–2604. doi:10.1039/d0cc08389e
52. Reetz, M. T. *Angew. Chem., Int. Ed. Engl.* **1982,** *21,* 96–108. doi:10.1002/anie.198200961
53. Caine, D. *Alkylations of Enols and Enolates*. *Comprehensive Organic Synthesis;* Pergamon Press: Oxford, UK, 1991; Vol. 3, pp 1–63. doi:10.1016/b978-0-08-052349-1.00058-5
54. Zhao, F.; Tan, B.; Li, Q.; Tan, Q.; Huang, H. *Molecules* **2022,** *27,* 8977. doi:10.3390/molecules27248977
55. Huang, F.; Liu, Z.; Yu, Z. *Angew. Chem., Int. Ed.* **2016,** *55,* 862–875. doi:10.1002/anie.201507521
56. Yang, D.-Y.; Wang, H.; Chang, C.-R. *Adv. Synth. Catal.* **2022,** *364,* 3100–3121. doi:10.1002/adsc.202200474
57. Peña-López, M.; Piehl, P.; Elangovan, S.; Neumann, H.; Beller, M. *Angew. Chem., Int. Ed.* **2016,** *55,* 14967–14971. doi:10.1002/anie.201607072
58. Barman, M. K.; Jana, A.; Maji, B. *Adv. Synth. Catal.* **2018,** *360,* 3233–3238. doi:10.1002/adsc.201800380

59. Chakraborty, S.; Daw, P.; Ben David, Y.; Milstein, D. *ACS Catal.* **2018,** *8,* 10300–10305. doi:10.1021/acscatal.8b03720
60. Kabadwal, L. M.; Das, J.; Banerjee, D. *Chem. Commun.* **2018,** *54,* 14069–14072. doi:10.1039/c8cc08010k
61. Sklyaruk, J.; Borghs, J. C.; El-Sepelgy, O.; Rueping, M. *Angew. Chem., Int. Ed.* **2019,** *58,* 775–779. doi:10.1002/anie.201810885
62. Bruneau-Voisine, A.; Pallova, L.; Bastin, S.; César, V.; Sortais, J.-B. *Chem. Commun.* **2019,** *55,* 314–317. doi:10.1039/c8cc08064j
63. Gawali, S. S.; Pandia, B. K.; Pal, S.; Gunanathan, C. *ACS Omega* **2019,** *4,* 10741–10754. doi:10.1021/acsomega.9b01246
64. Lan, X.-B.; Ye, Z.; Huang, M.; Liu, J.; Liu, Y.; Ke, Z. *Org. Lett.* **2019,** *21,* 8065–8070. doi:10.1021/acs.orglett.9b03030
65. Kaithal, A.; Gracia, L.-L.; Camp, C.; Quadrelli, E. A.; Leitner, W. *J. Am. Chem. Soc.* **2019,** *141,* 17487–17492. doi:10.1021/jacs.9b08832
66. Jana, A.; Das, K.; Kundu, A.; Thorve, P. R.; Adhikari, D.; Maji, B. *ACS Catal.* **2020,** *10,* 2615–2626. doi:10.1021/acscatal.9b05567
67. Waiba, S.; Jana, S. K.; Jati, A.; Jana, A.; Maji, B. *Chem. Commun.* **2020,** *56,* 8376–8379. doi:10.1039/d0cc01460e
68. Patra, K.; Laskar, R. A.; Nath, A.; Bera, J. K. *Organometallics* **2022,** *41,* 1836–1846. doi:10.1021/acs.organomet.2c00085
69. Thenarukandiyil, R.; Kamte, R.; Garhwal, S.; Effnert, P.; Fridman, N.; de Ruiter, G. *Organometallics* **2023,** *42,* 62–71. doi:10.1021/acs.organomet.2c00520
70. Jalwal, S.; Regina, A.; Atreya, V.; Paranjothy, M.; Chakraborty, S. *Dalton Trans.* **2024,** *53,* 3236–3243. doi:10.1039/d3dt04321e
71. Liu, T.; Wang, L.; Wu, K.; Yu, Z. *ACS Catal.* **2018,** *8,* 7201–7207. doi:10.1021/acscatal.8b01960
72. El-Sepelgy, O.; Matador, E.; Brzozowska, A.; Rueping, M. *ChemSusChem* **2019,** *12,* 3099–3102. doi:10.1002/cssc.201801660
73. Liu, Y.; Shao, Z.; Wang, Y.; Xu, L.; Yu, Z.; Liu, Q. *ChemSusChem* **2019,** *12,* 3069–3072. doi:10.1002/cssc.201802689
74. Schlagbauer, M.; Kallmeier, F.; Irrgang, T.; Kempe, R. *Angew. Chem., Int. Ed.* **2020,** *59,* 1485–1490. doi:10.1002/anie.201912055
75. Lan, X.-B.; Ye, Z.; Liu, J.; Huang, M.; Shao, Y.; Cai, X.; Liu, Y.; Ke, Z. *ChemSusChem* **2020,** *13,* 2557–2563. doi:10.1002/cssc.202000576
76. Sun, F.; Huang, J.; Wei, Z.; Tang, C.; Liu, W. *Angew. Chem., Int. Ed.* **2023,** *62,* e202303433. doi:10.1002/anie.202303433
77. Waiba, S.; Maji, K.; Maiti, M.; Maji, B. *Angew. Chem., Int. Ed.* **2023,** *62,* e202218329. doi:10.1002/anie.202218329
78. Jang, Y. K.; Krückel, T.; Rueping, M.; El-Sepelgy, O. *Org. Lett.* **2018,** *20,* 7779–7783. doi:10.1021/acs.orglett.8b03184
79. Rana, J.; Gupta, V.; Balaraman, E. *Dalton Trans.* **2019,** *48,* 7094–7099. doi:10.1039/c8dt05020a
80. Jana, A.; Reddy, C. B.; Maji, B. *ACS Catal.* **2018,** *8,* 9226–9231. doi:10.1021/acscatal.8b02998
81. Borghs, J. C.; Tran, M. A.; Sklyaruk, J.; Rueping, M.; El-Sepelgy, O. *J. Org. Chem.* **2019,** *84,* 7927–7935. doi:10.1021/acs.joc.9b00792
82. Horton, D. A.; Bourne, G. T.; Smythe, M. L. *Chem. Rev.* **2003,** *103,* 893–930. doi:10.1021/cr020033s
83. Somei, M.; Yamada, F. *Nat. Prod. Rep.* **2004,** *21,* 278–311. doi:10.1039/b212257j
84. Shiri, M. *Chem. Rev.* **2012,** *112,* 3508–3549. doi:10.1021/cr2003954
85. Elebiju, O. F.; Ajani, O. O.; Oduselu, G. O.; Ogunnupebi, T. A.; Adebiyi, E. *Front. Chem. (Lausanne, Switz.)* **2023,** *10,* 1074331. doi:10.3389/fchem.2022.1074331
86. Mastalir, M.; Pittenauer, E.; Allmaier, G.; Kirchner, K. *J. Am. Chem. Soc.* **2017,** *139,* 8812–8815. doi:10.1021/jacs.7b05253
87. Borghs, J. C.; Zubar, V.; Azofra, L. M.; Sklyaruk, J.; Rueping, M. *Org. Lett.* **2020,** *22,* 4222–4227. doi:10.1021/acs.orglett.0c01270
88. Jana, A.; Kumar, A.; Maji, B. *Chem. Commun.* **2021,** *57,* 3026–3029. doi:10.1039/d1cc00181g
89. Rana, J.; Nagarasu, P.; Subaramanian, M.; Mondal, A.; Madhu, V.; Balaraman, E. *Organometallics* **2021,** *40,* 627–634. doi:10.1021/acs.organomet.1c00009
90. Mondal, A.; Sharma, R.; Dutta, B.; Pal, D.; Srimani, D. *J. Org. Chem.* **2022,** *87,* 3989–4000. doi:10.1021/acs.joc.1c02702
91. Zhao, M.; Li, X.; Zhang, X.; Shao, Z. *Chem. – Asian J.* **2022,** *17,* e202200483. doi:10.1002/asia.202200483
92. Saini, P.; Dolui, P.; Nair, A.; Verma, A.; Elias, A. J. *Chem. – Asian J.* **2023,** *18,* e202201148. doi:10.1002/asia.202201148
93. Mondal, A.; Kumar, R.; Suresh, A. K.; Sahoo, M. K.; Balaraman, E. *Catal. Sci. Technol.* **2023,** *13,* 5745–5756. doi:10.1039/d3cy01044a
94. Deibl, N.; Kempe, R. *Angew. Chem., Int. Ed.* **2017,** *56,* 1663–1666. doi:10.1002/anie.201611318
95. Kallmeier, F.; Dudziec, B.; Irrgang, T.; Kempe, R. *Angew. Chem., Int. Ed.* **2017,** *56,* 7261–7265. doi:10.1002/anie.201702543
96. Borghs, J. C.; Azofra, L. M.; Biberger, T.; Linnenberg, O.; Cavallo, L.; Rueping, M.; El-Sepelgy, O. *ChemSusChem* **2019,** *12,* 3083–3088. doi:10.1002/cssc.201802416
97. Hofmann, N.; Homberg, L.; Hultzsch, K. C. *Org. Lett.* **2020,** *22,* 7964–7970. doi:10.1021/acs.orglett.0c02905
98. Liu, X.; Werner, T. *Adv. Synth. Catal.* **2021,** *363,* 1096–1104. doi:10.1002/adsc.202001209
99. Mondal, A.; Sharma, R.; Pal, D.; Srimani, D. *Chem. Commun.* **2021,** *57,* 10363–10366. doi:10.1039/d1cc03529k
100. Lu, L.; Luo, J.; Milstein, D. *ACS Catal.* **2023,** *13,* 5949–5954. doi:10.1021/acscatal.3c00369

License and Terms

BEILSTEIN JOURNAL OF ORGANIC CHEMISTRY

Generation of alkyl and acyl radicals by visible-light photoredox catalysis: direct activation of C–O bonds in organic transformations

Mithu Roy, Bitan Sardar, Itu Mallick and Dipankar Srimani*

Review

Open Access

Address:
Department of Chemistry, Indian Institute of Technology-Guwahati, Kamrup, Assam 781039, India

Email:
Dipankar Srimani* - dsrimani@iitg.ac.in

* Corresponding author

Keywords:
acyl radical; alkyl radical; sustainable catalysis; visible light

Beilstein J. Org. Chem. **2024,** *20,* 1348–1375.
https://doi.org/10.3762/bjoc.20.119

Received: 30 January 2024
Accepted: 27 May 2024
Published: 14 June 2024

This article is part of the thematic issue "Sustainable concepts in catalysis: nonprecious metals and visible light".

Guest Editor: O. El-Sepelgy

Abstract

Alkyl and acyl radicals play a critical role in the advancement of chemical synthesis. The generation of acyl and alkyl radicals by activation of C–O bonds using visible-light photoredox catalysis offers a mild and environmentally benign approach to useful chemical transformations. Alcohols, carboxylic acids, anhydrides, xanthates, oxalates, *N*-phthalimides, and thiocarbonates are some examples of alkyl and acyl precursors that can produce reactive radicals by homolysis of the C–O bond. These radicals can then go through a variety of transformations that are beneficial for the construction of synthetic materials that are otherwise difficult to access. This study summarizes current developments in the use of organic photocatalysts, transition-metal photoredox catalysts, and metallaphotocatalysts to produce acyl and alkyl radicals driven by visible light.

Introduction

The growing awareness of the necessity for sustainable developments has been heightened by the current energy crisis and the adverse impacts of industrialization. The development of green and energy-efficient methods in organic chemistry that use renewable sources of starting materials is considered highly sustainable [1-3]. Radical reactions have profound applications in organic synthesis [4-9]. In the context of sustainable catalysis, visible-light-mediated chemistry is becoming a prominent viable option for radical transformations in the synthesis of biologically useful compounds due to the energy efficiency and environmental friendliness [10,11]. Recently, the photocatalytic and electrochemical deoxygenation of acids and alcohols has attracted significant attention as the strategic cleavage of the C–O bond is quite challenging and opens up new possibilities for constructing useful compounds [12-14].

The use of photogenerated carbon-centered radicals, such as acyl and alkyl radicals, has shown great promise in the synthe-

sis and functionalization of various organic molecules [15,16]. These carbon radicals can be generated in several ways. The first and most straightforward method is the homolytic cleavage of labile C–heteroatom bonds, especially alkyl halides [17]. Due to growing concerns about the harmful effects of toxic compounds (e.g., some halides) on the environment, the scientific community is now looking for alternative chemicals that can form these radicals. Moreover, discovering mild strategic approaches for the generation of unstabilized alkyl and acyl radicals and maintaining a high degree of selectivity with respect to the desired outcome are key obstacles to the growth of alkyl and acyl radical chemistry. With this in mind, the emergence of new chemical transformations involving radicals generated via C–O bond cleavage by visible light becomes significant.

$C(sp^3)$–O bonds are ubiquitous in nature and can be easily found in biochemical feedstocks, such as alcohols and acids. On the other hand, alcohols and acids are easily accessible. Although the starting materials are abundant, the C–O bond strength and the high redox potential impede the progress of photoredox-mediated catalysis in this domain [18]. Conventional procedures, such as Barton–McCombie deoxygenation [19] and use of thiocarbonyl-based activating groups [20], are quite popular. However, they have certain limitations, such as the use of toxic reagents, high temperature, and UV light [21], among others. Recent advancements include the photoinduced deoxygenation of acids and alcohols by means of anhydride, xanthate, carboxylate, oxalate, and *N*-alkoxyphthalimide functionalization (Figure 1) and utilization in visible-light-mediated chemical transformations. Despite the great importance of these strategies, the direct use of acids or alcohols is more fascinating as this approach circumvents the additional synthesis of special functionalized compounds. The strategy involves in situ activation by appropriate reagent, followed by photochemical C–O bond scission to directly access acyl or alkyl radicals from carboxylic acids or alcohols, thereby eliminating the need for an extra step. As a result, such methods are continuously gaining popularity.

This review delves into the current state of deoxygenation processes, focusing on techniques that use visible-light irradiation to harness the reactivity of alcohols and acids both upon derivatization and through direct use. By exploring recent advancements in deoxygenation reactions and the design of potential reactants, we aim to give an overview of the diverse strategies that highlight the unique reaction design and promote green chemistry principles. In this regard, in 2019, Banerjee et al. published a review article on the generation of acyl radicals in the presence of visible light [22]. Therein, they discussed the various ways in which visible light can generate acyl radicals from different organic molecules to facilitate important chemical reactions. Thus, we will focus on the reports detailing organic transformations that proceed via visible-light-induced deoxygenative generation of acyl radicals from carboxylic acids and acid anhydrides that have appeared since 2019.

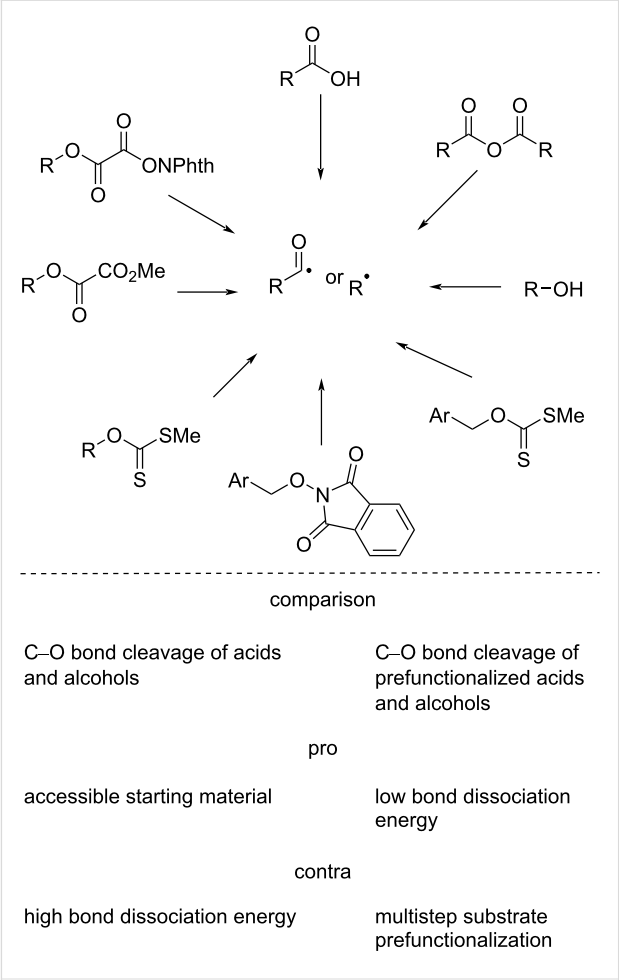

Figure 1: Generation of alkyl and acyl radicals via C–O bond breaking.

Review

General mechanism of photoredox catalysis

In recent times, visible-light-mediated photoredox chemistry has evolved as a unique tool for various organic transformations. In contrast to traditional catalysis, the photochemical process uses an electron or energy transfer mechanism to form reactive intermediates. Typically, a photocatalyst is triggered to carry out energy transfer and electron transfer or proton-coupled electron transfer when it absorbs light of an appropriate wavelength (Figure 2). These processes generate highly reactive species, such as radical cations or anions, which can initiate the desired organic transformations. Different photocatalysts, such as transition metal complexes [23,24], organic dyes [25], and semiconductors [26], can be employed for visible-light-induced chemical processes. The choice of photocatalyst depends on the

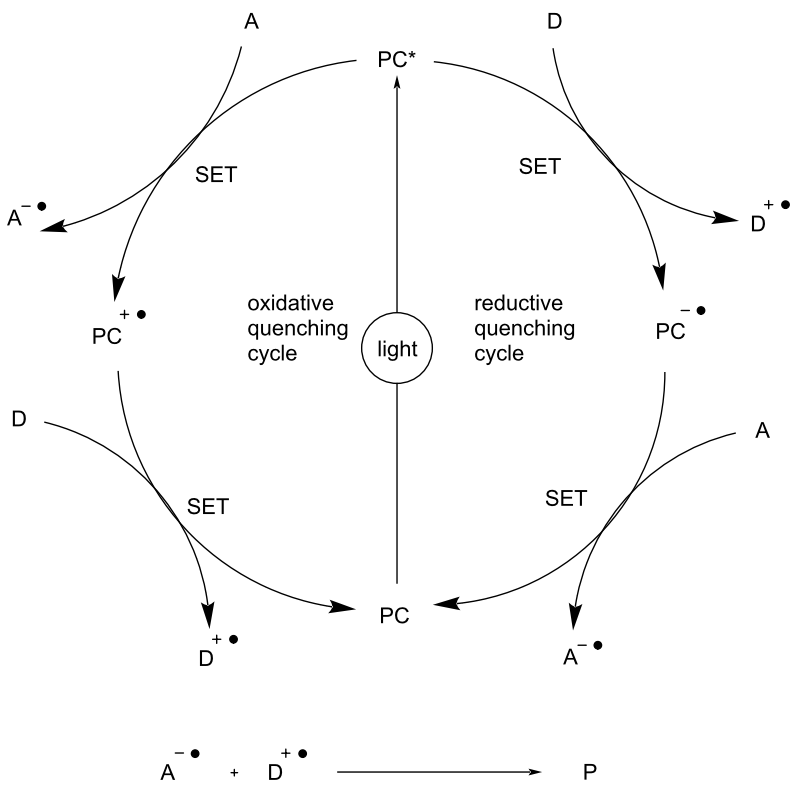

Figure 2: General photocatalytic mechanism.

specific requirements of the catalytic process, including the type of reaction, the targeted absorption wavelength, and the overall efficacy. Researchers continue to explore and design photocatalysts to enhance the performance in various photocatalytic applications.

Visible-light-induced photoredox catalysis has been used in a variety of chemical reactions, including C–C, C–N, C–O, and C–halogen bond formation, as well as C–H functionalization [27]. Some notable examples include C–H arylation, various cross-coupling reactions, oxidative coupling, and photocatalytic radical reactions. The advantages of visible-light-induced photoredox catalysis are due to the ability to utilize visible light, a sustainable and abundant energy source, to initiate chemical reactions. This approach offers milder reaction conditions, which often result in improved selectivity and functional group compatibility. Additionally, it allows the activation of typically inert bonds and can enable the development of novel synthetic strategies. It has expanded the scope of available synthetic methods and contributed to the synthesis of complex molecules with high efficiency and selectivity. Ongoing research in this field continues to explore new catalysts, photosensitizers, and reaction mechanisms to further advance the field of visible-light-mediated organic transformations.

This review describes techniques for the generation of alkyl and acyl radicals by breaking the C–O bonds of various reactants with visible light and how to use them in organic transformations.

Reactions involving acyl radicals obtained via C–O bond cleavage

Direct C–O bond activation of acids

In visible-light photoredox catalysis, simple and affordable carboxylic acids and acid anhydrides can be utilized as good acyl radical sources for the deoxygenation approach. Acyl radicals can be generated through the use of photocatalysts, such as iridium complexes or organic dyes, and activating agents, including dimethyl dicarbonate (DMDC) and PPh_3. Redox-active esters are created when activating agents and carboxylic acids react. These esters can then be reduced using a photoredox catalyst to produce the acyl radical. In 2019, Doyle [28] introduced the photoredox-catalyzed hydroacylation of styrene derivatives via deoxygenation of challenging aliphatic carboxylic acids (Scheme 1). The deoxygenation was promoted by phosphine reagents to form acyl radicals. The acyl radicals reacted with the C=C bond and formed the expected product. Appropriate selection of the phosphine reagent was the key to success in the process. Due to the lower oxidation potential, electron-rich

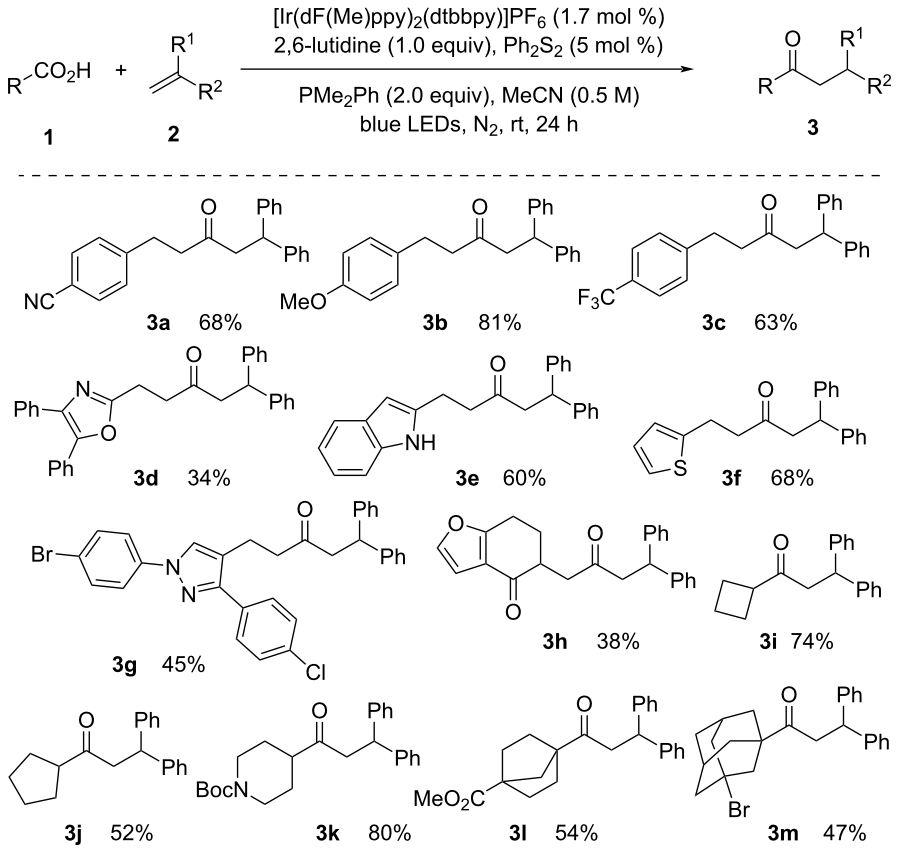

Scheme 1: Photoredox-catalyzed hydroacylation of olefins with aliphatic carboxylic acids.

PMe_2Ph preferentially transferred a single electron to the excited state of the photocatalyst rather than the alkene, which was essential for obtaining the desired product in a satisfactory yield.

Various hydrocinnamic acids having electron-donating and electron-withdrawing substituents provided the targeted products **3a**–**c** in good yield. Heterocycles containing carboxylic acids also provided the products **3d**–**g** in moderate to good yield. Aliphatic carboxylic acids, under optimized or slightly modified conditions, cyclic secondary, and tertiary alkyl carboxylic acids were smoothly coupled with 1,1-diphenylethylene to give **3i**–**m**.

α,α′-Diarylated ketones serve as crucial building blocks in the construction of both natural and synthetic compounds with significant biological relevance. In 2022, Yu et al. [29] showcased a very mild procedure for the effective synthesis of α,α′-diarylated ketones (Scheme 2). Compared to previous procedures, this methodology was a significant improvement as it did not require an excessive amount of additives or high temperature. The methodology was applicable to various carboxylic acids with electron-donating as well as electron-withdrawing substituents but unfortunately, aliphatic acids were not effective in this reaction. In addition, several control experiments, such as fluorescence quenching and Stern–Volmer studies, were done to analyze the SET transfer process of PPh_3 and quenching of photoexcited *$[Ir(dF(CF_3)ppy)_2(bpy)]PF_6$ by PPh_3.

Fluorinated organic compounds are widely used in pharmaceuticals and pesticides. Therefore, it is crucial to diversify organic scaffolds by addition of fluorinated groups or by defluorination. In 2020, Wang and co-workers [30] demonstrated the photomediated synthesis of γ,γ-difluoroallylic ketones by reacting trifluoromethyl alkenes and acids in the presence of PPh_3 additive and iridium photocatalyst in basic medium (Scheme 3). This methodology was suitable for a wide range of carboxylic acids in the presence of alkene, alkyne, halogen, and ether moieties. *N*-Boc-protected amines and esters also provided a good to excellent yield. Unfortunately, α,β-unsaturated carboxylic acids and aliphatic carboxylic acids were ineffective using this method.

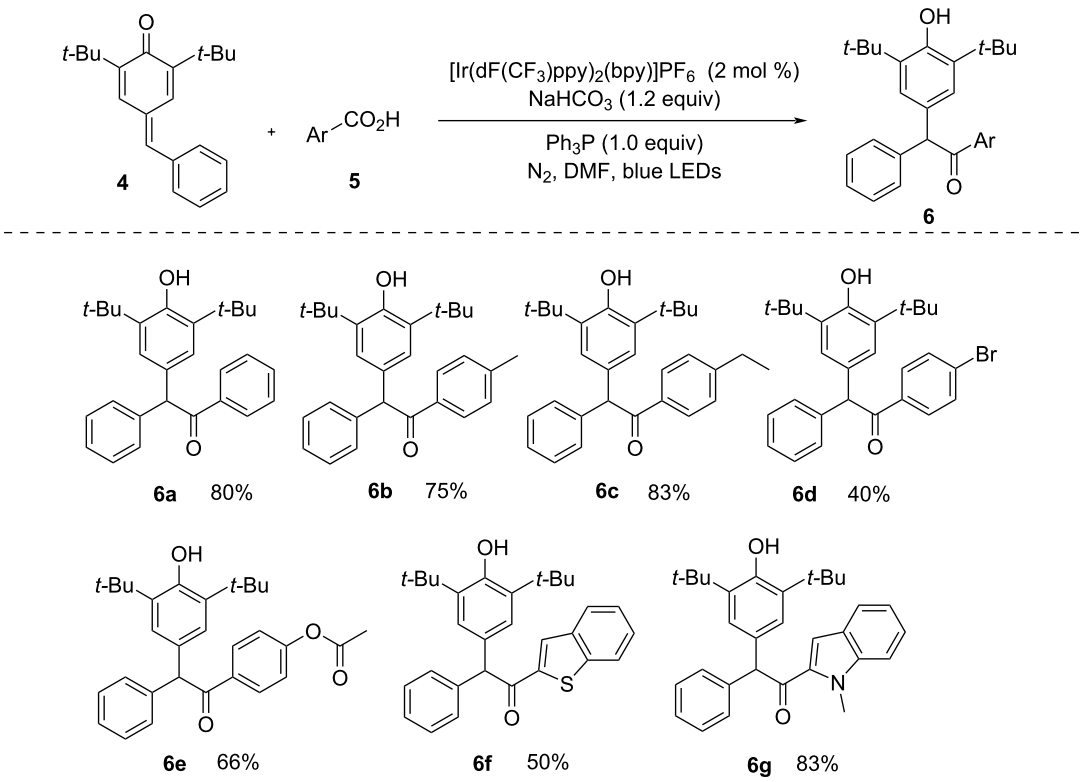

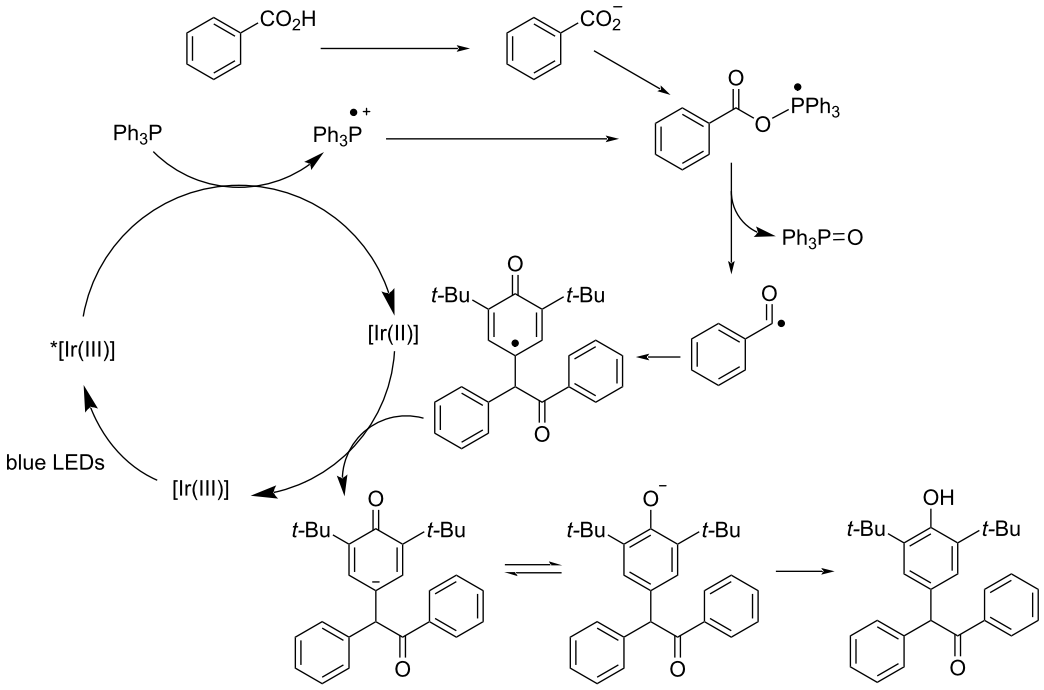

Scheme 2: Acylation–aromatization of *p*-quinone methides using carboxylic acids.

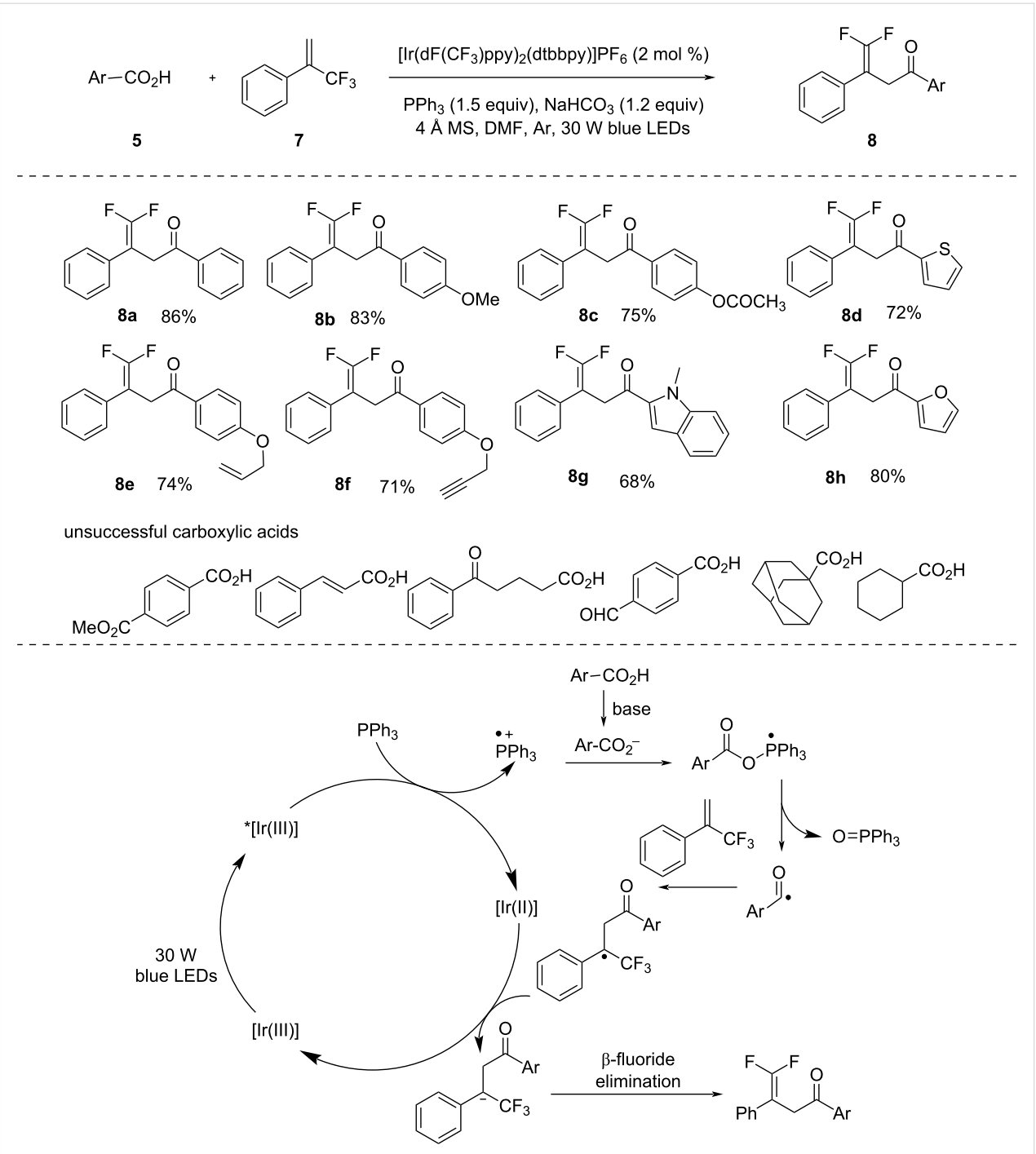

Scheme 3: Visible-light-induced deoxygenation–defluorination for the synthesis of γ,γ-difluoroallylic ketones.

In 2024, Liu and co-workers [31] introduced a photocatalytic hydroacylation of azobenzenes employing acids as hydroacylating reagents (Scheme 4). The reaction progressed smoothly, involving the cleavage of the C–O bond using a photogenerated phosphoranyl radical. The methodology demonstrated an excellent compatibility with a wide range of azobenzenes and carboxylic acids, yielding diverse *N*,*N*′-diarylhydrazides. This class of compounds is traditionally challenging to synthesize, making this approach a valuable alternative. The method offers a mild and effective way to create *N*,*N*′-diarylhydrazides using easily accessible starting materials.

Initially, photoexcitation of the iridium photocatalyst $[Ir(dF(CF_3)ppy)_2(dtbbpy)]PF_6$ leads to excited-state *[Ir(III)],

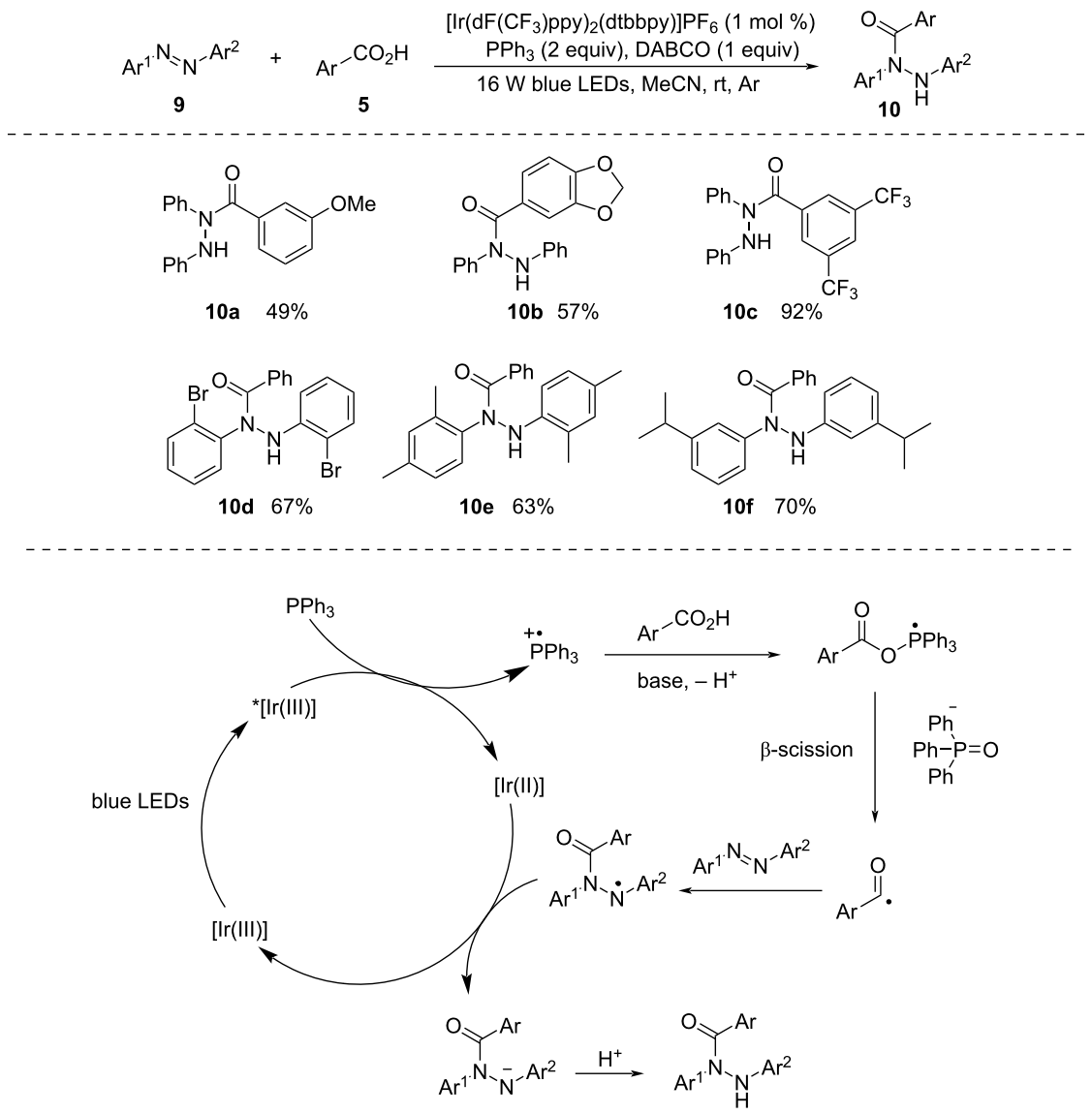

Scheme 4: Photochemical hydroacylation of azobenzenes with carboxylic acids.

E_{red} (*[Ir(III)]/[Ir(II)]) = +1.21 V, possessing sufficient energy to oxidize PPh_3, forming the triphenylphosphine radical cation. Subsequently, benzoic acid undergoes deprotonation facilitated by a base, producing benzoate. This benzoate then reacts with the triphenylphosphine radical cation, resulting in the formation of the phosphoranyl radical intermediate, which undergoes β-scission, leading to the formation of a benzoyl radical, accompanied by the liberation of a triphenylphosphine oxide molecule. After this, the addition of the benzoyl radical to azobenzene results in the generation of a nitrogen-centered radical. This radical is then subjected to reduction by the reduced photocatalyst, producing the nitrogen-centered anion intermediate. Ultimately, the protonation of this anion gives rise to the desired product.

The photomediated formation of acyl radicals directly from acids mostly employs DMDC or phosphines (e.g., PPh_3, PMe_2Ph) as additives and [Ir(III)] as photocatalyst. In 2022, Chu and co-workers [32] developed a protocol to form acyl radicals directly from acids utilizing Ph_2S as activator and the organic dye Mes–Acr–$MeClO_4$ as photocatalyst (Scheme 5). They demonstrated intermolecular radical cyclization of *o*-hydroxybenzoic acid derivatives with terminal alkynes to afford flavone derivatives. Here, functionally diverse flavonoids

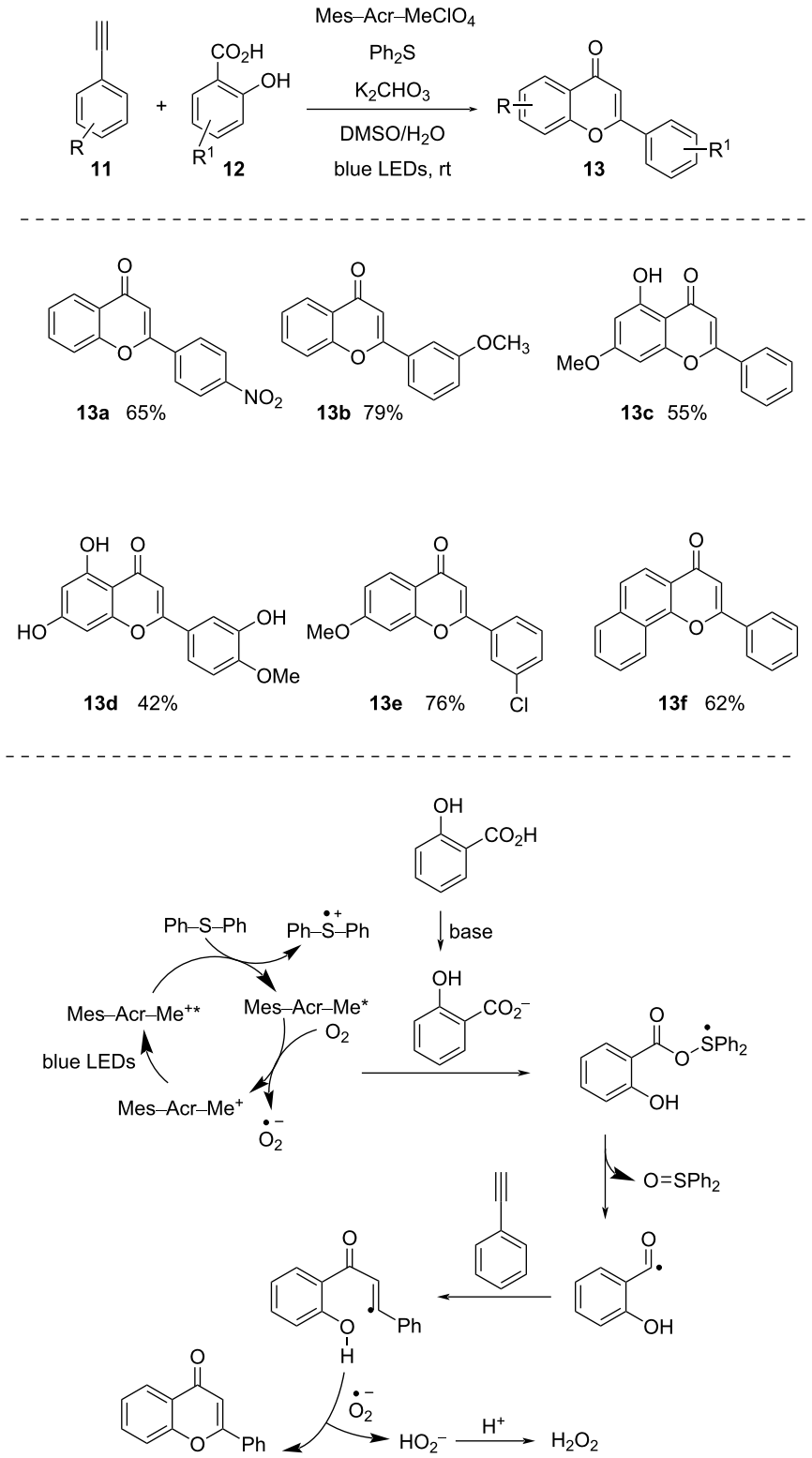

Scheme 5: Photoredox-catalyzed synthesis of flavonoids.

were synthesized in moderate to excellent yield by reacting various salicylic acid derivatives and aryl acetylenes.

Due to irradiation with blue light, Mes–Acr–Me^+ gets excited to Mes–Acr–Me^{+}* and takes up a single electron from Ph_2S. The reaction of the diphenyl sulfide radical cation with carboxylate and successive acyloxy C–O bond cleavage forms diphenyl sulfoxide and an acyl radical. This acyl radical eventually leads to the formation of expected product.

Reactions involving alkyl radical obtained via C–O bond cleavage

C–O bond activation of prefunctionalized alcohols

Alkyl radicals play a crucial role as intermediates in various chemical transformations involving C–H, C–C, and C–heteroatom bond formations. The best known technique for the creation of alkyl radicals is the homolytic cleavage of the C–X bond of alkyl halides by toxic tin hydride [17]. Later, various efforts have been made to replace toxic tin hydrides with other reagents [33-42]. However, these protocols have a limited scope and suffer from prefunctionalization and waste generation. Photons are considered the greenest reagent in organic synthesis. Thus, photomediated alkyl radical generation from easily accessible alcohols for organic synthesis is highly interesting. However, direct C–O bond activation of alcohols by visible light is limited due to the large redox potential and the high C–O bond energy. As such, the conversion of alcohols to redox-active groups is necessary to tackle this issue. In this section, we will discuss various types of prefunctionalized alcohols that are used under visible-light photoredox conditions to generate alkyl radicals by homolysis of C–O bonds.

Thiocarbonyl: In 2014, Ollivier and co-workers [43] demonstrated visible-light-mediated iridium-catalyzed reduction of thiocarbonyl derivatives derived from alcohols. The thiocarbonyl derivatives were prepared by reaction of thiocarbonyldiimidazole (TCDI, **15**) with alcohols in the presence of a catalytic amount of DMAP (0.4 equiv). TCDI is a very popular substrate for such reaction types and was first introduced by Barton and McCombie (Scheme 6) [20].

In this process, the catalyst is first excited and then transfers one electron to the thiocarbamate moiety to form a thiocarbamate radical anion, with change in oxidation state from III to IV. Next, the sacrificial electron donor Hünig base successfully converts [Ir(IV)] to [Ir(III)], with concurrent formation of an amine radical cation. Then, the photogenerated thiocarbamate radical anion forms the alkyl radical by homolytic cleavage of the C–O bond. Next, the H-atom abstraction from iPr2NEt or the from the corresponding radical cation furnishes the desired product.

In 2019, Aggarwal and co-workers [44] described a method to convert aliphatic alcohols into boronic esters. At first, aliphatic alcohols are functionalized into 2-iodophenyl thionocarbonates that can facilitate a visible-light-mediated Barton–McCombie radical deoxygenation (Scheme 7). The reaction is free from photocatalyst, radical initiators, or conventional metal hydrides, such as tin or silicon hydrides. The reaction mechanism is interesting since first, a Lewis acid–base adduct is generated by interaction of Et_3N with a boron atom of bis(catecholato)diboron (B_2cat_2, **19**). As a result, one of the catecholate ligands experiences an increase in electron density, which facilitates a π–π interactions with the aryl iodide system and ultimately results in the production of an electron donor–acceptor (EDA) complex **21**. Photoexcitation of this EDA complex furnishes an aryl iodide radical anion and a radical cation complex **22**. Then, the elimination of iodide leads to the formation of **23**, which further undergoes 5-*endo*-trig cyclization, followed by fragmentation to produce an alkyl radical and a cyclic thiocarbonate **25**. These alkyl radicals then interact with B_2cat_2 (**19**) to produce a variety of structurally intricate boronic esters. The reaction occurs in DMF solvent and requires ca. 18 h to finish upon irradiation with blue LEDs. The catecholboronic esters produced at first are transesterified into pinacol borane by addition of pinacol and triethylamine. The reaction proved to be useful for a wide variety of substrates, such as borneol, menthol, epiandrosterone, hecogenin, rockogenin, and tigogenin. All of them were successfully converted into boronic esters with high diastereoselectivity.

In 2021, Cook and co-workers [45] unveiled the photomediated trifluoromethylation of alcohols by converting alcohols into thiocarbonates (Scheme 8). This copper-mediated deoxygenative trifluoromethylation technique worked with both benzylic and unactivated thiocarbonates. The proposed mechanism starts with the homolysis of (bpy)Cu(III)$(CF_3)_3$ by blue-light irradiation, which produces CF_3 radicals and (bpy)Cu(II)$(CF_3)_2$. Subsequently, the interaction between the CF_3 radical and silane furnishes a Si-based radical, which in turn reacts with the thiocarbonate to form an alkyl radical. Finally, a coupling reaction of the alkyl radical with (bpy)Cu(III)$(CF_3)_3$ leads to the formation of the trifluoromethylation product and a Cu(I) species.

Oxalates: In 2015, Macmillan and co-workers [46] utilized oxalates as activating groups for alcohols. Alkyl oxalates were effectively converted into useful radicals, catalyzed by an iridium complex under visible-light photoredox conditions (Scheme 9). This new approach does not require any sacrificial use of reductants or oxidants and is entirely redox-neutral. The authors have shown that simple cesium alkyl oxalates of tertiary alcohols can easily couple with electron-deficient alkenes in the

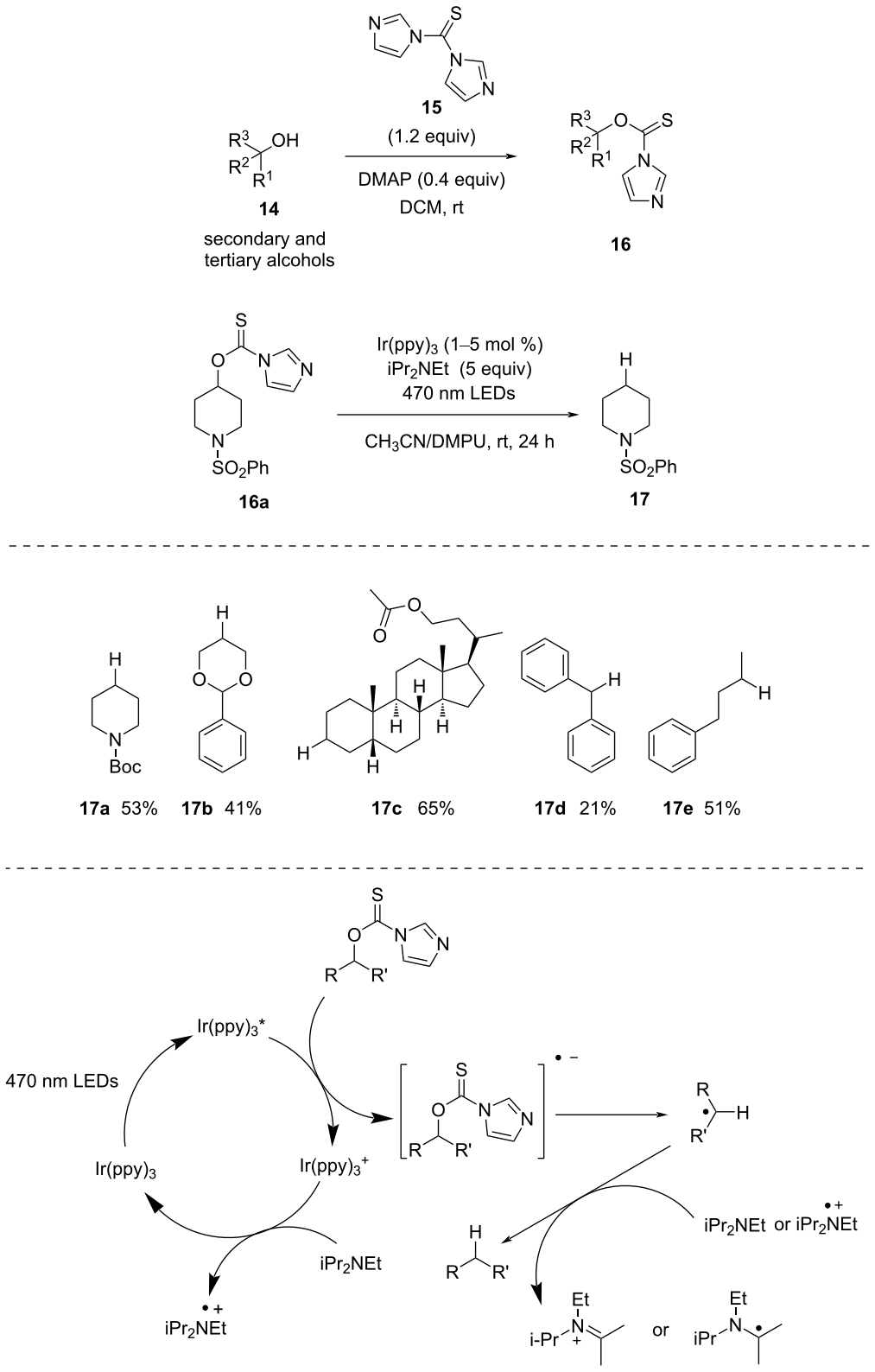

Scheme 6: Synthesis of *O*-thiocarbamates and photocatalytic reduction of *O*-thiocarbamates.

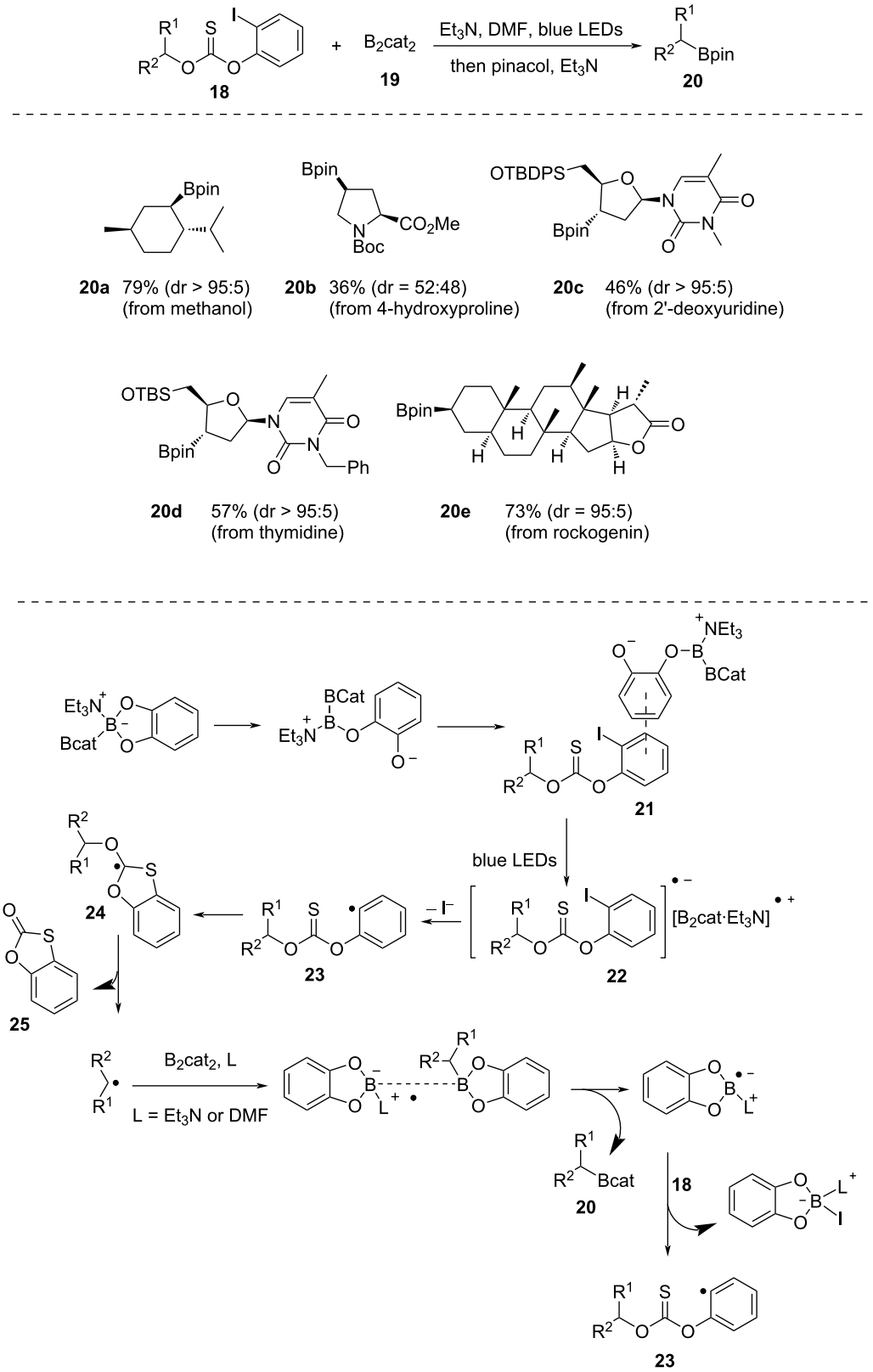

Scheme 7: Deoxygenative borylation of alcohols.

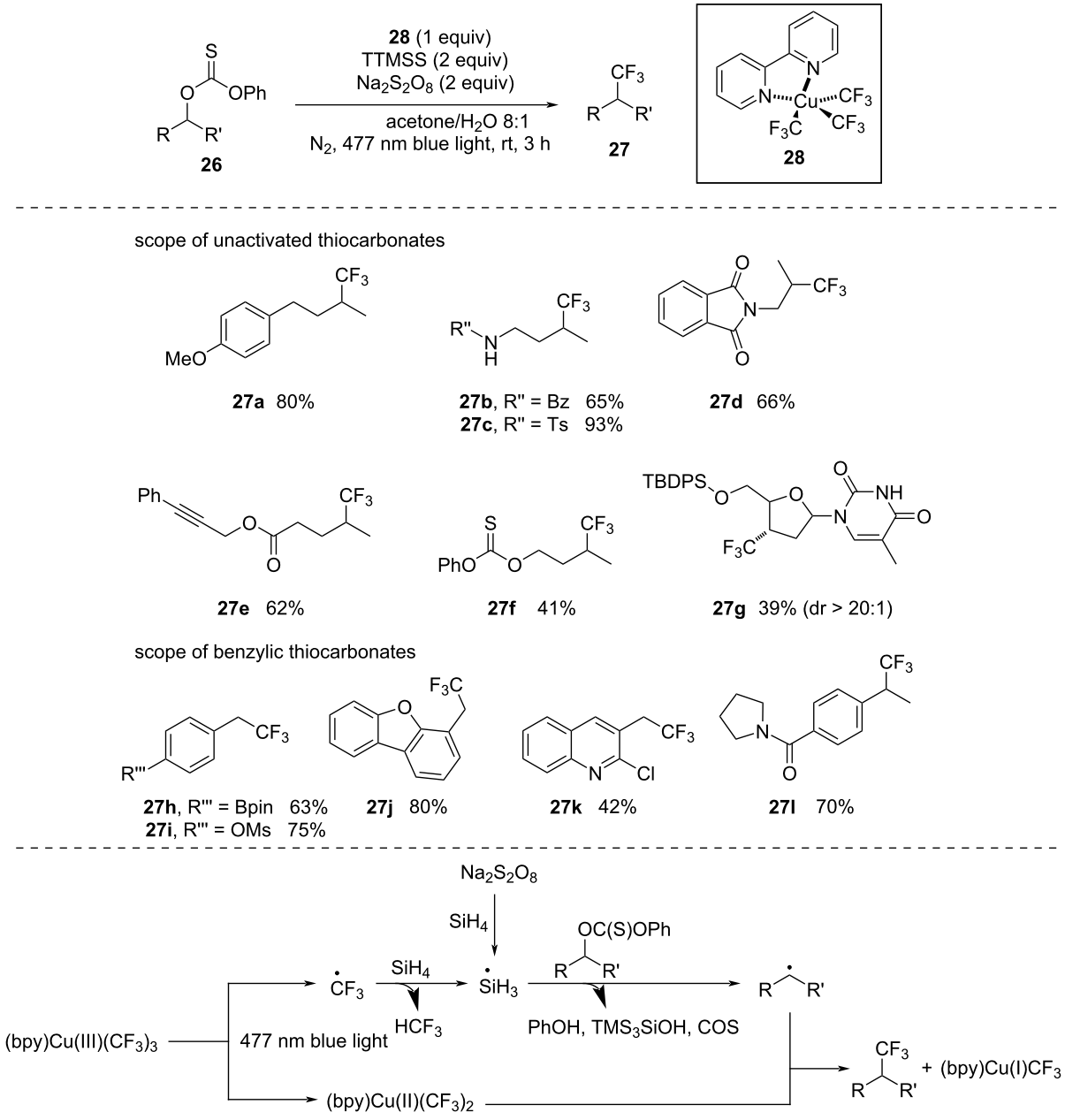

Scheme 8: Trifluoromethylation of *O*-alkyl thiocarbonyl substrates.

presence of visible light. Initially, the [Ir(III)] photocatalyst is excited to the long-lived higher-energy state *[Ir(III)]. Then, the excited-state photocatalyst oxidizes the cesium alkyl oxalate via SET, followed by elimination of two carbon dioxide molecules, generating a tertiary alkyl radical that easily combines with an electron-deficient alkene, providing the product. This protocol was well compatible with a wide range of acceptor components, such as various acrylates, α,β-unsaturated acids, enones, enals, acrylamides, vinyl phosphonates, and vinyl sulfones. Various cesium salts of oxalates also performed well using this protocol. Isopropyl and *tert*-butyl groups present in an adjacent position of oxalates do not disturb the reaction and provide the desired products with good yield. Cyclopentanol-derived oxalates, some heterocyclic oxalates, and natural-product-derived oxalates were also compatible with this method.

In 2018, Chu and co-workers [47] devised an elegant protocol for achieving *syn*-alkylarylation of terminal alkynes using tertiary alkyl oxalates and aryl bromides (Scheme 10). This is achieved through the synergistic combination of photoredox and nickel catalysis. This approach facilitates the formation of diverse trisubstituted olefins with outstanding regioselectivity

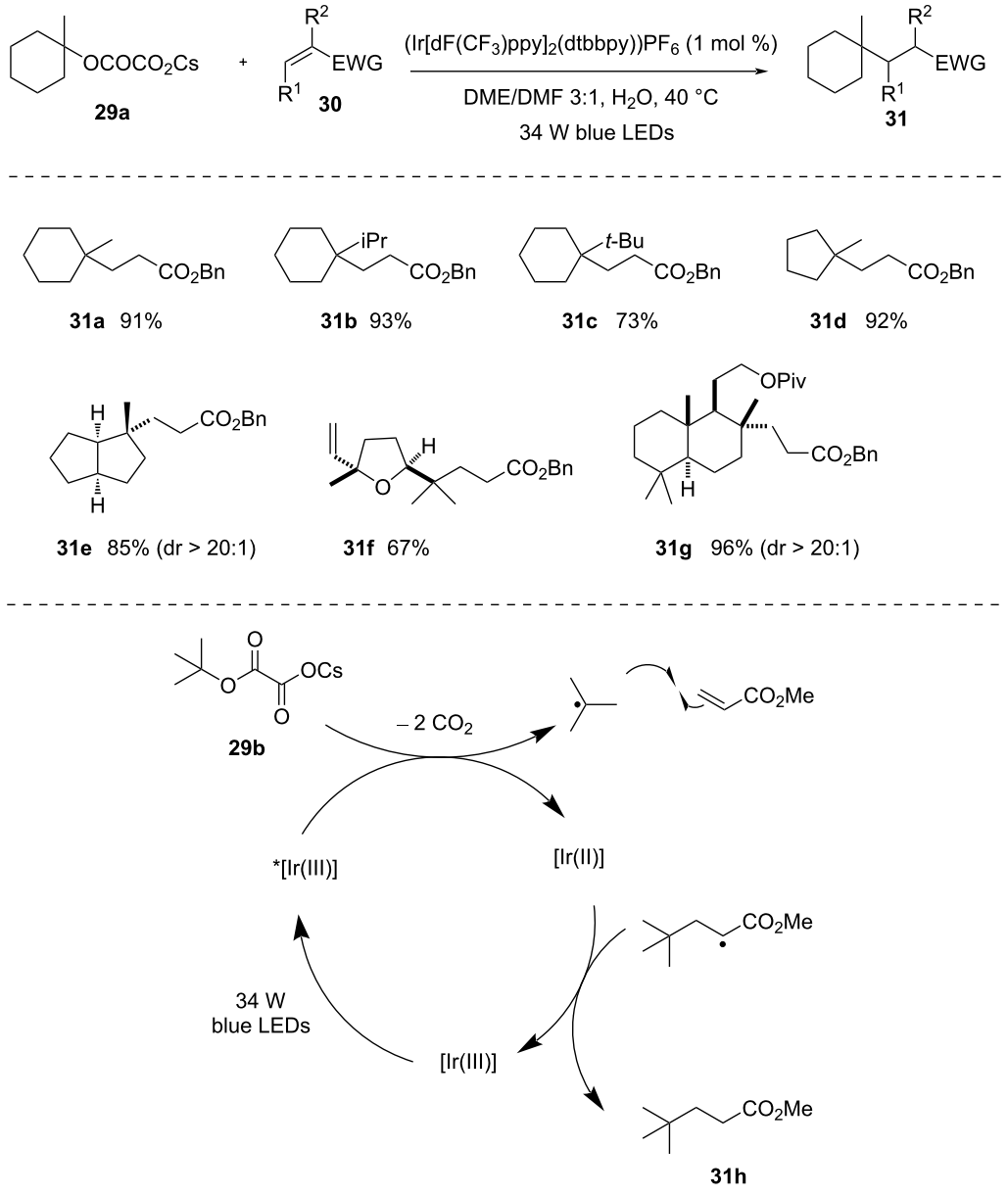

Scheme 9: Redox-neutral radical coupling reactions of alkyl oxalates and Michael acceptors.

and *syn*-stereoselectivity. The proposed mechanism involves C–O bond activation of tertiary oxalates. It requires $[Ir(dF(CF_3)ppy)_2(dtbbpy)]PF_6$ and $NiCl_2$·DME along with dtbbpy ligand. The reaction commences with single-electron oxidation of cesium oxalate initiated by *[Ir(III)] photocatalyst. This transfer leads to the elimination of two CO_2 molecules and results in a tertiary alkyl radical, which eventually reacts with an alkyne to yield a vinyl radical **35**. Later, the addition of Ni(0) and ligand to the vinyl radical **35** gives the intermediate **36**. This intermediate undergoes oxidative addition with aryl bromide to produce Ni(III) species **37**. A final reductive elimination gives the desired alkene and Ni(I). The two catalytic cycles are finally completed by single-electron reduction of [Ni(I)] by [Ir(II)], which regenerates [Ni(0)] and ground-state [Ir(III)]. Cyclic oxalates readily form the corresponding alkyl radicals under iridium photocatalysis. The generated alkyl radicals then undergo the desired addition with alkyne to produce alkenyl radicals that via Ni-catalysed coupling reactions with aryl bromides form trisubstituted alkenes *Z*-selectively. Internal alkynes are not suitable for this transformation due to the steric reason, but terminal arylalkynes bearing electron-donating and electron-withdrawing substituents were

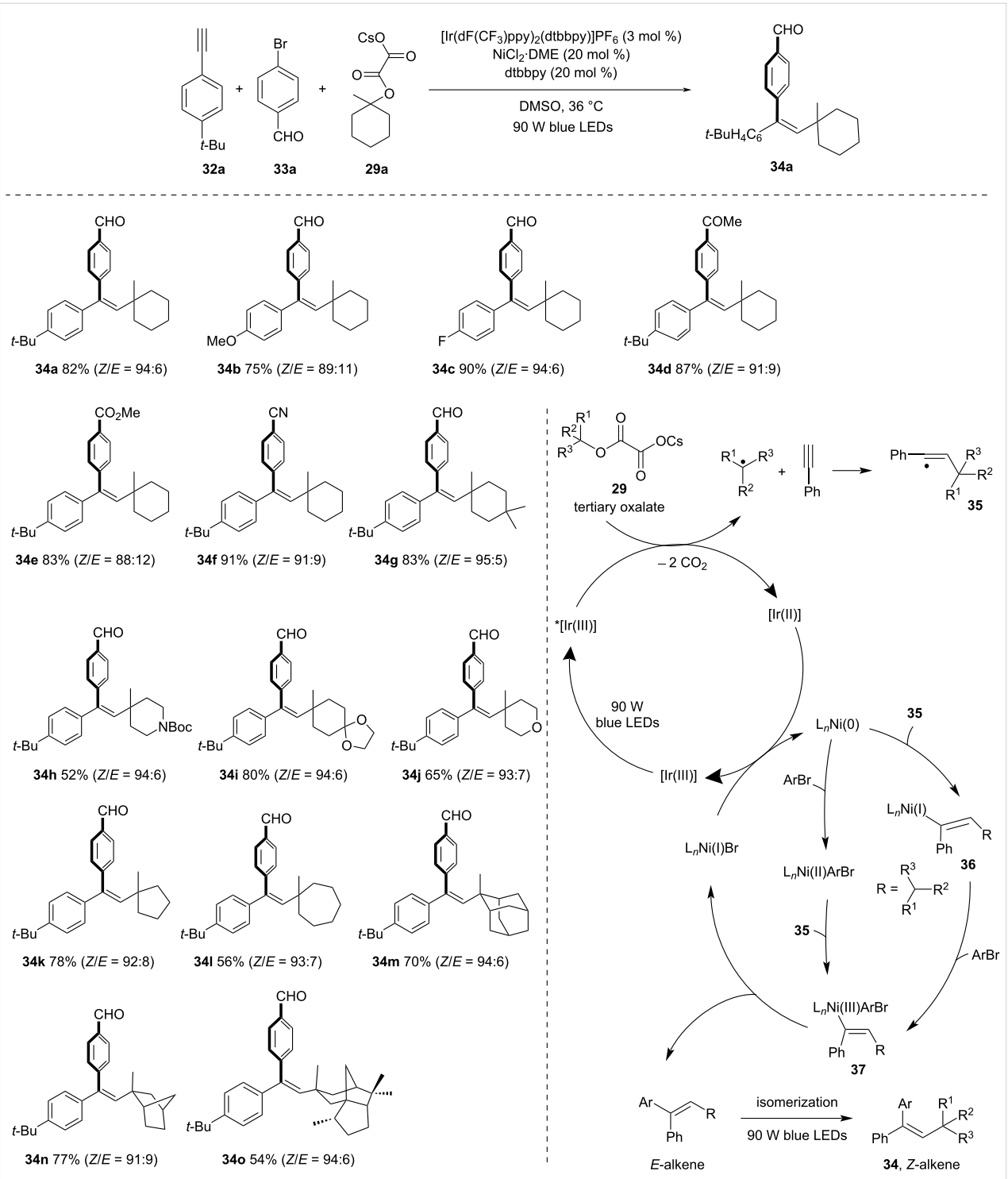

Scheme 10: Visible-light-catalyzed and Ni-mediated *syn*-alkylarylation of alkynes.

well compatible with this method. The procedure is limited to electron-withdrawing and electron-neutral aryl halides. The presence of a conjugated substituent in the *p*-position of an aryl halide is crucial for achieving good *syn*-stereoselectivity.

In 2019, using a similar concept, they reported 1,2-alkylarylation of alkenes with alkyl oxalates and aryl bromides under visible-light photoredox and Ni catalysis (Scheme 11) [48]. This protocol was applicable to a wide range of substrates, such as nonactivated alkenes, heteroatom-substituted alkenes, and

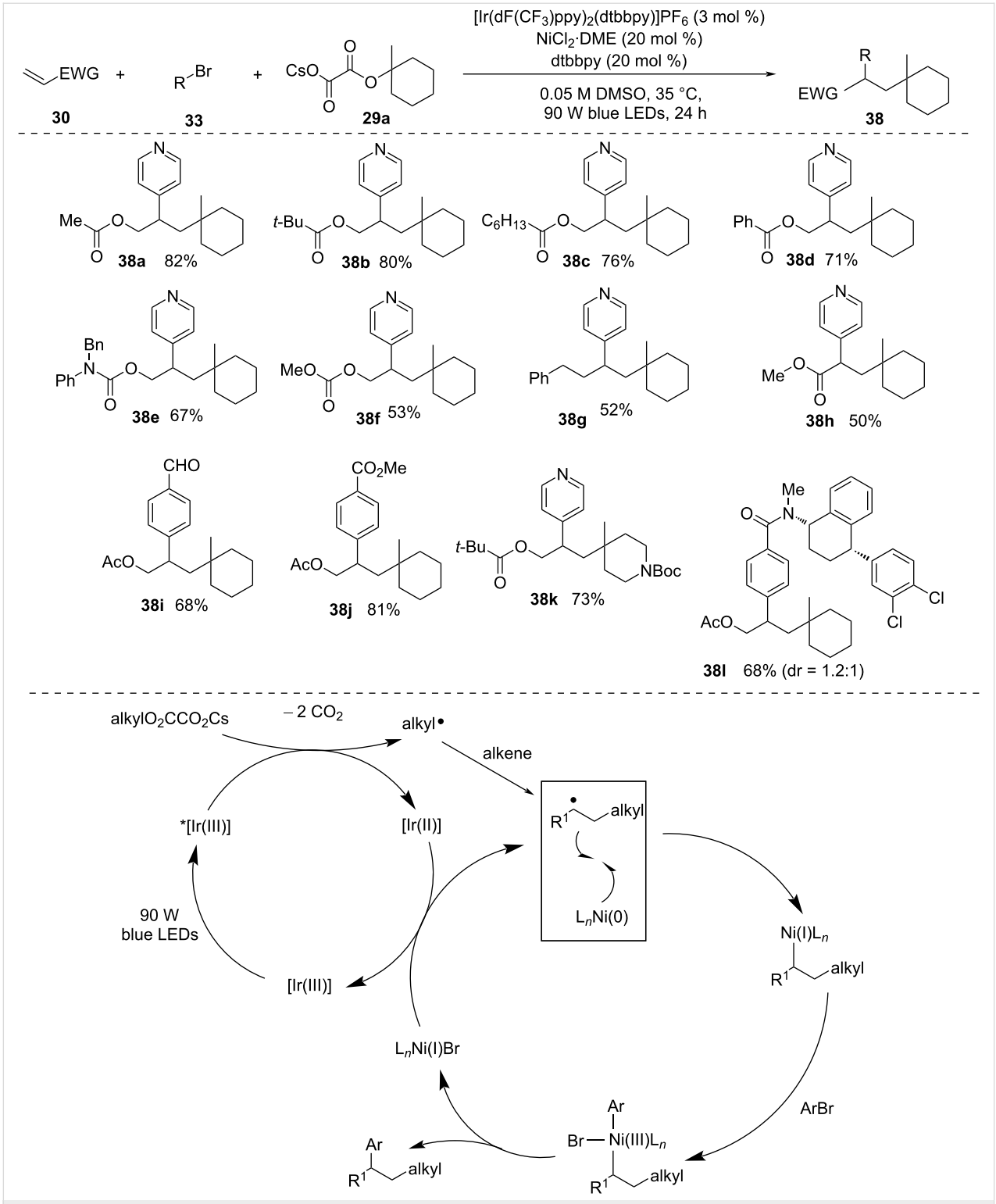

Scheme 11: 1,2-Alkylarylation of alkenes with aryl halides and alkyl oxalates.

conjugated alkenes. Using alkyl oxalates obtained from readily available alcohols facilitated the construction of intricate alkyl compounds. However, only tertiary alkyl oxalates were applicable to this methodology.

In 2019, Studer et al. [49] reported photoinduced C–O borylation of tertiary alcohols using oxalates as a radical source and $Ir(ppy)_3$ as a photocatalyst (Scheme 12). At first, the tertiary alcohols were functionalized using Barton pyridine-2-thione-*N*-

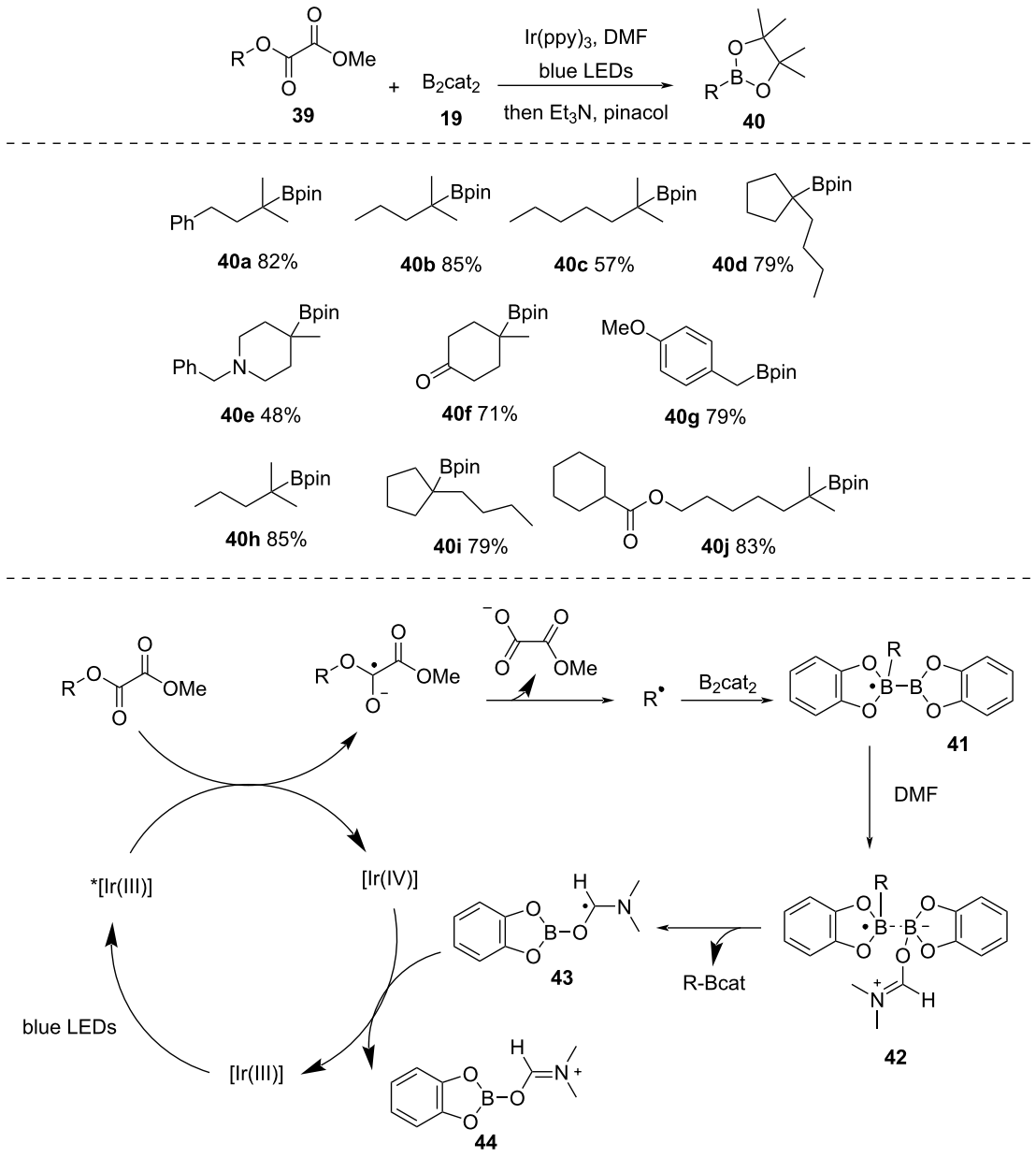

Scheme 12: Deoxygenative borylation of oxalates.

oxycarbonyl (PTOC) esters for *tert*-alkyl radical generation. Next, the oxalates were utilized for borylation in DMF with the help of photoexcited $Ir(ppy)_3$. The suggested mechanism begins with the formation of photoexcited *[Ir(III)], which promotes SET to oxalate and generates an oxalate radical anion and [Ir(IV)]. The fragmentation of the oxalate radical anion produces an alkyl radical. The radical subsequently undergoes addition to B_2cat_2 (**19**) to produce the boryl radical **41**. Here, the choice of solvent is also important. The interaction between DMF and the boryl radical **41** assists B–B bond scission to furnish the target borylated products and an intermediate **43**, which is oxidized by [Ir(IV)], regenerating the [Ir(III)] catalyst and completing the catalytic cycle.

Overman and co-workers [50] used *tert*-alkyl *N*-phthalimidoyl oxalates to produce alkyl radicals that were further reacted with various Michael acceptors (Scheme 13). The photocatalyst $Ru(bpy)_3^{2+}$ and Hantzsch ester were essential for the success of the reaction. The reaction was well compatible with various *N*-phthalimidoyl oxalates (i.e., **31h–k**) as well as electron-deficient alkenes (i.e., **31l–o**).

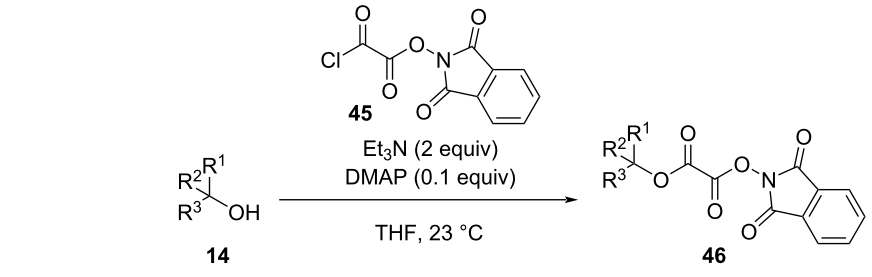

synthesis of *tert*-alkyl *N*-phthalimidoyl oxalates

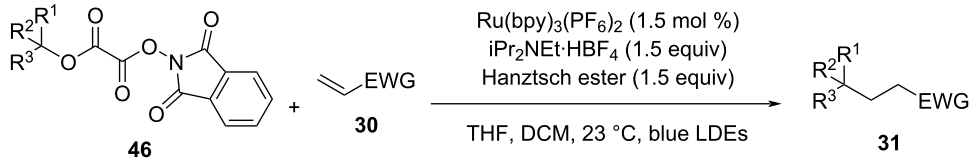

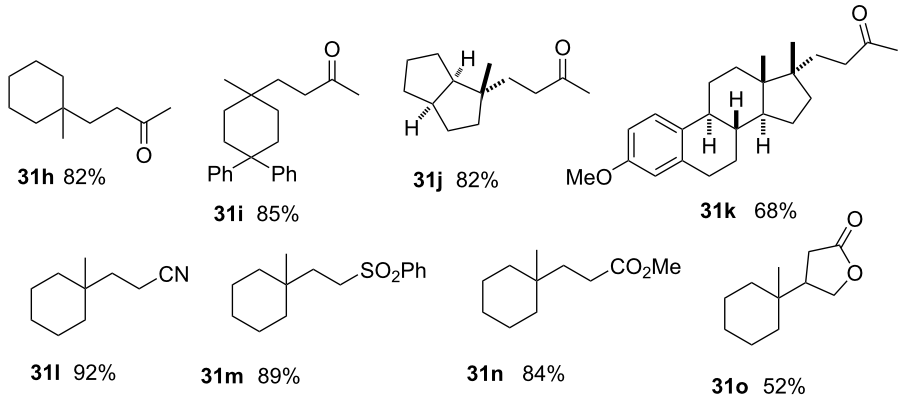

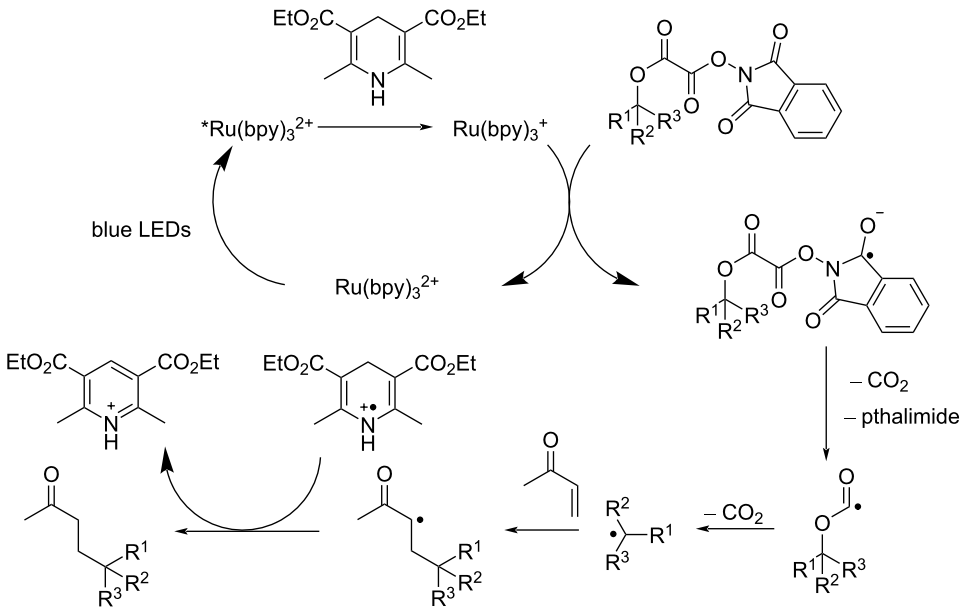

Scheme 13: Coupling of *N*-phthalimidoyl oxalates with various acceptors.

Xanthates: In 2017, Molander and co-workers [51] introduced a C(sp^3)–C(sp^2) cross-coupling reaction of benzyl radicals generated from *o*-benzyl xanthate esters with aryl bromides via dual photoredox and nickel catalysis (Scheme 14). *sec*-$BuBF_3K$ was found to be the best radical precursor for generating the alkyl radicals that initiated the C–O bond cleavage of *O*-benzyl xanthate esters to provide benzyl radicals. Next, the benzyl radicals underwent nickel-catalyzed cross-coupling reactions with aryl halides to deliver the desired cross-coupled products. Interestingly, in absence of any xanthate, *sec*-butyl radicals underwent cross-coupling reactions with aryl halides to form *sec*-butyl arenes, whereas in the presence of xanthate, no undesired *sec*-butyl arenes were generated. This underpinned the formation of *sec*-butyl radicals in the system that rapidly reacted with

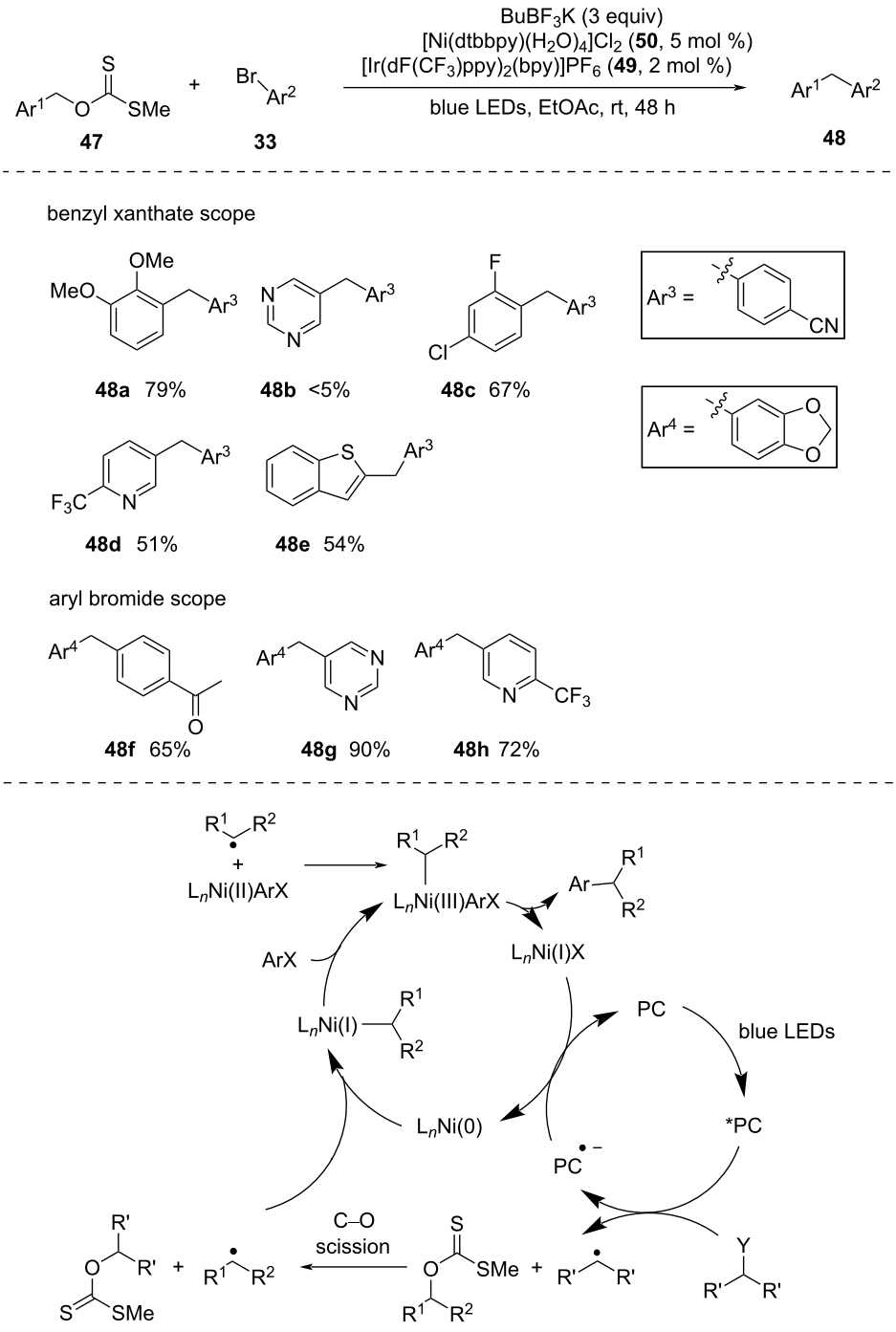

Scheme 14: Cross-coupling of *O*-alkyl xanthates with aryl halides via dual photoredox and nickel catalysis.

O-benzyl xanthates before participating in the nickel-catalyzed cross-coupling reactions. Precatalyst $[Ni(dtbbpy)(H_2O)_4]Cl_2$ (**50**) and photosensitizer $[Ir(dF(CF_3)ppy)_2(bpy)]PF_6$ (**49**) were found to be the best choices for a smooth reaction progress.

In 2019, Studer et al. [49] reported a borylation reaction of alcohols by conversion into xanthates that act as alkyl radical source via photocatalytic deoxygenation (Scheme 15). Therein, silane was used as radical agent for the reduction of xanthates. Under blue-light irradiation, xanthates were reacted with B_2cat_2 (**19**) in dimethylacetamide (DMAc), providing the borylated product in decent yield. The methodology was metal-free and did not require conventional heating. Nevertheless, the borylation process was limited to secondary alcohols. To address the instability of the catecholate products, they were converted in situ to the Bpin esters by introducing pinacol and Et_3N into the reaction mixture.

In 2021, Wu and co-workers [52] developed a method in which alkyl radicals were generated via photocatalytic deoxygenation of alcohols (Scheme 16). This one-pot strategy involved the reaction of xanthates formed in situ with electron-deficient alkenes under visible-light photoredox conditions in the presence of PPh_3. This approach did not require multistep synthesis of starting materials. In addition, alcohol groups in polyols could be converted rather selectively in the order tertiary alcohol< secondary alcohol < primary alcohol.

They also proposed a mechanism, which is outlined in Scheme 16. The first step involves deprotonation of alcohol in the presence of base and nucleophilic attack of CS_2 to generate a xanthate salt intermediate. Photocatalyst-induced SET from the xanthate intermediate gives rise to a sulfur-centered radical. The xanthate radical combines with PPh_3, resulting in a phosphoranyl radical. Later, a sequential β-scission and elimination of carbonyl sulfide generates the alkyl radical. This alkyl radical reacts with electrophilic alkene and forms the target product.

***N*-Alkoxyphthalimides:** In 2019, Tang and co-workers [53] utilized *N*-alkoxyphthalimides for the generation of alkyl radicals by reacting photogenerated alkoxyl radicals with $P(OMe)_3$ (Scheme 17). This strategy provided the alkylation of allyl and alkenyl sulfones with a wide range of *N*-alkoxyphthalimides produced from benzyl alcohols. The protocol also allowed to use *N*-alkoxyphthalimides derived from aliphatic alcohols. However, the reaction was less facile with benzyl alcohols derived *N*-alkoxyphthalimides. The plausible mechanism starts with blue-light excitation of [Ir(III)] to activated *[Ir(III)], which is then reduced by Hantzsch ester to form [Ir(II)]. After SET, the resultant [Ir(II)] species reduces *N*-alkoxyphthalimide to produce the *N*-alkoxyphthalimide radical anion. The Hantzsch ester radical cation further protonates this anion, promoting homolytic N–O bond breaking that yields phthalimide and an alkoxyl radical. This alkoxyl radical can easily extract hydrogen or undergo β-fragmentation. When $P(OMe)_3$ is present, the alkoxyl radical combines with it to generate a phosphoranyl radical. This radical easily undergoes β-scission, resulting in the production of an alkyl radical. After that, this alkyl radical reacts with allyl and alkenyl sulfones in an addition–elimination cycle to produce the required product and a benzenesulfonyl radical. The benzenesulfonyl radical abstracts a hydrogen radical from the Hantzsch ester radical to form $PhSO_2H$ and a pyridine species, thereby completing the catalytic cycle.

Direct C–O bond activation of alcohols

Alcohols have a high C–O bond strength and redox potential, making it difficult to directly activate the C–O bonds and

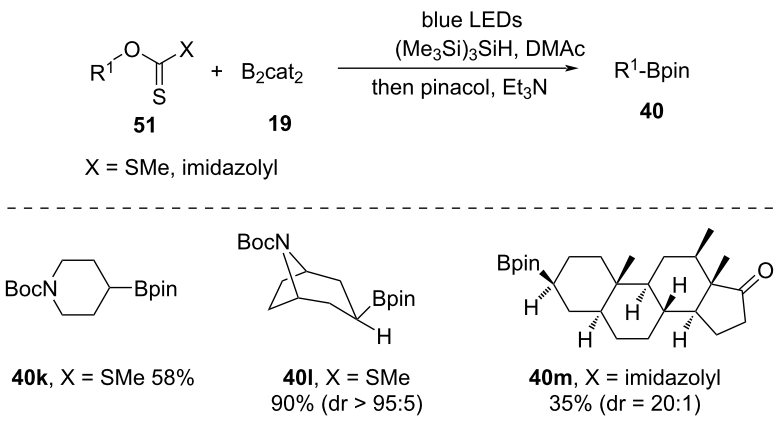

Scheme 15: Deoxygenative borylation of secondary alcohol.

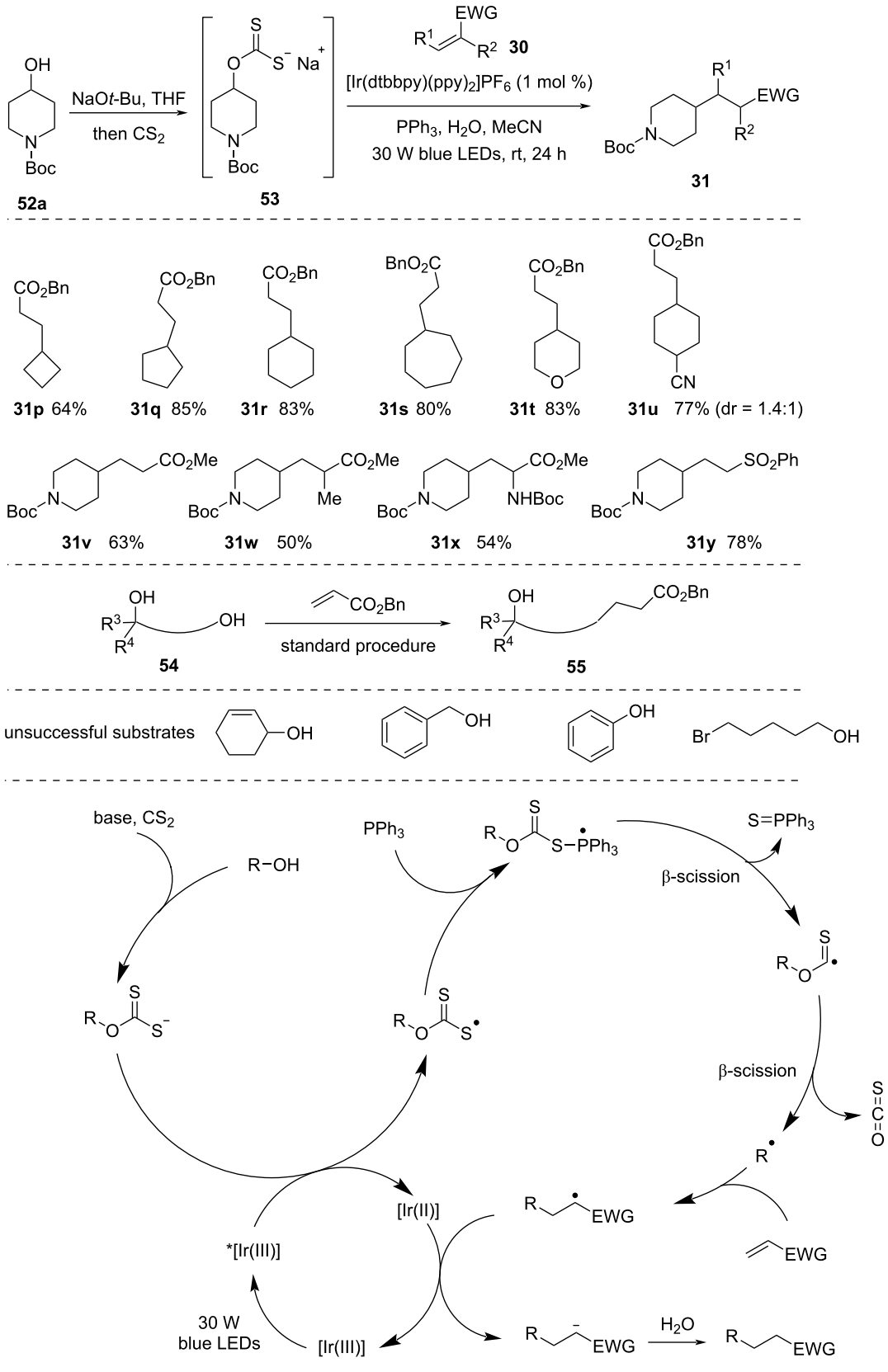

Scheme 16: Deoxygenative alkyl radical generation from alcohols under visible-light photoredox conditions.

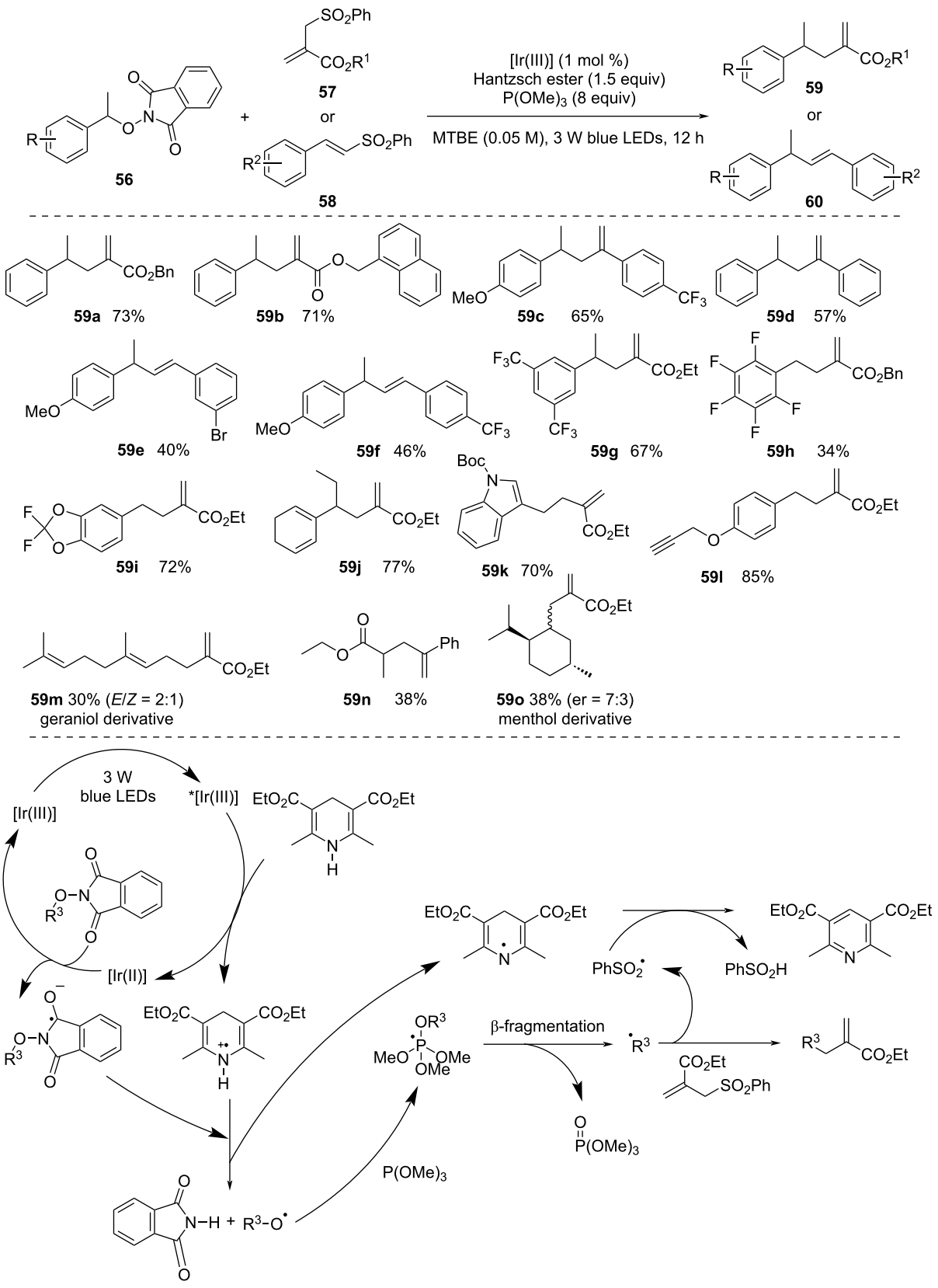

Scheme 17: Deoxygenative alkylation via alkoxy radicals against hydrogenation or β-fragmentation.

produce carbon-centered radicals. Thus, to generate carbon-centered radicals, functionalization of alcohols is required, which requires an additional step. Therefore, it is quite interesting to directly employ alcohols for creating carbon-centered radicals that facilitate photomediated organic transformations. In this section, we will discuss some methods where alcohol C–O bonds were directly activated via photoredox catalysis.

In 2018, Doyle and co-workers [54] documented a catalytic method for the deoxygenation of benzylic alcohols to toluenes, utilizing phosphines and photoredox catalyst under visible-light irradiation (Scheme 18). In this method, they were able to synthesize various hydrocarbons in good yield. Alcohols containing electron-deficient arenes delivered a comparably lower yield (i.e., **62b**–**d**, 52–63%), probably because of the lower

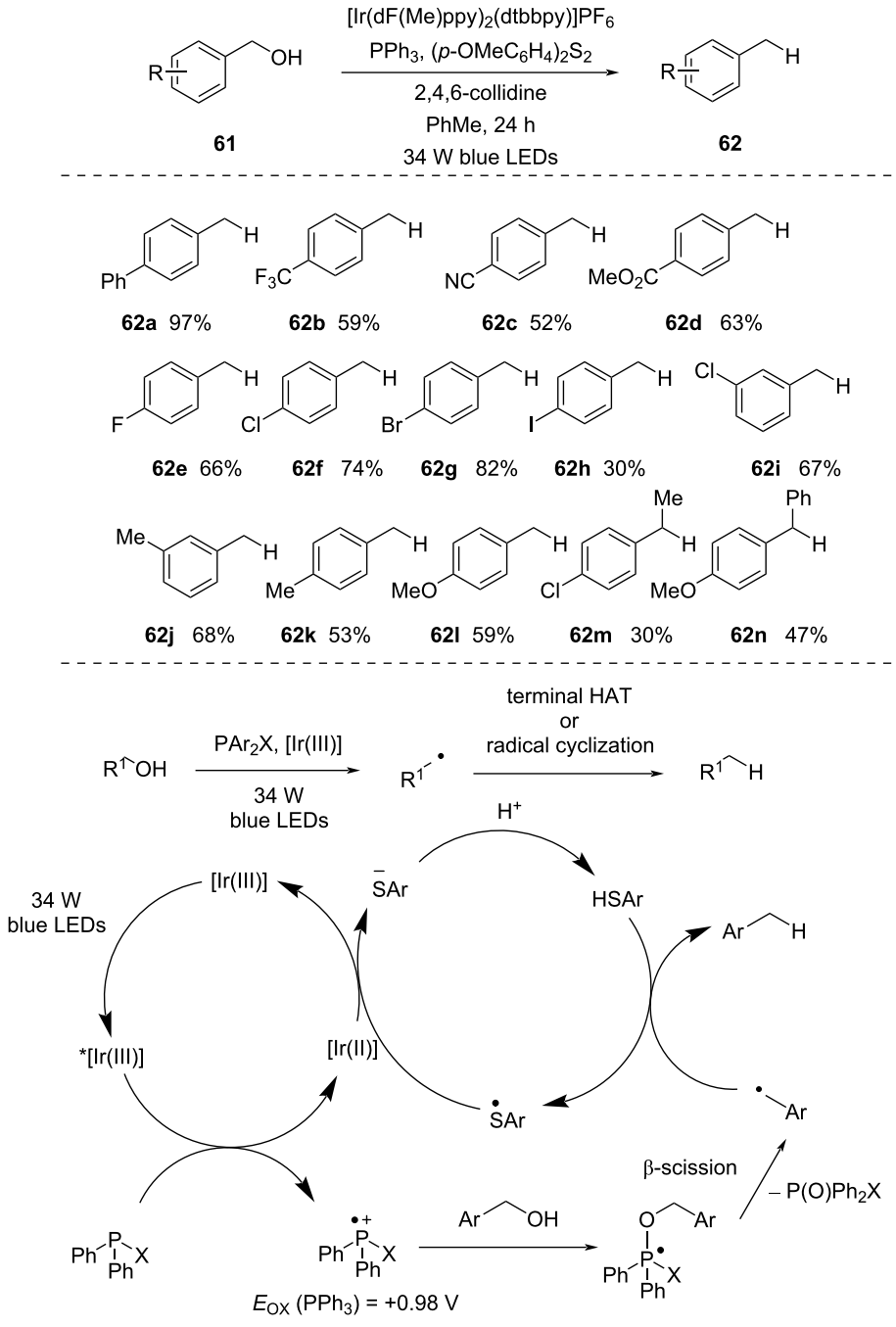

Scheme 18: Direct C–O bond activation of benzyl alcohols.

nucleophilicity of the alcohols. Halogen atoms present in the *p*-position of alcohols were tolerated well and provided a decent yield (i.e., **62e**–**h**, 30–82%) of the corresponding hydrocarbons. *m*-Substitution also provided a good product yield (i.e., **62i** and **62j**, 67 and 68%). Additionally, electron-rich benzylic alcohols yielded the product in a lower yield (i.e., **62k** and **62l**, 53 and 59%) compared to **62a**. This was due to the generation of electron-rich phosphoranyl radicals, which were more prone to oxidation before undergoing β-scission. The deoxygenation process of secondary benzylic alcohols occurred with decreased efficiency (i.e., **62m** and **62n**, 30 and 47%), in line with the slower addition of a more sterically hindered alcohol to a phosphine radical cation.

The proposed mechanism involves the formation of a phosphine radical cation via SET from photoexcited [Ir(III)] complex. Subsequently, the benzylic alcohol initiates a polar nucleophilic attack on the phosphine radical cation, forming a phosphoranyl radical. This phosphoranyl radical intermediate then undergoes β-cleavage, giving rise to a benzylic radical and triphenylphosphine oxide. A terminal hydrogen atom transfer (HAT), facilitated by an aryl thiol, results in the formation of the desired product with concurrent formation of the thiyl radical. The reduction of the thiyl radical by [Ir(II)] generates a thiolate anion and [Ir(III)]. Finally, the thiolate anion is converted to the aryl thiol via proton transfer to complete the catalytic cycle.

In 2021, MacMillan and co-workers [55] introduced a cross-coupling reaction of alcohols with aryl halides through metallaphotoredox catalysis (Scheme 19). Therein, alcohols were activated by the use of NHC salts. This activation facilitated the construction of C–C bonds when combined with aryl halide coupling partners. A diverse array of alcohols and various medicinally important aryl and heteroaryl halides reacted well in this protocol.

Under basic conditions, the mechanism involves the condensation of a benzoxazolium salt **80**, creating NHC–alcohol adduct **81**. The [Ir(III)] photocatalyst is excited when exposed to blue light, leading to the formation of a long-lived triplet-excited-state *[Ir(III)] complex.

This excited-state *[Ir(III)] complex can effectively oxidize the nitrogen atom of activated NHC–alcohol adduct **66** via SET. The resulting nitrogen radical cation intermediate **67** weakens the adjacent C–H bond, making it more acidic and susceptible to deprotonation by a suitable base, ultimately yielding an α-amino radical intermediate **68**. This carbon-centered radical, positioned near three heteroatoms, undergoes rapid β-cleavage to produce a carbamate **69** and a deoxygenated alkyl radical **70**. The formation of carbamate byproduct **69**, having a strong C=O double bond, acts as thermodynamic driving factor for the C–O bond homolysis.

In 2022, MacMillan and co-workers [56] outlined a comprehensive and direct deoxygenative hydroalkylation method for various types of electrophilic olefins (Scheme 20). This method involved primary, secondary, and tertiary alcohols and was facilitated by the use of a newly developed NHC-based activator. The deoxyalkylation was performed by initially stirring the alcohol substrate with NHC and pyridine in MTBE for 15 min. After that, Michael acceptor, sodium acetate, 1,1,3,3-tetramethylguanidine, and [Ir(III)] photocatalyst in MTBE/DMA were added to the mixture. Then, blue LEDs were used to irradiate the reaction mixture to produce the desired product. The developed protocol was highly attractive as it eliminated waste generation, which was essential for practical use, particularly in late-stage functionalization. For the deoxygenation of primary substrates, which underwent slower β-scission, NHC **72** was found to be most effective. Unstrained secondary alcohols were efficiently activated with the help of NHC **65**. Deoxygenation of sterically congested alcohols, which has been a longstanding challenge in organic synthesis, was achieved by using a more electrophilic alcohol activator NHC **73**. The mechanism was similar to the previous one. Therein, firstly, the alcohol is condensed with the benzoxazolium salt and generated the adduct **74** in situ. Then, the excited photocatalyst is reductively quenched by adduct **74**, followed by proton elimination, generating α-amino radical intermediate **75**. This subsequently undergoes β-cleavage to produce an alkyl radical **76** and an aromatized byproduct. This alkyl radical is then added to electron-deficient alkenes via Giese addition and is followed by reduction, providing the desired product.

Other related C–O bond cleavages

Recently, the photochemical C–O bond cleavage of ethers in organic transformations has attracted considerable interest. In this context, in 2018, Nicewicz and co-workers [57,58] reported a visible-light-photoredox-catalyzed single-step synthesis of polysubstituted aldehydes using easily accessible olefin substrates (Scheme 21). Styrenes selectively reacted with vinyl ethers in the presence of an acridinium photocatalyst and a diphenyl disulfide HAT catalyst to produce the aldehyde product when exposed to blue LED light. Differently substituted styrenes were examined using this protocol, which produced the aldehyde products in good yield (i.e., **80a**–**d**, 48–80%). Cyclic olefins also performed well under these conditions and generated products with a β-ring moiety (i.e., **80e**–**g**, 60–64%), which would have been challenging to synthesize otherwise. 2-Substituted ethyl vinyl ethers also provided α-branched aldehyde products in decent yield (i.e., **80h**–**k**, 49–66%). An α,β,γ-trisub-

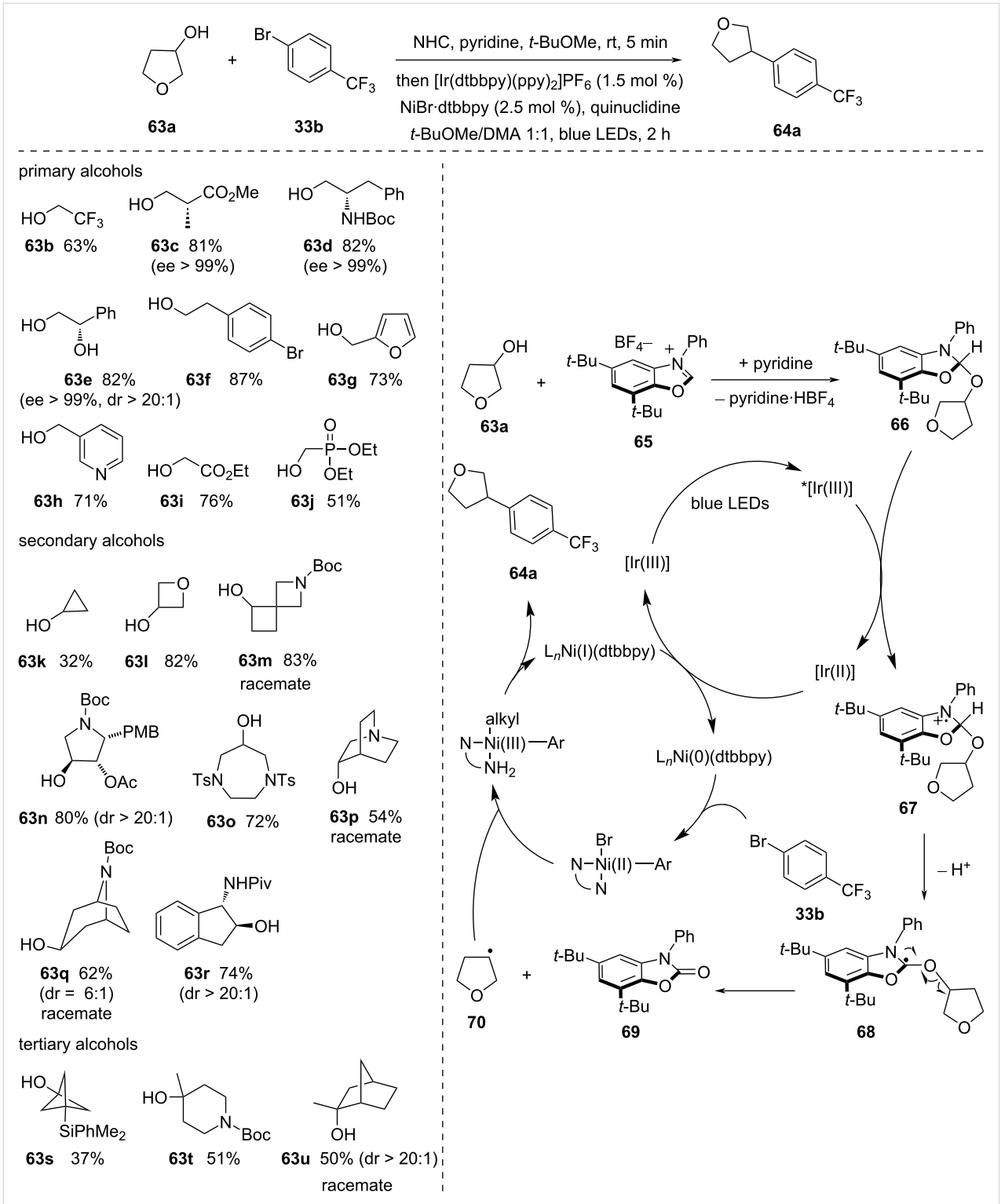

Scheme 19: Deoxygenative arylation of alcohols using NHC to activate alcohols.

stituted aldehyde (i.e., **80l**, 65%) was synthesized using an α,β-disubstituted styrene, which could not be produced using the conventional method. The excited photocatalyst *Mes–Acr$^+$ oxidized the styrene to produce the extremely electrophilic radical cation **81** and Mes–Acr because of the favorable π–π stacking. Ethyl vinyl ether, which is the most nucleophilic molecule in the reaction, combined with radical cation **81** to form the oxonium radical **82**, which could proceed in two directions:

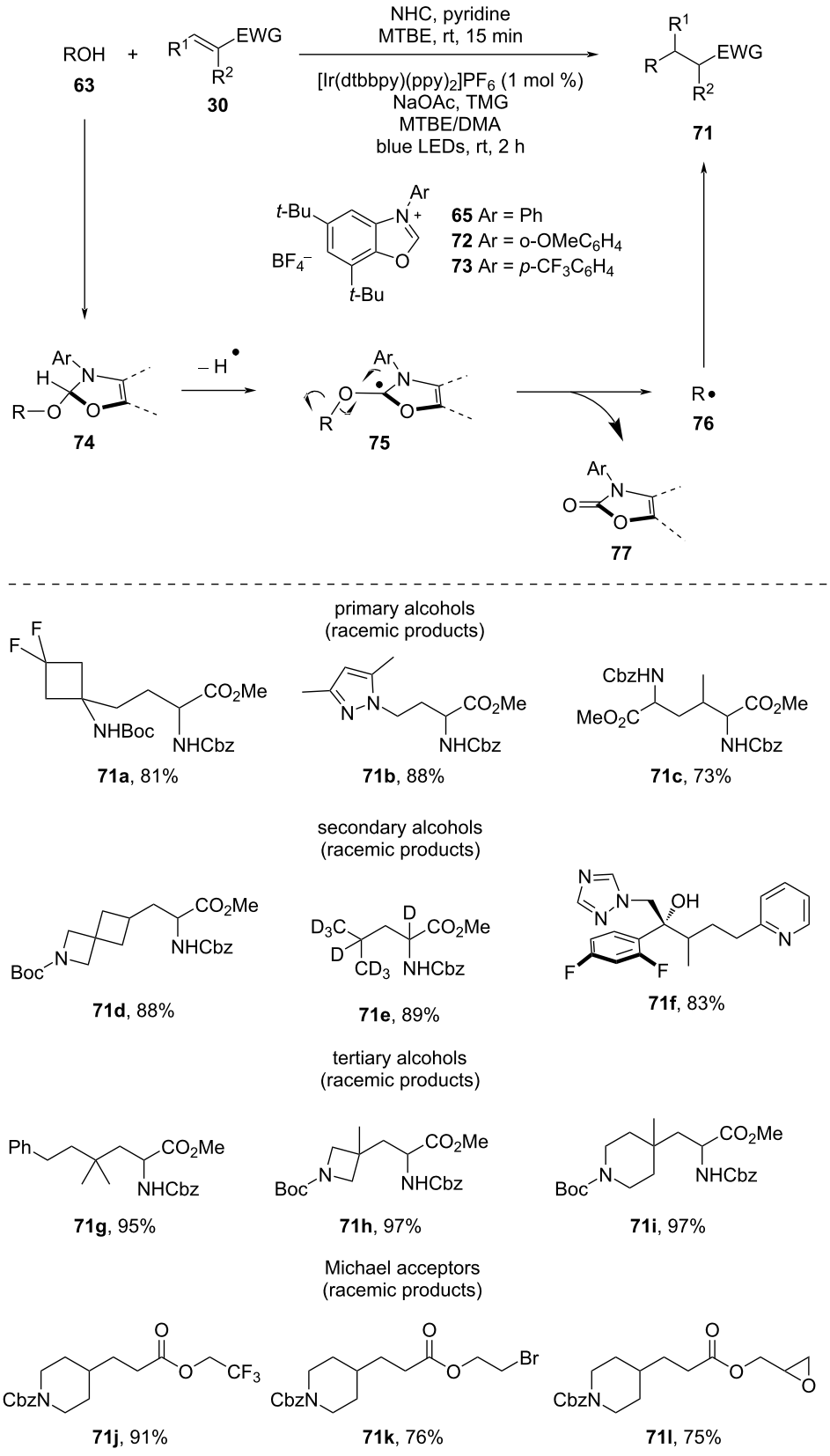

Scheme 20: Deoxygenative conjugate addition of alcohol using NHC as alcohol activator.

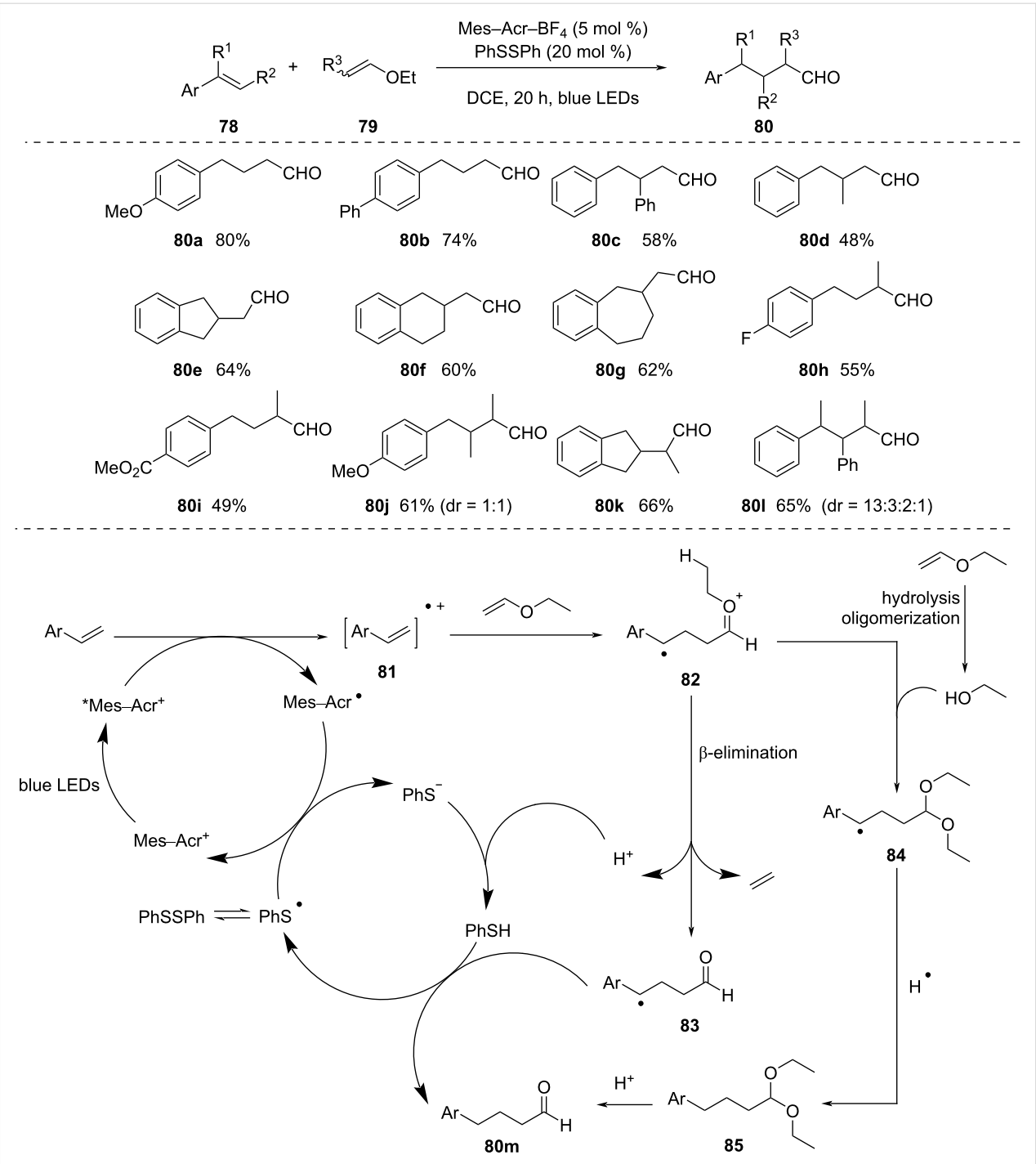

Scheme 21: Synthesis of polysubstituted aldehydes.

1) β-elimination, yielding radical **83** and 2) photoinduced breakdown of ethyl vinyl ether and trapping of ethanol, yielding radical **84**. To regenerate the photocatalyst, PhSSPh functioned as an oxidant. After protonation upon the β-elimination step, PhS^- contributed a hydrogen atom to both **83** and **84**, alongside regeneration of the HAT catalyst. Lastly, the acetal side product **85** was transformed into the aldehyde by acidic workup.

Conclusion

The techniques, catalysts, and mechanistic analyses of homogeneous catalytic deoxygenation processes for high-value products have advanced significantly over the last few years. This review presents an extensive overview of recent photocatalysis methodologies in the field of C–O bond activation. As conventional techniques, such as Barton decarboxylation, create

hazardous wastes, the use of alternative feedstocks, including alcohols and acids, has been encouraged to achieve sustainability. The recent advancements not only avoid the use of various halide-based reactants but also opened up C–O bond activations in terms of alcohol and acid functionalizations, choice of reactants, etc.

Consequently, in this review, we focused on the advancements in photocatalytic alkyl and acyl radial generation from alcohols and acids. It is highly expected that many groups will explore many new useful synthetic transformations based on renewable feedstocks, such as alcohols and acids, which will likely lead to even more exciting opportunities in the near future.

Funding

The author thanks SERB, India (CRG/2021/000402) for financial assistance.

Author Contributions

Mithu Roy: project administration; validation. Bitan Sardar: project administration; resources. Itu Mallick: resources; software. Dipankar Srimani: conceptualization; methodology; supervision.

ORCID® iDs

Dipankar Srimani - https://orcid.org/0000-0001-8826-9773

Data Availability Statement

Data sharing is not applicable as no new data was generated or analyzed in this study.

References

1. Morton, O. *Nature* **2006,** *443,* 19–22. doi:10.1038/443019a
2. Nocera, D. G. *Daedalus (Boston)* **2006,** *135,* 112–115. doi:10.1162/daed.2006.135.4.112
3. Lewis, N. S. *Science* **2007,** *315,* 798–801. doi:10.1126/science.1137014
4. Yu, X.-Y.; Chen, J.-R.; Xiao, W.-J. *Chem. Rev.* **2021,** *121,* 506–561. doi:10.1021/acs.chemrev.0c00030
5. Wang, P.; Zhao, Q.; Xiao, W.; Chen, J. *Green Synth. Catal.* **2020,** *1,* 42–51. doi:10.1016/j.gresc.2020.05.003
6. Srivastava, V.; Singh, P. K.; Srivastava, A.; Singh, P. P. *RSC Adv.* **2020,** *10,* 20046–20056. doi:10.1039/d0ra03086d
7. Bagdi, A. K.; Rahman, M.; Bhattacherjee, D.; Zyryanov, G. V.; Ghosh, S.; Chupakhin, O. N.; Hajra, A. *Green Chem.* **2020,** *22,* 6632–6681. doi:10.1039/d0gc02437f
8. Revathi, L.; Ravindar, L.; Fang, W.-Y.; Rakesh, K. P.; Qin, H.-L. *Adv. Synth. Catal.* **2018,** *360,* 4652–4698. doi:10.1002/adsc.201800736
9. Capaldo, L.; Ravelli, D.; Fagnoni, M. *Chem. Rev.* **2022,** *122,* 1875–1924. doi:10.1021/acs.chemrev.1c00263
10. Cannalire, R.; Pelliccia, S.; Sancineto, L.; Novellino, E.; Tron, G. C.; Giustiniano, M. *Chem. Soc. Rev.* **2021,** *50,* 766–897. doi:10.1039/d0cs00493f
11. Bellotti, P.; Huang, H.-M.; Faber, T.; Glorius, F. *Chem. Rev.* **2023,** *123,* 4237–4352. doi:10.1021/acs.chemrev.2c00478
12. Zhang, M.; Yuan, X.-A.; Zhu, C.; Xie, J. *Angew. Chem., Int. Ed.* **2019,** *58,* 312–316. doi:10.1002/anie.201811522
13. Guan, W.; Chang, Y.; Lin, S. *J. Am. Chem. Soc.* **2023,** *145,* 16966–16972. doi:10.1021/jacs.3c03418
14. Wang, H.; Wang, Z.; Zhao, G.; Ramadoss, V.; Tian, L.; Wang, Y. *Org. Lett.* **2022,** *24,* 3668–3673. doi:10.1021/acs.orglett.2c01286
15. Crespi, S.; Fagnoni, M. *Chem. Rev.* **2020,** *120,* 9790–9833. doi:10.1021/acs.chemrev.0c00278
16. Raviola, C.; Protti, S.; Ravelli, D.; Fagnoni, M. *Green Chem.* **2019,** *21,* 748–764. doi:10.1039/c8gc03810d
17. Kuivila, H. G.; Menapace, L. W. *J. Org. Chem.* **1963,** *28,* 2165–2167. doi:10.1021/jo01044a001
18. Roth, H. G.; Romero, N. A.; Nicewicz, D. A. *Synlett* **2016,** *27,* 714–723. doi:10.1055/s-0035-1561297
19. Lopez, R. M.; Hays, D. S.; Fu, G. C. *J. Am. Chem. Soc.* **1997,** *119,* 6949–6950. doi:10.1021/ja971400y
20. Barton, D. H. R.; McCombie, S. W. *J. Chem. Soc., Perkin Trans. 1* **1975,** 1574–1585. doi:10.1039/p19750001574
21. Albini, A.; Fagnoni, M., Eds. *Handbook of Synthetic Photochemistry;* Wiley-VCH: Weinheim, Germany, 2009. doi:10.1002/9783527628193
22. Banerjee, A.; Lei, Z.; Ngai, M. Y. *Synthesis* **2019,** *51,* 303–333. doi:10.1055/s-0037-1610329
23. Prier, C. K.; Rankic, D. A.; MacMillan, D. W. C. *Chem. Rev.* **2013,** *113,* 5322–5363. doi:10.1021/cr300503r
24. Cheung, K. P. S.; Sarkar, S.; Gevorgyan, V. *Chem. Rev.* **2022,** *122,* 1543–1625. doi:10.1021/acs.chemrev.1c00403
25. Romero, N. A.; Nicewicz, D. A. *Chem. Rev.* **2016,** *116,* 10075–10166. doi:10.1021/acs.chemrev.6b00057
26. Kisch, H. *Angew. Chem., Int. Ed.* **2013,** *52,* 812–847. doi:10.1002/anie.201201200
27. Shaw, M. H.; Twilton, J.; MacMillan, D. W. C. *J. Org. Chem.* **2016,** *81,* 6898–6926. doi:10.1021/acs.joc.6b01449
28. Martinez Alvarado, J. I.; Ertel, A. B.; Stegner, A.; Stache, E. E.; Doyle, A. G. *Org. Lett.* **2019,** *21,* 9940–9944. doi:10.1021/acs.orglett.9b03871
29. Li, G.-N.; Li, H.-C.; Wang, M.-R.; Lu, Z.; Yu, B. *Adv. Synth. Catal.* **2022,** *364,* 3927–3931. doi:10.1002/adsc.202200868
30. Guo, Y.-Q.; Wang, R.; Song, H.; Liu, Y.; Wang, Q. *Org. Lett.* **2020,** *22,* 709–713. doi:10.1021/acs.orglett.9b04504
31. Yang, J.; Wang, C.; Huang, B.; Zhou, H.; Li, J.; Liu, X. *Org. Lett.* **2024,** *26,* 498–502. doi:10.1021/acs.orglett.3c03875
32. Fan, X.; He, C.; Ji, M.; Sun, X.; Luo, H.; Li, C.; Tong, H.; Zhang, W.; Sun, Z.; Chu, W. *Chem. Commun.* **2022,** *58,* 6348–6351. doi:10.1039/d2cc01538b
33. Chatgilialoglu, C.; Ferreri, C.; Landais, Y.; Timokhin, V. I. *Chem. Rev.* **2018,** *118,* 6516–6572. doi:10.1021/acs.chemrev.8b00109
34. Gagosz, F.; Moutrille, C.; Zard, S. Z. *Org. Lett.* **2002,** *4,* 2707–2709. doi:10.1021/ol026221m
35. Tsai, L.-C.; You, M.-L.; Ding, M.-F.; Shu, C.-M. *Molecules* **2012,** *17,* 8056–8067. doi:10.3390/molecules17078056
36. Quiclet-Sire, B.; Zard, S. Z. *Chem. – Eur. J.* **2006,** *12,* 6002–6016. doi:10.1002/chem.200600510
37. Darmency, V.; Renaud, P. Tin-Free Radical Reactions Mediated by Organoboron Compounds. *Radicals in Synthesis I;* Springer: Berlin, Germany, 2006; pp 71–106. doi:10.1007/128_030
38. Studer, A.; Amrein, S. *Synthesis* **2002,** 835–849. doi:10.1055/s-2002-28507

39. Walton, J. C.; Studer, A. *Acc. Chem. Res.* **2005,** *38,* 794–802. doi:10.1021/ar050089j
40. Studer, A.; Amrein, S. *Angew. Chem., Int. Ed.* **2000,** *39,* 3080–3082. doi:10.1002/1521-3773(20000901)39:17<3080::aid-anie3080>3.0.co;2-e
41. Snider, B. B. *Chem. Rev.* **1996,** *96,* 339–364. doi:10.1021/cr950026m
42. Streuff, J. *Chem. Rec.* **2014,** *14,* 1100–1113. doi:10.1002/tcr.201402058
43. Chenneberg, L.; Baralle, A.; Daniel, M.; Fensterbank, L.; Goddard, J.-P.; Ollivier, C. *Adv. Synth. Catal.* **2014,** *356,* 2756–2762. doi:10.1002/adsc.201400729
44. Wu, J.; Bär, R. M.; Guo, L.; Noble, A.; Aggarwal, V. K. *Angew. Chem., Int. Ed.* **2019,** *58,* 18830–18834. doi:10.1002/anie.201910051
45. Liu, Z.-Y.; Cook, S. P. *Org. Lett.* **2021,** *23,* 808–813. doi:10.1021/acs.orglett.0c04039
46. Nawrat, C. C.; Jamison, C. R.; Slutskyy, Y.; MacMillan, D. W. C.; Overman, L. E. *J. Am. Chem. Soc.* **2015,** *137,* 11270–11273. doi:10.1021/jacs.5b07678
47. Guo, L.; Song, F.; Zhu, S.; Li, H.; Chu, L. *Nat. Commun.* **2018,** *9,* 4543. doi:10.1038/s41467-018-06904-9
48. Guo, L.; Tu, H.-Y.; Zhu, S.; Chu, L. *Org. Lett.* **2019,** *21,* 4771–4776. doi:10.1021/acs.orglett.9b01658
49. Friese, F. W.; Studer, A. *Angew. Chem., Int. Ed.* **2019,** *58,* 9561–9564. doi:10.1002/anie.201904028
50. Lackner, G. L.; Quasdorf, K. W.; Overman, L. E. *J. Am. Chem. Soc.* **2013,** *135,* 15342–15345. doi:10.1021/ja408971t
51. Vara, B. A.; Patel, N. R.; Molander, G. A. *ACS Catal.* **2017,** *7,* 3955–3959. doi:10.1021/acscatal.7b00772
52. Guo, H.-M.; Wu, X. *Nat. Commun.* **2021,** *12,* 5365. doi:10.1038/s41467-021-25702-4
53. Han, J.-B.; Guo, A.; Tang, X.-Y. *Chem. – Eur. J.* **2019,** *25,* 2989–2994. doi:10.1002/chem.201806138
54. Stache, E. E.; Ertel, A. B.; Rovis, T.; Doyle, A. G. *ACS Catal.* **2018,** *8,* 11134–11139. doi:10.1021/acscatal.8b03592
55. Dong, Z.; MacMillan, D. W. C. *Nature* **2021,** *598,* 451–456. doi:10.1038/s41586-021-03920-6
56. Wang, J. Z.; Sakai, H. A.; MacMillan, D. W. C. *Angew. Chem., Int. Ed.* **2022,** *61,* e202207150. doi:10.1002/anie.202207150
57. Wu, F.; Wang, L.; Chen, J.; Nicewicz, D. A.; Huang, Y. *Angew. Chem., Int. Ed.* **2018,** *57,* 2174–2178. doi:10.1002/anie.201712384
58. McManus, J. B.; Griffin, J. D.; White, A. R.; Nicewicz, D. A. *J. Am. Chem. Soc.* **2020,** *142,* 10325–10330. doi:10.1021/jacs.0c04422

License and Terms

BEILSTEIN JOURNAL OF ORGANIC CHEMISTRY

Visible-light-mediated flow protocol for Achmatowicz rearrangement

Joachyutharayalu Oja[1], Sanjeev Kumar[1,2] and Srihari Pabbaraja[*1,2]

Letter

Open Access

Address:
[1]Department of Organic Synthesis & Process Chemistry, CSIR-Indian Institute of Chemical Technology, Hyderabad-500007, India and [2]Academy of Scientific and Innovative Research (AcSIR), Ghaziabad 201002, India

Email:
Srihari Pabbaraja[*] - srihari@iict.res.in

* Corresponding author

Keywords:
Achmatowicz reaction; flow chemistry; furfuryl alcohols; photocatalyst; sunlight

Beilstein J. Org. Chem. **2024,** *20,* 2493–2499.
https://doi.org/10.3762/bjoc.20.213

Received: 02 August 2024
Accepted: 26 September 2024
Published: 08 October 2024

This article is part of the thematic issue "Sustainable concepts in catalysis: nonprecious metals and visible light".

Guest Editor: O. El-Sepelgy

Abstract

The batch processes of APIs/pharmaceutical synthesis are prone to suffer significant limitations, including longer process time, shortage of skilled manpower, laborious post-synthetic work-up, etc. To address the inherent limitations of batch processes, a novel approach was undertaken, resulting in the establishment and development of a visible light-assisted modular photo-flow reactor with a seamlessly integrated post-synthetic work-up procedure enabling the efficient synthesis of dihydropyranones from furfuryl alcohols. The reaction uses sun light as green energy source, and the novel photo-flow reactor platform developed with an integrated system enabling a downstream process in a time and labor-efficient manner which facilitates the Achmatowicz rearrangement, resulting in a fast (10 min) formation of the dihydropyranone products.

Introduction

The furan ring moiety is present in several natural products [1] and serves as a key precursor to 1,4-dicarbonyls [2], cyclopentanones [3], and carboxylic acids [4], in synthetic organic chemistry. Furfuryl alcohols, a family of 2-substituted furan molecules, are Achmatowicz rearrangement substrates for accessing highly decorated dihydropyranones [5]. In recent years, several groundbreaking approaches for the synthesis of dihydropyranones have been described by diverse groups of researchers [6]. These techniques do not require any pre-functionalization of non-prefunctionalized materials in order to proceed with the rearrangement. However, the Achmatowicz reaction or similar methodologies involve a catalytic to stoichiometric amount of oxidants such as *m*-CPBA [7], PCC [8], Br_2 [9], NBS [10], DMDO [11], KBr/Oxone [12], $Na_2S_2O_8$ [13], photosensitizers/O_2[1] [14], or Me_2S [15], spirulina [16], $Ti(OiPr)_4$/*t*-BuOOH [17], $VO(acac)_2$)/*t*-BuOOH [18], and enzymatic oxidation [19] etc., which may compromise the environmental benefits (Scheme 1a,b) and take longer reaction times. Alternatively, a

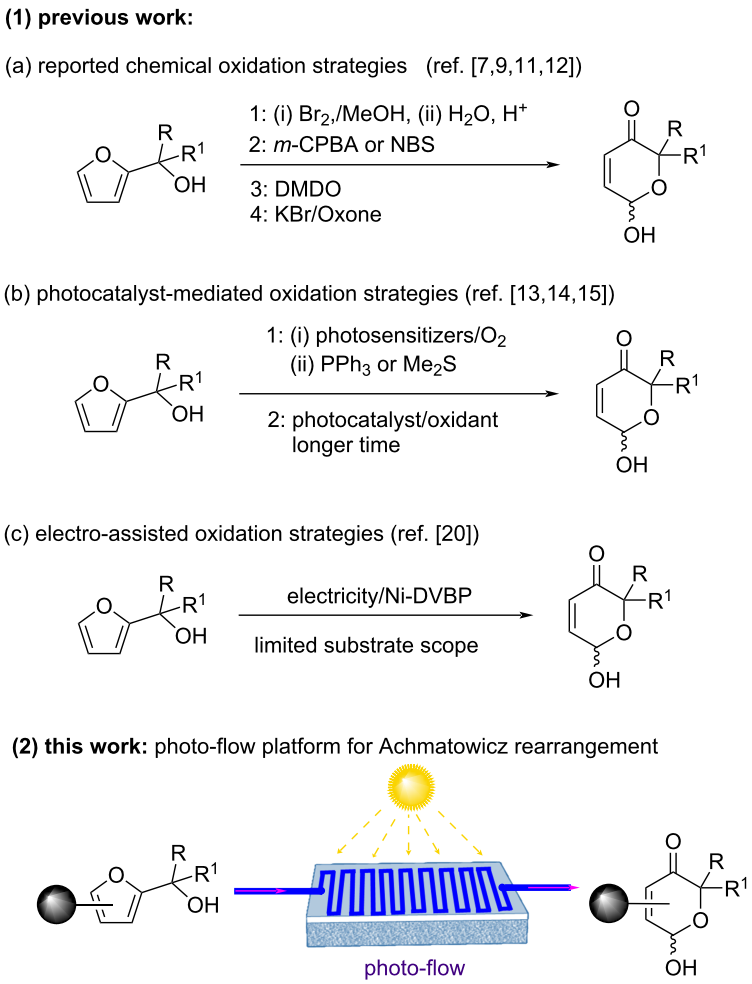

Scheme 1: Strategies for Achmatowicz rearrangement.

new green pathway is necessary for the Achmatowicz reaction to be performed in a faster and safer manner.

Towards this direction, few research groups have already reported the Achmatowicz reaction utilizing greener approaches, yet they suffered due to some limitations. Sun et al. [20] have successfully demonstrated an Achmatowicz rearrangement using electricity as a green oxidant (Scheme 1c) in a batch protocol. This electrochemical batch process utilizes electricity to enhance the vibrational energy of the substrate for the completion of the reaction and involves a noble metal, such as Ni-DVBP as an electrode. Also, the batch technique encounters a serious issue when considered for bulk production as a result of the expensive cost of Ni-DVBP and Ag/AgCl electrode, low surface-to-volume ratio, ineffective mixing, and sluggish heat exchange. The longer inter-electrode distances, may also lead to longer reaction times and poorer reaction selectivity and decreased yields [21]. Jeremy Robertson et al. [22] have demonstrated a combined use of flow and batch processes involving an electrochemical flow cell for the oxidation of furfuryl alcohols and subsequently utilizing the crude electrolysis mixture for hydrolysis in a traditional batch process to get the rearranged Achmatowicz product.

As a result, developing an alternative strategy would be an attractive solution to address the limitations described above. Flow chemistry was chosen as the most attractive alternative for the photo-induced (visible light) Achmatowicz rearrangement to convert furfuryl alcohol scaffolds into dihydropyranones due to its ability to better control of reaction conditions, including

more uniform light exposure and improved mixing efficiency, which result in higher reaction rates and more consistent product quality. Additionally, the flow system enhances mass transfer and reduces reaction times, leading to more efficient processes and potentially higher yields compared to the batch processes [23]. The first photoredox-mediated Achmatowicz reaction was reported by Gilmore et al. [13] in batch mode utilizing furfuryl alcohols with $Ru(bpy)_3Cl_2{\cdot}6H_2O$ as photocatalyst, $Na_2S_2O_8$ as an oxidant and H_2O/DMSO/MeCN as solvent system to get the product in 2 h excluding work-up procedure. However, safety concerns, long reaction time, downstream process in a time and labor-efficient manner and scalability of the product still arose and thus prompted us to initiate a flow process that could overcome the above challenges. To address these points, a novel continuous photo-flow platform for the Achmatowicz reaction including integrated post-synthetic work-up in a safe and faster manner with less intervention of human was developed (Scheme 1 (2)). This process involves a nature abundant energy source such as sun light and biomass-derived furfuryl alcohols as starting material making it more environmental benign.

Results and Discussion

A batch process Achmatowicz rearrangement mediated by less expensive rose bengal as photocatalyst (PC) was first reported by Vassilikogiannakis et al. [24] and was further developed by Guan-Ben Du et al. [14]. Very often, the photolysis reactions performed in batch process encounter issues that include ineffective illumination, improper mixing, prolonged reaction durations, low quantum efficiency and mass transfer, a limited surface-to-volume ratio, along with an inadequate reaction selectivity [25]. Continuous flow technology has emerged as an attractive solution for many of these challenges, gaining popularity for its ability to efficiently address these issues. Additionally, this platform offers the advantage of integrating multiple steps, i.e., performing multistep transformations, then reaction extraction and separation, into a single process, which are typically performed individually/separately in batch methods. This enhances the overall efficiency for obtaining the desired product(s) from the reaction mixture. In continuation to our efforts on developing flow-based platforms, we herein present a photo-flow platform for Achmatowicz reactions. A novel photo-flow solar panel reactor was fabricated to test and validate the Achmatowicz rearrangement reaction (Figure S1, Supporting Information File 1), and the reaction conditions were optimized with a ruthenium catalyst. As illustrated in Figure S1, Supporting Information File 1, a flat photo-flow reactor was predesigned comprising a wide-surface polystyrene sheet (length 50 cm × width 50 cm × height 5 cm) bearing a reactor (PFA tubing) that was manually put and hooked on the polystyrene surface (Figure S1b, Supporting Information File 1). This reactor was then exposed to sunlight/handmade LED to carry out the Achmatowicz rearrangement reaction. To test the model reaction's feasibility, a stock solution containing ethyl 3-(furan-2-yl)-3-hydroxypropanoate (**2a**)/$Ru(bpy)_3Cl_2{\cdot}6H_2O$/$K_2S_2O_8$/ACN (2 mL)/DMSO (2 mL)/$H_2O$ (4 mL) as a molar ratio of 1:1:0.005:70:54:408 was taken in one syringe and pumped to our fabricated photo-flow reactor (10 mL – PFR). The passing solution was then exposed to solar light (February to April sunlight in Hyderabad, India), to execute the Achmatowicz rearrangement, and a complete conversion was observed within 10 min (Table 1, entry 1). The Achmatowicz rearrangement product **3a** was obtained in 82% yield (Table 1, entry 1) using $Ru(bpy)_3Cl_2{\cdot}6H_2O$ as a PC under solar light at 28–34 °C, light intensity 330000–322000 lux [26] with a flow rate of 1.0 mL min^{-1} in 10 mL reactor (10 min duration). A light-off experiment was performed to examine the Achmatowicz rearrangement's dependence on light, and it was observed that continuous light irradiation was required (Table 1, entry 2). Next, we considered running the process without utilizing the $Ru(bpy)_3Cl_2{\cdot}6H_2O$ catalyst (Table 1, entry 3). There was no evidence of product formation, indicating that the Ru catalyst was required to pursue the photoinduced Achmatowicz rearrangement. Furthermore, it was observed that the product yield depended on resident time and it dropped over time as the residence time was reduced (see details in Supporting Information File 1, Table S1, entries 4–6) however, when the time was increased there was minimal enhancement in yield (see details in Supporting Information File 1, Table S1, entry 2). Following additional adjustment of the reaction conditions with various solvents, oxidants, lights, and photocatalysts, (see details in Supporting Information File 1, Table S1, entries 10–18), it was discovered that a combination of ACN/DMSO/H_2O solvent, $K_2S_2O_8$ oxidant, $Ru(bpy)_3Cl_2{\cdot}6H_2O$ photocatalyst, and 28–34 °C temperature were the best-suited and optimized reaction conditions. After optimization, our efforts were put towards investigating for the selective elimination of the waste solvent using an integrated one-flow work-up procedure to generate **3a** with maximum practicality. Initially, the individual stages of the liquid–liquid extraction was achieved using the droplet micro fluidic method for extracting the compound (see details in Supporting Information File 1, Table S2). In this context, our previously in-house-developed liquid–liquid extractor was utilized (see details in Supporting Information File 1, Figure S4) [27]. After few trials towards optimization of extraction and separation, the best yield (82%) was obtained when EtOAc (flow rate set at 2.5 mL/min), water (flow rate set at 4.5 mL/min) were taken with the extraction time of 0.25 min and separation time of 0.11 min (see details in Supporting Information File 1, Table S2, entry 5). To verify the steadiness of the newly constructed integrated photo-flow system, we performed the experiment continuously for one hour under our op-

Table 1: Optimization of continuous flow Achmatowicz reaction[a].

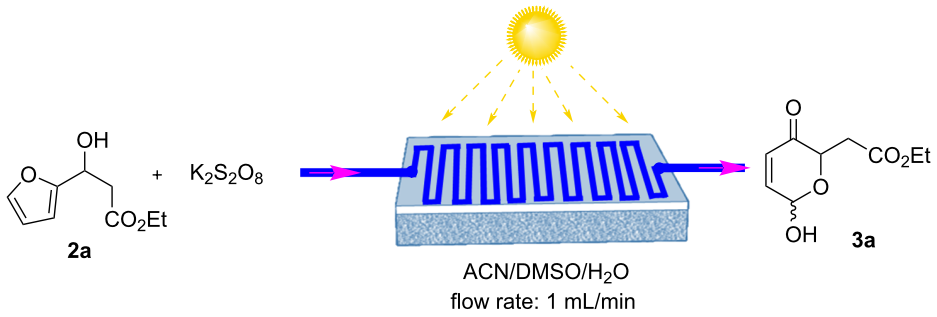

Entry	Deviation from standard conditions	% Yield[b]
1	none	82
2	without light	NR
3	without $Ru(bpy)_3Cl_2·6H_2O$	NR
4	without $K_2S_2O_8$	NR
5	$Na_2S_2O_8$ instead of $K_2S_2O_8$	82
6	blue LED (30 W)	70
7	white LED (30 W)	80
8	$RuCl_2·6H_2O$ instead of $Ru(bpy)_3Cl_2·6H_2O$	32
9	methylene blue or rose bengal	trace

[a]Reaction conditions: **2a** (100 mg, 0.54 mmol, 1.0 equiv)/$K_2S_2O_8$ (146 mg, 0.54 mmol, 1.0 equiv)/$Ru(bpy)_3Cl_2·6H_2O$ (2 mg, 2.6 μmol, 0.005 equiv)/ACN (2 mL)/DMSO (2 mL)/H_2O (4 mL) in molar ratio of 1:1:0.005:70:54:408 and a reactor volume of 10 mL at room temperature; [b]yields are based on isolated yields.

timized conditions, yielding 16.058 g day^{-1} production (see details in Supporting Information File 1, section 5.1). On the other hand, the traditional batch process requires longer durations to make an identical Achmatowicz rearrangement reaction [7-10,14,15].

With the established photo-flow platform and optimized conditions, we were interested in investigating the scope of this methodology using several substituted furfuryl alcohol substrates (**2a–p**) which were subjected to the Achmatowicz reaction utilizing our photo-flow platform to provide the corresponding dihydropyranone products (**3a**–**p**) with moderate to good yields (51–85%), Figure 1.

We investigated several furanol derivatives by altering the substituents at two critical positions: the hydroxymethyl carbon and the 5-position of the furan ring, that were essential for the Achmatowicz reaction. Figure 1 demonstrates that even when there was no substituent at the hydroxymethyl position (in **2b**), the reaction proceeded effectively, leading to the formation of **3b** with an 80% yield inferring that the absence of substituents at the hydroxymethyl group does not prevent the formation of the desired product. At the same position, introducing more substituents such as *n*-butyl (**2c**), dimethyl (**2d**), cyclohexyl (**2e**) and sterically crowded diphenyl (**2f**) groups also led to the corresponding products (**3c**–**f**) with average to good yields that were comparable to that obtained from the unsubstituted furfuryl alcohol **2b**. These findings highlight the robustness of the Achmatowicz reaction in accommodating variations at these key sites. Next, the effect of the *p*-substituted phenyl group was also investigated by evaluating substrates **2g**, **2h** showing not much variations in the yields of the products **3g** and **3h**. The more electron-withdrawing *m*-fluorophenyl (**2i**), *o*-chlorophenyl (**2j**), *o*-bromophenyl (**2k**), *o*-trifluoromethylphenyl (**2l**), and *o*-nitrophenyl (**2m**) groups also resulted in comparable yields of **3g–m**, respectively, indicating no significant effect of substitutents on the aryl ring. A similar result was also obtained with dimethoxy-substituted phenyl moiety (**2n**) affording **3n** with a slightly lower yield of 74%. The substitution at C5-position on the furan ring in furfuryl alcohol derivatives were further investigated. A methyl group at the 5-position (**2o**, **2p**) resulted in the corresponding products (**3o**, **3p**) in good yields. All the products obtained were characterized by ^{1}H NMR, ^{13}C NMR and mass spectrometry techniques.

A plausible catalytic cycle has been postulated based on a literature study [13], and is shown in Figure 2. With the exposure of photocatalyst to sunlight/LED light, $[Ru(bpy)_3]^{2+}$ undergoes transition to $[Ru(bpy)_3]^{2+*}$ which is quenched by persulfate resulting in $[Ru(bpy)_3]^{3+}$ along with the simultaneous generation

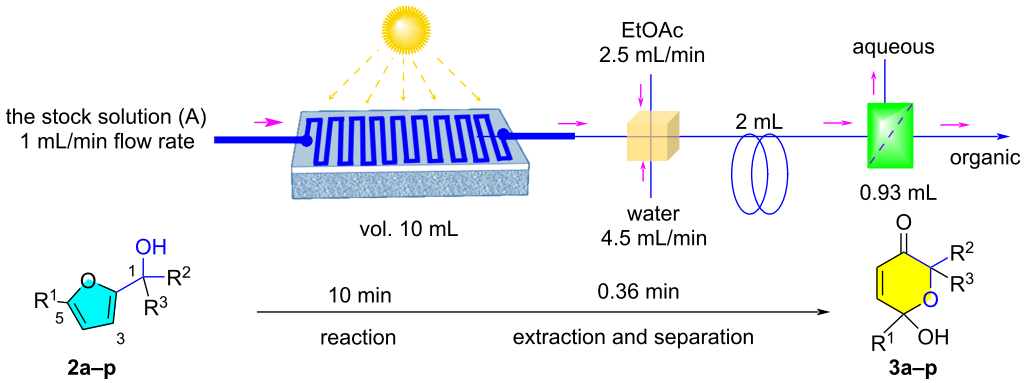

2a: R^1 = H, R^2 = H, R^3 = CH_2CO_2Et
2b: R^1 = H, R^2 = H, R^3 = H
2c: R^1 = H, R^2 = H, R^3 = *n*-butyl
2d: R^1 = H, R^2 = Me, R^3 = Me
2e: R^1 = H, R^2 = R^3 = cyclohexyl
2f: R^1 = H, R^2 = R^3 = Ph
2g: R^1 = H, R^2 = H, R^3 = 4-isopropylphenyl
2h: R^1 = H, R^2 = H, R^3 = 4-(methoxycarbonyl)phenyl
2i: R^1 = H, R^2 = H, R^3 = 3-fluorophenyl
2j: R^1 = H, R^2 = H, R^3 = 2-chlorophenyl
2k: R^1 = H, R^2 = H, R^3 = 2-bromophenyl
2l: R^1 = H, R^2 = H, R^3 = 2-trifluoromethylphenyl
2m: R^1 = H, R^2 = H, R^3 = 2-nitrophenyl
2n: R^1 = H, R^2 = H, R^3 = 3,4-dimethoxyphenyl
2o: R^1 = Me, R^2 = H, R^3 = H
2p: R^1 = Me, R^2 = H, R^3 = Me

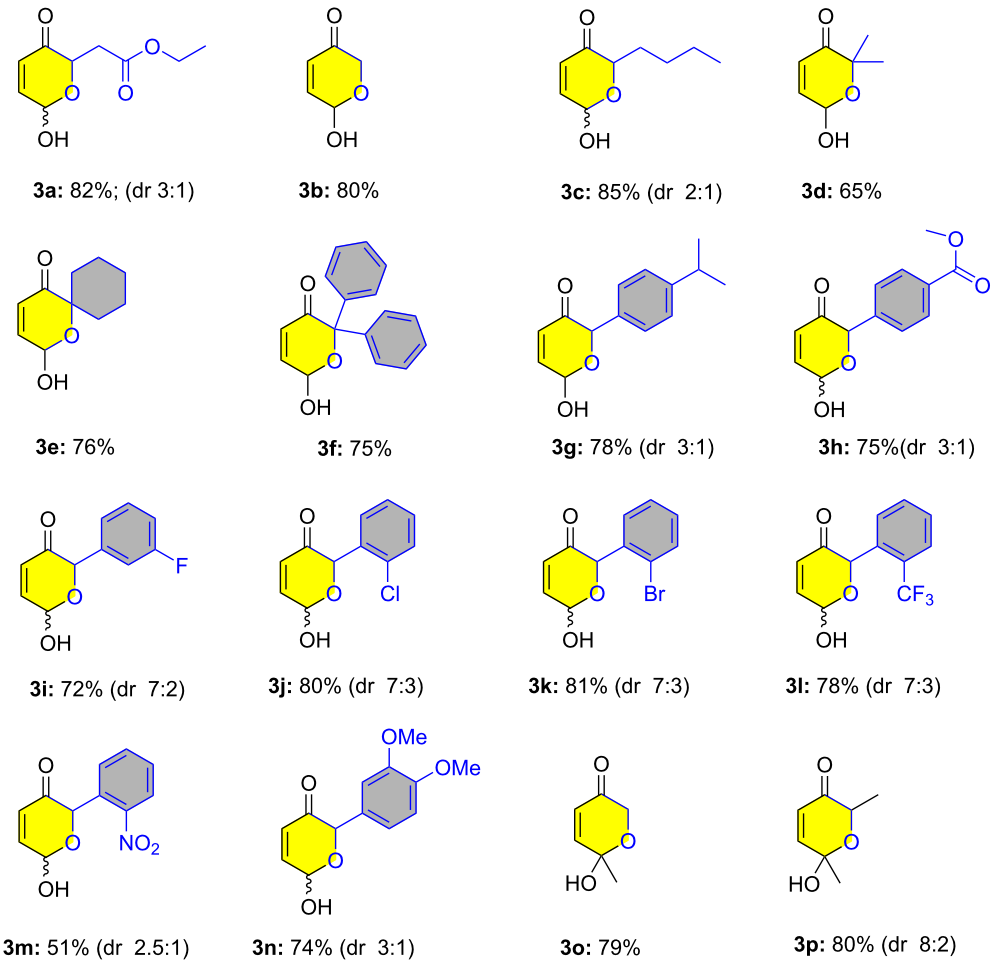

3a: 82%; (dr 3:1)
3b: 80%
3c: 85% (dr 2:1)
3d: 65%
3e: 76%
3f: 75%
3g: 78% (dr 3:1)
3h: 75%(dr 3:1)
3i: 72% (dr 7:2)
3j: 80% (dr 7:3)
3k: 81% (dr 7:3)
3l: 78% (dr 7:3)
3m: 51% (dr 2.5:1)
3n: 74% (dr 3:1)
3o: 79%
3p: 80% (dr 8:2)

Figure 1: Scope of the integrated continuous photo-flow (visible light)-induced Achmatowicz rearrangement reaction. Reaction conditions: Stock solution (A) comprise of **2**/$K_2S_2O_8$/$Ru(bpy)_3Cl{\cdot}6H_2O$/ACN/DMSO/H_2O in a molar ratio of 1:1:0.005:70:54:408; yields are based on isolated yields.

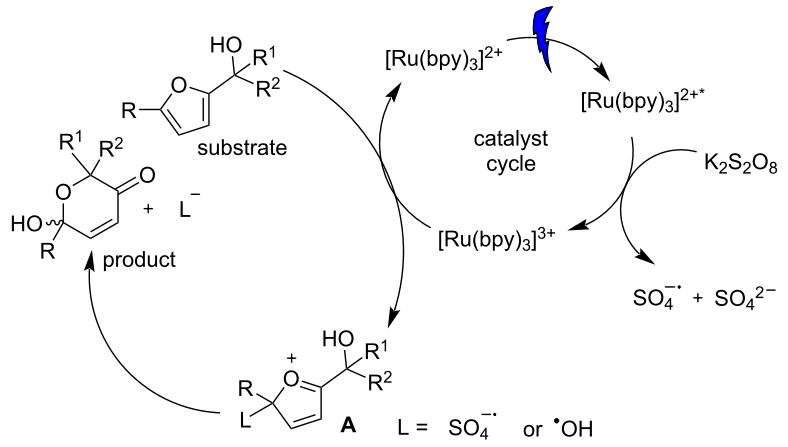

Figure 2: Proposed mechanism for the photochemically induced Achmatowicz rearrangement.

of sulfate and a sulfate radical. SET from furfuryl alcohol closes the catalytic cycle of the PC and an intermediate A is generated with L (L = $SO_4^{-\cdot}$ or OH). The Achmatowicz product is formed by addition of water to oxocarbenium intermediate A followed by elimination of L.

Conclusion

In conclusion, an integrated continuous PFR platform for photocatalytic functionalization of furfuryl alcohols to dihydropyranones through an Achmatowicz rearrangement is accomplished. The combined steps include fast reaction (10 min), and post-synthetic work-up (extraction time 0.25 min and separation time 0.11 min) in safe environment with minimal human intervention and avoiding hazardous chemical exposure. The process utilizes nature abundant energy sources such as sun light, as a greener approach and easily available biomass-derived furfuryl alcohols as starting materials. The flow platform with the developed protocol was utilized successfully to make several dihyropyranones that may find wide applications in medicinal and materials chemistry and natural product synthesis.

Supporting Information

Supporting Information File 1

Experimental section and NMR spectra.
[https://www.beilstein-journals.org/bjoc/content/supplementary/1860-5397-20-213-S1.pdf]

Supporting Information File 2

Video of the experimental set up.
[https://www.beilstein-journals.org/bjoc/content/supplementary/1860-5397-20-213-S2.mp4]

Acknowledgements

CSIR-IICT manuscript communication no. IICT/Pubs./2023/351.

Funding

One of the authors (SK) is thankful to the Council of Scientific & Industrial Research (CSIR), New Delhi, for providing a Senior Research Fellowship (CSIR-SRF). The authors OJ and PS thank SERB for financial assistance. Funding from SERB, New Delhi with sanction order no. CRG/2022/002136 under budget head GAP-0961 (internal).

Author Contributions

Joachyutharayalu Oja: investigation; visualization; writing – original draft. Sanjeev Kumar: investigation; visualization; writing – original draft. Srihari Pabbaraja: conceptualization; supervision; writing – review & editing.

ORCID® iDs

Srihari Pabbaraja - https://orcid.org/0000-0002-1708-6539

Data Availability Statement

All data that supports the findings of this study is available in the published article and/or the supporting information of this article.

References

1. Ochi, M.; Yamada, K.; Kawakami, H.; Tatsukawa, A.; Kotsuki, H.; Shibata, K. *Tetrahedron Lett.* **1992,** *33,* 7531–7534. doi:10.1016/s0040-4039(00)60816-x
2. Merino, P.; Tejero, T.; Delso, J. I.; Matute, R. *Curr. Org. Chem.* **2007,** *11,* 1076–1091. doi:10.2174/138527207781369245
3. Piancatelli, G.; D'Auria, M.; D'Onofrio, F. *Synthesis* **1994,** 867–889. doi:10.1055/s-1994-25591
4. Gutnov, A. *Chem. Heterocycl. Compd.* **2016,** *52,* 87–89. doi:10.1007/s10593-016-1836-4

5. Montagnon, T.; Tofi, M.; Vassilikogiannakis, G. *Acc. Chem. Res.* **2008,** *41,* 1001–1011. doi:10.1021/ar800023v
6. Liang, L.; Guo, L.-D.; Tong, R. *Acc. Chem. Res.* **2022,** *55,* 2326–2340. doi:10.1021/acs.accounts.2c00358
7. Georgiadis, M. P.; Couladouros, E. A.; Polissiou, M. G.; Filippakis, S. E.; Mentzafos, D.; Terzis, A. *J. Org. Chem.* **1982,** *47,* 3054–3058. doi:10.1021/jo00137a005
8. Piancatelli, G.; Scettri, A.; D'Auria, M. *Tetrahedron Lett.* **1977,** *18,* 2199–2200. doi:10.1016/s0040-4039(01)83720-5
9. Achmatowicz, O., Jr.; Bukowski, P.; Szechner, B.; Zwierzchowska, Z.; Zamojski, A. *Tetrahedron* **1971,** *27,* 1973–1996. doi:10.1016/s0040-4020(01)98229-8
10. Couladouros, E. A.; Georgiadis, M. P. *J. Org. Chem.* **1986,** *51,* 2725–2727. doi:10.1021/jo00364a020
11. Adger, B. M.; Barrett, C.; Brennan, J.; McKervey, M. A.; Murray, R. W. *J. Chem. Soc., Chem. Commun.* **1991,** 1553–1554. doi:10.1039/c39910001553
12. Zhao, G.; Tong, R. *Green Chem.* **2019,** *21,* 64–68. doi:10.1039/c8gc03030h
13. Plutschack, M. B.; Seeberger, P. H.; Gilmore, K. *Org. Lett.* **2017,** *19,* 30–33. doi:10.1021/acs.orglett.6b03237
14. Zhou, B.; Tao, Y.-F.; He, Y.-J.; Liu, L.-X.; Chang, Z.-H.; Li, X.-H.; Lin, T.; Du, G.-B. *Green Chem.* **2023,** *25,* 196–210. doi:10.1039/d2gc03344e
15. Lee, G. C. M.; Syage, E. T.; Harcourt, D. A.; Holmes, J. M.; Garst, M. E. *J. Org. Chem.* **1991,** *56,* 7007–7014. doi:10.1021/jo00025a012
16. Noutsias, D.; Alexopoulou, I.; Montagnon, T.; Vassilikogiannakis, G. *Green Chem.* **2012,** *14,* 601–604. doi:10.1039/c2gc16397g
17. Ho, T.-L.; Sapp, S. G. *Synth. Commun.* **1983,** *13,* 207–211. doi:10.1080/00397918308065990
18. Ji, Y.; Benkovics, T.; Beutner, G. L.; Sfouggatakis, C.; Eastgate, M. D.; Blackmond, D. G. *J. Org. Chem.* **2015,** *80,* 1696–1702. doi:10.1021/jo502641d
19. Thiel, D.; Doknić, D.; Deska, J. *Nat. Commun.* **2014,** *5,* 5278. doi:10.1038/ncomms6278
20. Liu, X.; Li, B.; Han, G.; Liu, X.; Cao, Z.; Jiang, D.-e.; Sun, Y. *Nat. Commun.* **2021,** *12,* 1868. doi:10.1038/s41467-021-22157-5
21. Noël, T.; Cao, Y.; Laudadio, G. *Acc. Chem. Res.* **2019,** *52,* 2858–2869. doi:10.1021/acs.accounts.9b00412
22. Syntrivanis, L.-D.; del Campo, J. F.; Robertson, J. *J. Flow Chem.* **2018,** *8,* 123–128. doi:10.1007/s41981-018-0016-3
23. Baumann, M.; Moody, T. S.; Smyth, M.; Wharry, S. *Org. Process Res. Dev.* **2020,** *24,* 1802–1813. doi:10.1021/acs.oprd.9b00524
24. Noutsias, D.; Kouridaki, A.; Vassilikogiannakis, G. *Org. Lett.* **2011,** *13,* 1166–1169. doi:10.1021/ol200027f
25. Cambié, D.; Bottecchia, C.; Straathof, N. J. W.; Hessel, V.; Noël, T. *Chem. Rev.* **2016,** *116,* 10276–10341. doi:10.1021/acs.chemrev.5b00707
26. Rana, A.; Malviya, B. K.; Jaiswal, D. K.; Srihari, P.; Singh, A. K. *Green Chem.* **2022,** *24,* 4794–4799. doi:10.1039/d2gc00649a
27. Sthalam, V. K.; Mahajan, B.; Karra, P. R.; Singh, A. K.; Pabbaraja, S. *RSC Adv.* **2023,** *13,* 1455. doi:10.1039/d2ra90133a

License and Terms